

**DESIGN AND APPLICATIONS OF PHOSPHINE
LIGANDS TO TRANSITION METAL-CATALYZED
REACTIONS**

JIANG CHUNHUI

NATIONAL UNIVERSITY OF SINGAPORE

2014

**DESIGN AND APPLICATIONS OF PHOSPHINE
LIGANDS TO TRANSITION METAL-CATALYZED
REACTIONS**

JIANG CHUNHUI
(M.Sc., Nanjing Univ.)

**A THESIS SUBMITTED FOR THE DEGREE
OF DOCTOR OF PHILOSOPHY**

DEPARTMENT OF CHEMISTRY

NATIONAL UNIVERSITY OF SINGAPORE

2014

Thesis Declaration

I hereby declare that this thesis is my original work and it has been written by me in its entirety Prof. Lu Yixin, Chemistry Department, National University of Singapore, between 08/2010 and 07/2014.

I have duly acknowledged all the sources of information which have been used in the thesis.

This thesis has not been submitted for any degree in any university previously.

The content of the thesis has been partly published in:

1. **Chunhui Jiang**, Yixin Lu*, Tamio Hayashi*, "High Performance of a Palladium-Phosphinooxazoline Catalyst in Asymmetric Arylation of Cyclic N-Sulfonyl Ketimines," *Angew. Chem. Int. Ed.* **2014**, Early View. (DOI: 10.1002/anie.201406147)

Jiang Chunhui
Name


Signature

24/01/2015
Date

Acknowledgements

I would like to express my sincere gratitude to all the people who have helped and inspired me during my PhD studies in the past 4 years. Without their supports, this thesis could not have been accomplished.

Foremost, I would like to thank my supervisor, Prof. Lu Yixin, for offering all his enthusiasm and guidance throughout my studies. His profound knowledge, patience and motivation inspire me a lot and will accompany me in my future career.

Besides my advisor, I am deeply indebted to Prof. Tamio Hayashi for his sharing of knowledge and intellectual discussions.

Every member of Prof. Lu's group has been extremely supportive and I really appreciate their support and encouragement. I especially thank Dr. Yao Weijun, Dr. Vasudeva Rao Gandi, Dr. Wang Tianli, Dr. Liu Xiaoqian, Dr Luo Jie, Dr. Han Xiaoyu, Dr. Zhong Fangrui, Dr. Chen Guoying, Dr. Jacek Kwiatkowski, Dr. Dou Xiaowei, Wen Shan, Wong Yee Lin, Zhou Xin, Zhou Bo and other labmates for their help during my PhD studies.

I also want to thank NUS for the research scholarship and financial support. Thanks also go to all the staff in NMR, Mass, and X-Ray labs for their help.

Last but not least, I am extremely grateful to my beloved wife, Li Qing, and my little angel, Jiang Run-xi, for always standing by me and supporting me wordlessly. I thank to my parents-in-law for taking care of my small family without me around. My gratitude also goes to my parents and sister for their endless love and support.

Table of Contents

Thesis Declaration	i
Acknowledgements	ii
Table of Contents	iii
Summary	vi
List of Tables	viii
List of Figures	ix
List of Schemes	x
List of Abbreviations	xiv
List of Publications	xvii
Chapter 1 Introduction	1
1.1 Historical background of asymmetric palladium catalysis	1
1.2 Palladium-catalyzed asymmetric additions	5
1.2.1 Asymmetric 1,4-additions	6
1.2.2 Asymmetric 1,2-additions	18
1.2.2.1 Imine substrates	18
1.2.2.2 Aldehydes and ketones as the substrates	24
1.2.2.3 Olefin substrates	29
1.2.3 Asymmetric cycloadditions	32
1.2.4 Asymmetric 1,6-additions	36
1.3 Project objectives	36
Chapter 2 High Performance of a Palladium Phosphinooxazoline Catalyst in Asymmetric Arylation of Cyclic N-Sulfonyl Ketimines	
2.1 Introduction	39

2.2	Results and discussions	44
2.2.1	Catalytic system comparison	44
2.2.2	Reaction monitoring	49
2.2.3	Substrate scope	51
2.2.4	Derivation	57
2.3	Conclusions	57
2.4	Experimental section	57
2.4.1	General information	57
2.4.2	Ketimines	58
2.4.3	Palladium-Catalyzed Asymmetric Arylation of Ketimines	61
 Chapter 3 Palladium(II)/PHOX Complex-Catalyzed Asymmetric Addition of Boron Reagents to Cyclic Trifluoromethyl Ketimines: An Efficient Preparation of Anti-HIV Drug Analogues		
3.1	Introduction	104
3.2	Results and discussions	110
3.2.1	Catalyst screening	110
3.2.2	Substrate scope	113
3.2.3	Determination of absolute configuration	116
3.3	Conclusions	116
3.4	Experimental section	117
3.4.1	General information	117
3.4.2	Synthesis of cyclic <i>N</i> -trifluoromethyl ketimine	118
3.4.3	Palladium-catalyzed asymmetric arylation of ketimines	118
3.4.4	X-ray crystallographic analysis of 3-23am	119
3.4.5	Analytical data of dihydroquinazoline 3-23	121

**Chapter 4 Development of New Phosphine Ligands Derived from Amino Acids
and Their Applications in Transition-Metal-Catalyzed Asymmetric
Reactions**

4.1	Introduction	139
4.2	Results and discussions	145
4.2.1	Phosphine-amide ligands	145
4.2.2	Phosphine-olefin ligands	154
4.2.3	Phosphine-imine ligands	156
4.3	Conclusions	161
4.4	Experimental section	161
4.4.1	General information	162
4.4.2	General procedure for preparation of ligands	162
4.4.2.1	Phosphine-amide ligands from L-valine	162
4.4.2.2	Phosphine-amide ligands from L-threonine	164
4.4.2.3	Phosphine-peptide ligands from L-threonine	165
4.4.2.4	Phosphine-thiourea ligands from L-threonine	166
4.4.2.5	Phosphine-olefin ligands	167
4.4.2.6	Phosphine-imine ligands	168
4.4.3	General procedure for transition-metal-catalyzed reactions	169
4.4.3.1	Pd-catalyzed AAA reaction	169
4.4.3.1	Ag-catalyzed Mannich reaction	170
4.4.3.1	Rh-catalyzed 1,4-addition	171
4.4.3.1	Pd-catalyzed 1,2-addition	172

Summary

This thesis mainly describes the development of asymmetric palladium catalysis in nucleophilic additions of organoboron reagents to cyclic ketimines to synthesize chiral nitrogen-containing compounds with tertiary carbon center. In addition, this thesis also depicts the attempts of developing new phosphine based ligands derived from amino acids and the preliminary results of their applications in different transition-metal-catalyzed asymmetric reactions.

Chapter 1 gave a brief historical background of asymmetric palladium catalysis. The Inventions of three most famous reactions, “Tsuji–Trost reaction, Mizoroki–Heck reaction and palladium-catalyzed cross-coupling,” were shortly introduced. Beside them, the recent progress of palladium asymmetric addition was also summarized and a selection of examples in this field were described in details, including 1,4-addition, 1,2 addition, cycloaddition and so on.

Chapter 2 demonstrated the high performance of palladium-phosphinooxazoline catalyst in asymmetric arylation of cyclic *N*-sulfonyl ketimines, giving high yields of chiral cyclic sulfonamides which bear tetra-substituted stereogenic center. A systematic comparison between this catalytic system with others was discussed in the main content.

Chapter 3 further studied the application of palladium-phosphinooxazoline catalyst in asymmetric addition of organoboron reagents to cyclic trifluoromethyl ketimines. This methodology provided an easy access to anti-HIV drug analogues with potential biological activity.

Chapter 4 presented the development of new phosphine based chiral ligands derived from amino acids, including phosphine-amide ligands, phosphine-peptide

ligands phosphine-olefin ligands and phosphine-imine ligands. These newly developed ligands were further screened in a series of transition-metal-catalyzed reactions.

List of Tables

Table 2.1	Catalytic Asymmetric Addition of Phenylboronic Acid (2-19m) to Cyclic <i>N</i> -Sulfonyl Aldimine 2-18a and Ketimine 2-18b	47
Table 2.2	Details of monitoring the reaction process of 2-18a	49
Table 2.3	Details of monitoring the reaction process of 2-18b	50
Table 2.4	Palladium-Catalyzed Asymmetric Addition of Arylboronic Acids 2-19m–z to Cyclic <i>N</i> -Sulfonyl Ketimines 2-18b–d .	52
Table 2.5	Condition screening for asymmetric addition of 2-19w to 2-18b	54
Table 2.6	Palladium-Catalyzed Asymmetric Addition of Arylboronic Acids to Cyclic <i>N</i> -Sulfonyl Aryl Ketimines 2-18e–g .	55
Table 3.1	Catalytic Asymmetric Addition of Phenylboronic Acid to Cyclic <i>N</i> -trifluoromethyl ketimine	110
Table 3.2	Catalytic Asymmetric Addition of Arylboronic Acid 3-22 to Cyclic <i>N</i> -trifluoromethyl ketimine 3-1a	113
Table 4.1	Phosphine ligands in Pd-catalyzed AAA reaction of malonate with allylic acetate	148
Table 4.2	Phosphine ligands in Pd-catalyzed AAA reaction of nitrophosphonate with allylic carbamate	150
Table 4.3	Phosphine ligands in Pd-catalyzed AAA reaction of α -fluoro- β -ketoester with allylic carbamate	151
Table 4.4	Phosphine ligands in Pd-catalyzed AAA reaction of phthalide derivative with allylic carbamate	151
Table 4.5	Phosphine ligands in Ag-catalyzed asymmetric Mannich reaction	153
Table 4.6	Phosphine-olefin ligands in Rh-catalyzed 1,4-addition	156
Table 4.7	Pd/phosphine-imine complex catalyzed asymmetric arylation of 6-membered cyclic imine	160

List of Figures

Figure 3.1	ORTEP structure of dihydroquinazoline 3-23am	116
Figure 4.1	³¹ P NMR study on coordination between Rh catalyst and phosphine-olefin ligand	157

List of Schemes

Scheme 1.1	The catalytic cycle of Wacker process	2
Scheme 1.2	The Tsuji-Trost reaction	2
Scheme 1.3	Palladium-catalyzed Mizoroki-Heck reaction	4
Scheme 1.4	Transition Metal-catalyzed cross-coupling	5
Scheme 1.5	First example of a Pd-catalyzed 1,4-addition of organoboronic acids	6
Scheme 1.6	Difference in reactivity between neutral Pd- and Rh- enolates	7
Scheme 1.7	Pd/dppe complex catalyzed 1,4-addition of boronic acids	7
Scheme 1.8	Pd-catalyzed asymmetric 1,4-addition of organoboron reagents to α,β -saturated ketones	8
Scheme 1.9	Miyaura's representative work on Pd-catalyzed asymmetric 1,4-additions	9
Scheme 1.10	Pd-catalyzed asymmetric arylations of α,β -unsaturated carbonyls	10
Scheme 1.11	Palladacycles as catalysts for asymmetric 1,4-addition	11
Scheme 1.12	NHC/Pd(II) complex catalyzed asymmetric 1,4-addition	11
Scheme 1.13	Pd/pyrox catalyzed 1,4-additions to β -substituted cyclic enones	12
Scheme 1.14	Pd-catalyzed asymmetric addition of Ph_2PH to β -aryl enone	13
Scheme 1.15	Pd-catalyzed asymmetric additions of diphenylphosphine to α,β -unsaturated carbonyl compounds	14
Scheme 1.16	Asymmetric 1,4-addition of HPPH_2 reported by Leong et al.	15
Scheme 1.17	Arylsiloxanes as nucleophiles in Pd-catalyzed 1,4-addition	15
Scheme 1.18	Anilines as nucleophiles in Pd-catalyzed asymmetric 1,4-additions	16
Scheme 1.19	Pd-catalyzed enantioselective protonation via 1,4-addition	17
Scheme 1.20	Pd-catalyzed enantioselective Friedel-Crafts alkylation	17

Scheme 1.21	Sodeoka's work on Pd-catalyzed asymmetric addition of β -ketoesters to imines	19
Scheme 1.22	Asymmetric arylations of imines by Lu et al.	20
Scheme 1.23	Shi's work on Pd-catalyzed asymmetric additions to Ts- and Boc-imines	21
Scheme 1.24	Bisoxazolines as ligands in Pd-catalyzed asymmetric additions to imines	22
Scheme 1.25	Pd-catalyzed enantioselective additions of nitriles to N-tosylimines	22
Scheme 1.26	Pd-catalyzed asymmetric allylation of imines	23
Scheme 1.27	Pd-catalyzed 1,2-addition of malonates to cyclic imines	24
Scheme 1.28	Pd-catalyzed enantioselective arylation of boronic acids to cyclic ketimines	24
Scheme 1.29	Qin's work on the asymmetric addition of boronic acids to isatins	25
Scheme 1.30	Shi's work on the asymmetric addition of boronic acids to isatins	25
Scheme 1.31	Pd-catalyzed enantioselective ene and aldol reactions	26
Scheme 1.32	Pd-catalyzed asymmetric hydroxymethylation of β -keto ester	27
Scheme 1.33	Comparison between NHC based ligands and P-imine ligands in Pd-catalyzed asymmetric allylations of aldehydes	28
Scheme 1.34	Pd-catalyzed enantioselective arylation of aldehydes with arylboronic acids	29
Scheme 1.35	Pd-catalyzed asymmetric addition of $B_2(\text{pin})_2$ to allenes	29
Scheme 1.36	Enantioselective Pd-catalyzed difunctionalizations of alkenes	30
Scheme 1.37	Pd-catalyzed intramolecular cyclization via asymmetric additions to olefins	31
Scheme 1.38	Pd-catalyzed asymmetric hydrocarbonation of allenes	32

Scheme 1.39	Pd-catalytic asymmetric addition of arylboronic acids to cumulenes	32
Scheme 1.40	Lu's work on Pd-catalyzed asymmetric cycloadditions	33
Scheme 1.41	Pd-catalyzed asymmetric arylation cyclization of allenyl aldehyde	34
Scheme 1.42	Pd-catalyzed enantioselective [2+2] cycloaddition	34
Scheme 1.43	Pd-catalytic enantioselective oxidative cascade cyclization	35
Scheme 1.44	Pd-catalyzed asymmetric [3+2] cyclization	35
Scheme 1.45	Duan's work on Pd-catalyzed asymmetric 1,6-addition	36
Scheme 2.1	Hayashi's work on Rh-catalyzed asymmetric addition to <i>N</i> -sulfonyl ketimines	40
Scheme 2.2	Lam's work on Rh-catalyzed asymmetric addition to <i>N</i> -sulfonyl cyclic imines	41
Scheme 2.3	Xu's Sulfur-olefin ligand in asymmetric addition to <i>N</i> -sulfonyl cyclic imines	41
Scheme 2.4	Zhang's work on Pd-catalyzed arylation of cyclic imines	42
Scheme 2.5	Reactivity and utility of cyclic <i>N</i> -sulfonyl imines	43
Scheme 2.6	Ring-opening of the asymmetric arylation products 2-20	44
Scheme 3.1	Structures of Efavirenz, DPC 961 and DPC 083	105
Scheme 3.2	Zn(OTf) ₂ promoted asymmetric alkynylation of ketimine	105
Scheme 3.3	Proline catalyzed asymmetric Mannich reaction of alkyl ketone and ketimine	106
Scheme 3.4	Bifunctional cinchona thiourea catalyzed asymmetric aza-Henry reaction of ketimines and derivation to DPC 083	107
Scheme 3.5	Ma's work on asymmetric reactions of ketimines and synthesis of DPC 083	108
Scheme 4.1	Kagan's DIOP and Knowles' DiPAMP ligands	140

Scheme 4.2	Examples of privileged chiral ligands	141
Scheme 4.3	Amino acid derived chiral ligands: rigid versus flexible	143
Scheme 4.4	Gilbertson's phosphorus containing peptide ligands	144
Scheme 4.5	Achiwa's phosphine-amidine ligand in Pd-catalyzed AAA reaction	144
Scheme 4.6	Morimoto's extension of Achiwa's phosphine-amidine ligand	144
Scheme 4.7	Phosphine-amide ligands derived from amino acids	147
Scheme 4.8	Phosphine-olefin ligands derived from amino acids	156
Scheme 4.9	Phosphine-olefin ligand in Pd-catalyzed AAA reaction	157
Scheme 4.10	Phosphine-imine ligands in Pd-catalyzed AAA reaction	158
Scheme 4.11	Pd/phosphine-imine complexes	159
Scheme 4.12	Pd/phosphine-imine complex catalyzed asymmetric arylation of tosyl imine	159
Scheme 4.13	Pd/phosphine-imine complex catalyzed asymmetric arylation of 5-membered cyclic imine	161
Scheme 4.14	Comparison between Pd/phosphine-imine and Pd/PHOX complexes	162

List of Abbreviations

Ac	Acetyl
Å	ångström
Aq	Aqueous
Ar	Aromatic
Bn	Benzyl
Boc	<i>tert</i> -Butyloxycarbonyl
br	broad
Bz	Benzoyl
Bu	Butyl
Cat.	Catalysts
Conc.	Concentrated
DABCO	1,4-diazabicyclo[2.2.2]octane
DCE	1,2-Dichloroethylene
DMAP	4-Dimethylaminopyridine
DMF	Dimethylformamide
DMSO	Dimethyl sulfoxide
DIPA	Diisopropylamine
d	doublet
<i>d.r.</i>	Diastereomeric ratio
ee	Enantiomeric excess
Et	Ethyl
EWG	Electron-withdrawing group

h	Hour
HPLC	High performance liquid chromatography
IPA	<i>iso</i> -Propanol
m	multiplet
m/z	mass-to-charge ratio
mmol	millimole
MBH	Morita–Bayliss–Hillman
Me	Methyl
Ms	Methyl sulfonyl
μL	microlitre
NR	No reaction
Nu	nucleophile
Ph	Phenyl
Pr	Propyl
ppm	parts per million
q	quartet
r.t.	Room temperature
s	singlet
TBDPS	<i>tert</i> -butyldiphenylsilyl
TBS	<i>tert</i> -butyldimethylsilyl
TDS	hexyldimethylsilyl
TEA	Triethylamine
TFA	Trifluoromethylacetic acid
THF	Tetrahydrofuran

TIPB	1,3,5-Triisopropylphenyl
TPS	Triphenylsilane
TS	Transition state
Ts (Tos)	<i>p</i> -Toluenesulfonyl
t	triplet
vs	versus

List of Publications

1. **Chunhui Jiang**, Yixin Lu*, Tamio Hayashi*, "High Performance of a Palladium-Phosphinooxazoline Catalyst in Asymmetric Arylation of Cyclic N-Sulfonyl Ketimines," *Angew. Chem. Int. Ed.* **2014**, Early View. (DOI: 10.1002/anie.201406147)
2. Xiaowei Dou, Bo Zhou, Weijun Yao, Fangrui Zhong, **Chunhui Jiang**, Yixin Lu*, "A Facile Approach for the Asymmetric Synthesis of Oxindoles with a 3-Sulphenyl-Substituted Quaternary Stereocenter," *Org. Lett.* **2013**, *15*, 4920-4923.
3. Jie Luo, **Chunhui Jiang**, Haifei Wang, Li-Wen Xu, Yixin Lu*, "Direct asymmetric Michael addition of phthalide derivatives to chalcones," *Tetrahedron Lett.* **2013**, *54*, 5261-5265.
4. Fangrui Zhong, **Chunhui Jiang**, Weijun Yao, Li-Wen Xu, Yixin Lu* , "Molecular sieve mediated decarboxylative Mannich and aldol reactions of β -ketoacids," *Tetrahedron Lett.* **2013**, *54*, 4333-4336.
5. **Chunhui Jiang**, Fangrui Zhong, Yixin Lu*, "Asymmetric organocatalytic decarboxylative Mannich reaction using β -keto acids: a new protocol for the synthesis of chiral β -amino ketones," *Beilstein J. Org. Chem.* **2012**, *8*, 1279-1283.

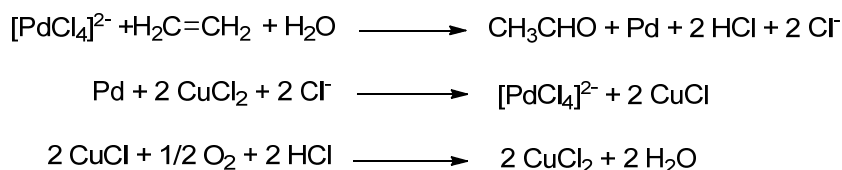
Chapter 1 Introduction

1.1 Historical background of asymmetric palladium catalysis

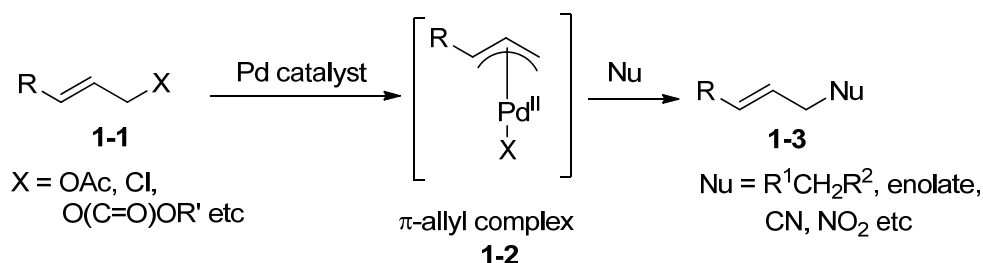
Palladium catalysis is a very important method for constructing carbon–carbon and carbon–heteroatom bonds in organic synthesis and has been widely used in both academia and industry for decades. As early as 1959, Wacker process for the oxidation of ethylene to acetaldehyde by oxygen in water in the presence of a tetra-chloropalladate(II) catalyst was invented (Scheme 1.1).¹ It was one of the most important milestones in the history of organopalladium chemistry and also the starting point of modern palladium chemistry.² Since then, tremendous efforts have been devoted to this area and many new reactions have been developed based on palladium catalysis. In recognition of the significance of this research field, the 2010 Nobel Prize in Chemistry was awarded jointly to Richard F. Heck, Ei-ichi Negishi and Akira Suzuki for their great contribution to palladium-catalyzed cross-coupling reactions. In palladium catalysis, palladium-catalyzed asymmetric reactions were undoubtedly very appealing and had drawn tremendous attention from synthetic chemists. With the development of different chiral ligands as catalyst partners, palladium-catalyzed reactions have been shown to be versatile in producing biologically important chiral molecules.

¹ J. Smidt, W. Hafner, R. Jira, J. Sedlmeier, R. Sieber, R. Ruttiger, and H. Kojer, *Angew. Chem.* **1959**, *71*, 176.

² J. Tsuji, *J. Organomet. Chem.* **1986**, *300*, 281.

Wacker process**Scheme 1.1** The catalytic cycle of Wacker process

Nearly ten years after the invention of Wacker process, Tsuji reported a carbon–carbon forming substitution reaction which was later known as Tsuji–Trost reaction by using (π -allyl)palladium complexes in 1965.³ Trost *et al.* further advanced this process by developing an asymmetric version later.⁴ The scope of this reaction has been greatly expanded to include many different C, N, or O based nucleophiles, and many electrophiles containing different leaving groups, as well as many P, N, or S based ligands. In Tsuji–Trost reaction, palladium catalyst firstly coordinates with the allyl group, the oxidative addition subsequently takes place to yield chiral π -allyl complex **1-2**, and attack by the nucleophile leads to the final substitution product **1-3** (Scheme 1.2).

Tsuji–Trost reaction**Scheme 1.2** The Tsuji-Trost reaction

³ J. Tsuji, H. Takahashi, M. Morikawa, *J. Am. Chem. Soc.* **1965**, *87*, 3275.

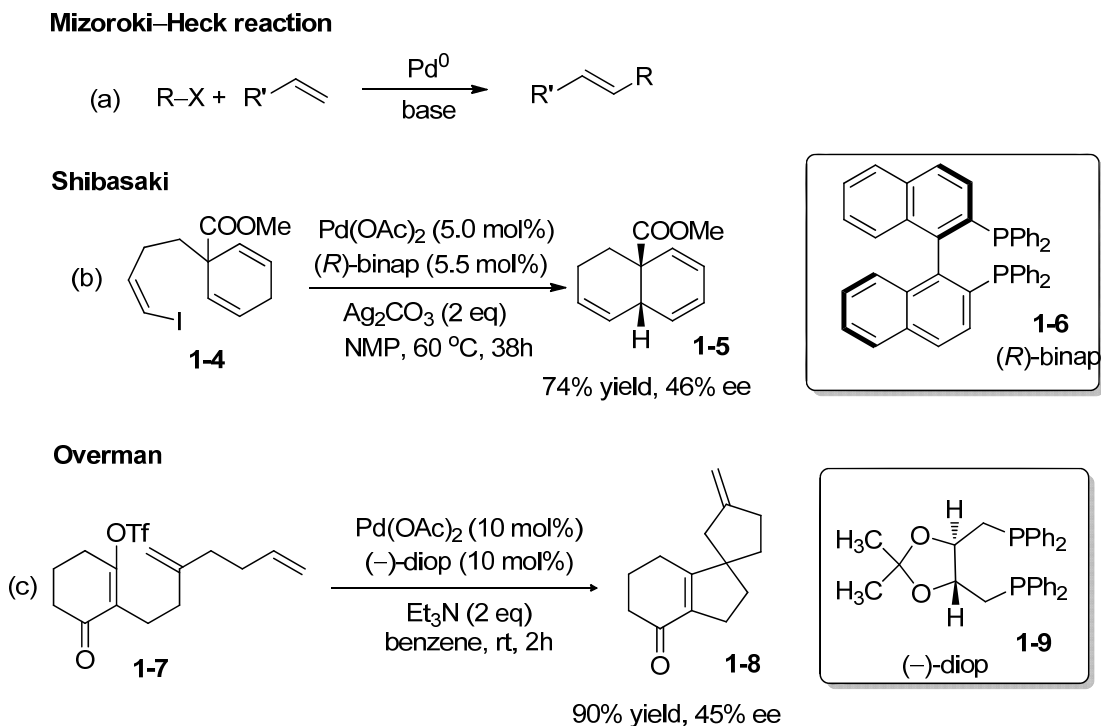
⁴ B. M. Trost, D. L. Van Vranken, *Chem. Rev.* **1996**, *96*, 395.

Another important carbon–carbon bond forming reaction in asymmetric palladium catalysis is asymmetric Mizoroki–Heck reaction (Scheme 1.3a). In the early 1970s, Mizoroki⁵ and Heck⁶ independently reported a new palladium-mediated crossing coupling of alkene with aryl halide. Interestingly, Shibasaki and Overman also reported asymmetric examples of Mizoroki–Heck reaction in 1989.⁷ They achieved intramolecular cyclization by using Pd(OAc)₂ as a catalyst and (*R*)-BINAP **1-6** or (*R, R*)-DIOP **1-9** as a chiral ligand (Scheme 1.3b and 1.3c). In this transformation, tertiary and quaternary chiral centers were generated although the enantioselectivities were low. Following their seminal work, various new substrates and chiral ligands were designed, and now asymmetric Mizoroki–Heck reaction is one of the most efficient methods for preparation of chiral structures containing a tertiary and quaternary stereogenic centers.

⁵ a) T. Mizoroki, K. Mori, A. Ozaki, *Bull. Chem. Soc. Jpn.* **1971**, *44*, 581; b) T. Mizoroki, K. Mori, A. Ozaki, *Bull. Chem. Soc. Jpn.* **1973**, *46*, 1505.

⁶ R. F. Heck, J. P. Nolley Jr., *J. Org. Chem.* **1972**, *37*, 2320.

⁷ a) Y. Sato, M. Sodeoka, M. Shibasaki, *J. Org. Chem.* **1989**, *54*, 4738; b) N. E. Carpenter, D. J. Kucera, L. E. Overman, *J. Org. Chem.* **1989**, *54*, 5846



Scheme 1.3 Palladium-catalyzed Mizoroki–Heck reaction

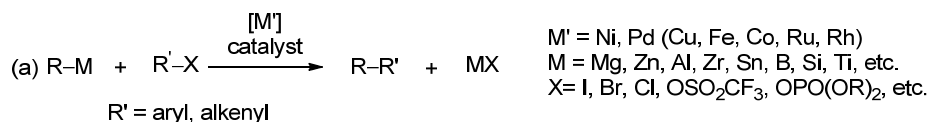
Despite palladium-catalyzed cross-coupling reaction arrived quite late in palladium catalysis, the impact however was significant. (Scheme 1.4a). Palladium overcomes the disadvantages of traditional Mg or Li-mediated cross coupling, such as limitation of unhindered alkyl halides as substrates, and the competing side reactions.^[9d] From 1975 to 1976, several other groups independently reported a number of palladium-catalyzed cross-coupling reactions.⁸ Subsequently that, Negishi and co-workers systematically studied this reaction and established the foundation for the palladium-catalyzed cross-coupling⁹ In the 1980s, Hayashi *et al.* developed

⁸ a) L. Cassar, *J. Organomet. Chem.* **1975**, 93, 253; b) M. Yamamura, I. Moritani, S. I. Murahashi, *J. Organomet. Chem.* **1975**, 91, C39; c) S. Baba, E. Negishi, *J. Am. Chem. Soc.* **1976**, 98, 6729; d) J. F. Fauvarque, A. Jutand, *Bull. Soc. Chim. Fr.* **1976**, 765; d) A. Sekiya, N. Ishikawa, *J. Organomet. Chem.* **1976**, 118, 349.

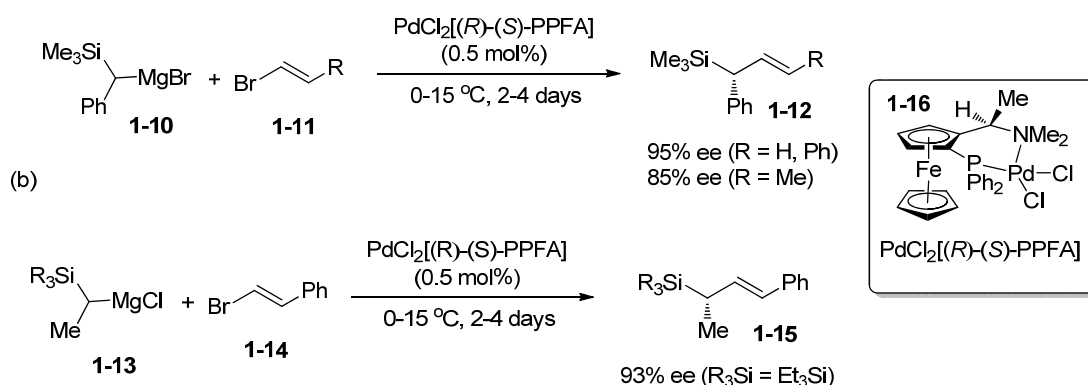
⁹ a) E. Negishi, A. O. King, N. Okukado, *J. Org. Chem.* **1977**, 42, 1821; b) A. O. King, N. Okukado, E. Negishi, *J. Chem. Soc. Chem. Commun.* **1977**, 683; c) A. O. King, E. Negishi, F. J. Villani, Jr., A. Silveira, Jr., *J. Org. Chem.* **1978**, 43, 358; d) N. Okukado, D. E. Van Horn, W. L. Klima, E. Negishi, *Tetrahedron Lett.* **1978**, 1027; e) E. Negishi, N. Okukado, A. O. King, D. E. Van Horn, B. I. Spiegel, *J. Am. Chem. Soc.* **1978**, 100, 2254; d) E. Negishi, in *Aspects of Mechanism and Organometallic Chemistry*, J. H. Brewster, Ed., Plenum Press, New York,

palladium-catalyzed enantioselective cross-coupling reactions by using phosphorus based chiral ligands¹⁰ (Scheme 1.4b).

Metal-catalyzed cross-coupling



Hayashi



Scheme 1.4 Transition Metal-catalyzed cross-coupling

In addition to the above three most important palladium-catalyzed asymmetric reactions, some other important reactions also appeared. One of them is palladium-catalyzed asymmetric addition, which is becoming more and more popular, and recent progresses in this field will be summarized in section 1.2.

1.2 Palladium-catalyzed asymmetric additions

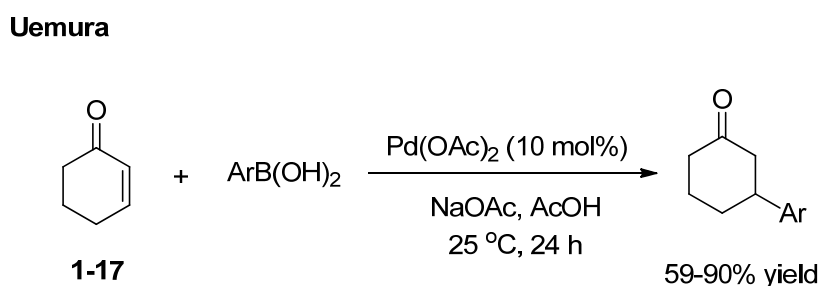
Palladium-catalyzed asymmetric addition is a versatile method for enantioselective formation of carbon-carbon and carbon-heteroatom bonds.

1978, 285-317; f) E. Negishi, *Acc. Chem. Res.* **1982**, *15*, 340.

¹⁰ T. Hayashi, M. Konishi, H. Ito, M. Kumada, *J. Am. Chem. Soc.* **1982**, *104*, 4962.

1.2.1 Asymmetric 1,4-additions

The first example of conjugated additions of organotin and organomercury reagents to α,β -unsaturated ketones by using palladium catalyst in an acidic two-phase condition was reported by Cacchi and co-workers.¹¹ In 1995, Uemura group reported another example of palladium catalyzed 1,4-addition to enones **1-17** in which organoboronic acids was first employed as nucleophiles, and higher catalyst loading and acidic solvent system were required in that reaction (Scheme 1.5).¹²



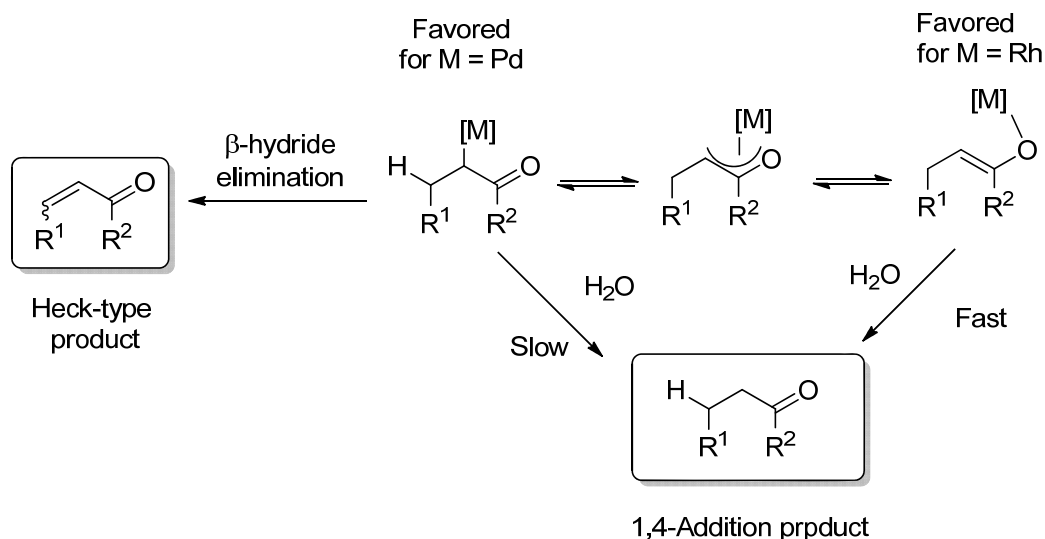
Scheme 1.5 The first example of a Pd-catalyzed 1,4-addition of organoboronic acids

However, rhodium catalysis is more favorable than palladium catalysis in the 1,4-addition, likely due to is the tendency of formed palladium enonate intermeidates to undergo β -hydride elimination, leading to the heck-type products and palladium(0) black rather than hydrolysis (Scheme 1.6).¹³

¹¹ a) S.Cacchi, D. Misiti, G.Palmieri, *Tetrahedron*, **1981**, 37, 2941; b) S.Cacchi, F. F. Latorre, D. Misiti *Tetrahedron Lett.* **1979**, 4591.

¹² C. S. Cho, S. Motofusa, K. Ohe, S. Uemura, *J. Org. Chem.* **1995**, 60, 883.

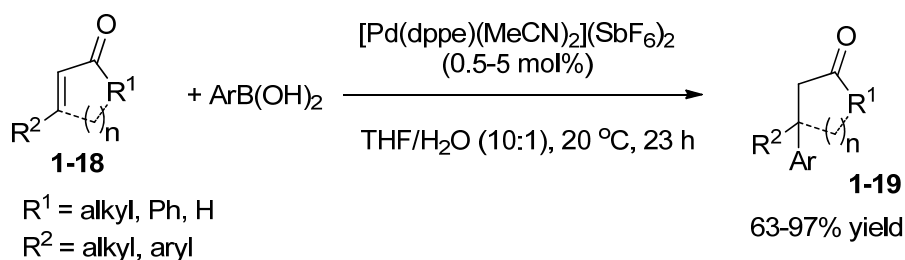
¹³ G. Berthon, T. Hayashi, *Rhodium- and Palladium-Catalyzed Asymmetric Conjugate Additions*, in *Catalytic Asymmetric Conjugate Reactions* (ed A. Córdova), Wiley-VCH, Weinheim, **2010**, chap. 1, pp. 1-70.



Scheme 1.6 Difference in reactivity between neutral Pd- and Rh- enolates

In 2003, Miyaura and co-workers developed a new catalytic system by using $[\text{Pd}(\text{dppe})(\text{MeCN})_2](\text{SbF}_6)_2$ as catalyst to dramatically increase the hydrolysis rate and obtain the desired additive products in high yields (Scheme 1.7).¹⁴

Miyaura



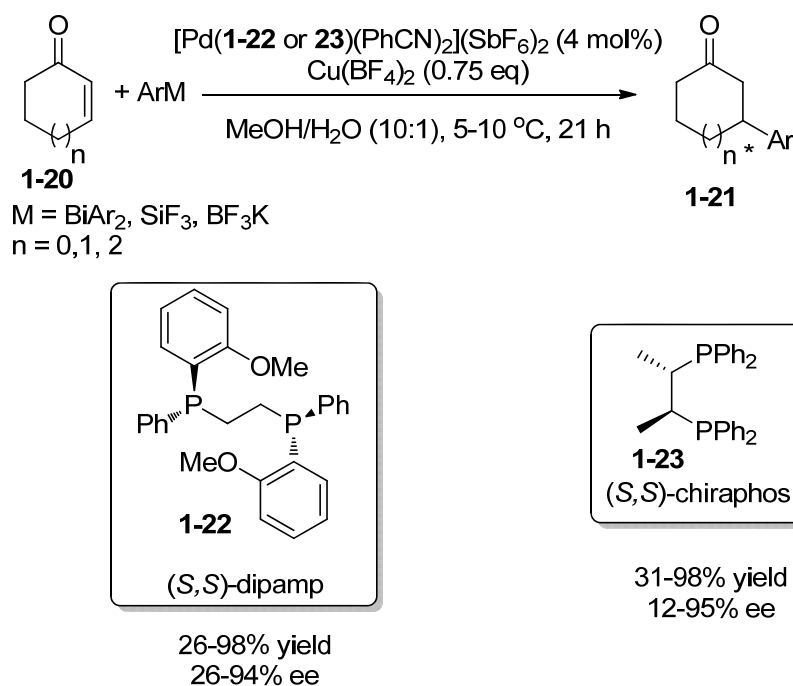
Scheme 1.7 Pd/dppe complex catalyzed 1,4-addition of boronic acids

In 2004, Miyaura and co-workers reported the first asymmetric version of 1,4-addition to α,β -saturated ketones **1-20**. In this reaction, the same palladium

¹⁴ T. Nishikata, Y. Yamamoto, N. Miyaura, *Angew. Chem. Int. Ed.* **2003**, 42, 2768.

catalyst, in combination with (*S,S*)-dipamp **1-22** and (*S,S*)-chiraphos **1-23** ligands were utilized to introduce asymmetry (Scheme 1.8).¹⁵

Miyaura



Scheme 1.8 Pd-catalyzed asymmetric 1,4-addition of organoboron reagents to

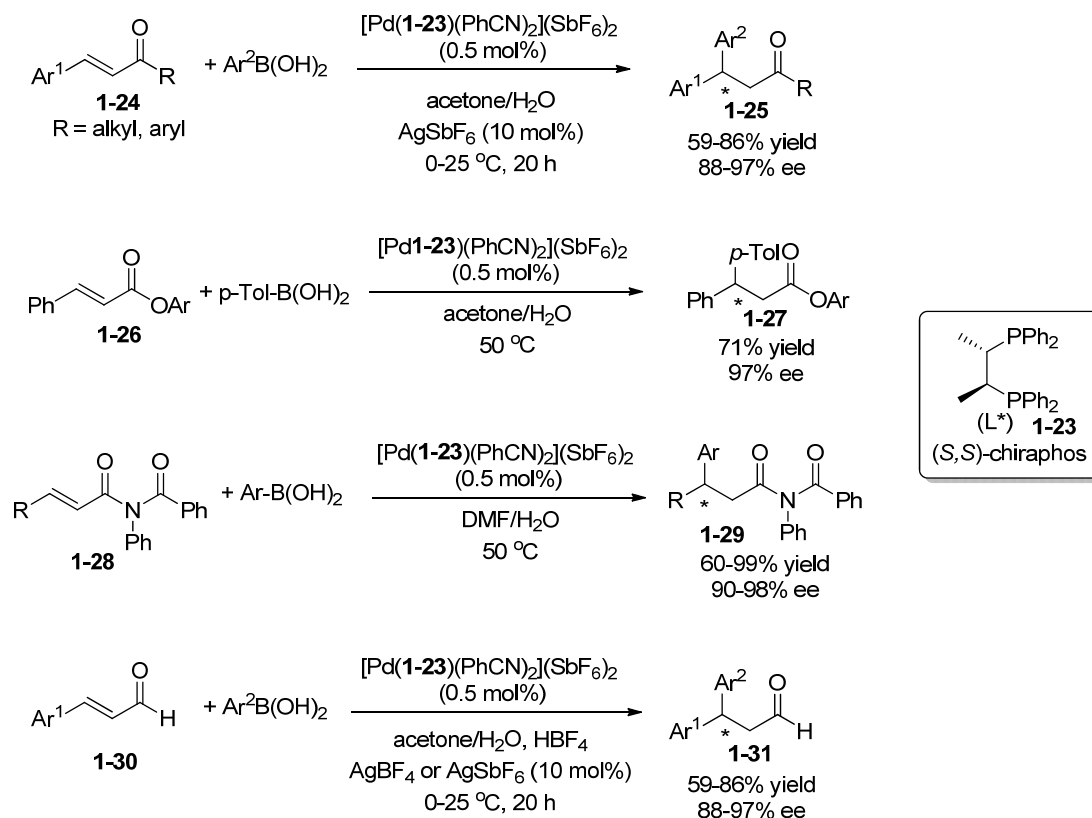
α,β -saturated ketones

Subsequently, the Miyaura group found $[\text{Pd}(\text{PhCN})_2](\text{SbF}_6)_2$ and (*S,S*)-chiraphos **1-23** were the best catalyst partners in 1,4-asymmetric additions of α,β -saturated ketones **1-24**, esters **1-26**, amides **1-28** and β -aryl enals **1-30** (Scheme 1.9).¹⁶

¹⁵ T. Nishikata, Y. Yamamoto, N. Miyaura, *Chem. Commun.* **2004**, 1822.

¹⁶ a) T. Nishikata, S. Kiyomura, Y. Yamamoto, N. Miyaura, *Synlett* **2008**, 2487; b) T. Nishikata, Y. Yamamoto, N. Miyaura, *Chem. Lett.* **2007**, 36, 1442; c) T. Nishikata, Y. Yamamoto, N. Miyaura, *Tetrahedron Lett.* **2007**, 48, 4007.

Miyaura

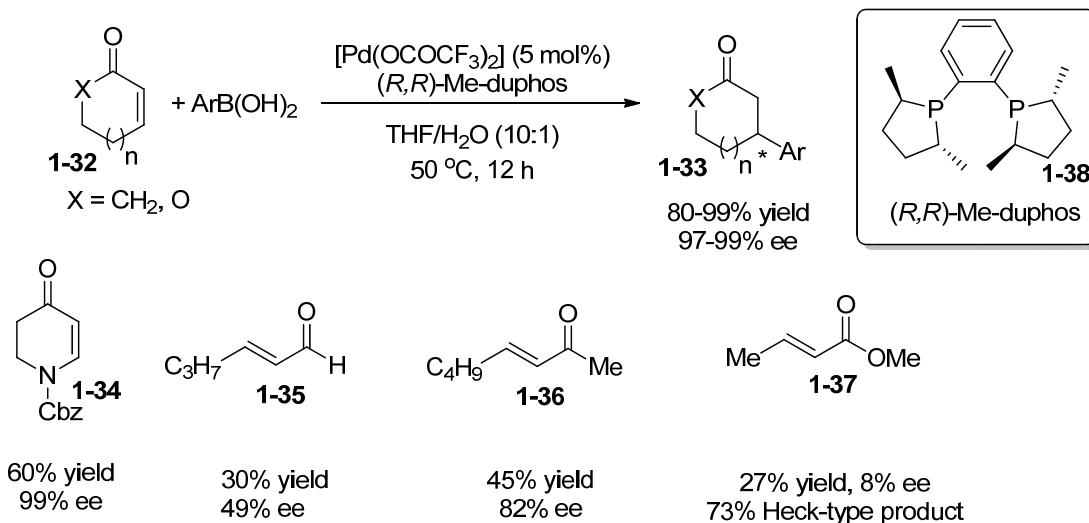


Scheme 1.9 Miyaura's representative work on Pd-catalyzed asymmetric 1,4-additions

In 2005, another catalytic system combining Pd(OCOCF₃)₂ and (*R,R*)-Me-duphos **1-38** was reported by Minnaard and co-workers. This catalytic system was proven to be most efficient for cyclic α,β -unsaturated ketone and esters **1-32** (Scheme 1.10).¹⁷

¹⁷ F. Gini, B. Hessen, A. J. Minnaard, *Org. Lett.* **2005**, 7, 5309.

Minnaard

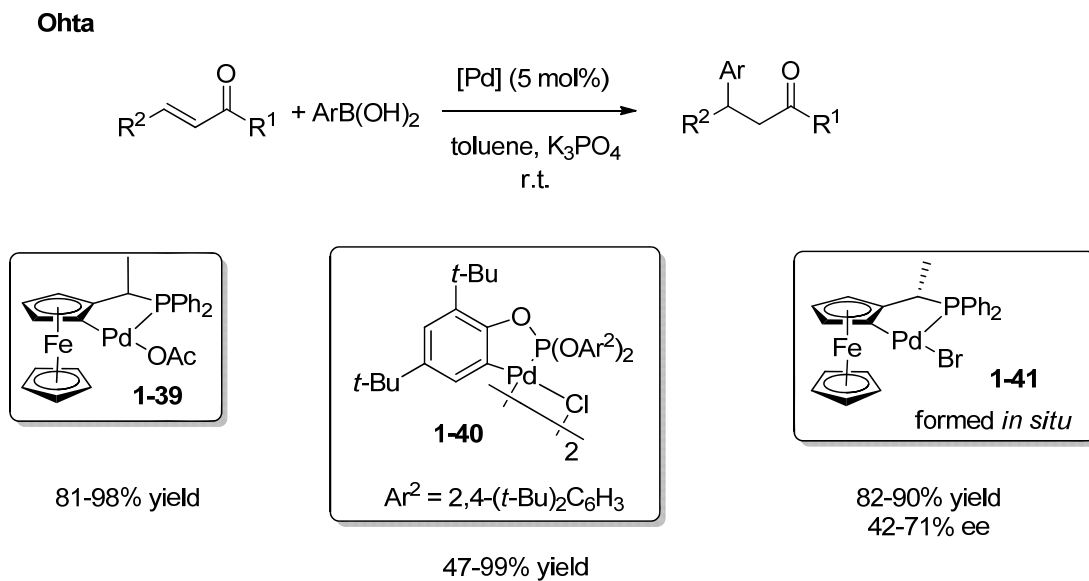


Scheme 1.10 Pd-catalyzed asymmetric arylations of α,β -unsaturated carbonyl compounds

In 2007, palladacycle was shown to be highly reactive for the addition of organoboronic acids to enones by Hu and co-workers.¹⁸ In contrast to dicationic Pd catalysts, strong Lewis acid AgSbF₆ or HBF₄ is not necessary for the addition reactions, likely due to the extreme stability and robust nature of palladacycle species. In 2009, Ohta group disclosed an enantioselective version in which the products were obtained in good yields and promising ee values (Scheme 1.11).¹⁹

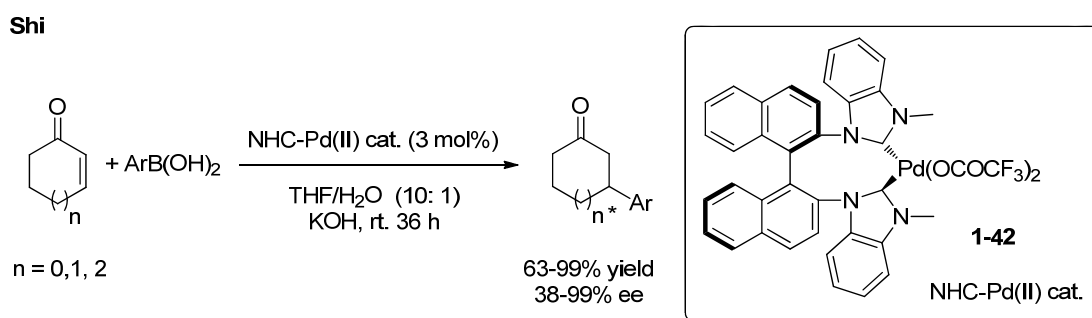
¹⁸ P. He, Y. Lu, C. Dong, Q. Hu, *Org. Lett.* **2007**, 9, 343.

¹⁹ Y. Suzuma, T. Yamamoto, T. Ohta, Y. Ito, *Chem. Lett.* **2007**, 36, 470.



Scheme 1.11 Palladacycles as catalysts for asymmetric 1,4-addition

The Shi group reported in 2008 that a cationic palladium (II) NHC diaqua complex **1-42** is a good catalyst for the asymmetric conjugated addition of arylboronic acids to cyclic enones (Scheme 1.12).²⁰



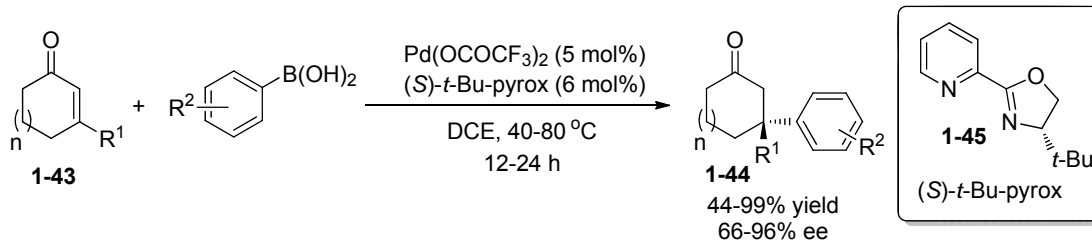
Scheme 1.12 NHC/Pd(II) complex catalyzed asymmetric 1,4-addition

In 2011, the Stoltz group employed a palladium catalyst prepared from $Pd(OCOCF_3)_2$ and pyridine-oxazoline ligand **1-45** for enantioselective construction of

²⁰ T. Zhang, M. Shi, *Chem. Eur. J.* **2008**, *14*, 3759.

quaternary stereogenic carbon centers *via* 1,4-addition of arylboronic acids to α,β -substituted cyclic enones **1-43** (Scheme 1.13).²¹

Stoltz



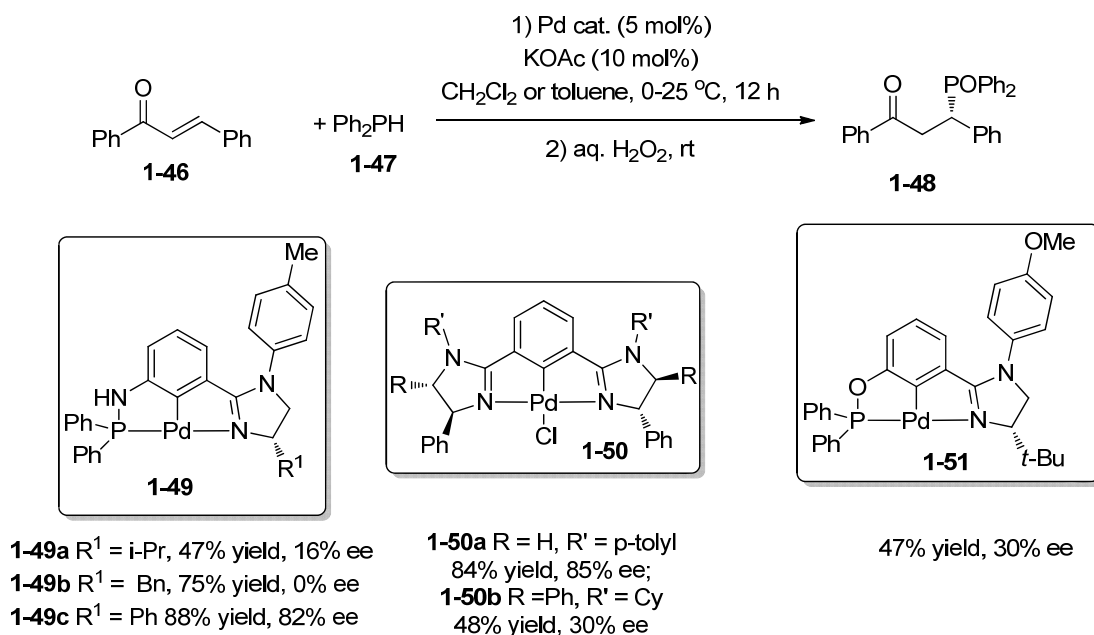
Scheme 1.13 Pd/pyrox catalyzed 1,4-additions to β -substituted cyclic enones

In addition to organoboron reagents, diphenylphosphines are also commonly used as nucleophiles in palladium catalyzed asymmetric 1,4-additions. The Song group developed a series of Pd pincer-type catalysts **1-49**, **1-50**, **1-51** and realized an efficient 1,4-addition of diphenylphosphines **1-47** to β -aryl enones **1-46** (Scheme 1.14).²²

²¹ K. Kikushima, J. C. Holder, M. Gatti B. M. Stoltz, *J. Am. Chem. Soc.* **2011**, *133*, 6902.

²² M.-J. Yang, Y.-J. Liu, J.-F. Gong, M.-P. Song, *Organometallics* **2011**, *30*, 3793.

Song

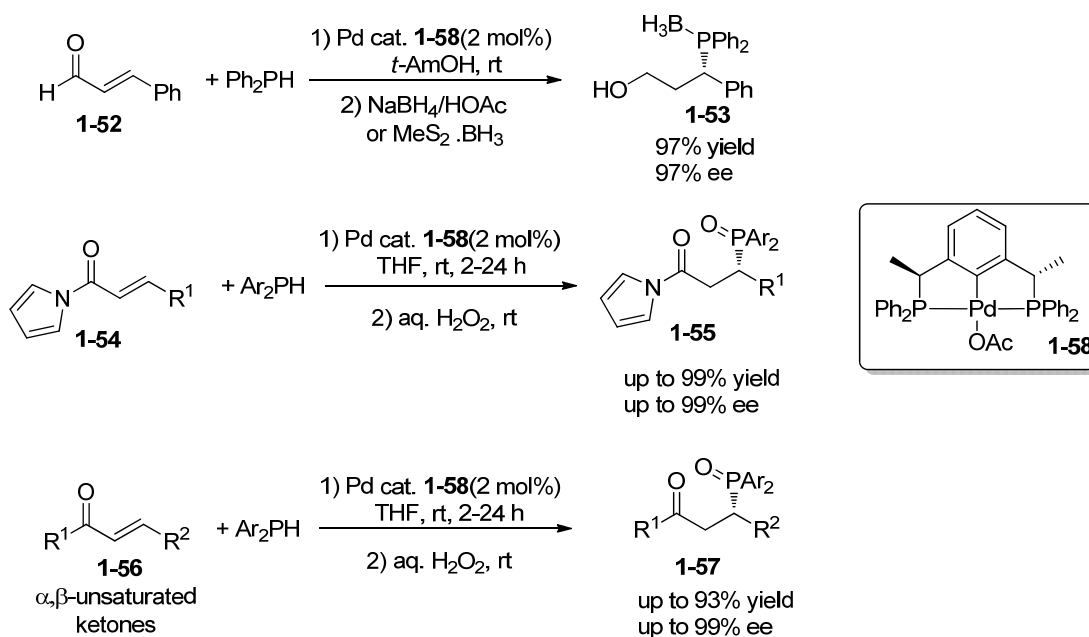


Scheme 1.14 Pd-catalyzed asymmetric addition of Ph_2PH to β -aryl enone

Recently, Duan and co-workers described highly enantioselective additions of diphenylphosphines to α,β -unsaturated aldehydes **1-52**, α,β -unsaturated *N*-acylpyrrole **1-54** and α,β -unsaturated ketones **1-56**, using a phosphorous–carbon–phosphorous pincer palladium catalyst **1-58** (Scheme 1.15).²³

²³ a) Y.-R. Chen, W.-L. Duan, *Org. Lett.* **2011**, *13*, 5824; b) J.-J. Feng, X.-F. Chen, M. Shi, W.-L. Duan, *J. Am. Chem. Soc.* **2010**, *132*, 5562; c) D. Du, W.-L. Duan, *Chem. Commun.* **2011**, *47*, 11101.

Duan



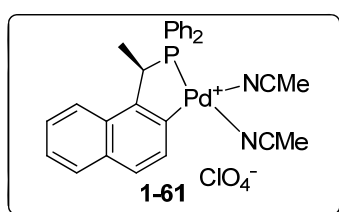
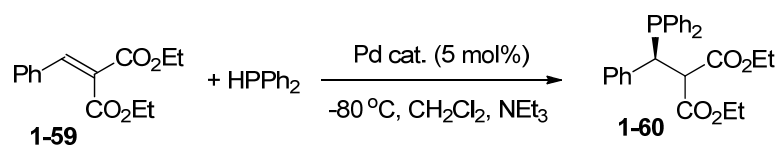
Scheme 1.15 Pd-catalyzed asymmetric additions of diphenylphosphine to α,β -unsaturated carbonyl compounds

Around the same time, the Leung group reported a chiral palladacycle catalyzed enantioselective hydrophosphination of substituted methyldiene-malonate esters **1-59** by applying diphenylphosphine nucleophilic reagents, representing a good method to access chiral tertiary phosphines **1-60** (Scheme 1.16).²⁴ Subsequently, the same group reported a few other efficient asymmetric addition reactions of diphenylphosphines to α,β -unsaturated carbonyl compounds and α,β -unsaturated imines.²⁵

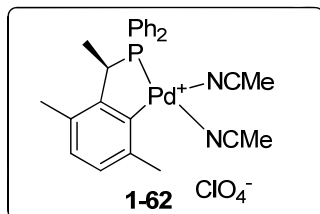
²⁴ C. Xu, G. J. H. Kennard, F. Hennesdorf, Y. Li, S. A. Pullarkat, P.-H. Leung, *Organometallics* **2012**, *31*, 3022.

²⁵ a) Y. Huang, S. A. Pullarkat, Y. Li, P.-H. Leung, *Chem. Commun.* **2010**, *46*, 6950; b) Y. Huang, R. J. Chew, Y. Li, S. A. Pullarkat, P.-H. Leung, *Org. Lett.* **2011**, *13*, 5862; c) Y. Huang, S. A. Pullarkat, S. Teong, R. J. Chew, Y. Li, P.-H. Leung, *Organometallics* **2012**, *31*, 4871; d) Y. Huang, R. J. Chew, S. A. Pullarkat, Y. Li, P.-H. Leung, *J. Org. Chem.* **2012**, *77*, 6849.

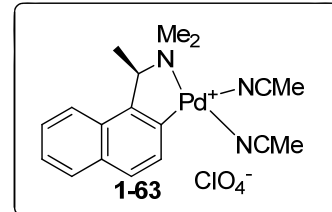
Leung



99% conv., 96% ee



99% conv., 65% ee

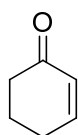
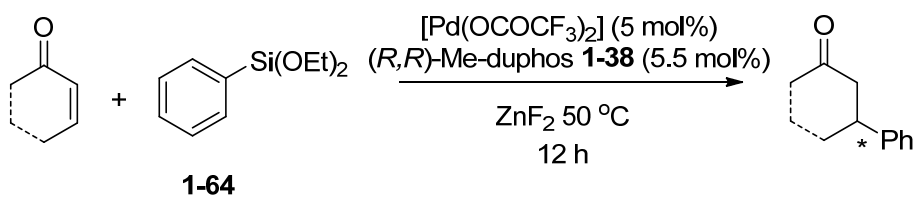
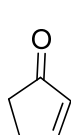
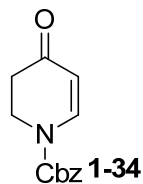
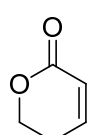
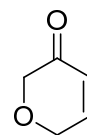
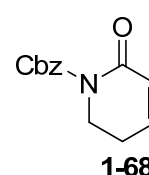


99% conv., 86% ee

Scheme 1.16 Asymmetric 1,4-addition of HPPH₂ reported by Leong et al.

Compared with wide utilization of organoboron reagents and diphenylphosphines, the reports on other nucleophiles are less common. In a report by Minnaard, arylsiloxanes **1-64** was employed to replace arylboronic acids, and good results were also obtained (Scheme 1.17).²⁶

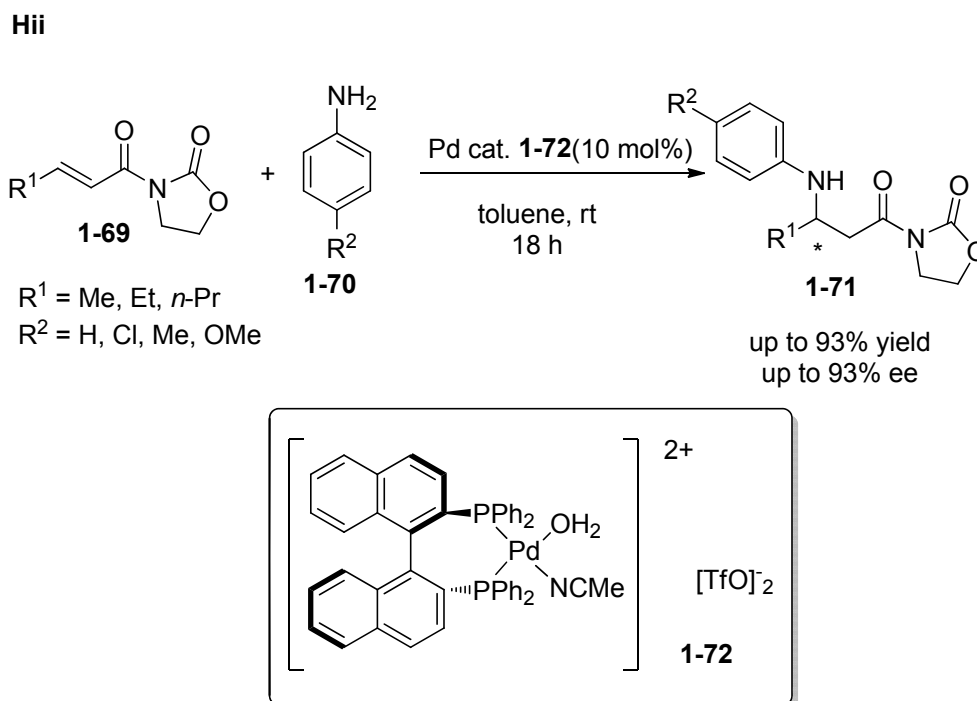
Minnaard

75% yield
99% ee80% yield
90% ee84% yield
99% ee20% yield
88% ee40% yield
78% ee60% yield
94% ee

Scheme 1.17 Arylsiloxanes as nucleophiles in Pd-catalyzed 1,4-addition

²⁶ F. Gini, B. Hessen, B. L. Feringa and A. J. Minnaard, *Chem. Commun.* **2007**, 43, 710.

Amines are also suitable nucleophiles for the above asymmetric 1,4-additions. Hii and co-workers screened 1,4-additions of amines to different α,β -unsaturated compounds by using binap-based Pd complex **1-72**, and discovered alkenoyl-*N*-oxazolidinones **1-69** were essential for achieving high enantioselectivity (Scheme 1.18).²⁷



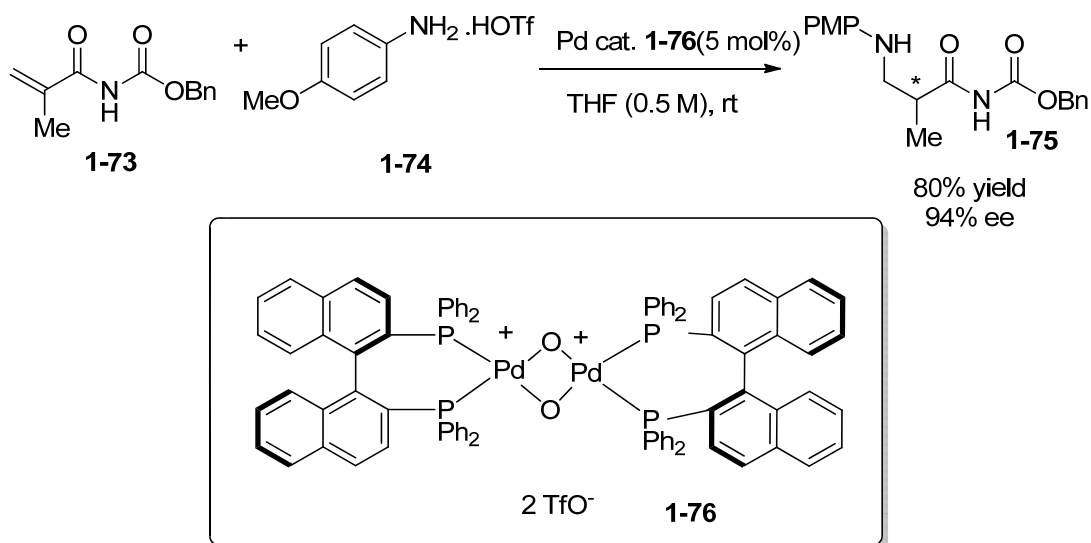
Scheme 1.18 Anilines as nucleophiles in Pd-catalyzed asymmetric 1,4-additions

The Sodoka group demonstrated that binap-based Pd complex **1-76** was efficient in catalyzing 1,4-additions of anilines to α,β -unsaturated amide **1-73**, affording the desired products **1-75** in excellent enantioselectivities (Scheme 1.19).²⁸

²⁷ K. Li, P. H. Phua, K. K. Hii, *Tetrahedron* **2005**, *61*, 6237.

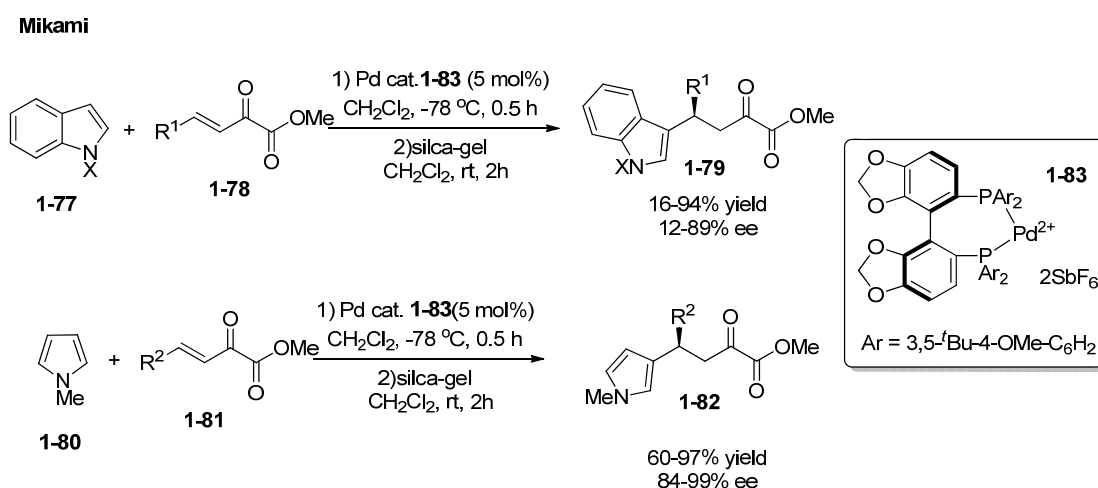
²⁸ Y. Hamashima, T. Tamura, S. Suzuki, M. Sodeoka, *Synlett* **2009**, *10*, 1631.

Sodeoka



Scheme 1.19 Pd-catalyzed enantioselective protonation via 1,4-addition

In 2001, the Mikami group reported asymmetric Friedel-Crafts alkylations of indole **1-77** and pyrrole **1-80** with α,β -unsaturated ketoesters **1-78** by employing chiral dicationic Pd complexes **1-83** (Scheme 1.20).²⁹



Scheme 1.20 Pd-catalyzed enantioselective Friedel-Crafts alkylation

²⁹ K. Aikawa, K. Honda, S. Mimura, K. Mikami, *Tetrahedron Lett.* **2011**, 52, 6682

1.2.2 Asymmetric 1,2-additions

Asymmetric 1,2-additions of different nucleophiles to imines, aldehydes and ketones are powerful methods to synthesize chiral amines, secondary and tertiary alcohols, and many transition-metals such as Rh, Cu and Pd can be used as a catalyst for these reactions. Compared with Rh and Cu, Pd catalyzed 1,2-addition was less developed owing to the competitive reductive elimination and β -hydride elimination of palladium species during the reaction.

1.2.2.1 Imine substrates

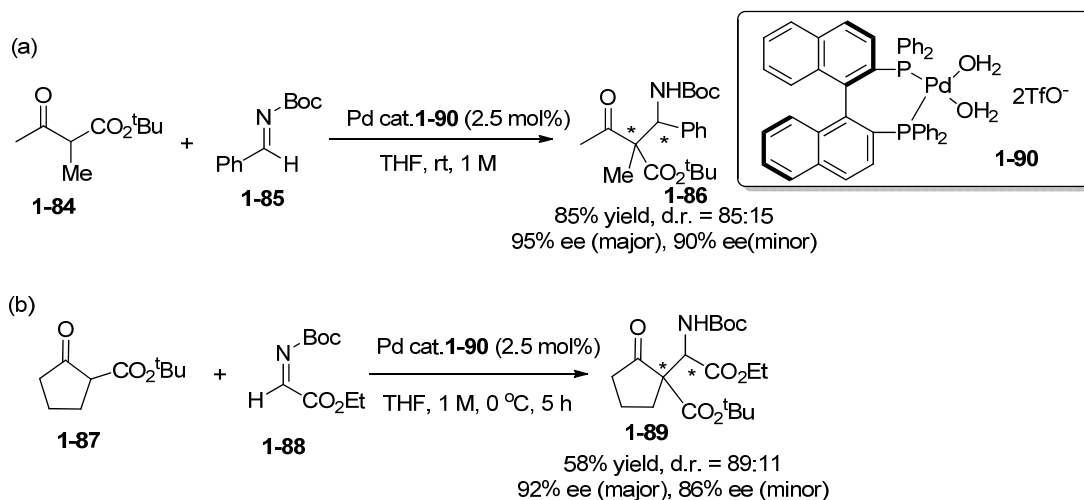
Imines are important and practically useful substrates in organic synthesis. The difficulties associated with additions to imines are their poor electrophilicity and the tendency of enolizable imines to undergo deprotonation. Back to just a few years ago, only few examples on palladium-catalyzed 1,2-addition to imines were reported.³⁰

In 2008, the Sodeoka group disclosed a highly enantioselective catalytic Mannich-type reaction of β -ketoesters with *N*-Boc imines, using Pd²⁺ diaqua complex **1-90** (Scheme 1.21).³¹

³⁰ a) H. Nakamura, K. Nakamura, Y. Yamamoto, *J. Am. Chem. Soc.* **1998**, *120*, 4242; b) M. Shimizu, M. Kimura, T. Watanabe, Y. Tamaru, *Org. Lett.* **2005**, *7*, 637; (c) N. Solin, O. Wallner, K. Szabó, *Org. Lett.* **2005**, *7*, 689

³¹ Y. Hamashima, N. Sasamoto, N. Umebayashi, M. Sodeoka, *Chem.-Asian J.* **2008**, *3*, 1443.

Sodeoka

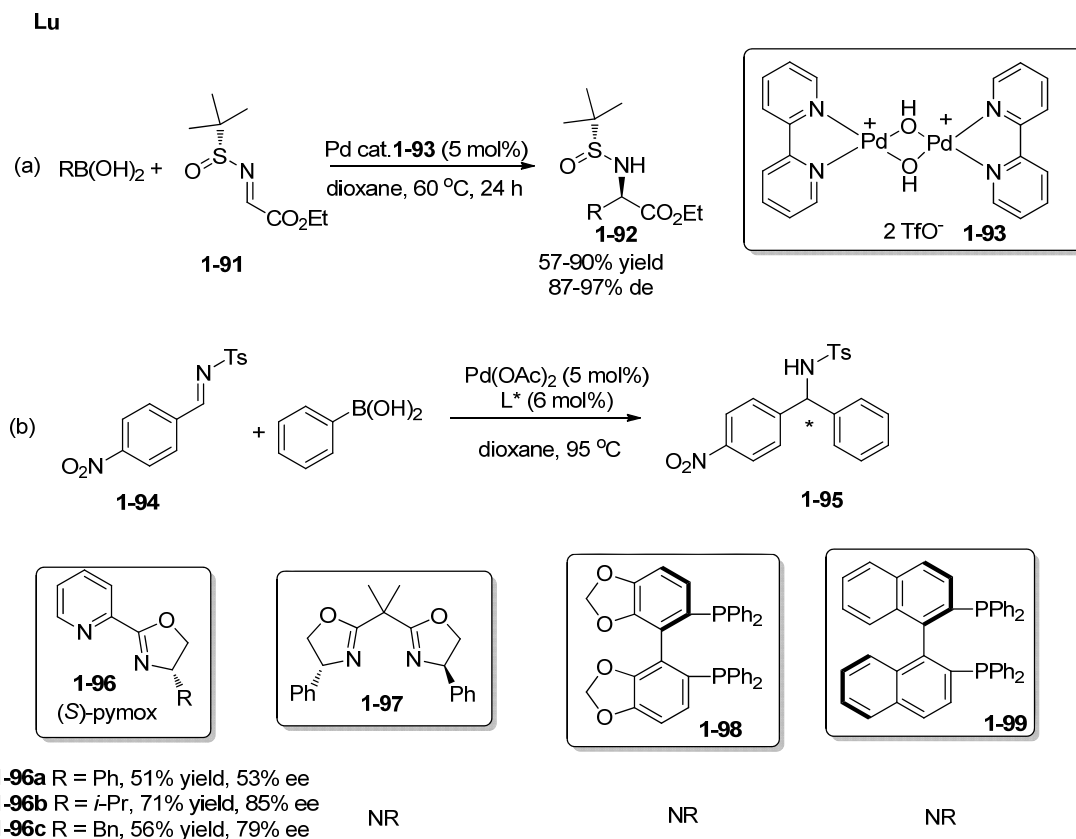


Scheme 1.21 Sodeoka's work on Pd-catalyzed asymmetric addition of β -ketoesters to imines

In 2007, a cationic palladium-complex **1-93**-catalyzed was employed by Lu and co-workers to catalyze the addition of arylboronic acids to *N*-tert-butanesulfinyl iminoacetates **1-91**, and optically active arylglycine derivatives **1-92** with moderate to good yield and high diastereoselectivity were obtained. (Scheme 1.22a).³² This example represents the first arylation of imines via palladium catalysis. Shortly after this report, the same group utilized pymox **1-96** as chiral ligand to achieve an asymmetric addition of arylboronic acids to *N*-tosylimine **1-94** to yield diarylmethylamines **1-95**. A number of other ligands based on biphenyl **1-98**, binaphthyl **1-99** and bis(oxazoline) **1-97** scaffolds were also screened, however, only pymox **1-96** led to moderate yield and good enantioselectivity (Scheme 1.22b).³³

³² H. Dai, X. Lu, *Org. Lett.* **2007**, *9*, 3077

³³ H. Dai, X. Lu, *Tetrahedron Lett.* **2009**, *50*, 3478.

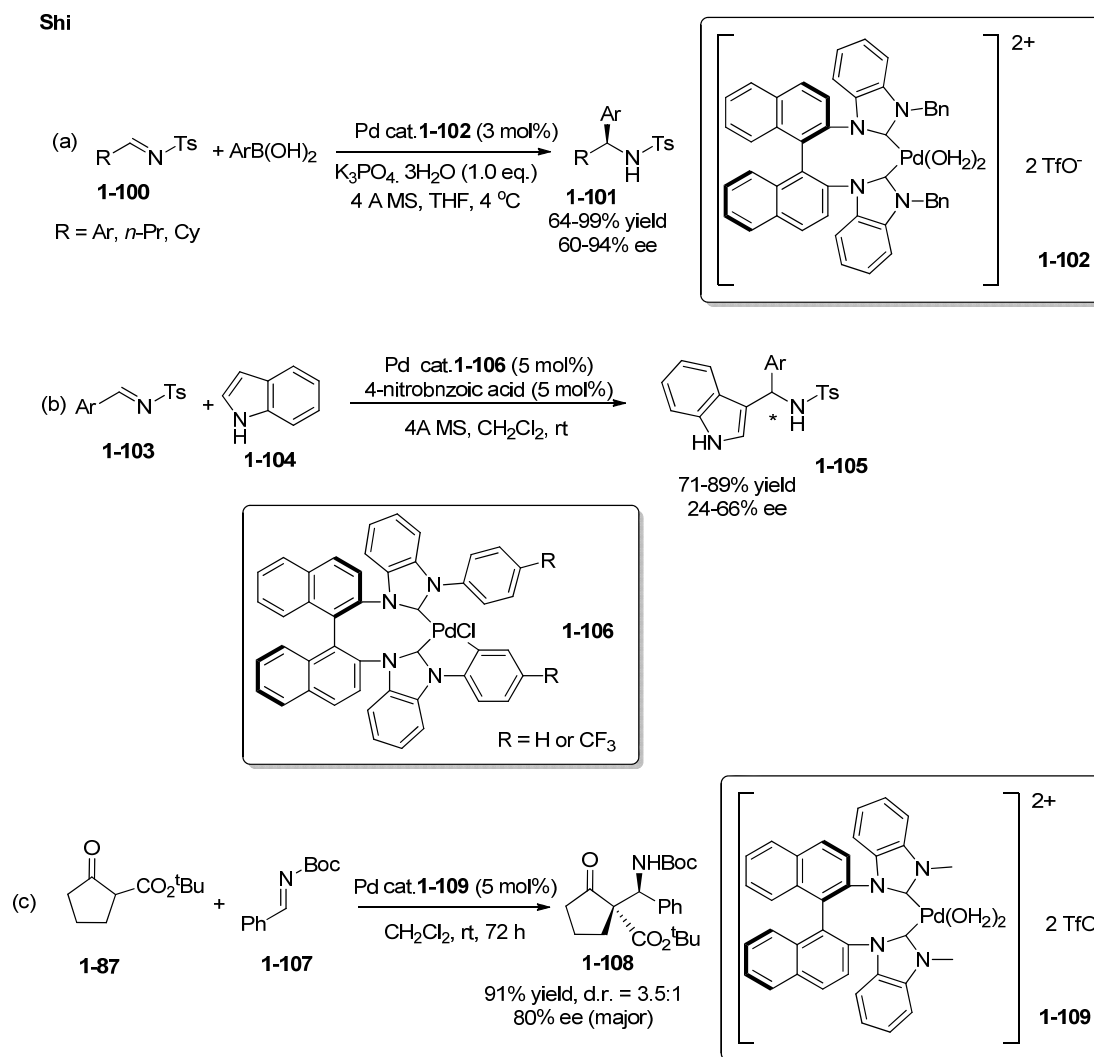


Scheme 1.22 Asymmetric arylations of imines by Lu et al.

In 2009, the Shi group disclosed 1,2-additions of arylboronic acids and indoles **1-104** to *N*-tosylimine, employing NHC based Pd^{2+} catalysts **1-102** and **1-106**, affording the desired products in moderate yields and good enantioselectivities (Scheme 1.23a and 1.23b).³⁴ One year later, the same group reported the asymmetric addition of cyclic β -keto esters to *N*-Boc imines catalyzed by a cationic Pd(II) NHC complex **1-109** (Scheme 1.23c).³⁵

³⁴ a) G.-N. Ma, T. Zhang, M. Shi, *Org. Lett.* **2009**, *4*, 875; b) Z. Liu, M. Shi, *Tetrahedron: Asymmetry* **2009**, *20*, 119.

³⁵ a) R. Zhang, D. Wang, Q. Xu, J. Jiang, M. Shi, *Chin. J. Chem.* **2012**, *30*, 1295; b) R. Zhang, Q. Xu, L.-Y. Mei, S.-K. Li, M. Shi, *Tetrahedron* **2012**, *68*, 3172.



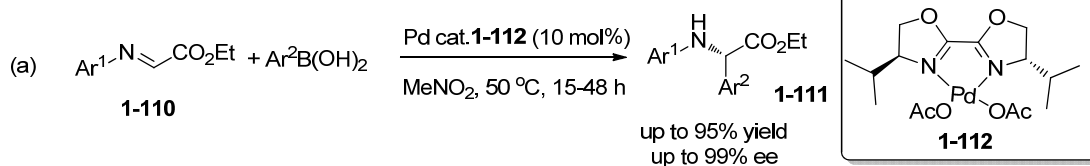
Scheme 1.23 Shi's work on Pd-catalyzed asymmetric additions to Ts- and Boc- imines

In 2012, Zeng and co-workers developed a method for Pd(II)-catalyzed asymmetric arylation of *N*-aryl imino esters **1-110**, in which Pd(II)-bisoxazoline complex **1-112** was proved to be efficient (Scheme 1.24a).³⁶ In the same year, the Lam group used another novel Pd(II)-bisoxazoline complex **1-116** for catalytic enantioselective addition of alkylazaarenes **1-113** to *N*-Boc imines (Scheme 1.24b).³⁷

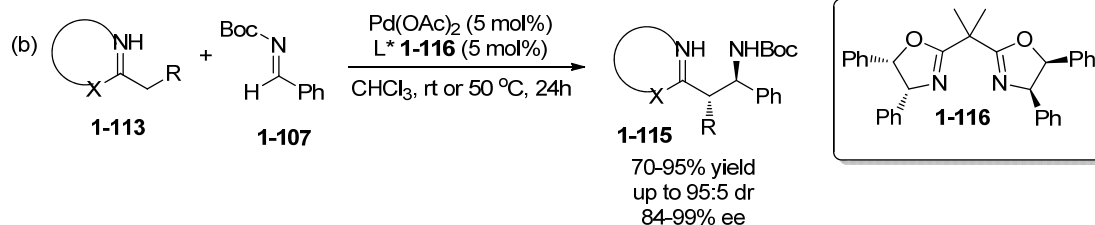
³⁶ J. Chen, X. Lu, W. Lou, Y. Ye, H. Jiang, W. Zeng, *J. Org. Chem.* **2012**, *77*, 8541

³⁷ D. Best, S. Kujawa, H. W. Lam, *J. Am. Chem. Soc.* **2012**, *134*, 18193

Zeng



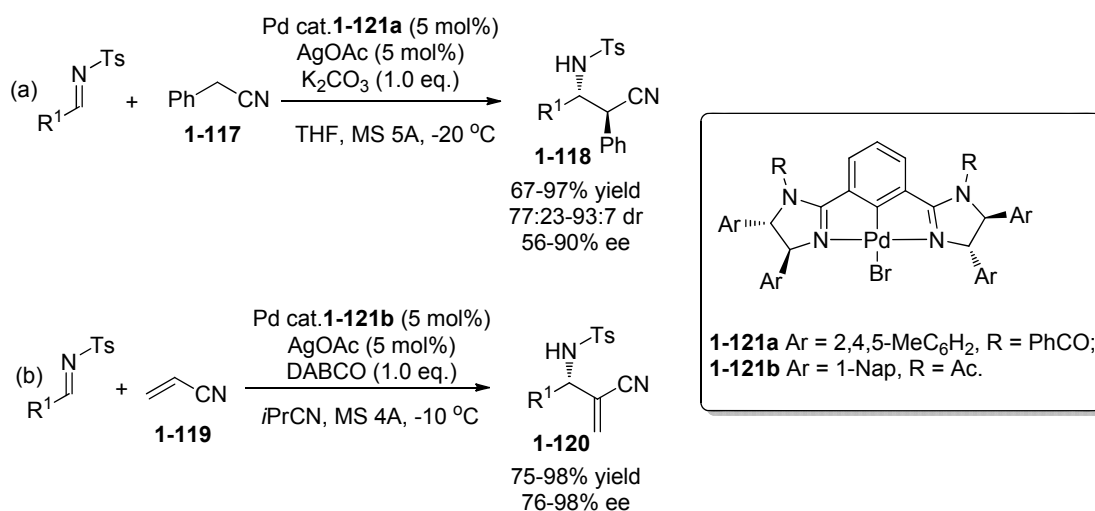
Lam



Scheme 1.24 Bisoxazolines as ligands in Pd-catalyzed asymmetric additions to imines

The Shibata group used novel Pd pincer-type catalyst **1-121a** in the asymmetric reactions of benzyl nitriles **1-117** and *N*-tosylimines (Scheme 1.25a).³⁸ Subsequently, the same group described asymmetric aza-MBH reactions of acrylonitriles **1-119** with *N*-tosylimines using a similar Pd catalyst **1-121b** (Scheme 1.25b).³⁹

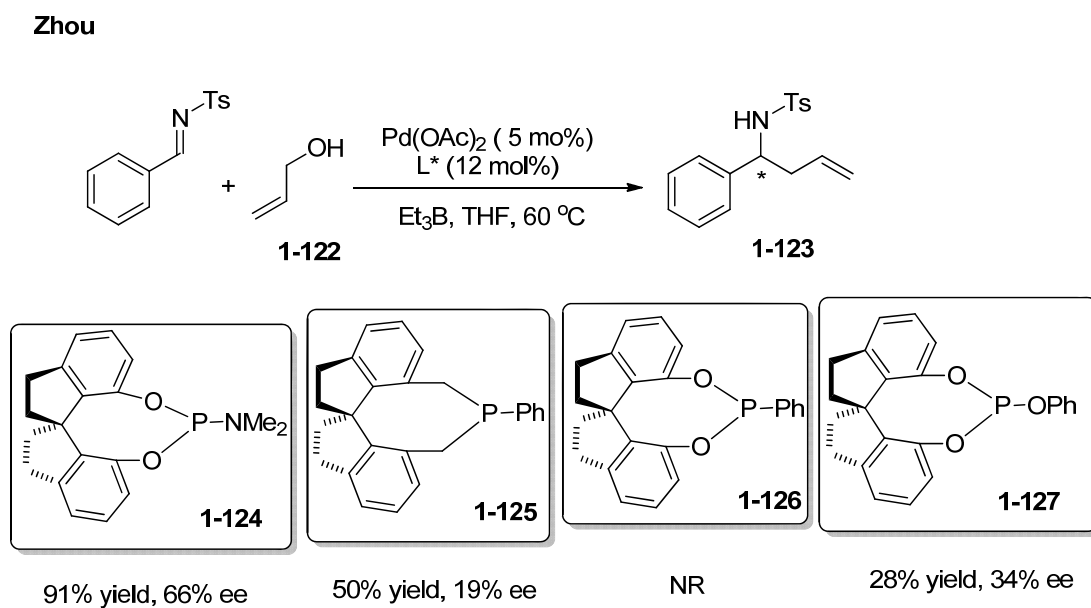
Shibata

Scheme 1.25 Pd-catalyzed enantioselective additions of nitriles to *N*-tosylimines

³⁸ K. Hyodo, S. Nakamura, K. Tuji, T. Ogawa, Y. Funahashi, N. Shibata, *Adv. Synth. Catal.* **2011**, 353, 3385.

³⁹ K. Hyodo, S. Nakamura, N. Shibata, *Angew. Chem. Int. Ed.* **2012**, 51, 10337.

Recently, Zhou and co-workers reported a palladium-catalyzed allylation of imines, using allylic alcohols **1-122** as allylic reagents. The newly developed spiro monodentated phosphoramidite based palladium complex **1-124** showed high catalytic activity. (Scheme 1.26).⁴⁰



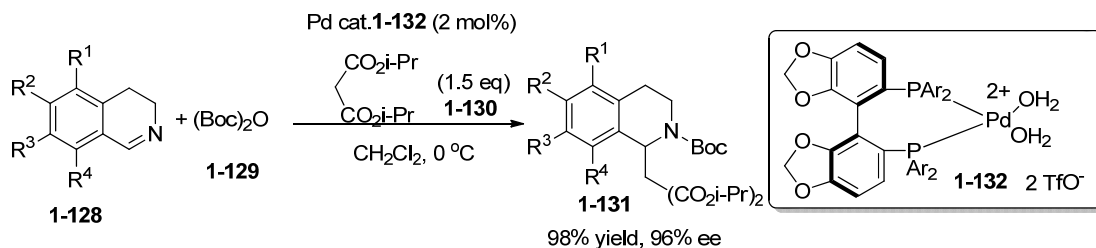
Scheme 1.26 Pd-catalyzed asymmetric allylation of imines

Compared with branched imines, cyclic imines were less investigated in the palladium catalytic asymmetric 1, 2-addition reactions. In one of the early reports in 2006, the Sodeoka group employed Pd catalyst **1-132** to promote addition of manolate **1-130** cyclic imines DHIQs **1-128**, affording the desired additive productz **1-131** in high yields and good to excellent enantioselectivities (Scheme 1.27).⁴¹

⁴⁰ X.-C. Qiao, S.-F. Zhu, W.-Q. Chen, Q.-L. Zhou, *Tetrahedron: Asymmetry* **2010**, *21*, 1216.

⁴¹ N. Sasamoto, C. Dubs, Y. Hamashima, M. Sodeoka, *J. Am. Chem. Soc.* **2006**, *128*, 14010.

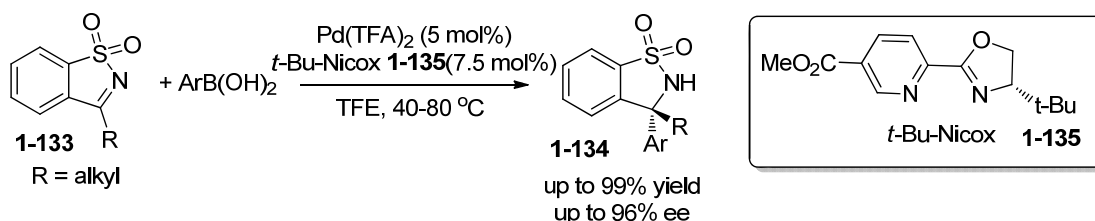
Sodeoka



Scheme 1.27 Pd-catalyzed 1,2-addition of malonates to cyclic imines

Very recently, the Zhang group reported a palladium/pyrox **1-135**-catalyzed addition of arylboronic acids to ketimines **1-133**, the products **1-134** were obtained in up to 99% yield and 96% ee. The reactions could be run under aerobic conditions and with trifluoroethanol as the solvent (Scheme 1.28).⁴²

Zhang



Scheme 1.28 Pd-catalyzed enantioselective arylation of boronic acids to cyclic ketimines

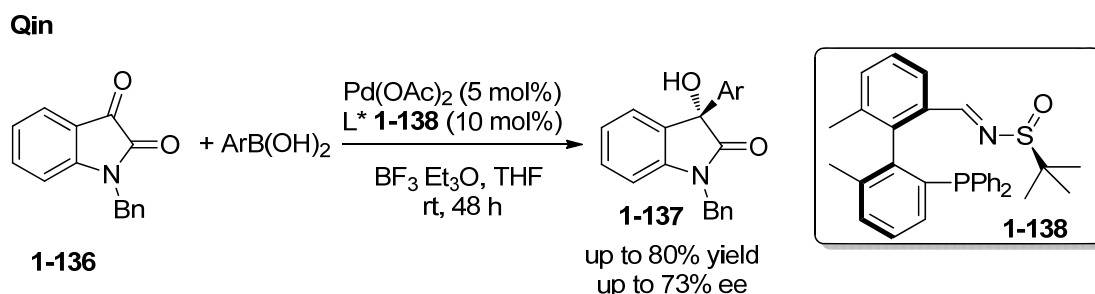
1.2.2.2 Aldehydes and ketones as the substrates

Besides imines, aldehydes and ketones are also widely used substrates in 1,2-addition reactions.

In 2009, Qin and co-workers reported an asymmetric addition of arylboronic acids to *N*-benzylisatins **1-136** catalyzed by Pd(OAc)₂ and phosphine-schiff base type

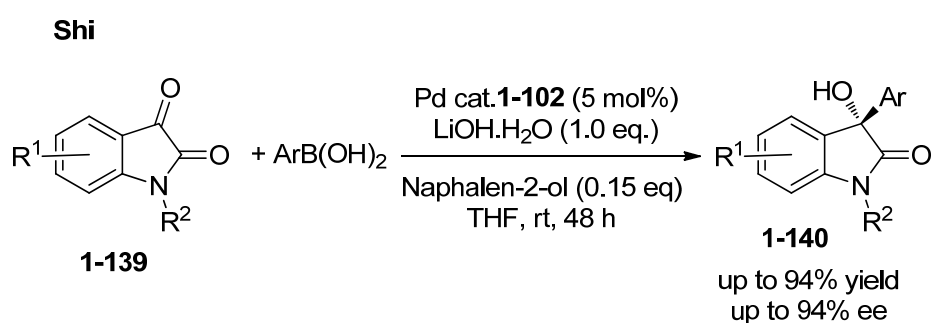
⁴² G. Yang, W. Zhang, *Angew. Chem. Int. Ed.* **2013**, *52*, 7540.

ligand **1-138**, giving the 3-aryl-3-hydroxyoxindoles **1-137** in moderate yields and ee values. A strong Lewis acid $\text{BF}_3 \cdot \text{Et}_2\text{O}$ was crucial for this transformation (Scheme 1.29).⁴³



Scheme 1.29 Qin's work on the asymmetric addition of boronic acids to isatins

In 2011, the Shi group examined the same reaction by using their (NHC) Pd^{2+} diaqua complex **1-102** as the catalyst, both reactivities and enantioselectivities were improved to excellent levels (Scheme 1.30).⁴⁴



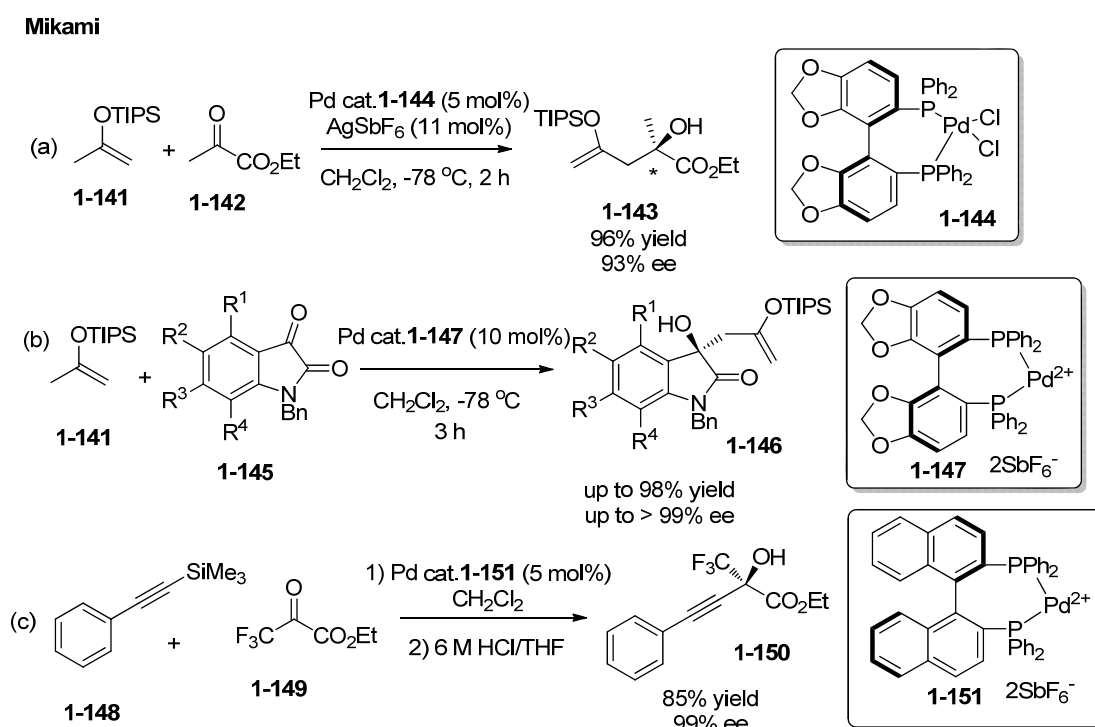
Scheme 1.30 Shi's work on the asymmetric addition of boronic acids to isatins

The Mikami group developed a SEGPHOS-Pd complex **1-144** catalytic system

⁴³ H. Lai, Z. H. Huang, Q. Wu, Y. Qin, *J. Org. Chem.* **2009**, *74*, 283.

⁴⁴ Z. Liu, P. Gu, M. Shi, P. McDowell, G. Li, *Org. Lett.* **2011**, *13*, 2314.

and applied it in the asymmetric ketoester-ene reaction, providing optically active β -hydroxy silyl enol ether **1-143** in good yields and high ee values (Scheme 1.31a).⁴⁵ Subsequently, the same group reported dicationic Pd complex **1-147** catalyzed enantioselective ene and aldol reactions with isatin derivatives (Scheme 1.31b).⁴⁶ In 2010, they also disclosed that dicationic (*S*)-BINAP-Pd complex **1-151** was efficient in catalyzing asymmetric addition of alkynylsilanes **1-148** to trifluoropyruvate **1-149** (Scheme 1.31c).⁴⁷



Scheme 1.31 Pd-catalyzed enantioselective ene and aldol reactions

Chiral Pd(II)-BINAP complex **1-90** was also used by the Sodeoka group for enantioselective aldol reaction of β -keto esters with formaldehyde, and the

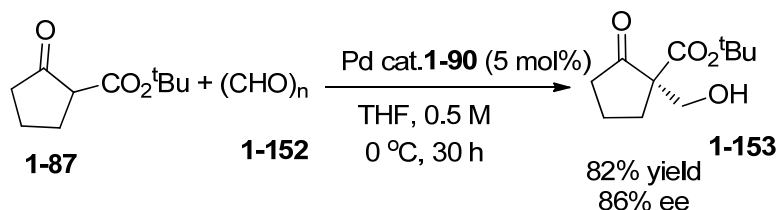
⁴⁵ K. Mikami, Y. Kawakami, K. Akiyama, K. Aikawa, *J. Am. Chem. Soc.* **2007**, *129*, 12950.

⁴⁶ K. Aikawa, S. Mimura, Y. Numata, K. Mikami, *Eur. J. Org. Chem.* **2011**, 62.

⁴⁷ K. Aikawa, Y. Hioki, K. Mikami, *Org. Lett.* **2010**, *12*, 5716.

desired adducts **1-153** were obtained with moderate to good yields and with good ee values (Scheme 1.32).⁴⁸

Sodeoka



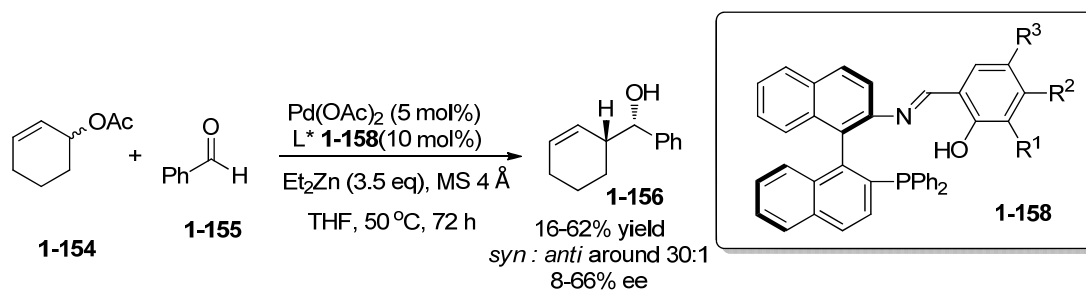
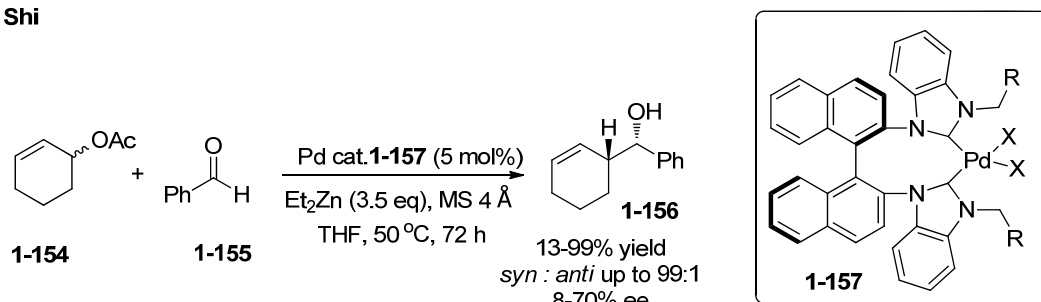
Scheme 1.32 Pd-catalyzed asymmetric hydroxymethylation of β -keto ester

In 2009, the Shi group examined a series of (NHC) Pd²⁺ complexes **1-157** in the enantioselective allylation of aldehydes **1-155** with cyclohexenyl acetate **1-154** in the presence of Et₂Zn as additive, producing homoallylic alcohols **1-156** in moderate to high yields, with modest ee values, and up to 99:1 *syn* to *anti*. A good number of phosphine-schiff base type ligands **1-158** were also screened in the same reaction and proved to be inferior to NHC based ligands (scheme 1.33).⁴⁹

⁴⁸ I. Fukuchi, Y. Hamashima, M. Sodeoka, *Adv. Synth. Catal.* **2007**, *349*, 509.

⁴⁹ a) W. Wang, T. Zhang, M. Shi, *Organometallics* **2009**, *28*, 2640; b) J.-J. Jiang, D. Wang, W.-F. Wang, Z.-L. Yuan, M.-X. Zhao, F.-J. Wang, M. Shi, *Tetrahedron: Asymmetry* **2010**, *21*, 2050.

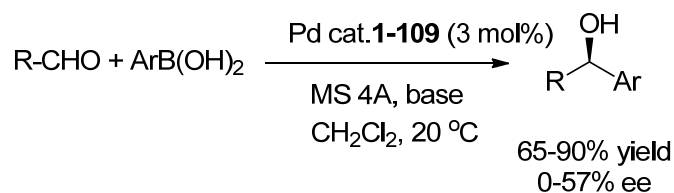
Shi



Scheme 1.33 Comparison between NHC based ligands and P-imine ligands in Pd-catalyzed asymmetric allyations of aldehydes.

Although the asymmetric addition of arylboronic acids to arylaldehydes have been widely reported, the application of chiral Pd catalysts has not been very successful. In 2010, the Shi group reported asymmetric arylation of arylaldehydes with arylboronic acid by using (NHC) Pd²⁺ complex **1-109** as catalyst, giving the adducts with promising results (Scheme 1.34).⁵⁰

Shi



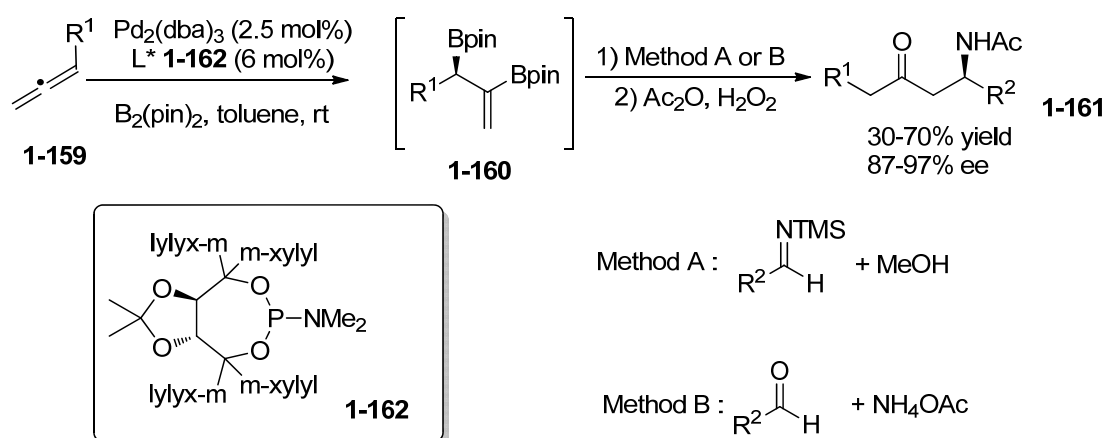
⁵⁰ R. Zhang, Q. Xu, X. Zhang, T. Zhang, M. Shi, *Tetrahedron: Asymmetry* **2010**, *21*, 1928.

Scheme 1.34 Pd-catalyzed enantioselective arylation of aldehydes with arylboronic acids

1.2.2.3 Olefin substrates

In 2006, the Morken group developed a one-pot synthesis of β -amidoketones **1-161** from allenes **1-159**, using tartaric acid based phosphorus ligand **1-162** and $\text{Pd}_2(\text{dba})_3$ catalyst. In this reaction, the chiral Pd catalyst was proved to be very efficient, giving rise to the formation of key intermediates **1-160** in optically active forms (Scheme 1.35).⁵¹

Morken



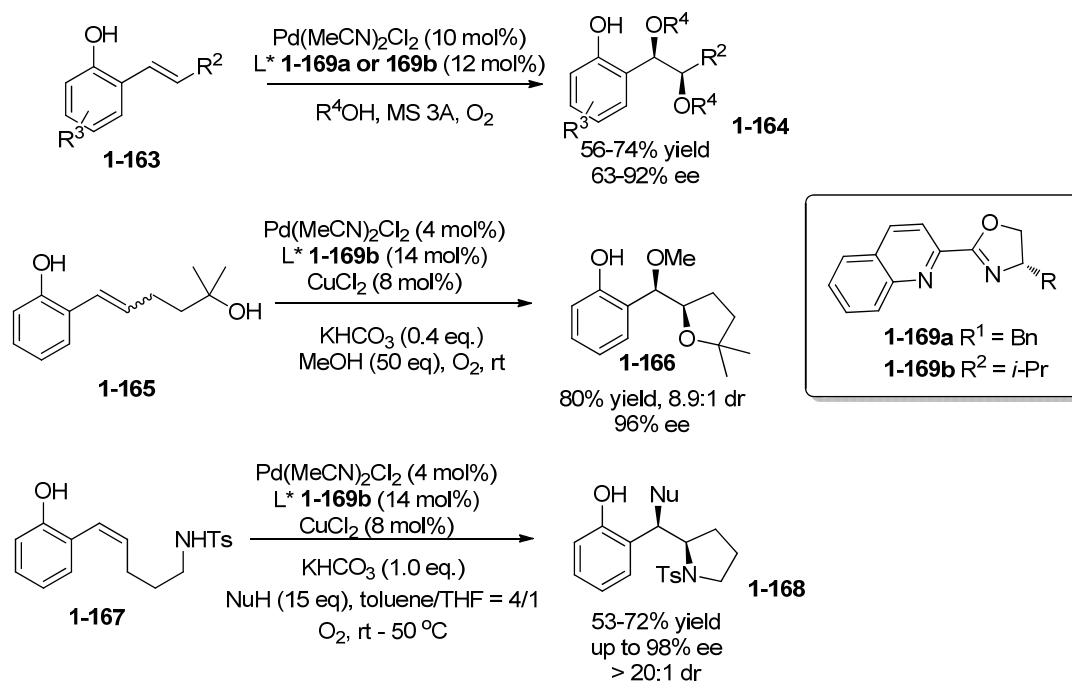
Scheme 1.35 Pd-catalyzed asymmetric addition of $\text{B}_2(\text{pin})_2$ to allenes

From 2007 to 2012, Sigman and co-workers developed a catalytic system comprising $\text{Pd}(\text{MeCN})_2\text{Cl}_2$ and (*S*)-ⁱPr-Quinox **1-169**, and showed its effectiveness in enantioselective difunctionalizations of alkenes involving the addition of two distinct

⁵¹ J. D. Sieber, J. P. Morken, *J. Am. Chem. Soc.* **2006**, *128*, 74.

nucleophiles(Scheme 1.36).⁵²

Sigman



Scheme 1.36 Enantioselective Pd-catalyzed difunctionalizations of alkenes

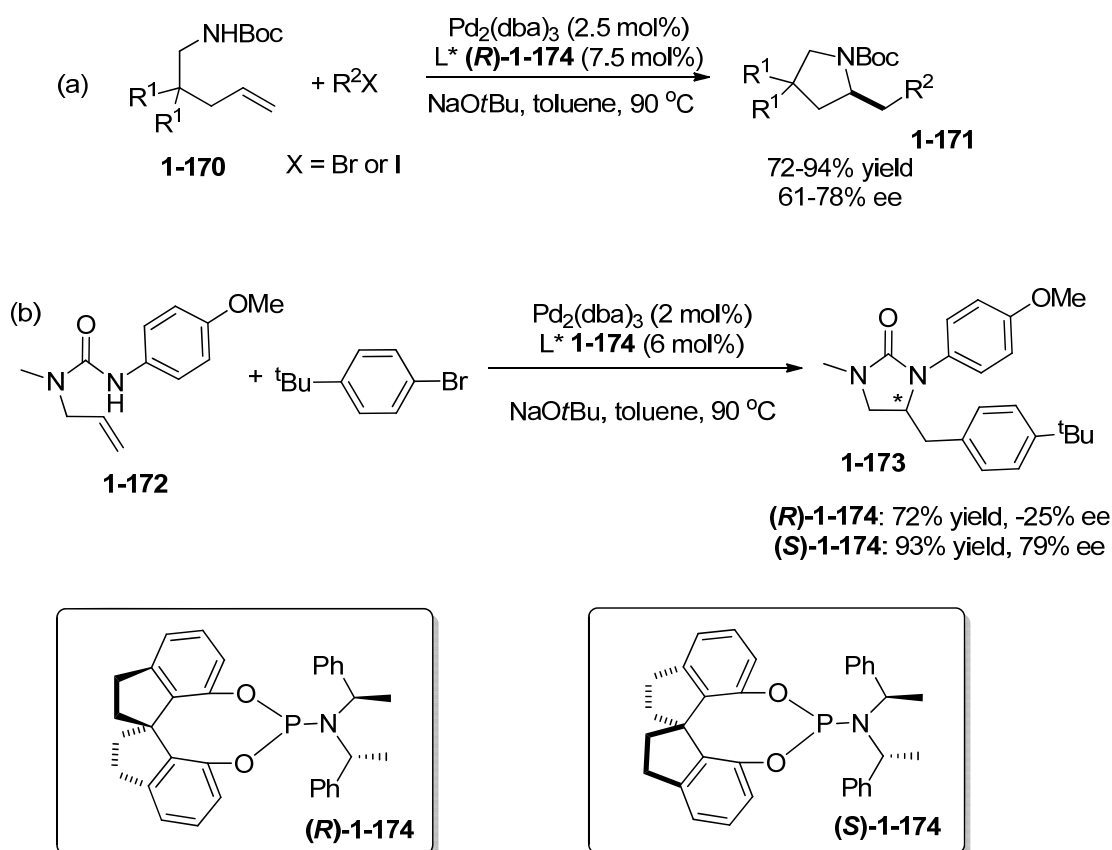
A combination of (*S*)-Siphos-PE **1-174** and Pd₂(dba)₃ was used by the Wolfe group in 2010 to catalyzed asymmetric alkene carboamination reactions of *N*-*boc*-pent-4-enylamines **1-170** with alkenyl or aryl bromide, and the products **1-171** were obtained in good to excellent yields and with moderate to good enantioselectivities (Scheme 1.37a).⁵³ Subsequently, the same group further applied the same catalytic system to enantioselective carboamination reaction of urea

⁵² a) Y. Zhang, M. S. Sigman, *J. Am. Chem. Soc.* **2007**, *129*, 3076; b) K. H. Jensen, T. P. Pathak, Y. Zhang and M. S. Sigman, *J. Am. Chem. Soc.* **2009**, *131*, 17074; (c) R. Jana, T. P. Pathak, K. H. Jensen, M. S. Sigman, *Org. Lett.* **2012**, *14*, 4074.

⁵³ D. N. Mai, J. P. Wolfe, *J. Am. Chem. Soc.* **2010**, *132*, 12157.

derivatives **1-172** to produce chiral cyclic compounds **1-173** in good yields and moderate ee values (Scheme 1.37b).⁵⁴

Walfe

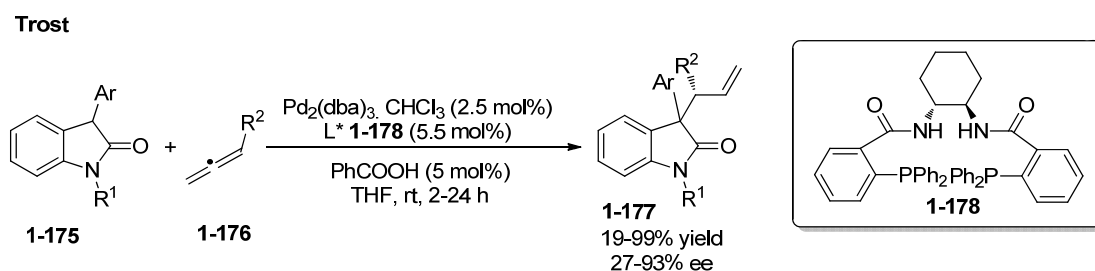


Scheme 1.37 Pd-catalyzed intramolecular cyclization *via* asymmetric additions to olefins

In 2011, Trost and co-workers reported an asymmetric Pd-catalyzed hydrocarbonation of allenes between benzyloxyallene **1-176** and oxindole **1-175** with the employment of the Trost ligand **1-178**, forming the desired products **1-177** bearing a quaternary stereocenter in excellent chemo-, regio-, diastereo- and

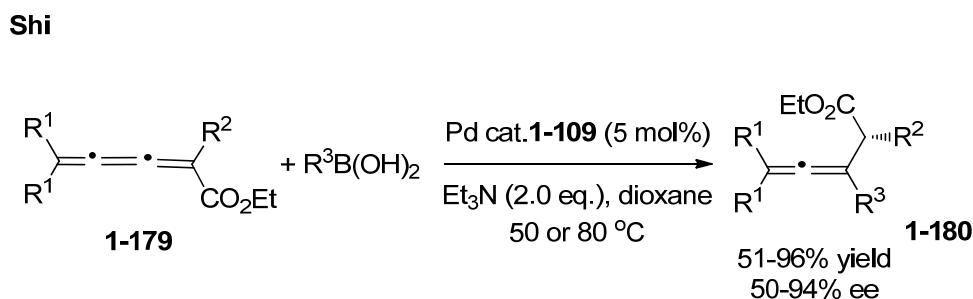
⁵⁴ B. A. Hopkins, J. P. Wolfe, *Angew. Chem. Int. Ed.* **2012**, *51*, 9886.

enantioselectivities (Scheme 1.38).⁵⁵



Scheme 1.38 Pd-catalyzed asymmetric hydrocarbonation of allenes

The Shi group developed the asymmetric addition of arylboronic acids to cumulene derivatives **1-179** catalyzed by chiral cationic Pd^{2+} diaqua complex **1-109** in 2011, affording allenic esters **1-180** in good to excellent yields and moderate to good enantioselectivities (Scheme 1.39).⁵⁶



Scheme 1.39 Pd-catalytic asymmetric addition of arylboronic acids to cumulenes

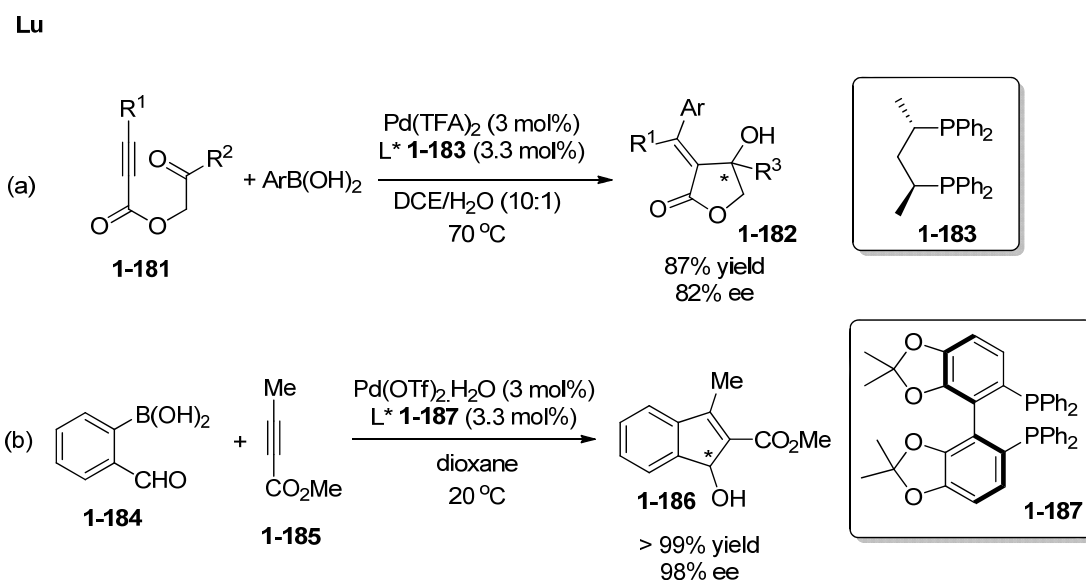
1.2.3 Asymmetric cycloadditions

In 2007, the Lu group reported a palladium-catalyzed asymmetric intramolecular addition of vinyl-palladium species to ketones under mild conditions, producing the corresponding cycloaddition products **1-182** in high yields and high

⁵⁵ B. M. Trost, J. Xie, J. D. Sieber, *J. Am. Chem. Soc.* **2011**, *133*, 20611.

⁵⁶ Z. Liu, P. Gu, M. Shi, *Chem. Eur. J.* **2011**, *17*, 5796.

enantioselectivities. Among all the screened bisphosphine ligands, (*S,S*)-BDPP **1-183** was identified as the best catalyst (Scheme 1.40a).⁵⁷ In the same year, the Lu group also developed an enantioselective tandem [3+2] annulation of 2-acylarylboronic acids **1-184** with substituted alkynes **1-185**, affording chiral 1-indenols **1-186** in high yields and excellent enantioselectivities. This time, Pd(OTf)₂·2H₂O/**1-187** system was found to be the best (Scheme 1.40b).⁵⁸



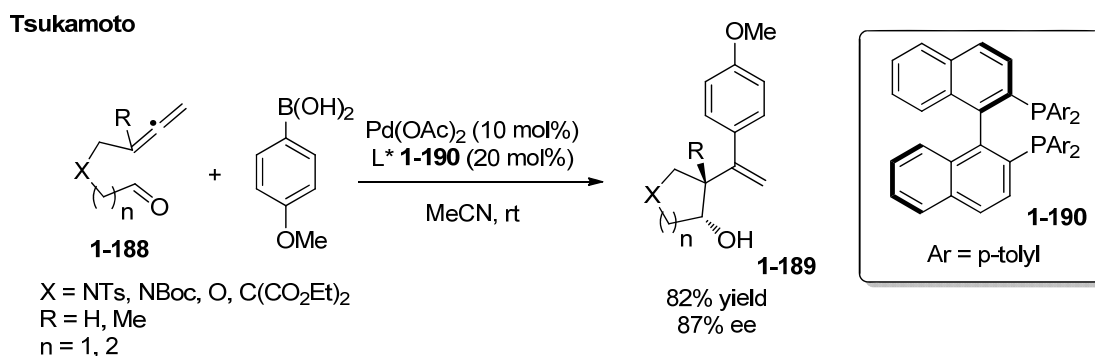
Scheme 1.40 Lu's work on Pd-catalyzed asymmetric cycloadditions

In 2008, a Pd-catalyzed enantioselective arylation cyclization of allenyl aldehydes **1-188** with arylboronic acids was demonstrated by the Tsukamoto group, and *cis*-fused five- and six-membered cyclic homoallylic alcohols **1-189** were obtained. A series of bisphosphine ligands were screened and only BINAP based

⁵⁷ J. Song, Q. Shen, F. Xu, X. Lu, *Org. Lett.* **2007**, *9*, 2947.

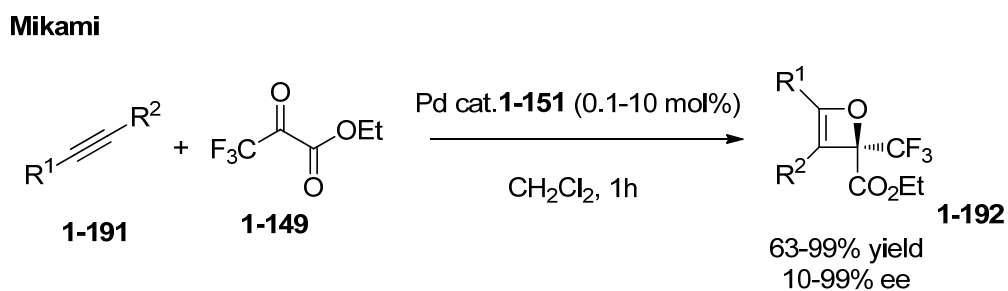
⁵⁸ M. Yang, X. Zhang and X. Lu, *Org. Lett.* **2007**, *9*, 5131.

ligands **1-190** showed good catalytic activities (Scheme 1.41).⁵⁹



Scheme 1.41 Pd-catalyzed asymmetric arylation cyclization of allenyl aldehyde

Very recently, the Mikami group reported a highly enantioselective [2+2] cycloaddition of alkynes **1-191** with trifluoropyruvate **1-149** by using a chiral dicationic BINAP/Pd catalyst **1-151**, affording oxetene derivatives **1-192** in good to excellent yields and high ee values (Scheme 1.42).⁶⁰



Scheme 1.42 Pd-catalyzed enantioselective [2+2] cycloaddition

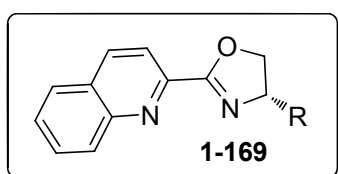
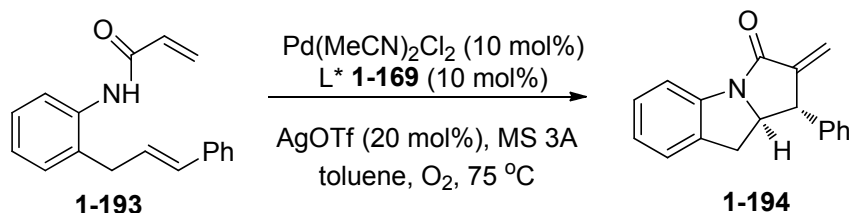
The Yang group reported a palladium(II)-catalyzed enantioselective oxidative cascade cyclization of olefinic substrates **1-193**, using Pd(MeCN)₂Cl₂/AgOTf as catalyst. Only Quinox type ligands **1-169** were shown to be effective in this study

⁵⁹ H. Tsukamoto, T. Matsumoto, Y. Kondo, *Org. Lett.* **2008**, 10, 1047

⁶⁰ K. Aikawa, Y. Hioki, N. Shimizu, K. Mikami, *J. Am. Chem. Soc.* **2011**, 133, 20092.

(Scheme 1.43).⁶¹

Yang

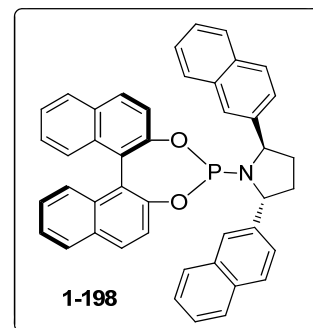
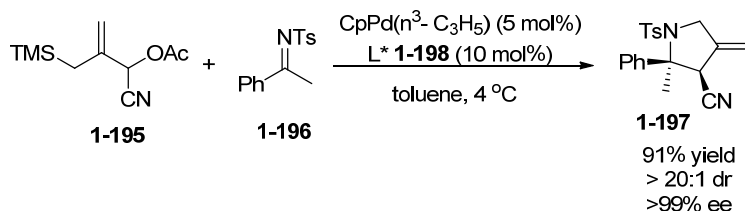


1-169a R = Bn, 80% yield, 76% ee
1-169b R = iPr, 66% yield, 72% ee
1-169c R = tBu, 62% yield, 93% ee
1-169d R = Ph, 44% yield, 36% ee

Scheme 1.43 Pd-catalytic enantioselective oxidative cascade cyclization

In 2010, the Trost group employed phosphoramidite ligands **1-198** in palladium(II)-catalyzed asymmetric [3+2] cyclization between trimethylenemethane **1-195** and imines **1-196**, generating highly optically active substituted pyrrolidines **1-197** (Scheme 1.44).⁶²

Trost



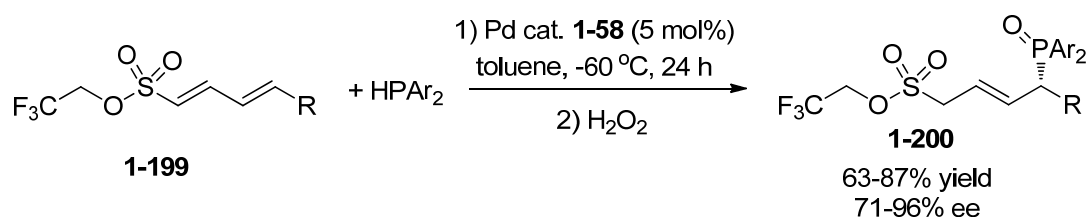
Scheme 1.44 Pd-catalyzed asymmetric [3+2] cyclization

⁶¹ W. He, K.-T. Yip, N.-Y. Zhu, D. Yang, *Org. Lett.* **2009**, *11*, 5626.⁶² B. M. Trost, S. M. Silverman, *J. Am. Chem. Soc.* **2010**, *132*, 8238.

1.2.4 Asymmetric 1,6-additions

Although asymmetric 1,6-addition have been successfully achieved by rhodium, iridium, copper as well as organic catalysis, the reports of palladium-catalyzed asymmetric 1,6-addition are very rare. Very recently, Duan and co-workers developed a palladium-catalyzed asymmetric 1,6-addition of diarylphosphines to electron-deficient dienes **1-199**, furnishing the optically active allylic phosphine derivatives **1-200** in good yields with high enantioselectivities (Scheme 1.45).⁶³

Duan



Scheme 1.45 Duan's work on Pd-catalyzed asymmetric 1,6-addition

1.3 Project objectives

Asymmetric palladium catalysis is a well established method for enantioselective synthesis of chiral molecules. Since the initial report, many palladium catalyzed asymmetric reactions have been developed over the decades, including asymmetric allylic alkylations, asymmetric Heck reactions, asymmetric cross-couplings, and asymmetric additions, among others. Pd-catalyzed asymmetric additions of various nucleophiles to C=X bonds (X= C, N, O) are becoming more and more important, due

⁶³ J. Lu, J. Ye, W.-L. Duan, *Chem. Commun.* **2014**, 50, 698.

to their high efficiency, flexible substrate scopes and mild reaction conditions. However, Pd-catalyzed asymmetric additions lagged well behind the reactions mediated by other transition metals such as rhodium, iridium and copper. Owing to the tendency of palladium species to undergo competitive reductive elimination and β -H elimination, palladium catalyzed asymmetric additions are much less developed.^[13] We therefore decided to focus on this potentially promising research area and intended to develop some new catalytic reactions. Specifically, we would like to tackle asymmetric additions of organoboron reagents to imines by palladium catalysis as good examples are rare. During the progress of our research, Zhang and co-workers reported a palladium-catalyzed asymmetric addition to cyclic imines. However, the scope of their reaction was unfortunately narrow, only five-membered imines could be used, and the reaction was not applicable to six-membered ring cyclic imine substrates.^[42]

Another objective of our research concerns with the development of chiral ligands. Chiral ligands are extremely important in transition metal catalysis, and majority of known ligands are not easily prepared. In this context, chiral ligands that can be readily derived from natural chiral building blocks are certainly very appealing. Many new kinds of chiral ligands are synthesized based on rational design and applied in metal catalyzed reactions every year. Actually, great progress has been achieved in this field and some of the developed chiral ligands which are called “privileged ligands,”⁶⁴ are proved to have good enantioselectivity and high efficiency

⁶⁴ a) T. P. Yoon, E. N. Jacobsen, *Science* **2003**, 299, 1691; b) A. Pfaltz, W. J. Drury III, *Proc. Natl. Acad. Sci. USA* **2004**, 101, 5723.

over a wide range of different reactions. Recently, our group developed a new class of mono-phosphine catalysts showing excellent reactivity and enantioselectivity in many organocatalytic asymmetric reactions.⁶⁵ These catalysts were all readily derived from natural amino acids, and their utilization as chiral ligands in transition metal catalysis is unknown. Another objective of this thesis is to design and synthesize amino acid-based chiral phosphine ligands, and employ them in the palladium catalyzed asymmetric reactions.

In chapter 2, the high performance of palladium-phosphinooxazoline catalyst in asymmetric arylation of cyclic *N*-sulfonyl ketimines will be described in detail. In chapter 3, the application of palladium-phosphinooxazoline catalyst in asymmetric addition of organoboron reagents to cyclic trifluoromethyl ketimines to synthesize anti-HIV drug analogues will be disclosed. In chapter 4, our efforts to prepare various types of amino acid-based phosphine-schiff base ligands and their applications to asymmetric reactions will be described.

⁶⁵ a) X. Han, Y. Wang, F. Zhong, Y. Lu, *J. Am. Chem. Soc.* **2011**, *133*, 1726; b) F. Zhong, X. Han, Y. Wang, Y. Lu, *Angew. Chem. Int. Ed.* **2011**, *50*, 7837; c) F. Zhong, X. Han, Y. Wang, Y. Lu, *Chem. Sci.* **2012**, *3*, 1231; d) X. Han, F. Zhong, Y. Wang, Y. Lu, *Angew. Chem. Int. Ed.* **2012**, *51*, 767.

Chapter 2 High Performance of a Palladium Phosphinooxazoline Catalyst in Asymmetric Arylation of Cyclic *N*-Sulfonyl Ketimines

2.1 Introduction

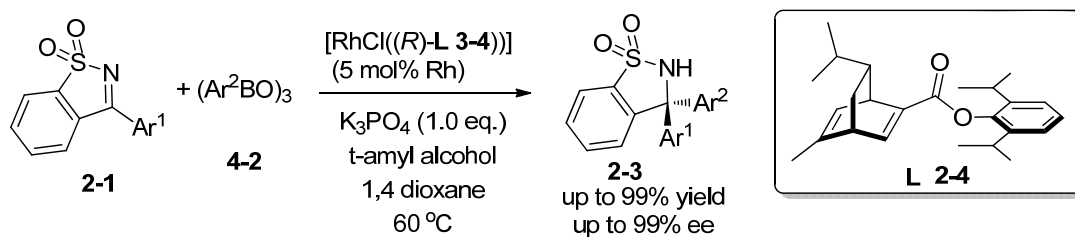
Rhodium- or palladium-catalyzed asymmetric addition of arylboron reagents to imines is one of the most efficient methods of producing chiral disubstituted and tri-substituted methylamines.⁶⁶ Among the imines used for the asymmetric arylation, cyclic *N*-sulfonyl imines have recently attracted considerable attention owing to their advantages over others in that they have generally higher reactivity towards the catalytic arylation and their cyclic structure makes enantioface differentiation of imine easier and simpler because of no *syn-anti* equilibration.

In 2012, Hayashi and co-workers reported the first example of asymmetric addition of arylbroxines **2-2** to cyclic *N*-sulfonyl ketimines **2-1** in the presence of a rhodium catalyst coordinated with a chiral diene ligand **2-4**, affording benzosultams **2-3** in excellent yields and enantioselectivity (Scheme 2.1).⁶⁷

⁶⁶ For reviews on the transition metal-catalyzed asymmetric addition of organometallic reagents to imines, see: a) S. Kobayashi, Y. Mori, J. S. Fossey, M. M. Salter, *Chem. Rev.* **2011**, *111*, 2626; b) C. S. Marques, A. J. Burke, *ChemCatChem* **2011**, *3*, 635; c) K. Yamada, K. Tomioka, *Chem. Rev.* **2008**, *108*, 2874; d) G. K. Friestad, A. K. Mathies, *Tetrahedron* **2007**, *63*, 2541. For recent examples of the transition metal-catalyzed asymmetric addition of organometallic reagents to imines, see: a) S. Hirner, A. Kolb, J. Westmeier, S. Gebhardt, S. Middel, K. Harms, P. von Zezschwitz, *Org. Lett.* **2014**, *16*, 3162; b) Z. Cui, Y.-J. Chen, W.-Y. Gao, C.-G. Feng, G.-Q. Lin, *Org. Lett.* **2014**, *16*, 1016; c) B. Gopula, C.-W. Chiang, W.-Z. Lee, T.-S. Kuo, P.-Y. Wu, J. P. Henschke, H.-L. Wu, *Org. Lett.* **2014**, *16*, 632.

⁶⁷ a) T. Nishimura, A. Noishiki, G. C. Tsui, T. Hayashi, *J. Am. Chem. Soc.* **2012**, *134*, 5056. See, also: b) T. Nishimura, A. Noishiki, Y. Ebe, T. Hayashi, *Angew. Chem. Int. Ed.* **2013**, *52*, 1777; c) T. Nishimura, A. Y. Ebe, H. Fujimoto, T. Hayashi, *Chem. Commun.* **2013**, *49*, 5504.

Hayashi



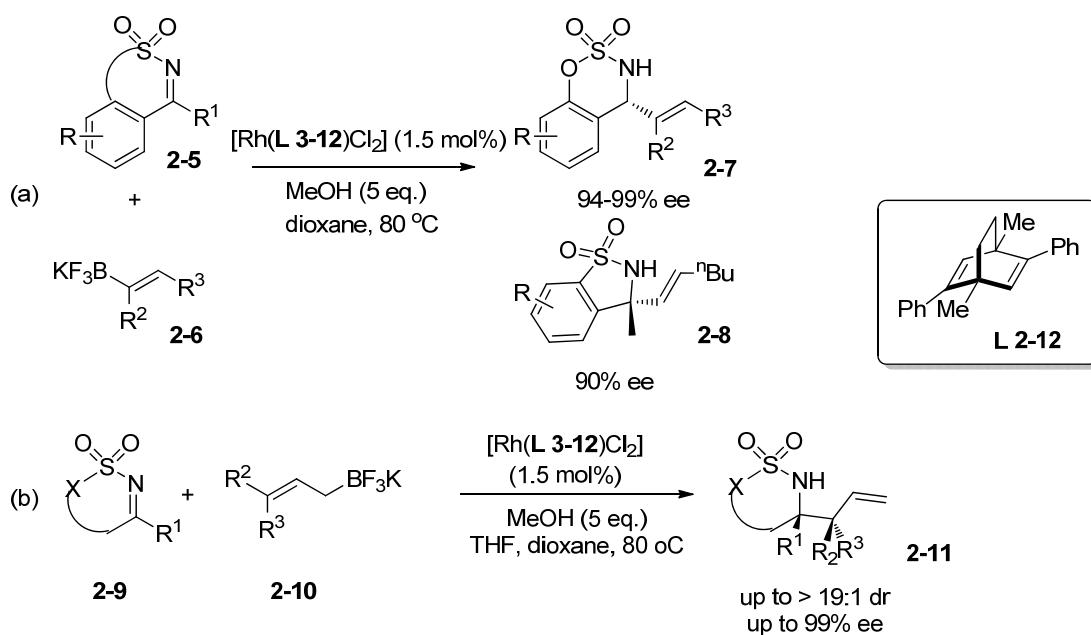
Scheme 2.1 Hayashi's work on Rh-catalyzed asymmetric addition to *N*-sulfonyl ketimines

Shortly after that, Lam group disclosed an Rh-catalyzed enantioselective addition of alkenylboron reagents **2-6** to cyclic imines **2-5** employing a rhodium complex based on chiral diene ligands **2-12** (Scheme 2.2a).⁶⁸ They also applied the same catalytic system in the enantioselective nucleophilic allylations of cyclic imines using potassium allyltrifluoroborates **2-10** as nucleophiles and proceeded high enantioselectivity and distereoselectivity (Scheme 2.2b).⁶⁹

⁶⁸ a) Y. Luo, A. J. Carnell, H. W. Lam, *Angew. Chem. Int. Ed.* **2012**, *51*, 6762

⁶⁹ b) Y. Luo, H. B. Hepburn, N. Chotsaeng, H. W. Lam, *Angew. Chem. Int. Ed.* **2012**, *51*, 8309.

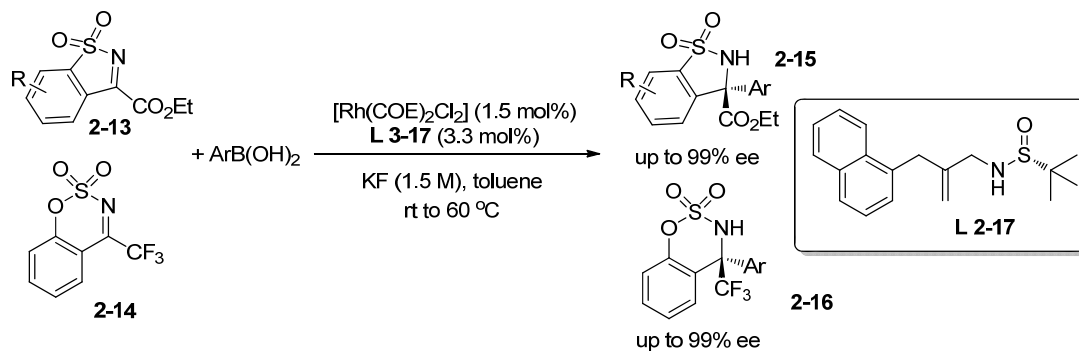
Lam



Scheme 2.2 Lam's work on Rh-catalyzed asymmetric addition to *N*-sulfonyl cyclic imines

Xu group in 2013 developed a new, simple sulfonamide-based olefin ligand **2-17** and used it in the asymmetric Rh-catalyzed arylations of cyclic ketimines, achieving high enantioselective products with stereogenic quaternary carbon center (Scheme 2.3).⁷⁰

Xu

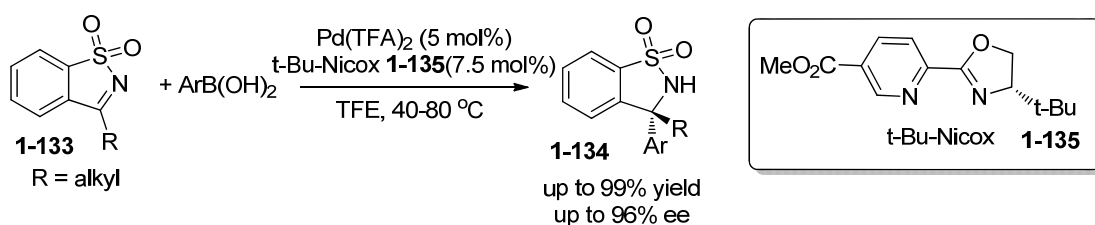


Scheme 2.3 Xu's Sulfur-olefin ligand in asymmetric addition to *N*-sulfonyl cyclic imines

⁷⁰ a) H. Wang, T. Jiang, M.-H. Xu, *J. Am. Chem. Soc.* **2013**, *135*, 971; b) H. Wang, M.-H. Xu, *Synthesis* **2013**, 45, 2125.

In addition to rhodium catalysis, Zhang and co-workers reported a palladium-catalyzed asymmetric addition of organoboronic acids to cyclic imines. This catalytic system showed high efficiency and excellent enantioselectivity under aerobic conditions and with unpurified solvent (scheme 2.4).⁷¹

Zhang

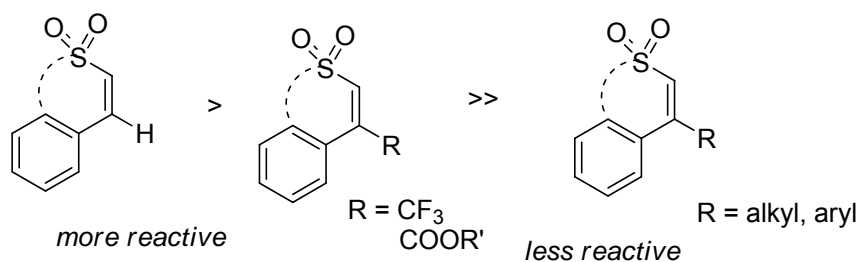
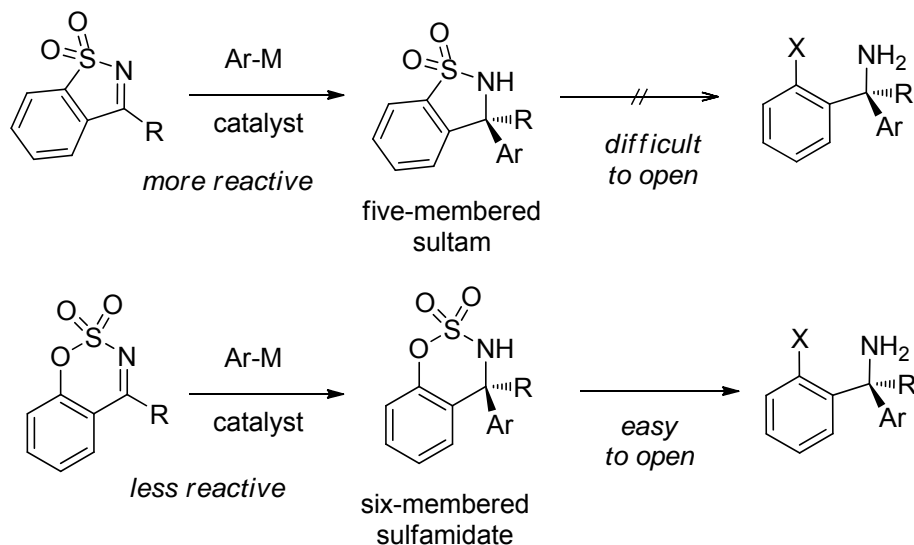


Scheme 2.4 Zhang's work on Pd-catalyzed arylation of cyclic imines

A summary of the catalytic asymmetric arylation of cyclic *N*-sulfonyl imines reported to date with rhodium (Hayashi, Lam, Xu) and palladium (Zhang) complexes as catalysts is illustrated in Scheme 2.5.

⁷¹ G. Yang, W. Zhang, *Angew. Chem. Int. Ed.* **2013**, *52*, 7540.

(a) Aldimines versus Ketimines

(b) Five-membered versus six-membered cyclic *N*-sulfonyl imines**Scheme 2.5** Reactivity and utility of cyclic *N*-sulfonyl imines

The cyclic *N*-sulfonyl imines used as the arylation substrates are classified into aldimines and ketimines, where the former is more reactive than the latter in general and some of the ketimines substituted with electron-withdrawing groups such as ester and CF_3 are as reactive as aldimines. The basic structure of the cyclic *N*-sulfonyl imines so far used is either 5-membered ring imine leading to benzosultam or 6-membered one **1** leading to benzosulfamidate. Although the 5-membered ring imines have high reactivity giving the corresponding sultams upon arylation even for ketimines, the ring cleavage giving chiral methylamines without loss of enantiomeric

purity is not trivial^{67a}. On the other hand, the 6-membered ring imines are less reactive towards the arylation while the resulting sulfamidates are known to undergo ring opening without loss of their enantiomeric purity.⁷² As a result there have been very few reports on the catalytic asymmetric addition to the 6-membered ring ketimines **1** (R = alkyl, aryl) in high yields.

2.2 Results and discussions

During our studies on the catalytic asymmetric addition of organoboron reagents to carbon–carbon and carbon–hetero atom double bonds,⁷³ it was found that a cationic palladium complex coordinated with a chiral phosphine-oxazoline ligand showed high catalytic activity and high enantioselectivity in the asymmetric addition of arylboronic acids to cyclic *N*-sulfonyl ketimines (R = alkyl, aryl) to give high yields of chiral cyclic sulfonamides which bear tetra-substituted stereogenic center.⁷⁴

2.2.1 Catalytic system comparison

The results obtained for the addition of phenylboronic acid (**2m**) to *N*-sulfonyl aldimine **2-18a** (R = H) and ketimine **2-18b** (R = Me) in the presence of a cationic

⁷² Ring opening of benzosulfamidate with nickel-catalyzed Grignard cross-coupling, see: a) P. M. When, J. Du Bois, *Org. Lett.* **2005**, *7*, 4685. Ring opening with LiAlH₄ reduction, see: b) Y.-Q. Wang, C.-B. Yu, D.-W. Wang, X.-B. Wang, Y.-G. Zhou, *Org. Lett.* **2008**, *10*, 2071.

⁷³ For reviews on the rhodium-catalyzed asymmetric addition of arylboron reagents, see: a) T. Hayashi, K. Yamasaki, *Chem. Rev.* **2003**, *103*, 2829; b) S. Darses, J.-P. Genet, *Eur. J. Org. Chem.* **2003**, 4313; c) J. Christoffers, G. Koripelly, A. Rosiak, M. Rössle, *Synthesis* **2007**, 1279; d) N. Miyaura, *Bull. Chem. Soc. Jpn.* **2008**, *81*, 1535; e) J. D. Hargrave, J. C. Allen, C. G. Frost, *Chem. Asian J.* **2010**, *5*, 386; f) H. J. Edwards, J. D. Hargrave, S. D. Penrose, C. G. Frost, *Chem. Soc. Rev.* **2010**, *39*, 2093; g) P. Tian, H.-Q. Dong, G.-Q. Lin, *ACS Catal.* **2012**, *2*, 95. For a review on the palladium-catalyzed asymmetric addition of arylboron reagents, see: Y.-W. Sun, P.-L. Zhu, Q. Xu, M. Shi, *RSC Advances* **2013**, *3*, 3153.

⁷⁴ A chiral phosphino-oxazoline–palladium complex has been used as a catalyst for the asymmetric addition of arylboronic acids to isatins: Q. Li, P. Wan, S. Wang, Y. Zhuang, L. Lia, Y. Zhou, Y. He, R. Cao, L. Qiu, Z. Zhou, *Appl. Catal. A: General* **2013**, *458*, 201.

palladium complex coordinated with (*S*)-*i*-Pr-phox⁷⁵ are summarized in Table 2.1, which also contains, for comparison, those for the reaction in the presence of other palladium and rhodium complexes so far reported as effective catalysts for the asymmetric arylation of *N*-sulfonyl imines. The best result was obtained with the catalyst generated in situ from PdCl₂((*S*)-*i*-Pr-phox)⁷⁶ and AgBF₄ in dichloroethane. Thus, aldimine **2-18a** was allowed to react with **2-19m** (2 eq to **2-18a**) in the presence of 5 mol% of the cationic palladium catalyst in dichloroethane at 65–70 °C for 12 h to give a quantitative yield of the phenylation product **2-20am**, which is an *R* isomer of 99.6% ee (entry 1). The same reaction conditions were successfully applied to the reaction of ketimine **2-18b**, which gave the corresponding phenylation product (*R*)-**2-20bm**^[6] of 99.5% ee in a quantitative yield (entry 1). The generation of cationic palladium species is essential for the high catalytic activity. In the absence of AgBF₄, no phenylation was observed for either aldimine **2-18a** or ketimine **2-18b** (entry 2). AgOTf is not a choice of the silver salt which gave only a low yield (10%) of **3am** and no **2-20bm** (entry 3). A palladium complex generated from Pd(OCOCF₃)₂ and (*S*)-*i*-Pr-phox catalyzed the phenylation of aldimine **2-18a** efficiently in CF₃CH₂OH at 80 °C, but its catalytic activity was lower for ketimine **1b** giving a modest yield (58%) of (*R*)-**2-20bm** although the enantioselectivity was high (99.8% ee) (entry 4). Cationic palladium bisphosphine complexes⁷⁷ generated by mixing

⁷⁵ a) P. von Matt, A. Pfaltz, *Angew. Chem., Int. Ed. Engl.* **1993**, 32, 566; b) J. Sprinz, G. Helmchen, *Tetrahedron Lett.* **1993**, 34, 1769; c) G. J. Dawson, C. G. Frost, J. M. J. Williams, S. J. Coote, *Tetrahedron Lett.* **1993**, 34, 3149.

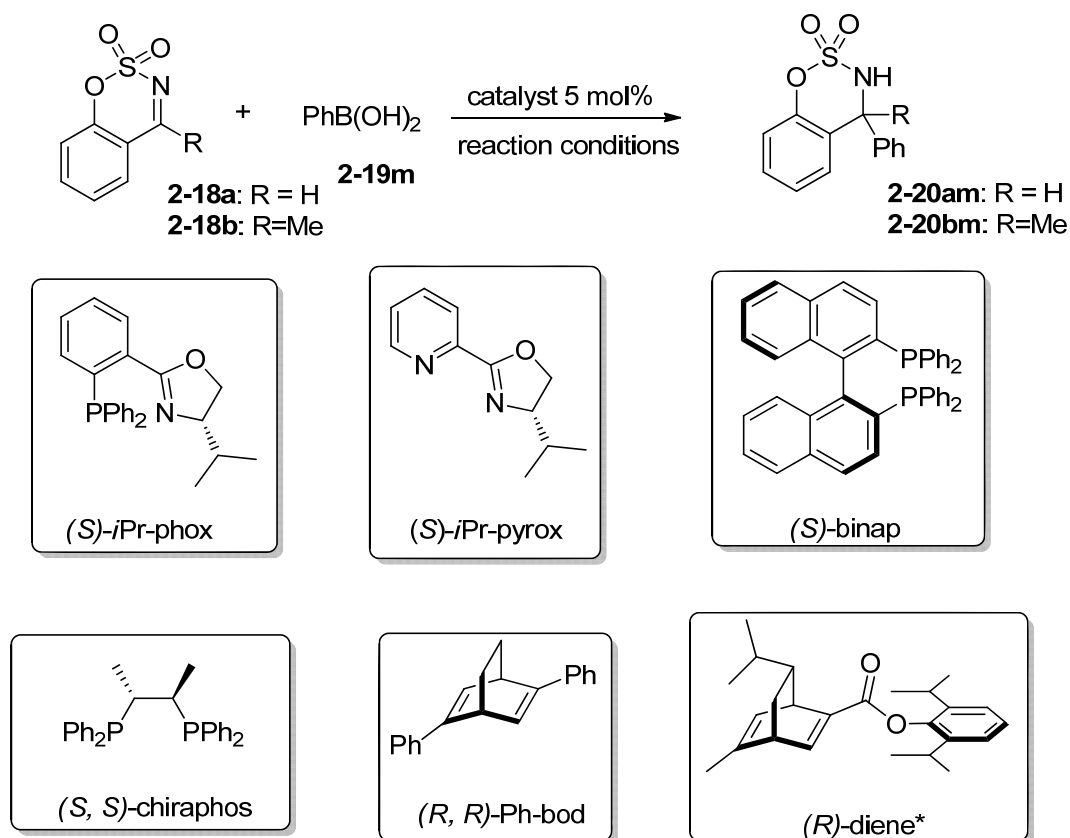
⁷⁶ a) Y. Uozumi, K. Kato, T. Hayashi, *Tetrahedron: Asymmetry* **1998**, 9, 1065; b) A. J. Blacker, M. L. Clarke, M. S. Loft, M. F. Mahon, M. E. Humphries, J. M. J. Williams, *Chem. Eur. J.* **2000**, 6, 353.

⁷⁷ Cationic bisphosphine-palladium catalysts have been used for conjugate addition to α,β -unsaturated carbonyl compounds: For reviews: a) A. Gutnov, *Eur. J. Org. Chem.* **2008**, 4547; b) Y. Yamamoto, T. Nishikata, N. Miyaura, *J. Synth. Org. Chem. Jpn.* **2006**, 64, 1112; c) G. Berthon-Gelloz, T. Hayashi in *Boronic Acids, Second*,

$\text{PdCl}_2[(S,S)\text{-chiraphos}]$ and $\text{PdCl}_2[(S)\text{-binap}]$ with AgBF_4 were not so catalytically active as that with the phosphine-oxazoline, $(S)\text{-iPr-phox}$, as a ligand. They catalyzed the phenylation of aldimine **2-18a** to some extent, but they were not catalytically active for ketimine **2-18b** (entries 5 and 6). Palladium complexes coordinated with chiral oxazoline-pyridine ligands, $(S)\text{-iPr-pyrox}$ and its derivatives, have been reported by Zhang to be catalytically active for the addition to 5-membered-ring ketimines. In our hands, his palladium catalyst system, $\text{Pd}(\text{OCOCF}_3)_2$ and $(S)\text{-iPr-pyrox}$ in $\text{CF}_3\text{CH}_2\text{OH}$, did not catalyze the phenylation of ketimine **2-18b** well,⁷⁸ while it is highly active for the phenylation of aldimine **2-18a** (entry 7). A cationic palladium complex generated by the addition of AgBF_4 to $\text{PdCl}_2[(S)\text{-iPr-pyrox}]$ also catalyzed the addition to aldimine **2-18a** very efficiently, but it is not active for ketimine **2-18b** in either $\text{CF}_3\text{CH}_2\text{OH}$ or dichloroethane (entries 8 and 9). Chiral diene/rhodium catalysts, which we previously reported to be most active for the asymmetric arylation of ketimines including the 5-membered-ring ones, catalyzed the phenylation of aldimine **2-18a** to give **2-20am** of high % ee in a quantitative yield (entries 10 and 11). They also catalyzed the asymmetric phenylation of ketimine **1b** with high enantioselectivity, but the yields of **3bm** are not so high as those observed with the present cationic palladium/ $(S)\text{-iPr-phox}$ catalyst. The binap–rhodium catalyst was less active than the diene-rhodium as reported

Completely Revised Edition (Ed.: D. G. Hall), Wiley-VCH: Weinheim, **2011**; Vol. 1, Chap. 5, pp 263–313.

⁷⁸ Zhang reported (ref 6) that the addition of $\text{PhB}(\text{OH})_2$ to **1b** ($\text{R} = \text{Me}$) catalyzed by a chiral pyridyloxazoline-palladium complex in a sealed tube charged with oxygen at 80 °C for 48 h gave 58% yield of the corresponding benzosulfamidate (95% ee); A palladium complex coordinated with chiral pyridinooxazoline ligand was reported to be an efficient catalyst for asymmetric conjugate addition to cyclic enones: a) K. Kikushima, J. C. Holder, M. Gatti, B. M. Stoltz, *J. Am. Chem. Soc.* **2011**, *133*, 6902; b) J. C. Holder, A. N. Marziale, M. Gatti, B. Mao, B. M. Stoltz, *Chem. Eur. J.* **2013**, *19*, 74.

Table 2.1 Catalytic Asymmetric Addition of Phenylboronic Acid (**2-19m**) to Cyclic*N*-Sulfonyl Aldimine **2-18a** and Ketimine **2-18b**^[a]

	Catalyst (5 mol%)	Solvent	2-20am	2-20bm
	additives	T [°C], t [h]	Yield ^[b] (<i>ee</i> ^[c])	Yield ^[b] (<i>ee</i> ^[c])
1	PdCl ₂ [(<i>S</i>)- <i>i</i> Pr-phox]	ClCH ₂ CH ₂ Cl	99%	99%
	AgBF ₄	65-70, 12	(99.6% <i>ee</i> , <i>R</i>)	(99.5% <i>ee</i> , <i>R</i>)
2	PdCl ₂ [(<i>S</i>)- <i>i</i> Pr-phox]	ClCH ₂ CH ₂ Cl	0%	0%
		65-70, 12	(-)	(-)
3	PdCl ₂ [(<i>S</i>)- <i>i</i> Pr-phox]	ClCH ₂ CH ₂ Cl	10%	0%
	AgOTf	65-70, 12	(-)	(-)

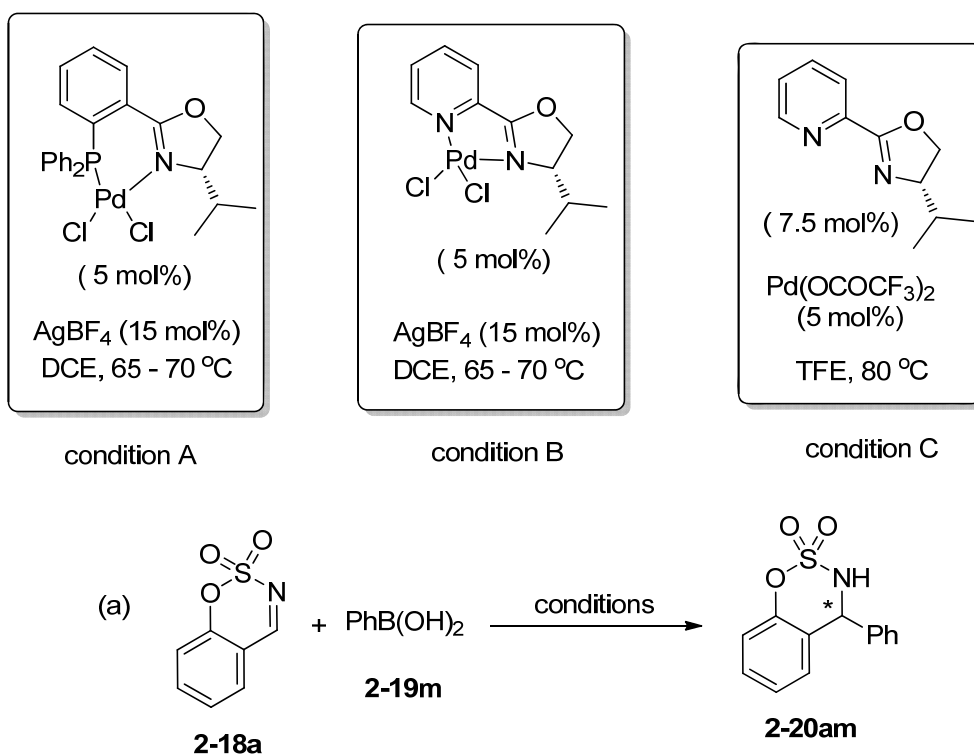
4	Pd(OCOFCF ₃) ₂	CF ₃ CH ₂ OH	99%	0%
	(<i>S</i>)- <i>i</i> Pr-phox	80, 20	(92% <i>ee</i> , <i>R</i>)	(-)
5	PdCl ₂ [(<i>S,S</i>)-chiraphos]	ClCH ₂ CH ₂ Cl	50%	0%
	AgBF ₄	65-70, 12	(84% <i>ee</i> , <i>S</i>)	(-)
6	PdCl ₂ [(<i>S</i>)-binap]	ClCH ₂ CH ₂ Cl	42%	0%
	AgBF ₄	65-70, 12	(94% <i>ee</i> , <i>S</i>)	(-)
7	Pd(OCOFCF ₃) ₂	CF ₃ CH ₂ OH	90%	7%
	(<i>S</i>)- <i>i</i> Pr-pyrox	80, 20	(68% <i>ee</i> , <i>R</i>)	(-)
8	PdCl ₂ [(<i>S</i>)- <i>i</i> Pr-pyrox]	CF ₃ CH ₂ OH	99%	0%
	AgBF ₄	80, 20	(77% <i>ee</i> , <i>R</i>)	(-)
9	PdCl ₂ [(<i>S</i>)- <i>i</i> Pr-pyrox]	ClCH ₂ CH ₂ Cl	99%	0%
	AgBF ₄	65-70, 12	(80% <i>ee</i> , <i>R</i>)	(-)
10	[RhCl((<i>R,R</i>)-Ph-Bod)] ₂	dioxane	99%	76%
	K ₃ PO ₄ , <i>t</i> -amyl alcohol	60, 12	(98.0% <i>ee</i> , <i>R</i>)	(97.0% <i>ee</i> , <i>R</i>)
11	[RhCl((<i>R</i>)-diene*)] ₂	dioxane	99%	30%
	K ₃ PO ₄ , <i>t</i> -amyl alcohol	60, 12	(99.6% <i>ee</i> , <i>R</i>)	(99.3% <i>ee</i> , <i>R</i>)
12	[RhCl((<i>S</i>)-binap)] ₂	dioxane	26%	< 3%
	K ₃ PO ₄ , <i>t</i> -amyl alcohol	60, 12	(89% <i>ee</i> , <i>S</i>)	(-)

[a] Reaction conditions: **2-18a** (0.10 mmol), **2-19m** (0.20 mmol), catalyst (5 mol%), additive, solvent (1.0 mL) at a given temperature for 12 h. [b] Isolated yield of **2-20am** or **2-20bm**. [c] Determined by HPLC analysis with chiral columns. The absolute configurations of **2-20am** and **2-20bm** were determined by comparison of their optical rotations with those reported.^[5a,6]

2.2.2 Reaction monitoring

By monitoring the reaction progress of the palladium-catalyzed addition to ketimine **2-18b** for comparison of the Pd/phox catalyst with Pd/pyrox catalyst (entries 1 vs 7), it was revealed that the low yield with the Pd/pyrox catalyst is due mainly to a short life of the catalyst system. Thus, the reaction with Pd/pyrox catalyst gave 7% yield the product **2-20bm** within 10 min, but the yield was not increased after 10 min. In contrast, the Pd/phox catalyst was found to keep its high catalytic activity for at least one hour to give high yield of **2-20bm** (Table 2.2 and 2.3).

Table 2.2 Details of monitoring the reaction process of **2-18a**^[a]



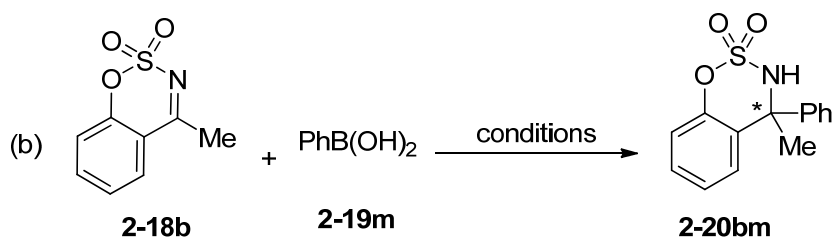
t [min]

Yield^[b] of condition AYield^[b] of condition B

10	83%	78%
20	88%	79%
30	93%	83%
60	98%	90%
120	99%	98%
240	99%	99%

[a] Reaction conditions: **2-18a** (0.10 mmol), **2-19m** (0.20 mmol), catalyst (5 mol%), additive, solvent (1.0 mL). [b] Isolated yield of **2-20am**.

Table 2.3 Details of monitoring the reaction process of **2-18b**^[a]



t [min]	Yield ^[b] of condition A	Yield ^[b] of condition B	Yield ^[b] of condition C
10	88	0	6
20	94	0	7
30	97	0	7
60	99	0	7
120	99	0	7
240	99	0	7

[a] Reaction conditions: **2-18b** (0.10 mmol), **2-19m** (0.20 mmol), catalyst (5 mol%), additive, solvent (1.0 mL). [b] Isolated yield of **2-20bm**.

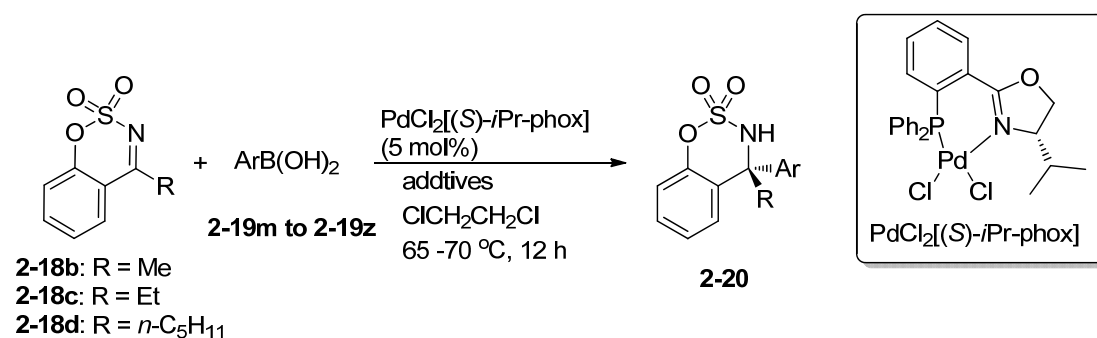
2.2.3 Substrate scope

The cationic palladium catalyst generated from PdCl₂[(*S*)-*i*-Pr-phox] and AgBF₄ was found to have wide applicability in the asymmetric addition of arylboronic acids to the methyl-substituted ketimine **2-18b** (Table 2.4). The addition of phenylboronic acids substituted at para position with methyl, phenyl, phenoxy, and halides all gave the corresponding arylation products with high enantioselectivity (>98% ee) in high yields (entries 3, 5–8). For those arylboronic acids which are not reactive enough to give high yields of the arylation products under the standard condition (condition **A**), the use of AgSbF₆ and K₃PO₄ as additives (condition **B**) improved the chemical yields with keeping the high enantioselectivity. The effects of the additives are summarized in entries 12–15 and details are shown in Table 2.5 for the addition of 2-MeOC₆H₄B(OH)₂ (**2-19w**) to ketimine **2-18b**. The reaction under the condition **A** (AgBF₄) gave only a modest yield (56%) of the arylation product **2-20bw**, though the enantioselectivity is high (99.5% ee). With AgSbF₆ (condition **C**) the yield was improved to 90%, but the product was racemic. This is probably due to an acid contaminated in AgSbF₆ which causes racemization of the product by way of a benzylic cation intermediate. Addition of K₃PO₄ as a weak base together with AgSbF₆ inhibited the racemization to give a high yield of **2-20bw** with high % ee. Combination of K₃PO₄ and AgBF₄ did not improve the yield of the product. Under the condition **B**, meta- and ortho-substituted phenylboronic acids gave the arylation products with high % ee (entries 16–18). The high catalytic activity and high

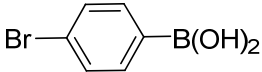
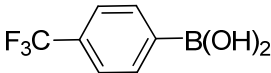
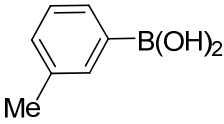
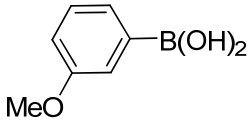
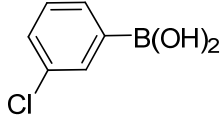
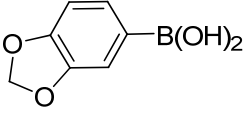
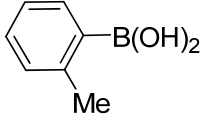
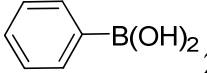
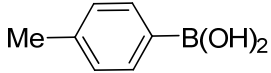
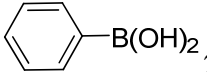
enantioselectivity were also observed in the addition to cyclic ketimines **2-18c** and **2-18d**, which are ethyl and pentyl imines, respectively (entries 19–21).

Table 2.4 Palladium-Catalyzed Asymmetric Addition of Arylboronic Acids **2-19m–z** to

Cyclic *N*-Sulfonyl Ketimines **2-18b–d**.^[a]



	2-18 , conditions ^[b]	ArB(OH) ₂ 2-19	2-20 , yield [%] ^[c]	ee [%] ^[d]
1	2-18b , A	2-19m	2-20bm , 99	99.5 (<i>R</i>)
2	2-18b , B	2-19m	2-20bm , 99	99.6 (<i>R</i>)
3	2-18b , A	2-19n	2-20bn , 99	98.1 (<i>R</i>)
4	2-18b , A	2-19o	2-20bo , 99	98.8 (<i>R</i>)
5	2-18b , B	2-19p	2-20bp , 99	99.9 (<i>R</i>)
6	2-18b , A	2-19q	2-20bq , 99	98.6 (<i>R</i>)
7	2-18b , A	2-19r	2-20br , 87	98.4 (<i>R</i>)
8	2-18b , A	2-19s	2-20bs , 88	99.4 (<i>R</i>)

9	2-18b, A	 2-19t	2-20bt, 95	99.9 (<i>R</i>)
10	2-18b, B	 2-19u	2-20bu, 51	99.4 (<i>R</i>)
11	2-18b, A	 2-19v	2-20bv, 99	99.4 (<i>R</i>)
12	2-18b, A	 2-19w	2-20bw, 56	99.5 (<i>R</i>)
13	2-18b, B		2-20bw, 88	99.9 (<i>R</i>)
14	2-18b, C^[e]		2-20bw, 90	0
15	2-18b, D^[e]		2-20bw, 48	99.7 (<i>R</i>)
16	2-18b, B	 2-19x	2-20bx, 95	99.7 (<i>R</i>)
17	2-18b, B	 2-19y	2-20by, 98	99.9 (<i>R</i>)
18	2-18b, B	 2-19z	2-20bz, 51	99.9 (<i>R</i>)
19	2-18c, B	 2-19m	2-20cm, 99	99.5 (<i>R</i>)
20	2-18c, A	 2-19n	2-20cn, 99	99.5 (<i>R</i>)
21	2-18d, A	 2-19m	2-20dm, 99	99.4 (<i>R</i>)

[a] Reaction conditions: **1** (0.10 mmol), **2** (0.20 mmol), PdCl₂[(*S*)-*i*-Pr-phox] (5 mol%), additive,

dichloroethane (1.0 mL) at 65–70 °C for 12 h. [b] **A**: AgBF₄ (15 mol%). **B**: AgSbF₆ (15 mol%) and

K₃PO₄ (15 mol%). [c] Isolated yield. [d] Determined by HPLC analysis with chiral columns. The

absolute configurations are proposed to be *R* by similarity of the stereochemical pathway to that giving

(*R*)-**3bm**. [e] **C**: AgSbF₆ (15 mol%). **D**: AgBF₄ (15 mol%) and K₃PO₄ (15 mol%).

Table 2.5 Condition screening for asymmetric addition of **2-19w** to **2-18b**^[a]

	Conditions	2-20bw , yield ^[b] [%]	<i>ee</i> ^[c] [%]
1	15% AgBF ₄ , ClCH ₂ CH ₂ Cl	56	99.9
2	10% AgSbF ₆ (<i>pre-formed</i>), ClCH ₂ CH ₂ Cl	80	55
3	10% AgBF ₄ (<i>pre-formed</i>), ClCH ₂ CH ₂ Cl	0	-
4	10% AgSbF ₆ (<i>pre-formed</i>), 1eq. K ₂ HPO ₄ , ClCH ₂ CH ₂ Cl	0	-
5	15% AgSbF ₆ , 1eq. K ₂ HPO ₄ , ClCH ₂ CH ₂ Cl	~20	-
6	15% AgBF ₄ , EtOH	0	-
7	15% AgBF ₄ , Dioxane	0	-
8	15% AgBF ₄ , TFE	66	n. d.
9	15% AgBF ₄ , toluene	23	n. d.
10	15% AgSbF ₆ , 30% K ₃ PO ₄ , ClCH ₂ CH ₂ Cl	88	99.9

11	5% AgSbF ₆ , ClCH ₂ CH ₂ Cl	0	-
----	--	---	---

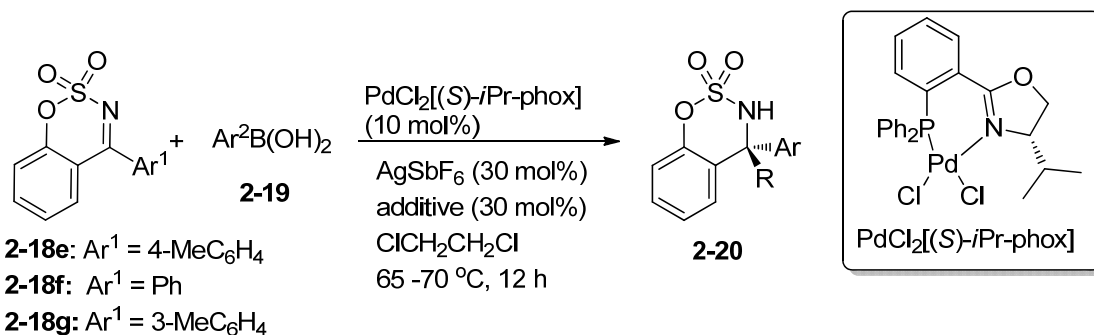
[a] Reaction conditions: **2-18b** (0.10 mmol), **2-19w** (0.20 mmol), catalyst (5 mol%), additive, solvent (1.0 mL). [b] Isolated yield of **2-20bw**. [c] Determined by HPLC analysis with chiral columns.

The asymmetric addition to cyclic ketimines with aryl groups on the imine carbon are more challenging because they are less reactive than those with alkyl groups, and the arylation products, triarylmethylamines, are more likely to undergo racemization under the reaction conditions (Table 2.6). The reaction of ketimine **2-18e** with 4-methoxyphenylboronic acid (**2-19p**) in the presence of PdCl₂((*S*)-*i*-Pr-phox) (10 mol%) and AgSbF₆ (30 mol%) proceeded well to give the corresponding arylation product **2-20ep** in 75% yield, but it was racemic (entry 1). The formation of racemic product was also observed in the presence of inorganic base K₃PO₄ (30 mol%), which corresponds to condition **B** in Table 2, or K₂CO₃ (entries 2 and 3).⁷⁹ Finally, it was found that the addition of proton sponge prevents the product from racemization under the reaction conditions (entry 5). In the presence of proton sponge, several triarylmethylamine products were obtained with high enantioselectivity (entries 6–8).

Table 2.6 Palladium-Catalyzed Asymmetric Addition of Arylboronic Acids to Cyclic

N-Sulfonyl Aryl Ketimines **2-18e–g**.^[a]

⁷⁹ The racemization of arylation product **3ep** under the reaction conditions was confirmed experimentally by exposing enantiomerically enriched **3ep** (99.2% ee) to the reaction conditions of entry 3 in Table 2.6, which resulted in complete racemization of **3ep**.



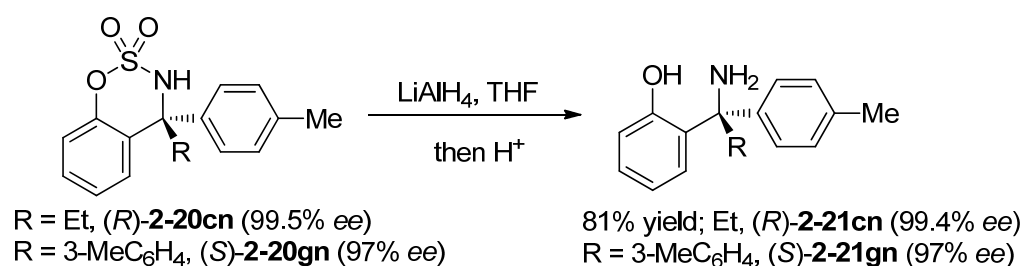
	2-18, additive	Ar ² B(OH) ₂ 2-19	2-20, yield [%] ^[b]	ee [%] ^[c]
1	2-18e , -		2-20ep , 75	0
2	2-18e , K ₃ PO ₄	2-19p	2-20ep , 73	0
3	2-18e , K ₂ CO ₃		2-20ep , 70	0
4	2-18e , NEt ₃		2-20ep , 63	81
5	2-18e , proton sponge		2-20ep , 80	99.2
6	2-18f , proton sponge		2-20fp , 65	99.6
		2-19p		
7	2-18g , proton sponge		2-20gp , 75	96
		2-19p		
8	2-18g , proton sponge		2-20gn , 68	97
		2-19n		

[a] Reaction conditions: **1** (0.10 mmol), **2** (0.20 mmol), PdCl₂[(*S*)-*i*Pr-phox] (10 mol%), AgSbF₆ (30 mol%), additive (30 mol%), dichloroethane (1.0 mL) at 65–70 °C for 12 h. [b] Isolated yield. [c]

Determined by HPLC analysis with chiral columns.

2.2.4 Derivation

Treatment of the asymmetric arylation products **2-20cn** and **2-20gn** with LiAlH_4 gave the corresponding 2-hydroxyphenylmethyamines **2-21cn** and **2-21gn**, respectively, without loss of their enantiomeric purities (Scheme 2.6).^[7b]



Scheme 2.6 Ring-opening of the asymmetric arylation products **2-20**

2.3 Conclusions

To summarize, a cationic palladium complex coordinated with chiral phosphine-oxazoline ligand (*i*Pr-phox) showed high catalytic activity and enantioselectivity in the asymmetric addition of arylboronic acids to 6-membered cyclic *N*-sulfonyl ketimines to give high yields of chiral cyclic sulfamidates with 96–99.9% ee which bear tetra-substituted stereogenic center.

2.4 Experimental section

2.4.1. General Information

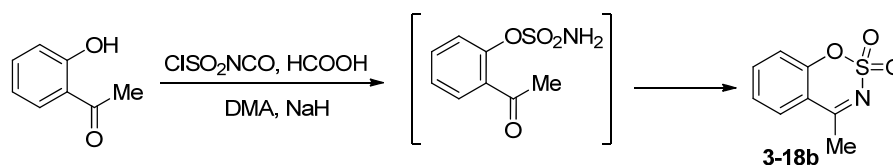
All the starting materials were obtained from commercial sources and used without further purification unless otherwise stated. THF was dried and distilled

from sodium benzophenone ketyl prior to use. DME and CH₂Cl₂ were distilled from CaH₂ prior to use. ¹H and ¹³C NMR spectra were recorded on a Bruker AMX500 (500 MHz) spectrometer. Chemical shifts were reported in parts per million (ppm), and the residual solvent peak was used as an internal reference: proton (chloroform δ 7.26), carbon (chloroform δ 77.0). Multiplicity was indicated as follows: s (singlet), d (doublet), t (triplet), q (quartet), m (multiplet), dd (doublet of doublet), and br s (broad singlet). Coupling constants were reported in Hertz (Hz). Low resolution mass spectra were obtained on a Finnigan/MAT LCQ spectrometer in ESI mode, and a Agilent Tech. 5975C inert MSD. All high resolution mass spectra were obtained on a Finnigan/MAT 95XL-T spectrometer. For thin layer chromatography (TLC), Merck pre-coated TLC plates (Merck 60 F254) were used, and compounds were visualized with a UV light at 254 nm. Further visualization was achieved by staining with iodine, or ceric ammonium molybdate followed by heating on a hot plate. Flash chromatographic separations were performed on Merck 60 (0.040-0.063 mm) mesh silica gel. The Enantiomerically excesses of products were determined by chiral-phase HPLC analysis, using a Daicel Chiralpak IC column (250 x 4.6 mm), Chiralpak AD-H column (250 x 4.6 mm), or Chiralcel OD-H column (250 x 4.6 mm).

All the aryboronic acids are commercially available and used as received. The palladium complex PdCl₂[(*S*)-*i*Pr-phox]^[76a] was prepared from PdCl₂(MeCN)₂ and (*S*)-*i*Pr-phox (CAS: 148461-14-7, Strem Chemicals Inc.) in benzene according to the reported procedure.^[76a]

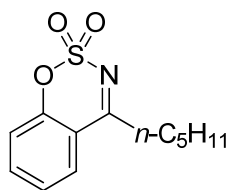
2.4.2 Ketimines

All the cyclic *N*-sulfonyl ketimines **2-18a-g** were prepared according to the literature procedures.^[72b] A typical procedure is given for the synthesis of **2-18b**.

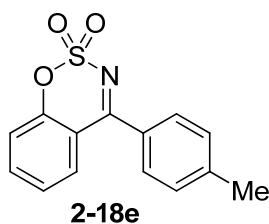


The preparation of cyclic ketimine 2-18b: Anhydrous formic acid (20.0 mmol, 921 mg, 0.75 mL) was added dropwise to neat chlorosulfonyl isocyanate (20.0 mmol, 2.83 g, 1.74 mL) at 0 °C with rapid stirring. Vigorous gas evolution was observed during the addition process. The resulting viscous suspension was stirred at room temperature until gas evolution ceased (1-2 h). To the resulting sulfamoyl chloride (ClSO₂NH₂) was added 2'-hydroxyacetophenone (10.0 mmol). After the mixture was cooled under ice-cooling, 15 mL of DMA (N,N-dimethyl-acetamide) was slowly added. Caution: a mild exotherm was noted upon combining these reagents. After the ice-cooling was removed, the mixture was stirred for 10 min, and sodium hydride (480 mg of 60% dispersion in mineral oil, 12.0 mmol) was added in portions. After stirring at rt for 30 min, another sodium hydride (480 mg of 60% dispersion in mineral oil, 12.0 mmol) was added in portions again. After stirring for 1 hour at rt the reaction mixture was allowed to stir overnight (8-12 h) at 50 °C. The reaction was quenched by the addition of H₂O and the aqueous layer was extracted with EtOAc. The combined organic layers were washed with brine, and concentrated under reduced pressure. The residue was purified by chromatography on silica gel (hexane/ethyl acetate = 3/1) to give compound **2-18b** as a colorless solid (1.13 g, 57% yield).

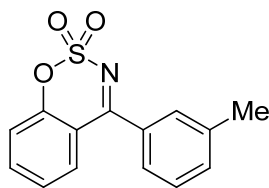
The ketimines, **2-18d**, **2-18e**, and **2-18g**, are new compounds. Their analytical data are shown below.

**2-18d**

Compound 2-18d. 53% yield; A colorless oil. ¹H NMR (500 MHz, CDCl₃) δ 7.81 (dd, *J* = 8.0, 1.5 Hz, 1H), 7.70 (td, *J* = 7.5, 1.6 Hz, 1H), 7.68 (td, *J* = 7.6, 1.6 Hz, 1H), 7.30 (dd, *J* = 8.3, 0.9 Hz, 1H), 2.02 (t, *J* = 7.5 Hz, 2H), 1.83 (quintet, *J* = 7.5 Hz, 2H), 1.47–1.33 (m, 4H), 0.93 (t, *J* = 7.2 Hz, 3H). ¹³C NMR (125 MHz, CDCl₃) δ 180.3, 152.6, 136.8, 127.9, 125.8, 119.3, 116.2, 35.9, 31.2, 25.7, 22.3, 12.9. HRMS (ESI) *m/z* calcd for C₁₂H₁₅NO₃S (M-H) 252.0695, found 252.0700.

**2-18e**

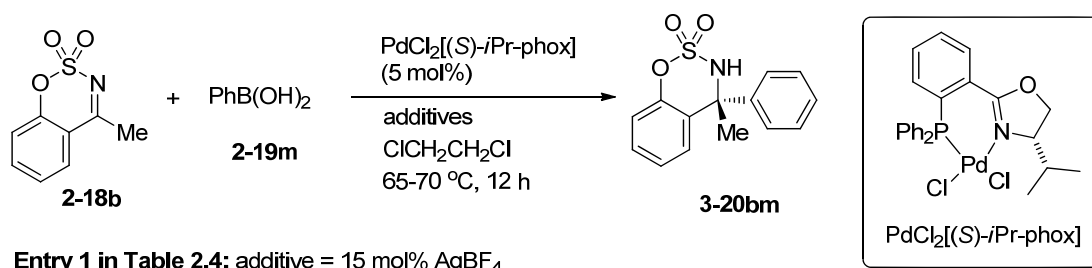
Compound 2-18e. 45% yield; A colorless solid. ¹H NMR (500 MHz, CDCl₃) δ 7.74 (td, *J* = 7.5, 1.6 Hz, 1H), 7.68 (d, *J* = 8.2 Hz, 2H), 7.67 (dd, *J* = 7.9, 1.6 Hz, 1H), 7.40 (d, *J* = 8.4 Hz, 1H), 7.37 (d, *J* = 8.0 Hz, 2H), 7.37 (td, *J* = 7.3, 1.1 Hz, 1H), 2.49 (s, 3H). ¹³C NMR (125 MHz, CDCl₃) δ 176.2, 154.6, 144.4, 136.7, 131.8, 130.9, 130.8, 129.6, 125.5, 119.4, 116.7, 21.7. HRMS (EI) *m/z* calcd for C₁₄H₁₁NO₃S 272.0460, found 272.0455.

**2-18g**

Compound 2-18g. 37% yield; A colorless solid. ^1H NMR (500 MHz, CDCl_3) δ 7.75 (td, $J = 7.9, 1.5$ Hz, 1H), 7.66 (dd, $J = 7.9, 1.4$ Hz, 1H), 7.61 (s, 1H), 7.53 (d, $J = 7.5$ Hz, 1H), 7.49 (d, $J = 7.6$ Hz, 1H), 7.45 (d, $J = 7.5$ Hz, 1H), 7.41 (t, $J = 6.8$ Hz, 1H), 7.38 (td, $J = 7.4, 1.0$ Hz, 1H), 2.46 (s, 3H). ^{13}C NMR (125 MHz, CDCl_3) δ 176.5, 154.6, 139.0, 136.8, 134.0, 132.7, 131.8, 130.9, 128.6, 127.9, 125.6, 119.4, 116.7, 21.4. HRMS (EI) m/z calcd for $\text{C}_{14}\text{H}_{11}\text{NO}_3\text{S}$ 272.0460, found 272.0458.

2.4.3 Palladium-Catalyzed Asymmetric Arylation of Ketimines

As representative experimental procedures, those for entries 1 and 2 in Table 2.4 and entry 5 in Table 2.6, are shown below.



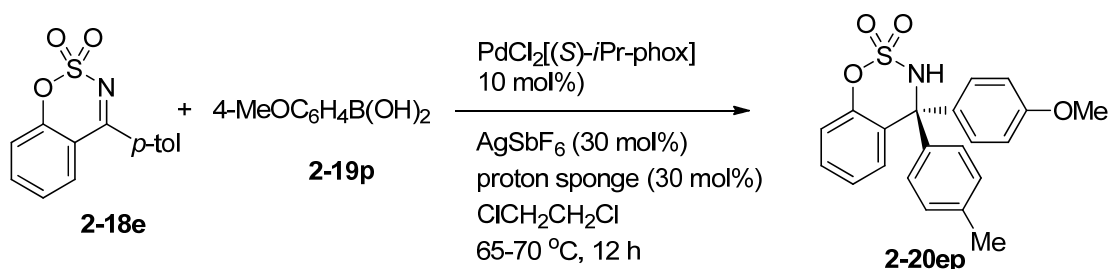
Entry 1 in Table 2.4: additive = 15 mol% AgBF_4

Entry 2 in Table 2.4: additive = 15 mol% AgSbF_6 and 15 mol% K_3PO_4

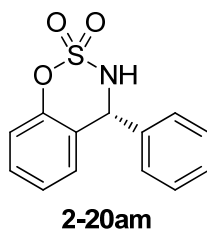
Entry 2 in Table 2.4: $\text{PdCl}_2[(S)\text{-}i\text{Pr-phox}]$ (2.9 mg, 0.0050 mmol), ketimine **2-18b** (19.7 mg, 0.100 mmol), and benzeneboronic acid (**2-19m**) (24.4 mg, 0.200 mmol) were placed in Schlenk tube under nitrogen. To the tube, 1,2-dichloroethane (0.5 mL) was added, and then AgBF_4 (2.9 mg, 0.015 mmol) in 1,2-dichloroethane (0.5 mL) was added. The reaction mixture was stirred at 65–70 °C for 12 h, and the mixture was

directly subjected to flash chromatography on silica gel using hexane/ethyl acetate (4:1) as an eluent to give **2-20bm** as a colorless solid (27.2 mg, 99% yield).

Entry 2 in Table 2.4: PdCl₂[(*S*)-*i*Pr-phox] (2.9 mg, 0.005 mmol), ketimine **2-18b** (19.7 mg, 0.100 mmol), benzeneboronic acid (**2-19m**) (24.4 mg, 0.200 mmol), and K₃PO₄ (2.2 mg, 0.015 mmol) were placed in Schlenk tube under nitrogen. To the tube, 1,2-dichloroethane (0.5 mL) was added, and then AgSbF₆ (5.2 mg, 0.015 mmol) in 1,2-dichloroethane (0.5 mL) was added dropwise to the resulting mixture over 1 min. The reaction mixture was stirred at 65–70 °C for 12 h, and it was directly subjected to flash chromatography on silica gel using hexane/ethyl acetate (4:1) as an eluent to give **2-20bm** as a colorless solid (27.3 mg, 99% yield).

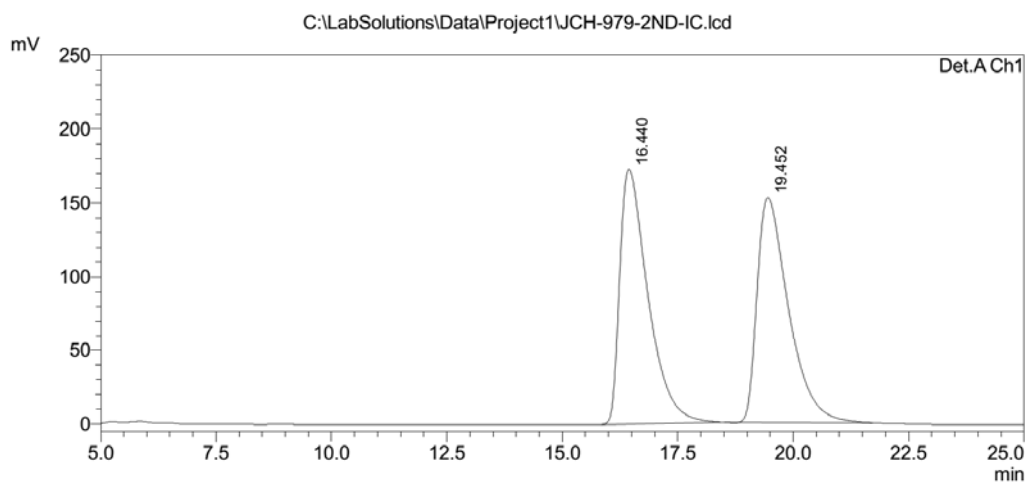


Entry 5 in Table 2.6: PdCl₂[(*S*)-*i*Pr-phox] (5.8 mg, 0.010 mmol), ketimine **2-18e** (27.3 mg, 0.100 mmol), 4-methoxyphenylboronic acid (**2-19p**) (60.8 mg, 0.400 mmol), and proton sponge (6.4 mg, 0.030 mmol) were placed in Schlenk tube under nitrogen. To the tube, 1,2-dichloroethane (0.5 mL) was added, and then AgSbF₆ (10.3 mg, 0.030 mmol) in 1,2-dichloroethane (0.5 mL) was added dropwise to the resulting mixture over 1 min. The reaction mixture was stirred at 65–70 °C for 12 h, and it was directly subjected to flash chromatography on silica gel using hexane/ethyl acetate (5:1) as an eluent to give **2-20ep** as a colorless solid (30.4 mg, 80% yield).



Compound 2-20am. A colorless solid. $[\alpha]_D^{25} +17$ (*c* 0.51, CHCl_3). [Ref.^[72b]: **98% ee**, $[\alpha]_D^{25} -24.2$ (*c* 0.60, CHCl_3), ***S* configuration**]. ^1H NMR (500 MHz, CDCl_3) δ 7.49–7.41 (m, 3H), 7.38–7.30 (m, 3H), 7.10 (td, *J* = 7.6, 1.0 Hz, 1H), 7.08 (d, *J* = 8.2 Hz, 1H), 6.83 (d, *J* = 7.7 Hz, 1H), 5.91 (d, *J* = 8.7 Hz, 1H), 4.72 (d, *J* = 8.5 Hz, 1H). ^{13}C NMR (125 MHz, CDCl_3) δ 151.5, 137.8, 129.7, 129.6, 129.5, 128.8, 128.6, 125.2, 122.0, 118.8, 62.0. The *ee* value was 99.6%, t_R (major) = 16.6 min, t_R (minor) = 20.2 min (Chiralpak IC, λ = 220 nm, hexane/*i*-PrOH = 9/1, flow rate = 1.0 mL/min). HRMS (ESI) *m/z* calcd for $\text{C}_{13}\text{H}_{11}\text{NO}_3\text{S}$ (M-H)⁻ 260.0387, found 260.0392.

<Chromatogram>

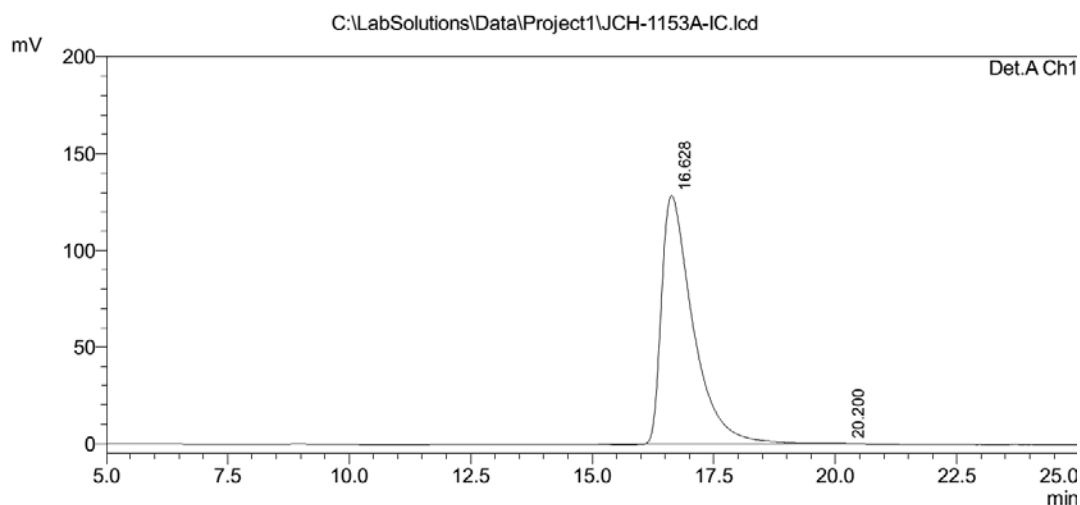


PeakTable

Detector A Ch1 220nm					
Peak#	Ret. Time	Area	Height	Area %	Height %
1	16.440	7326804	172619	50.254	53.075
2	19.452	7252879	152615	49.746	46.925
Total		14579683	325234	100.000	100.000

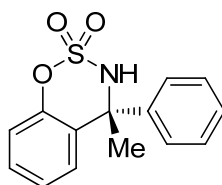
Racemic **2-20am**

<Chromatogram>



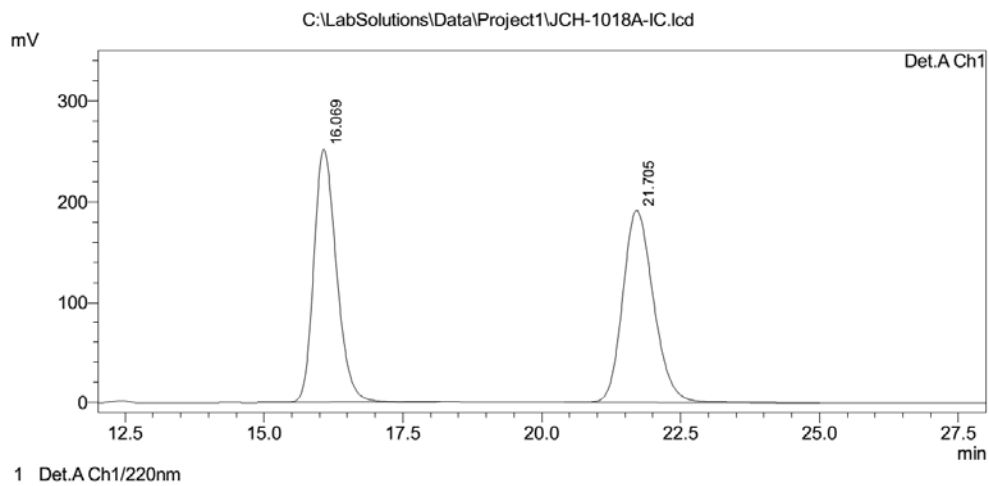
PeakTable

Peak#	Ret. Time	Area	Height	Area %	Height %
1	16.628	5875045	128984	99.814	99.627
2	20.200	10939	483	0.186	0.373
Total		5885984	129468	100.000	100.000

Enantiomerically enriched **2-20am****2-20bm**

Compound 2-20bm. A colorless solid. $[\alpha]_D^{25} +18$ (c 0.46, CHCl_3). [Ref.^[66]: 95% ee, $[\alpha]_D^{25} +12.7$ (c 0.18, CHCl_3), *R* configuration]. ^1H NMR (500 MHz, CDCl_3) δ 7.40–7.32 (m, 6H), 7.18 (td, $J = 7.7, 1.2$ Hz, 1H), 7.12 (dd, $J = 8.2, 1.2$ Hz, 1H), 7.02 (dd, $J = 7.9, 1.6$ Hz, 1H), 4.86 (s, 1H), 2.16 (s, 3H). ^{13}C NMR (125 MHz, CDCl_3) δ 150.2, 142.6, 129.5, 128.9, 128.7, 128.6, 127.4, 126.7, 125.5, 119.4, 65.3, 28.9. The ee value was 99.6%, t_R (minor) = 15.7 min, t_R (major) = 21.2 min (Chiralpak IC, $\lambda = 220$ nm, hexane/*i*-PrOH = 9/1, flow rate = 1.0 mL/min). HRMS (ESI) m/z calcd for $\text{C}_{14}\text{H}_{13}\text{NO}_3\text{S}$ (M-H)⁻ 274.0543, found 274.0540.

<Chromatogram>



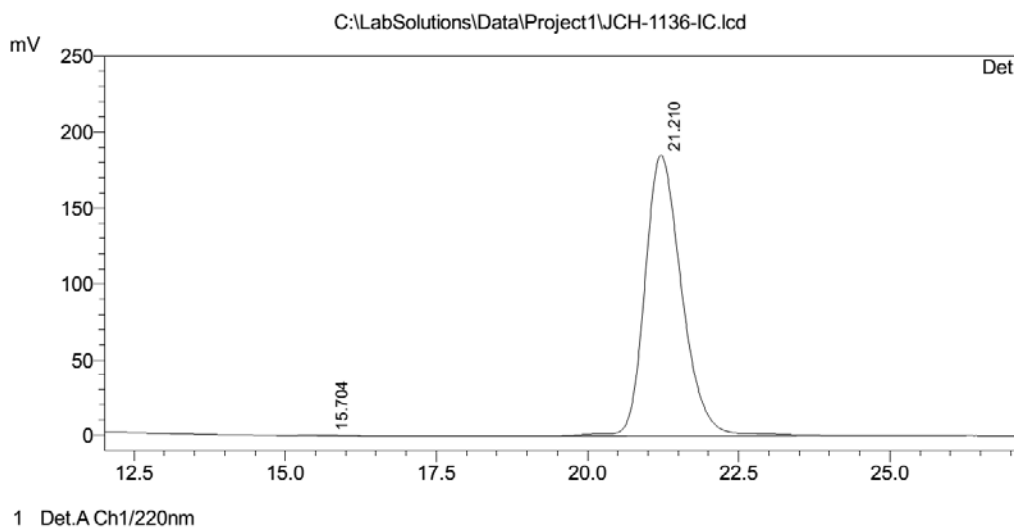
PeakTable

Detector A Ch1 220nm

Peak#	Ret. Time	Area	Height	Area %	Height %
1	16.069	7147279	251915	49.109	56.791
2	21.705	7406643	191671	50.891	43.209
Total		14553922	443586	100.000	100.000

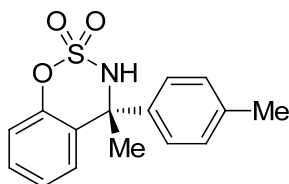
Racemic 2-20bm

<Chromatogram>



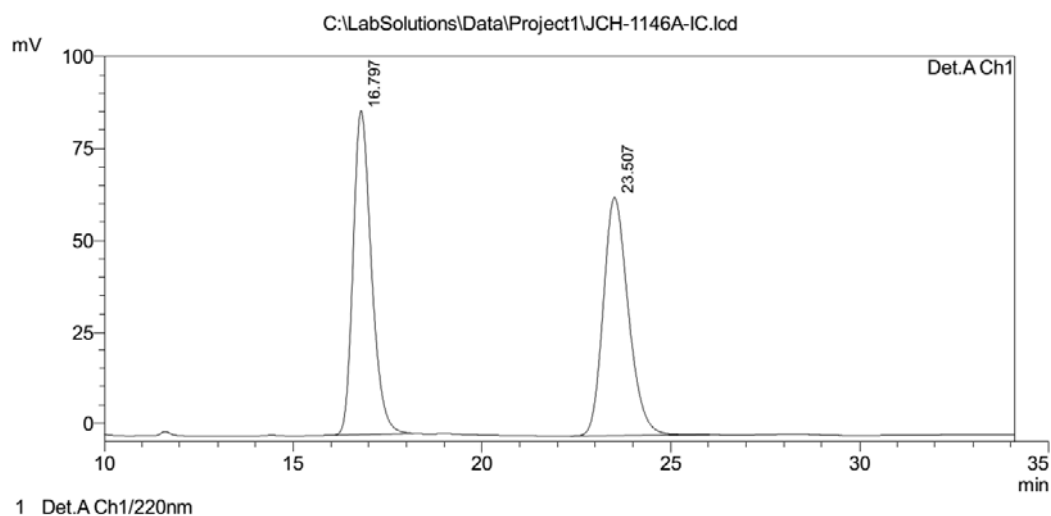
Peak Table

Detector A Ch1 220nm					
Peak#	Ret. Time	Area	Height	Area %	Height %
1	15.704	16309	355	0.207	0.191
2	21.210	7880322	184958	99.793	99.809
Total		7896632	185313	100.000	100.000

Enantiomerically enriched **2-20bm****2-20bn**

Compound 2-20bn. A colorless solid. $[\alpha]_D^{25} +17$ (c 0.57, CHCl_3). ^1H NMR (500 MHz, CDCl_3) δ 7.33 (td, $J = 7.5, 1.4$ Hz, 1H), 7.23 (d, $J = 8.2$ Hz, 2H), 7.17 (d, $J = 7.3$ Hz, 2H), 7.16 (t, $J = 6.4$ Hz, 1H), 7.10 (d, $J = 8.3$ Hz, 1H), 7.00 (d, $J = 7.9$ Hz, 1H), 4.86 (s, 1H), 2.34 (s, 3H), 2.14 (s, 3H). ^{13}C NMR (125 MHz, CDCl_3) δ 150.1, 140.7, 138.5, 129.5, 129.4, 128.6, 127.5, 126.6, 125.5, 119.3, 65.1, 28.8, 21.0. The ee value was 98.1%, t_R (minor) = 16.9 min, t_R (major) = 22.7 min (Chiralpak IC, $\lambda = 220$ nm, hexane/ i -PrOH = 9/1, flow rate = 1.0 mL/min). HRMS (ESI) m/z calcd for $\text{C}_{15}\text{H}_{15}\text{NO}_3\text{S}$ (M-H) $^-$ 288.0700, found 288.0701.

<Chromatogram>

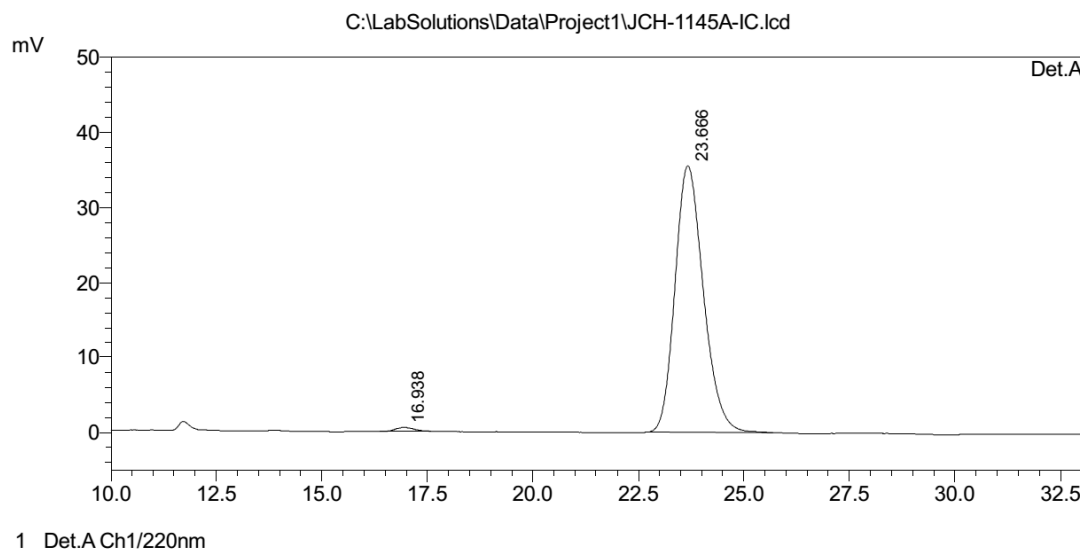


PeakTable

Peak#	Ret. Time	Area	Height	Area %	Height %
1	16.797	2977399	88318	49.790	57.625
2	23.507	3002564	64945	50.210	42.375
Total		5979963	153263	100.000	100.000

Racemic **2-20bn**

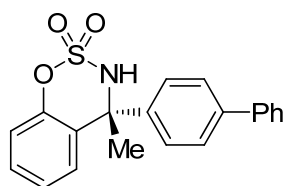
<Chromatogram>



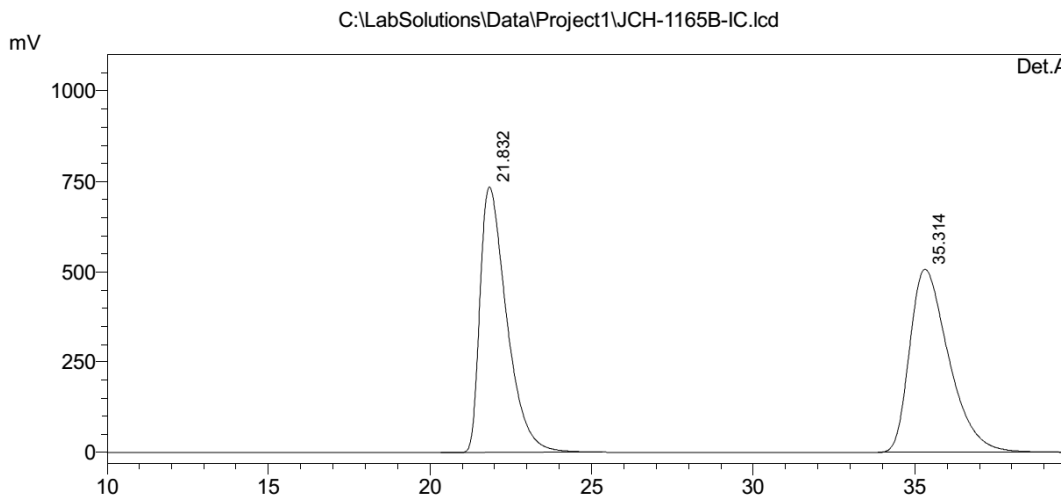
PeakTable

Peak#	Ret. Time	Area	Height	Area %	Height %
1	16.938	16108	523	0.960	1.451
2	23.666	1662347	35531	99.040	98.549
Total		1678455	36054	100.000	100.000

Enantiomerically enriched **2-20bn**

**2-20bo**

Compound 2-20bo. A colorless solid. $[\alpha]_D^{25} +6$ (c 0.83, CHCl_3). ^1H NMR (500 MHz, CDCl_3) δ 7.61–7.55 (m, 4H), 7.48–7.41 (m, 4H), 7.40–7.33 (m, 2H), 7.21 (td, $J = 7.7$, 1.2 Hz, 1H), 7.12 (dd, $J = 8.3$, 0.9 Hz, 1H), 7.10 (dd, $J = 7.9$, 1.5 Hz, 1H), 5.04 (s, 1H), 2.18 (s, 3H). ^{13}C NMR (125 MHz, CDCl_3) δ 150.2, 142.4, 141.5, 140.0, 129.6, 128.8, 128.6, 127.7, 127.5, 127.3, 127.2, 127.1, 125.6, 119.4, 65.1, 29.0. The *ee* value was 98.8%, t_R (minor) = 22.1 min, t_R (major) = 35.6 min (Chiralpak IC, $\lambda = 254$ nm, hexane/*i*-PrOH = 9/1, flow rate = 1.0 mL/min). HRMS (ESI) m/z calcd for $\text{C}_{20}\text{H}_{17}\text{NO}_3\text{S}$ (M-H) $^-$ 350.0856, found 350.0857.

<Chromatogram>

1 Det.A Ch1/254nm

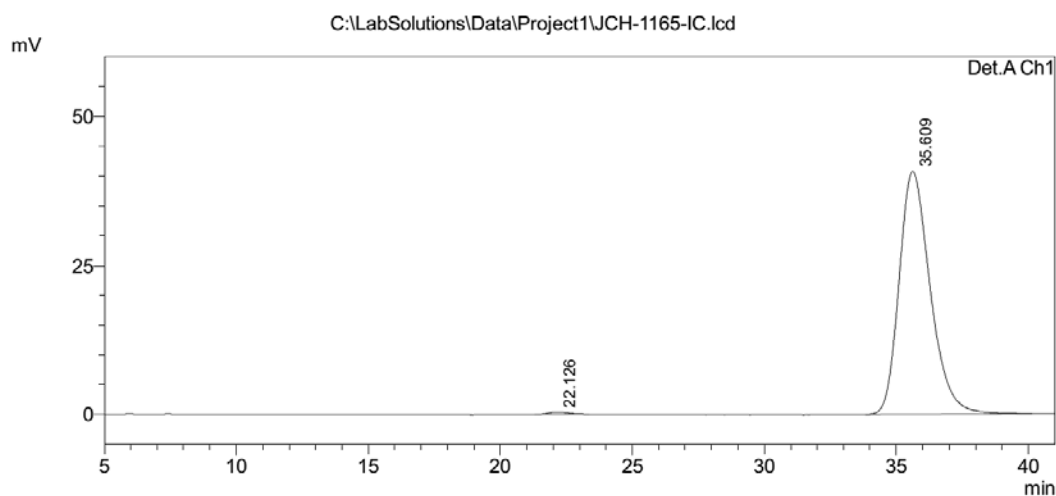
Peak Table

Detector A Ch1 254nm

Peak#	Ret. Time	Area	Height	Area %	Height %
1	21.832	42214379	735078	49.672	59.143
2	35.314	42772544	507799	50.328	40.857
Total		84986923	1242877	100.000	100.000

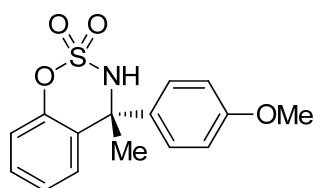
Racemic 2-20bo

<Chromatogram>



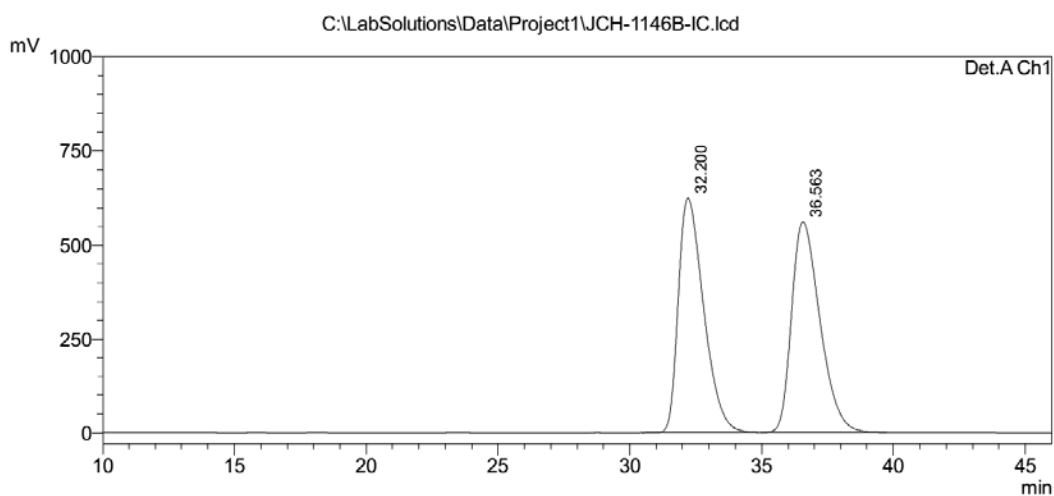
PeakTable

Peak#	Ret. Time	Area	Height	Area %	Height %
1	22.126	21065	399	0.628	0.970
2	35.609	3334911	40723	99.372	99.030
Total		3355976	41122	100.000	100.000

Enantiomerically enriched **2-20bo****2-20bp**

Compound 2-20bp. A colorless solid. $[\alpha]_D^{25} +20$ (c 0.53, CHCl_3). ^1H NMR (500 MHz, CDCl_3) δ 7.33 (td, $J = 7.5, 1.5$ Hz, 1H), 7.26 (d, $J = 8.8$ Hz, 2H), 7.16 (td, $J = 7.5, 1.1$ Hz, 1H), 7.10 (d, $J = 8.2$ Hz, 1H), 7.00 (dd, $J = 7.9, 1.5$ Hz, 1H), 6.86 (d, $J = 8.9$ Hz, 2H), 4.86 (s, 1H), 2.80 (s, 3H), 2.13 (s, 3H). ^{13}C NMR (125 MHz, CDCl_3) δ 159.5, 150.1, 135.7, 129.4, 128.6, 128.1, 127.6, 125.5, 119.3, 114.0, 64.9, 55.3, 28.9. The *ee* value was 99.9%, t_R (minor) = 31.3 min, t_R (major) = 37.3 min (Chiralpak IC, $\lambda = 220$ nm, hexane/*i*-PrOH = 9/1, flow rate = 1.0 mL/min). HRMS (ESI) m/z calcd for $\text{C}_{15}\text{H}_{15}\text{NO}_4\text{S}$ (M-H) $^-$ 304.0649, found 304.0655.

<Chromatogram>



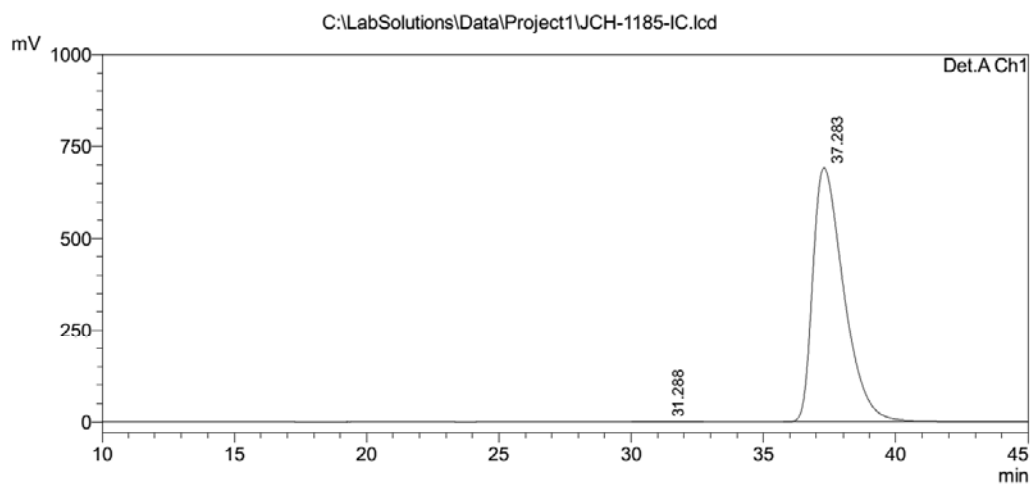
PeakTable

Detector A Ch1 220nm

Peak#	Ret. Time	Area	Height	Area %	Height %
1	32.200	41806336	624360	49.844	52.636
2	36.563	42067388	561818	50.156	47.364
Total		83873724	1186178	100.000	100.000

Racemic 2-20bp

<Chromatogram>

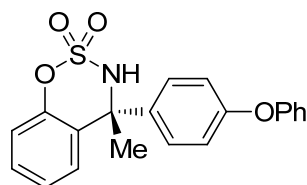


PeakTable

Detector A Ch1 220nm

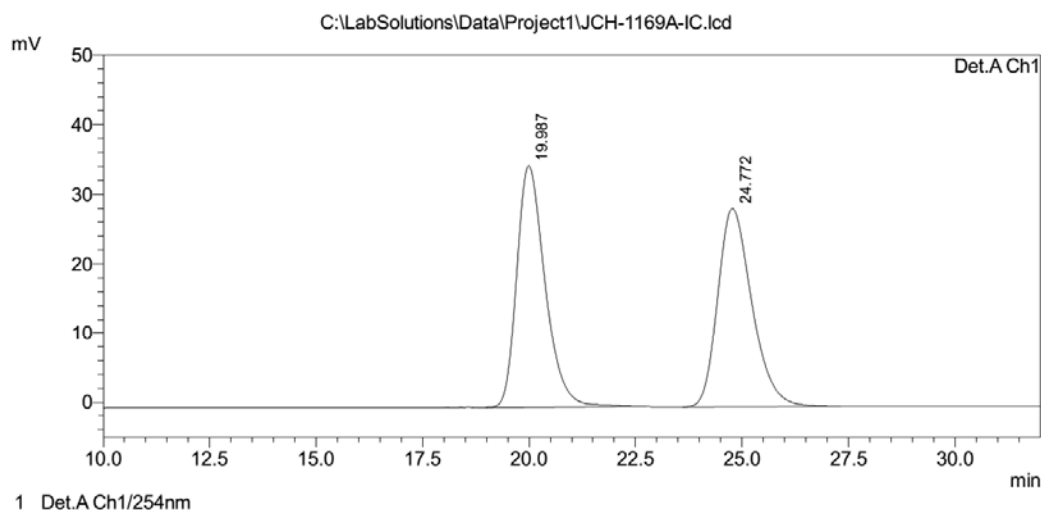
Peak#	Ret. Time	Area	Height	Area %	Height %
1	31.288	24077	397	0.043	0.057
2	37.283	56411249	692320	99.957	99.943
Total		56435326	692717	100.000	100.000

Enantiomerically enriched 2-20bp

**2-20bq**

Compound 2-20bq. A colorless solid. $[\alpha]_D^{25} +9$ (*c* 0.63, CHCl₃). ¹H NMR (500 MHz, CDCl₃) δ 7.38–7.32 (m, 3H), 7.29 (d, *J* = 8.8 Hz, 2H), 7.19 (t, *J* = 7.2 Hz, 1H), 7.14 (t, *J* = 7.4 Hz, 1H), 7.10 (d, *J* = 8.2 Hz, 1H), 7.06 (dd, *J* = 7.9, 1.4 Hz, 1H), 7.02 (d, *J* = 7.8 Hz, 2H), 6.95 (d, *J* = 8.8 Hz, 2H), 4.98 (s, 1H), 2.13 (s, 3H). ¹³C NMR (125 MHz, CDCl₃) δ 157.7, 156.2, 150.2, 137.9, 129.9, 129.6, 128.6, 128.3, 127.3, 125.5, 122.9, 119.5, 119.4, 118.3, 64.9, 29.2. The *ee* value was 98.6 %, *t_R* (minor) = 20.5 min, *t_R* (major) = 25.3 min (Chiralpak IC, λ = 254 nm, hexane/*i*-PrOH = 9/1, flow rate = 1.0 mL/min). HRMS (ESI) *m/z* calcd for C₂₀H₁₇NO₄S (M-H)⁻ 366.0806, found 366.0802.

<Chromatogram>

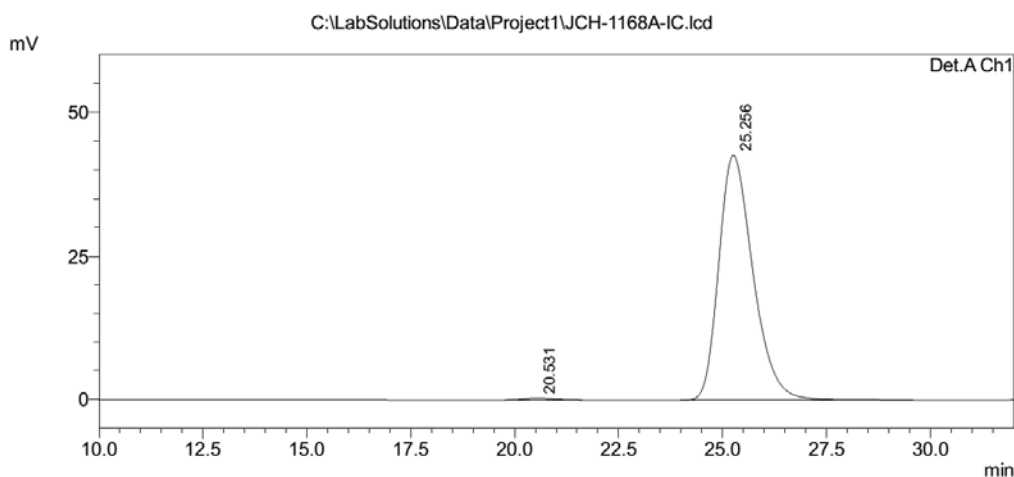


PeakTable

Peak#	Ret. Time	Area	Height	Area %	Height %
1	19.987	1612973	34809	50.135	54.857
2	24.772	1604294	28645	49.865	45.143
Total		3217268	63454	100.000	100.000

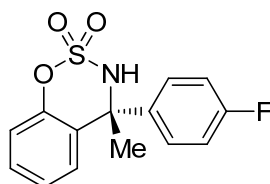
Racemic 2-20bp

<Chromatogram>



PeakTable

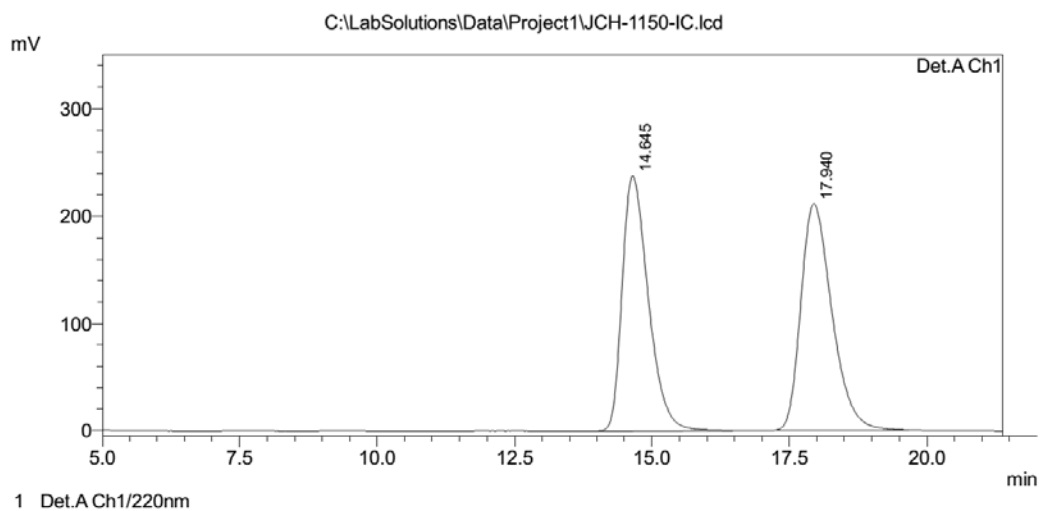
Peak#	Ret. Time	Area	Height	Area %	Height %
1	20.531	17295	346	0.699	0.803
2	25.256	2457956	42705	99.301	99.197
Total		2475251	43050	100.000	100.000

Enantiomerically enriched **2-20bq****2-20br**

Compound 2-20br. A colorless solid. $[\alpha]_D^{25} +34$ (c 0.68, CHCl_3). ^1H NMR (500 MHz, CDCl_3) δ 7.36 (td, $J = 7.9, 1.7$ Hz, 1H), 7.33 (dd, $J = 9.0, 5.2$ Hz, 2H), 7.21 (td, $J = 7.7, 1.2$ Hz, 1H), 7.09 (dd, $J = 7.3, 1.1$ Hz, 1H), 7.07 (dd, $J = 7.8, 1.4$ Hz, 1H), 7.04 (t, $J = 8.6$ Hz, 2H), 5.08 (s, 1H), 2.10 (s, 3H). ^{13}C NMR (125 MHz, CDCl_3) δ 162.4 (d, $J_{\text{F-C}} = 249$ Hz), 150.1, 139.2 (d, $J_{\text{F-C}} = 3$ Hz), 129.7, 128.7 (d, $J_{\text{F-C}} = 8$ Hz), 128.4, 127.0, 125.6, 119.5, 115.6 (d, $J_{\text{F-C}} = 22$ Hz), 64.7, 29.6. The ee value was 98.4%, t_R (minor) = 14.8 min, t_R (major) = 18.0 min (Chiralpak IC, $\lambda = 220$ nm, hexane/ i -PrOH = 9/1, flow rate = 1.0 mL/min). HRMS (ESI) m/z calcd for $\text{C}_{14}\text{H}_{11}\text{NFO}_3\text{S}$ (M-H) $^-$

292.0449, found 292.0450.

<Chromatogram>



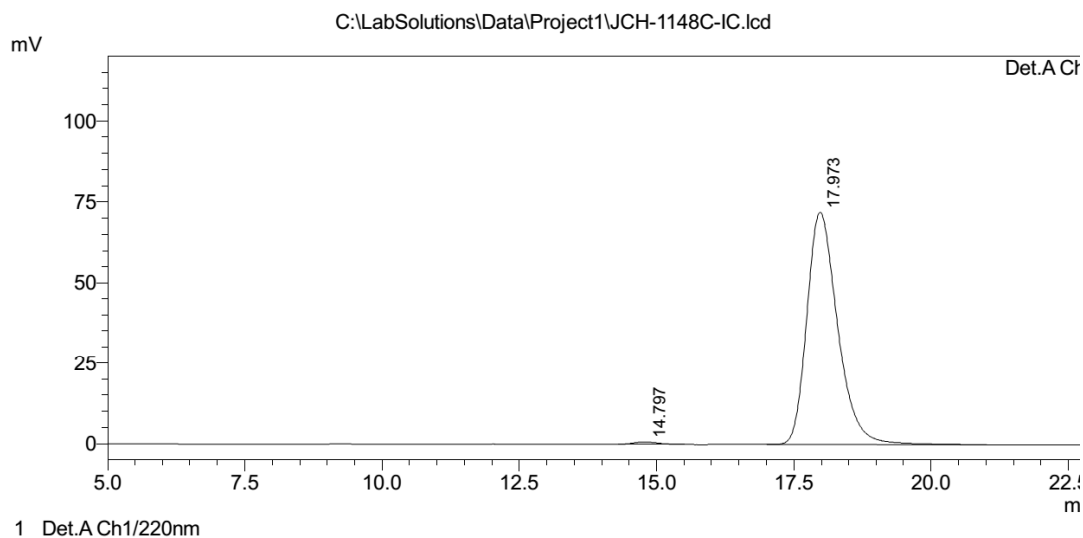
PeakTable

Detector A Ch1 220nm

Peak#	Ret. Time	Area	Height	Area %	Height %
1	14.645	7869187	237742	48.658	52.960
2	17.940	8303417	211165	51.342	47.040
Total		16172603	448906	100.000	100.000

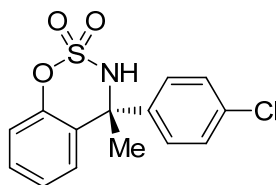
Racemic 2-20br

<Chromatogram>



PeakTable

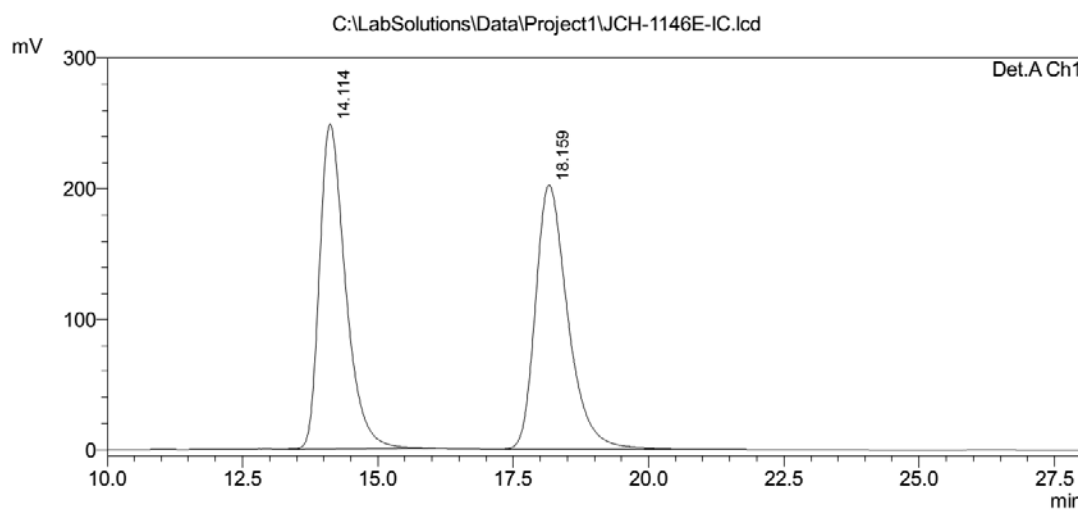
Peak#	Ret. Time	Area	Height	Area %	Height %
1	14.797	23492	758	0.827	1.041
2	17.973	2818026	72098	99.173	98.959
Total		2841518	72856	100.000	100.000

Enantiomerically enriched **2-20br****2-20bs**

Compound 2-20bs. A colorless solid. $[\alpha]_D^{25} +27$ (c 0.53, CHCl_3). ^1H NMR (500 MHz, CDCl_3) δ 7.37 (td, $J = 7.8, 1.6$ Hz, 1H), 7.32 (d, $J = 8.8$ Hz, 2H), 7.28 (d, $J = 8.8$ Hz, 2H), 7.22 (td, $J = 7.7, 1.2$ Hz, 1H), 7.11 (dd, $J = 8.3, 1.1$ Hz, 1H), 7.07 (dd, $J = 7.9, 1.5$ Hz, 1H), 4.95 (s, 1H), 2.10 (s, 3H). ^{13}C NMR (125 MHz, CDCl_3) δ 150.2, 141.8, 134.5, 129.8, 128.9, 128.3, 128.2, 126.7, 125.6, 119.6, 64.7, 29.6. The *ee* value was 99.4%, t_R (minor) = 14.3 min, t_R (major) = 18.2 min (Chiralpak IC, $\lambda = 220$ nm, hexane/*i*-PrOH = 9/1, flow rate = 1.0 mL/min). HRMS (ESI) m/z calcd for

$C_{13}H_{12}ClNO_3S (M-H)^-$ 308.0154, found 308.0146.

<Chromatogram>



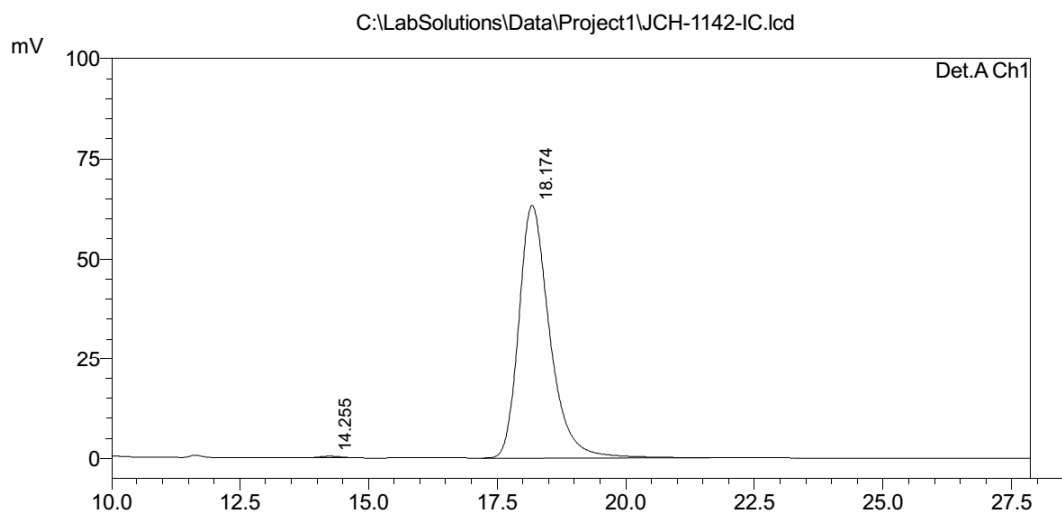
PeakTable

Detector A Ch1 220nm

Peak#	Ret. Time	Area	Height	Area %	Height %
1	14.114	8322337	248732	49.712	55.102
2	18.159	8418801	202667	50.288	44.898
Total		16741138	451399	100.000	100.000

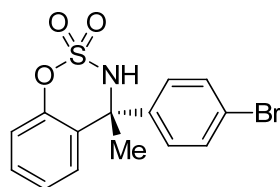
Racemic **2-20bs**

<Chromatogram>



PeakTable

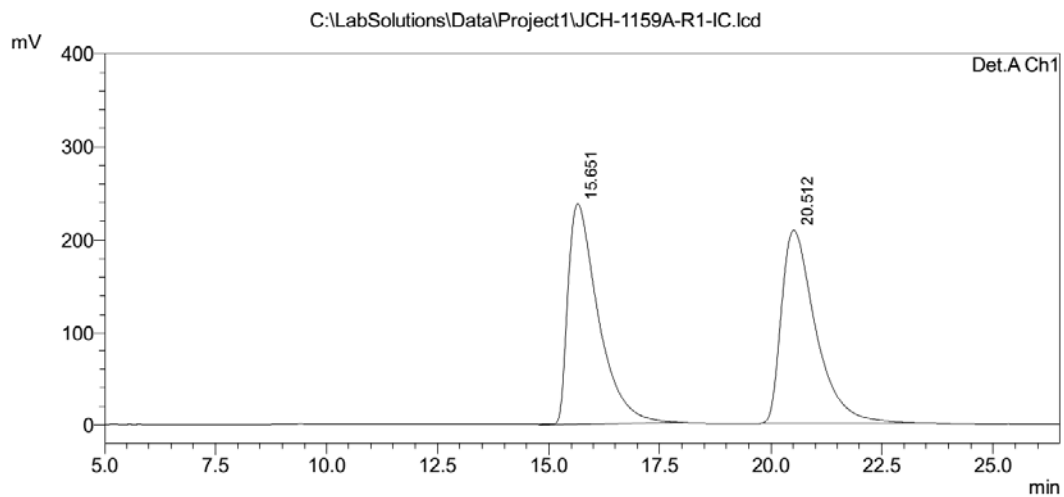
Peak#	Ret. Time	Area	Height	Area %	Height %
1	14.255	11572	403	0.436	0.632
2	18.174	2643826	63290	99.564	99.368
Total		2655399	63692	100.000	100.000

Enantiomerically enriched **2-20bs****2-20bt**

Compound 2-20bt. A colorless solid. $[\alpha]_D^{25} +23$ (c 0.71, CHCl_3). ^1H NMR (500 MHz, CDCl_3) δ 7.48 (d, J = 8.7 Hz, 2H), 7.37 (td, J = 7.5, 1.6 Hz, 1H), 7.22 (d, J = 8.6 Hz, 2H), 7.22 (td, J = 8.7, 1.2 Hz, 1H), 7.12 (dd, J = 8.3, 1.1 Hz, 1H), 7.06 (dd, J = 7.9, 1.5 Hz, 1H), 4.90 (s, 3H), 2.09 (s, 3H). ^{13}C NMR (125 MHz, CDCl_3) δ 150.2, 142.3, 131.9, 129.9, 128.5, 128.3, 126.6, 125.6, 122.8, 119.6, 64.8, 29.5. The ee value was 99.9%, t_R (minor) = 15.7 min, t_R (major) = 20.0 min (Chiralcel IC, λ = 220 nm, hexane/ i -PrOH = 9/1, flow rate = 1.0 mL/min). HRMS (ESI) m/z calcd for

$C_{14}H_{12}BrNO_3S (M-H)^-$ 351.9649, found 351.9644.

<Chromatogram>



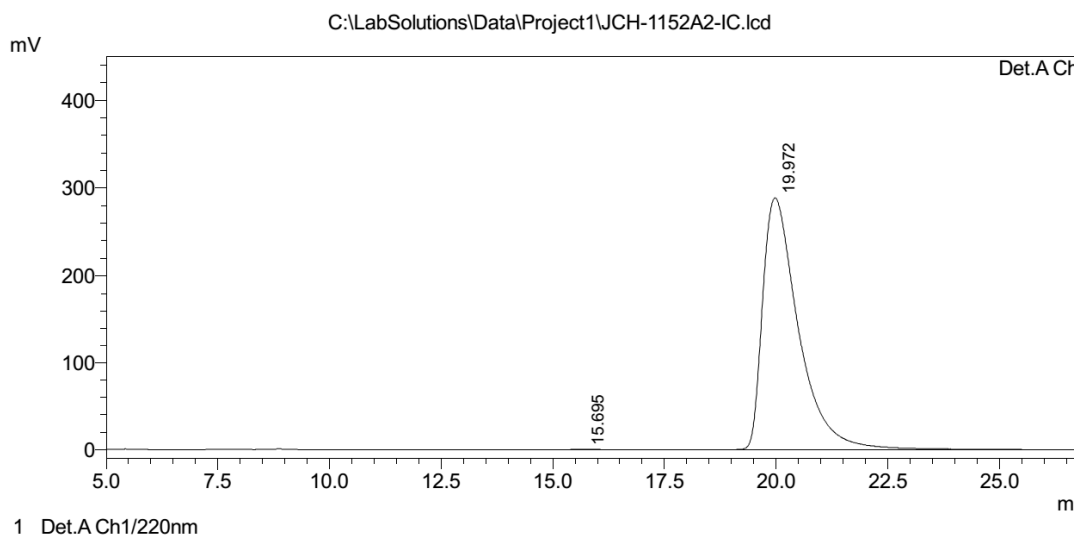
Detector A Ch1 220nm

PeakTable

Peak#	Ret. Time	Area	Height	Area %	Height %
1	15.651	11289997	237589	49.927	53.179
2	20.512	11322972	209181	50.073	46.821
Total		22612969	446770	100.000	100.000

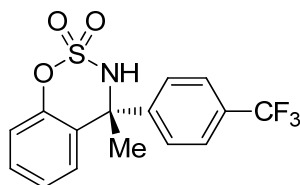
Racemic 2-20bt

<Chromatogram>



PeakTable

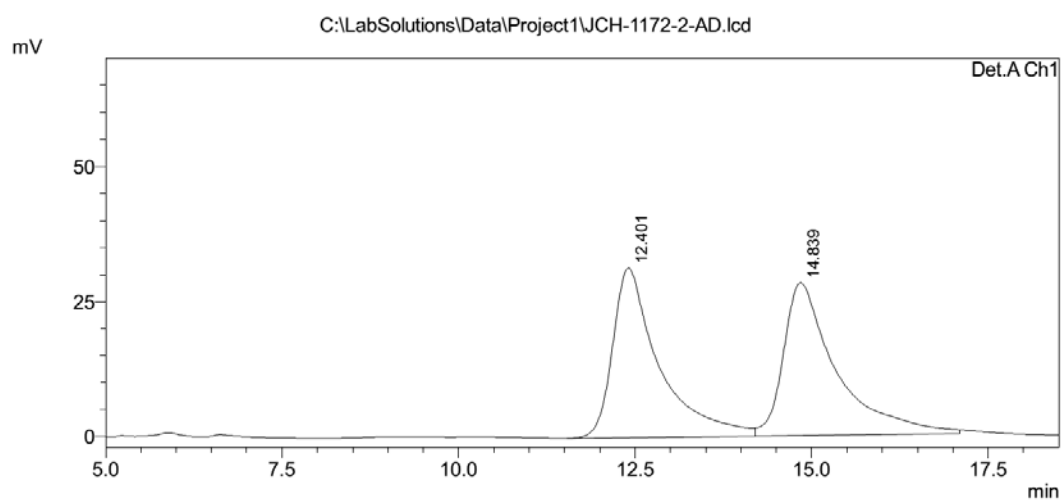
Detector A Ch1 220nm					
Peak#	Ret. Time	Area	Height	Area %	Height %
1	15.695	9682	283	0.060	0.098
2	19.972	16196350	288707	99.940	99.902
Total		16206032	288989	100.000	100.000

Enantiomerically enriched **2-20bt****2-20bu**

Compound 2-20bu. A colorless solid. $[\alpha]_D^{25} +63$ (c 0.34, CHCl_3). ^1H NMR (500 MHz, CDCl_3) δ 7.61 (d, $J = 8.4$ Hz, 2H), 7.49 (d, $J = 8.4$ Hz, 2H), 7.40 (td, $J = 8.1, 1.4$ Hz, 1H), 7.26 (td, $J = 7.7, 1.2$ Hz, 1H), 7.14 (dd, $J = 7.8, 1.5$ Hz, 1H), 7.12 (d, $J = 7.8$ Hz, 1H), 5.11 (s, 1H), 2.10 (s, 3H). ^{13}C NMR (125 MHz, CDCl_3) δ 150.3, 146.9, 130.6 (q, $J_{\text{F-C}} = 33$ Hz), 130.1, 128.3, 127.2, 126.3, 125.7, 125.7 (q, $J_{\text{F-C}} = 4$ Hz), 122.8 (q, $J_{\text{F-C}} = 272$ Hz), 119.7, 64.8, 30.0. The *ee* value was 99.4%, t_R (minor) = 12.3 min, t_R (major) = 17.0 min (Chiralpak AD-H, $\lambda = 220$ nm, hexane/*i*-PrOH = 9/1, flow rate = 1.0 mL/min). HRMS (ESI) m/z calcd for $\text{C}_{15}\text{H}_{11}\text{F}_3\text{NO}_3\text{S}$ (M-H) $^-$ 342.0417, found

342.0425.

<Chromatogram>

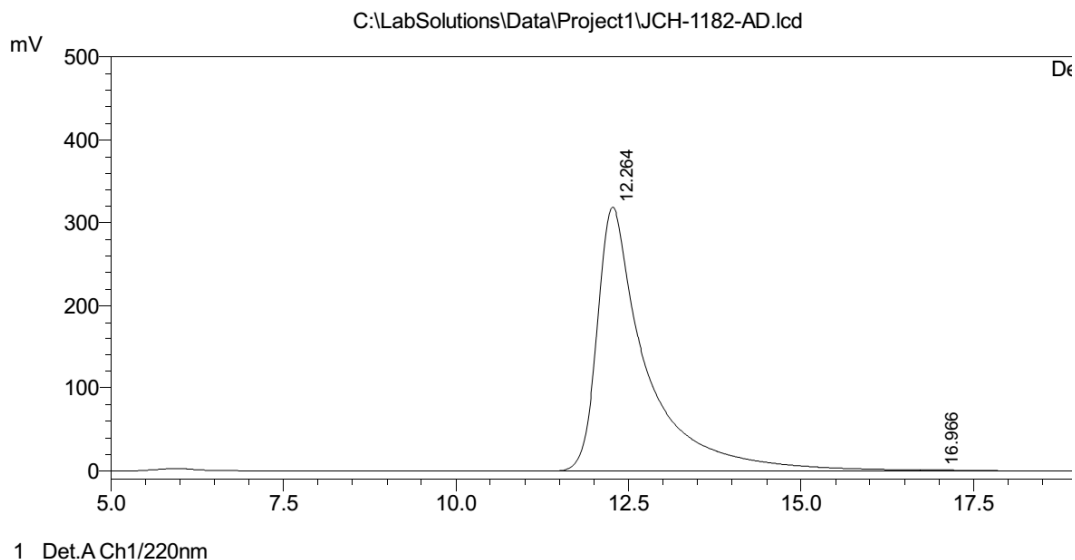


PeakTable

Peak#	Ret. Time	Area	Height	Area %	Height %
1	12.401	1441562	31491	49.348	52.585
2	14.839	1479662	28395	50.652	47.415
Total		2921225	59887	100.000	100.000

Racemic 2-20bu

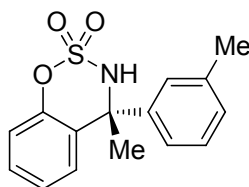
<Chromatogram>



PeakTable

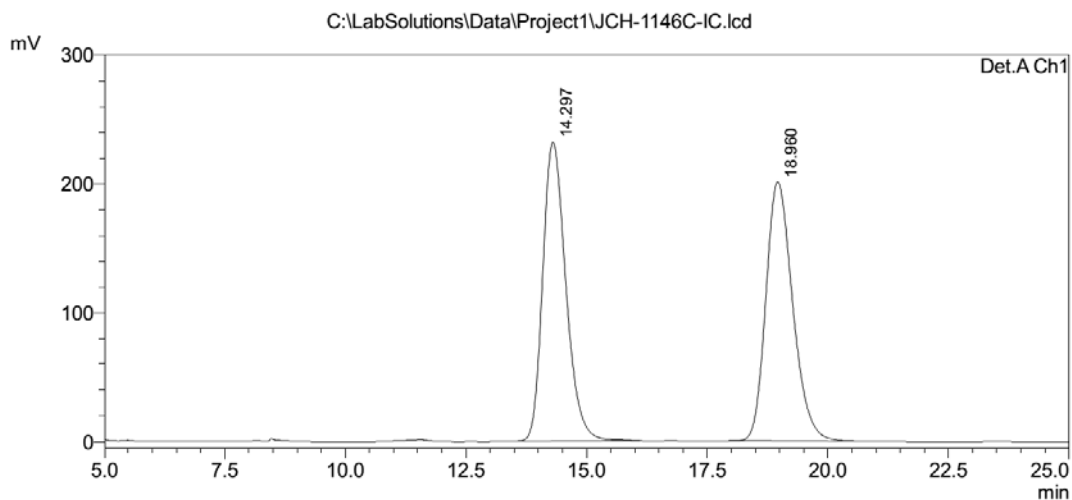
Detector A Ch1 220nm

Peak#	Ret. Time	Area	Height	Area %	Height %
1	12.264	15880114	318806	99.686	99.652
2	16.966	50087	1113	0.314	0.348
Total		15930202	319919	100.000	100.000

Enantiomerically enriched **2-20bu****2-20bv**

Compound 2-20bv. A colorless solid. $[\alpha]_D^{25} +6$ (c 0.53, CHCl_3). ^1H NMR (500 MHz, CDCl_3) δ 7.33 (td, $J = 7.8, 1.6$ Hz, 1H), 7.25 (td, $J = 7.8, 1.6$ Hz, 1H), 7.18–7.15 (m, 3H), 7.14 (s, 1H), 7.11 (dd, $J = 8.3, 1.2$ Hz, 1H), 7.00 (dd, $J = 7.9, 1.6$ Hz, 1H), 4.87 (s, 1H), 2.34 (s, 3H), 2.15 (s, 3H). ^{13}C NMR (125 MHz, CDCl_3) δ 150.1, 142.6, 138.7, 129.37, 129.36, 128.7, 128.6, 127.5, 127.3, 125.5, 122.7, 119.3, 65.2, 28.7, 21.5. The *ee* value was 99.4%, t_R (minor) = 14.4 min, t_R (major) = 18.8 min (Chiralpak IC, $\lambda = 220$ nm, hexane/*i*-PrOH = 9/1, flow rate = 1.0 mL/min). HRMS (ESI) m/z calcd for $\text{C}_{15}\text{H}_{15}\text{NO}_3\text{S}$ ($\text{M}-\text{H}$) $^-$ 288.0700, found 288.0700.

<Chromatogram>



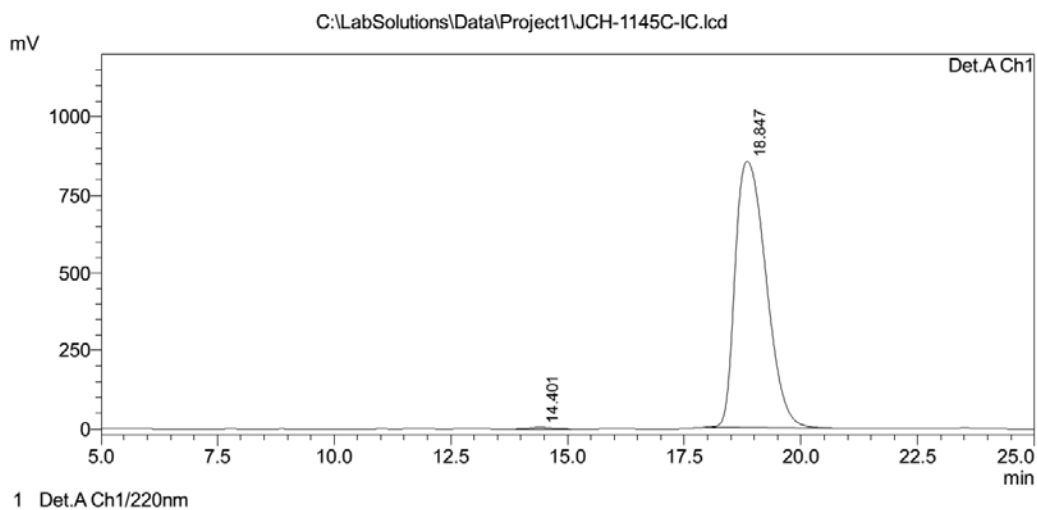
PeakTable

Detector A Ch1 220nm

Peak#	Ret. Time	Area	Height	Area %	Height %
1	14.297	7755319	232149	49.798	53.560
2	18.960	7818309	201287	50.202	46.440
Total		15573628	433436	100.000	100.000

Racemic **2-20bv**

<Chromatogram>

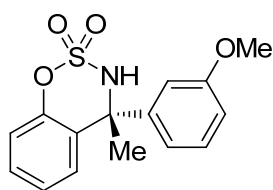


PeakTable

Detector A Ch1 220nm

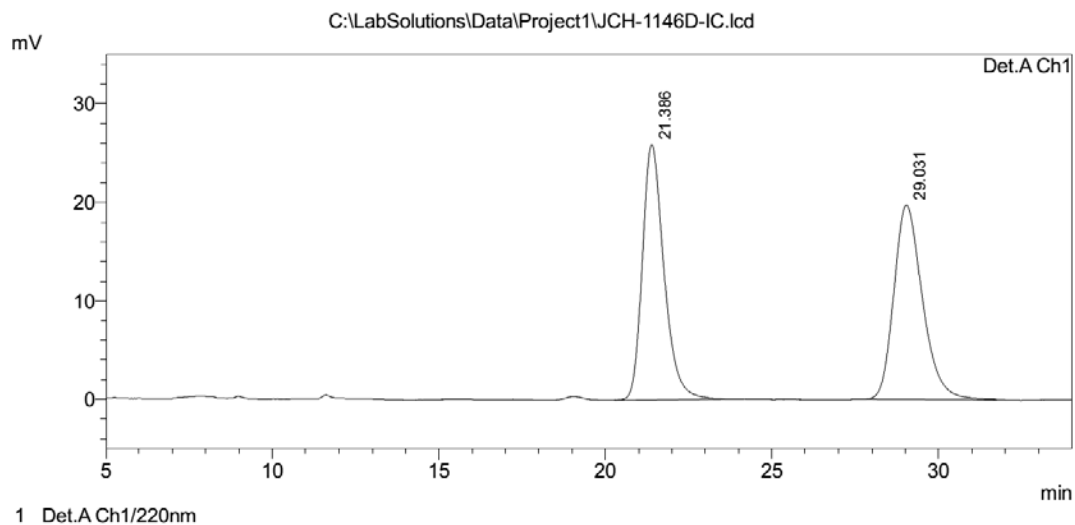
Peak#	Ret. Time	Area	Height	Area %	Height %
1	14.401	112730	4045	0.285	0.471
2	18.847	39450862	855016	99.715	99.529
Total		39563593	859061	100.000	100.000

Enantiomerically enriched **2-20bv**

**2-20bw**

Compound 2-20bw. A colorless solid. $[\alpha]_D^{25} +18$ (c 0.55, CHCl_3). ^1H NMR (500 MHz, CDCl_3) δ 7.33 (td, $J = 7.5, 1.6$ Hz, 1H), 7.28 (t, $J = 8.0$ Hz, 1H), 7.17 (td, $J = 7.7, 1.2$ Hz, 1H), 7.10 (dd, $J = 8.3, 1.1$ Hz, 1H), 7.03 (dd, $J = 7.9, 1.5$ Hz, 1H), 6.97–6.88 (m, 2H), 6.86 (dd, $J = 8.2, 2.4$ Hz, 1H), 4.92 (s, 1H), 2.78 (s, 3H), 2.13 (s, 3H). ^{13}C NMR (125MHz, CDCl_3) δ 159.8, 150.1, 145.2, 130.0, 129.5, 128.6, 127.3, 125.5, 119.4, 118.9, 112.32, 112.27, 65.2, 55.3, 28.8. The ee value was 99.9%, t_R (minor) = 21.5 min, t_R (major) = 28.9 min (Chiralpak IC, $\lambda = 220$ nm, hexane/*i*-PrOH = 9/1, flow rate = 1.0 mL/min). HRMS (ESI) m/z calcd for $\text{C}_{15}\text{H}_{15}\text{NO}_4\text{S}$ (M-H^-) 304.0649, found 304.0650.

<Chromatogram>



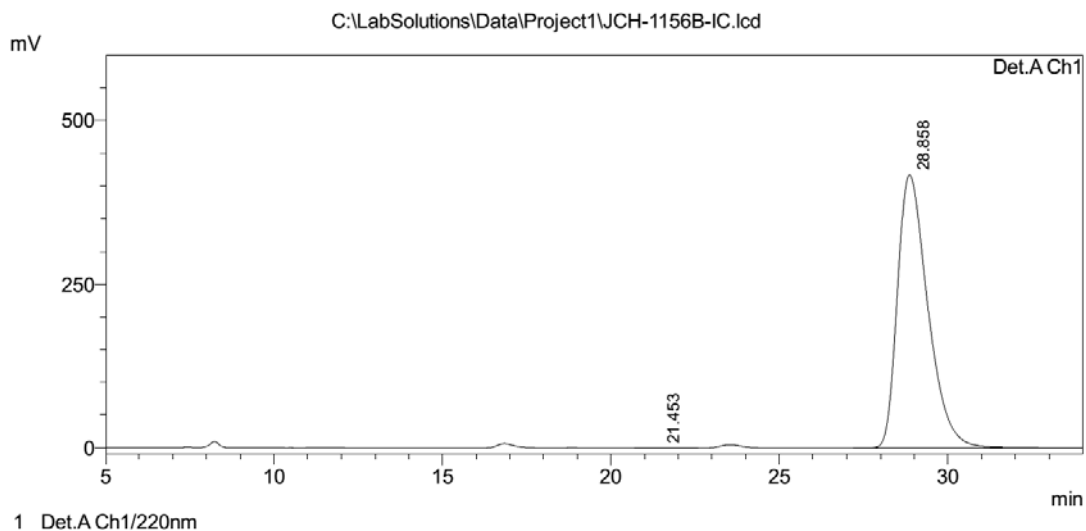
PeakTable

Detector A Ch1 220nm

Peak#	Ret. Time	Area	Height	Area %	Height %
1	21.386	1175740	25984	49.895	56.780
2	29.031	1180697	19779	50.105	43.220
Total		2356437	45763	100.000	100.000

Racemic **2-20bw**

<Chromatogram>

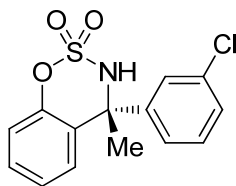


PeakTable

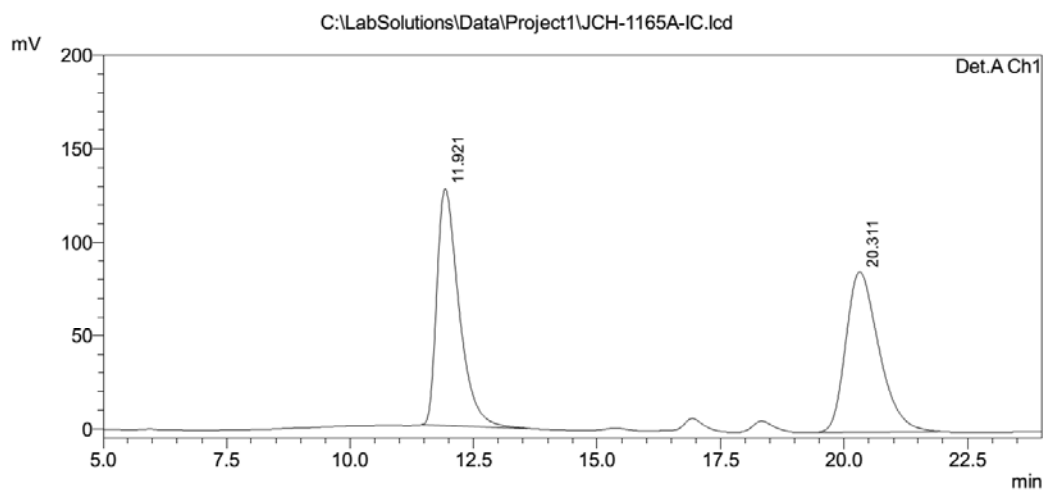
Detector A Ch1 220nm

Peak#	Ret. Time	Area	Height	Area %	Height %
1	21.453	13066	287	0.049	0.068
2	28.858	26493940	418698	99.951	99.932
Total		26507006	418985	100.000	100.000

Enantiomerically enriched **2-20bw**

**2-20bx**

Compound 2-20bx. A colorless solid. $[\alpha]_D^{25} +31$ (c 0.81, CHCl_3). ^1H NMR (500 MHz, CDCl_3) δ 7.33 (td, $J = 7.8, 1.6$ Hz, 1H), 7.31 (s, 1H), 7.28–7.24 (m, 2H), 7.22 (t, $J = 8.3$ Hz, 1H), 7.20 (td, $J = 7.6, 1.4$ Hz, 1H), 7.08 (dd, $J = 9.5, 1.2$ Hz, 1H), 7.06 (dd, $J = 7.9, 1.4$ Hz, 1H), 5.05 (s, 1H), 2.07 (s, 3H). ^{13}C NMR (125 MHz, CDCl_3) δ 150.2, 145.3, 134.7, 130.0, 129.9, 128.7, 128.4, 127.0, 126.4, 125.7, 125.0, 119.6, 64.8, 29.5. The ee value was 99.7%, t_R (minor) = 12.7 min, t_R (major) = 20.5 min (Chiralpak IC, $\lambda = 220$ nm, hexane/ i -PrOH = 9/1, flow rate = 1.0 mL/min). HRMS (ESI) m/z calcd for $\text{C}_{14}\text{H}_{12}\text{ClNO}_3\text{S}$ (M-H) $^-$ 308.0154, found 308.0162.

<Chromatogram>

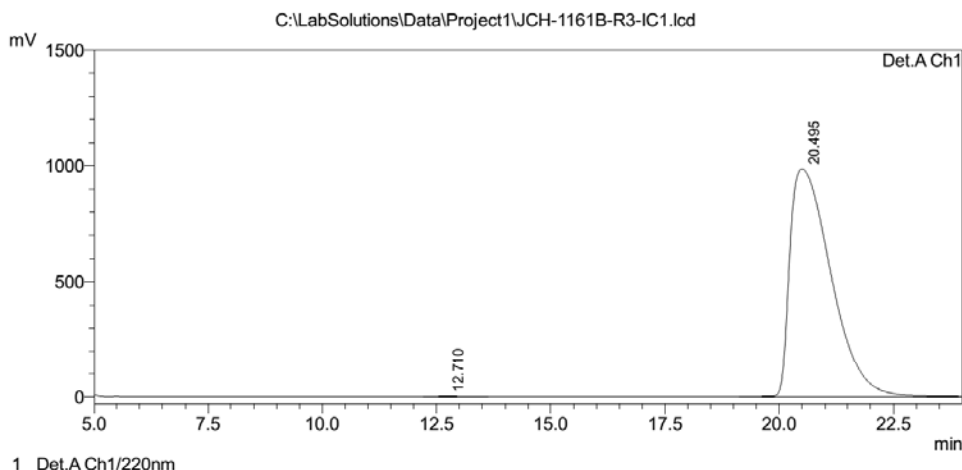
PeakTable

Detector A Ch1 220nm

Peak#	Ret. Time	Area	Height	Area %	Height %
1	11.921	3952839	126964	49.642	59.596
2	20.311	4009931	86079	50.358	40.404
Total		7962771	213043	100.000	100.000

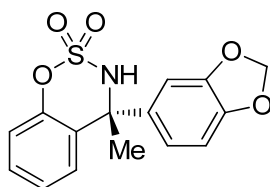
Racemic 2-20bx

<Chromatogram>



PeakTable

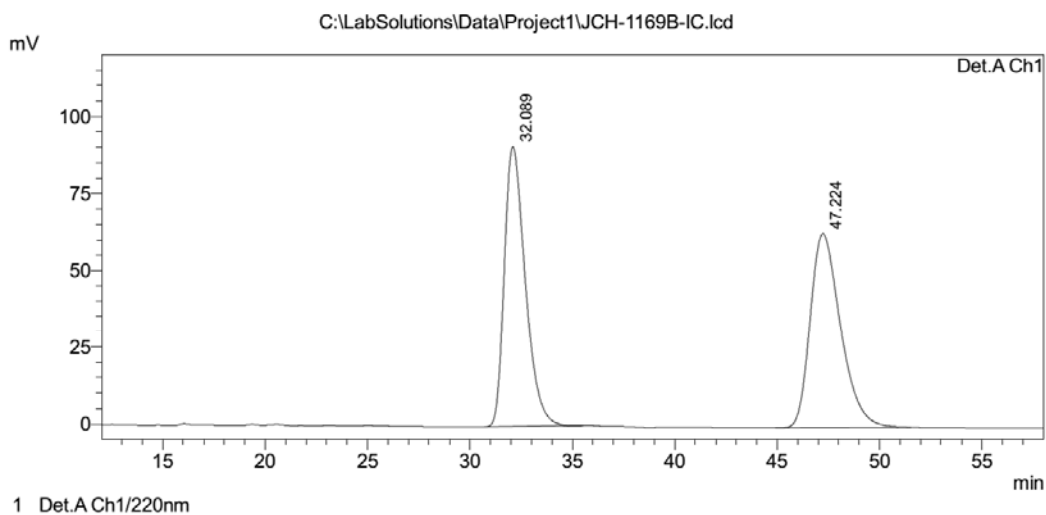
Peak#	Ret. Time	Area	Height	Area %	Height %
1	12.710	89610	2543	0.144	0.256
2	20.495	62274498	988853	99.856	99.744
Total		62364108	991395	100.000	100.000

Enantiomerically enriched **2-20bx****2-20by**

Compound 2-20by. A colorless solid. $[\alpha]_D^{25} +22$ (c 1.0, CHCl_3). ^1H NMR (500 MHz, CDCl_3) δ 7.33 (td, $J = 7.8, 1.5$ Hz, 1H), 7.18 (td, $J = 7.7, 1.2$ Hz, 1H), 7.09 (dd, $J = 8.2, 1.0$ Hz, 1H), 7.04 (dd, $J = 7.9, 1.6$ Hz, 1H), 6.81 (s, 1H), 6.80 (dd, $J = 7.4, 1.7$ Hz, 1H), 6.75 (dd, $J = 7.4, 1.5$ Hz, 1H), 5.96 (s, 2H), 4.94 (s, 1H), 2.09 (s, 3H). ^{13}C NMR (126 MHz, CDCl_3) δ 150.1, 148.1, 147.7, 137.5, 129.6, 128.5, 127.5, 125.6, 120.4, 119.4, 108.1, 107.5, 101.5, 65.2, 29.1. The ee value was 99.9%, t_R (minor) = 32.7 min, t_R (major) = 49.0 min (Chiralpak IC, $\lambda = 220$ nm, hexane/ i -PrOH = 9/1, flow rate =

1.0 mL/min). HRMS (ESI) m/z calcd for $C_{15}H_{13}NO_5S$ (M-H)⁻ 318.0442, found 318.0446.

<Chromatogram>

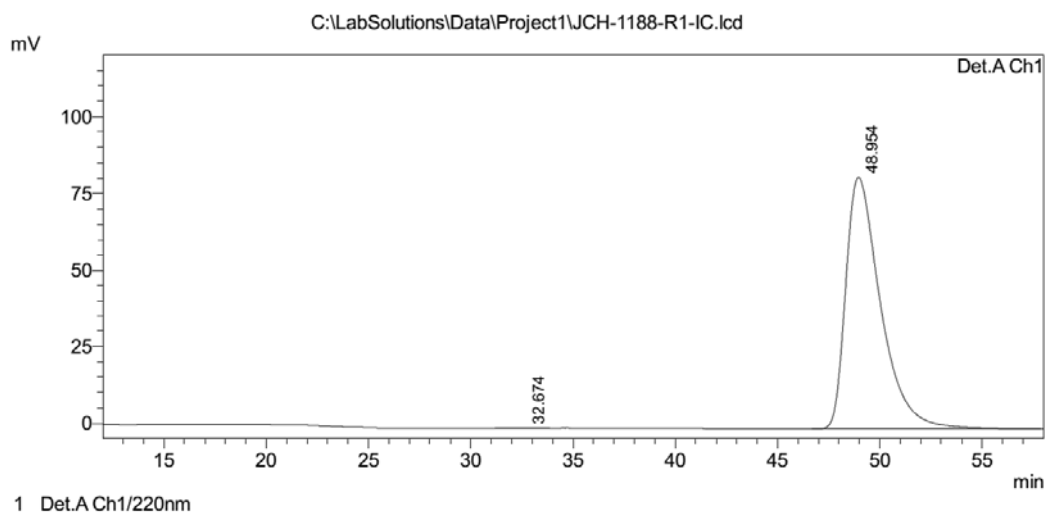


PeakTable

Peak#	Ret. Time	Area	Height	Area %	Height %
1	32.089	6479073	91087	49.842	59.036
2	47.224	6520183	63203	50.158	40.964
Total		12999256	154290	100.000	100.000

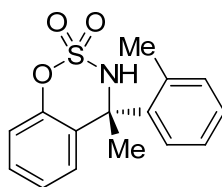
Racemic 2-20by

<Chromatogram>



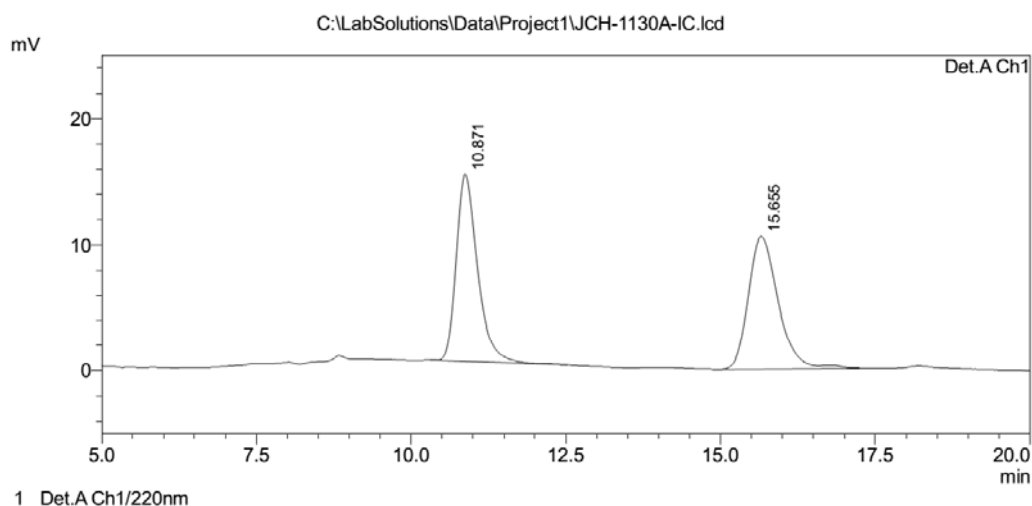
PeakTable

Peak#	Ret. Time	Area	Height	Area %	Height %
1	32.674	1039	32	0.011	0.039
2	48.954	9722663	82130	99.989	99.961
Total		9723702	82162	100.000	100.000

Enantiomerically enriched **2-20bz****2-20bz**

Compound 2-20bz. A colorless solid. $[\alpha]_D^{25} -85$ (c 0.64, CHCl_3). ^1H NMR (500 MHz, CDCl_3) δ 7.63 (dd, $J = 6.9, 2.3$ Hz, 1H), 7.31-7.27 (m, 3H), 7.16 (dd, $J = 6.3, 2.5$ Hz, 1H), 7.10 (td, $J = 7.5, 1.2$ Hz, 1H), 7.07 (dd, $J = 8.2, 1.0$ Hz, 1H), 6.82 (dd, $J = 7.8, 1.5$ Hz, 1H), 4.92 (s, 1H), 2.23 (s, 3H), 2.05 (s, 3H). ^{13}C NMR (125 MHz, CDCl_3) δ 149.8, 140.4, 136.7, 132.6, 129.3, 129.2, 127.8, 127.5, 126.8, 126.3, 125.9, 117.0, 65.0, 29.5, 20.6. The ee value was 99.9%, t_R (minor) = 11.6 min, t_R (major) = 16.6 min (Chiralpak IC, $\lambda = 220$ nm, hexane/ i -PrOH = 9/1, flow rate = 1.0 mL/min). HRMS (ESI) m/z calcd for $\text{C}_{15}\text{H}_{15}\text{NO}_3\text{S}$ (M-H) $^-$ 288.0700, found 288.0697.

<Chromatogram>

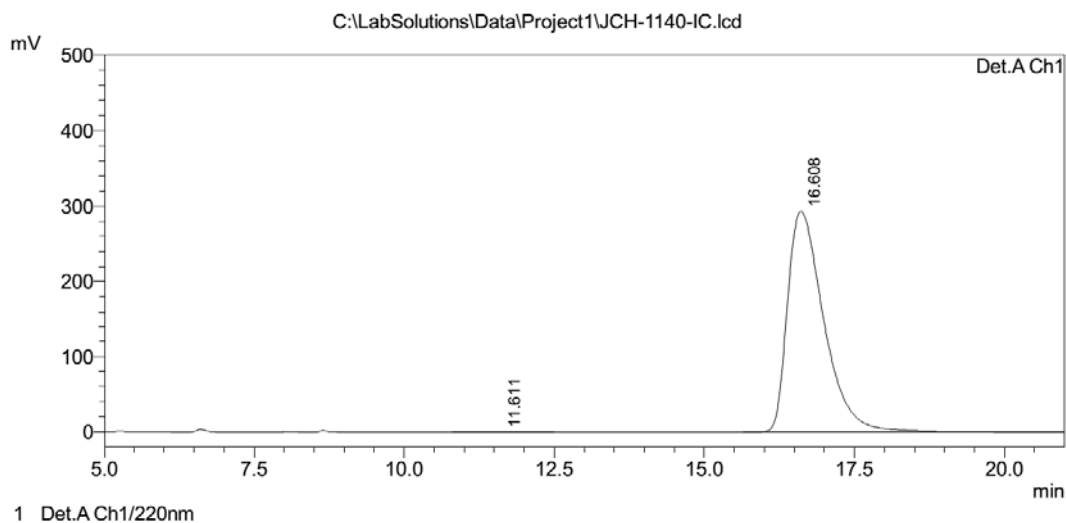


PeakTable

Peak#	Ret. Time	Area	Height	Area %	Height %
1	10.871	358712	14912	50.069	58.456
2	15.655	357726	10598	49.931	41.544
Total		716438	25510	100.000	100.000

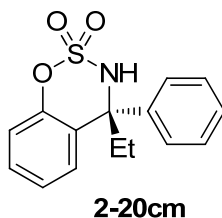
Racemic **2-20bz**

<Chromatogram>



PeakTable

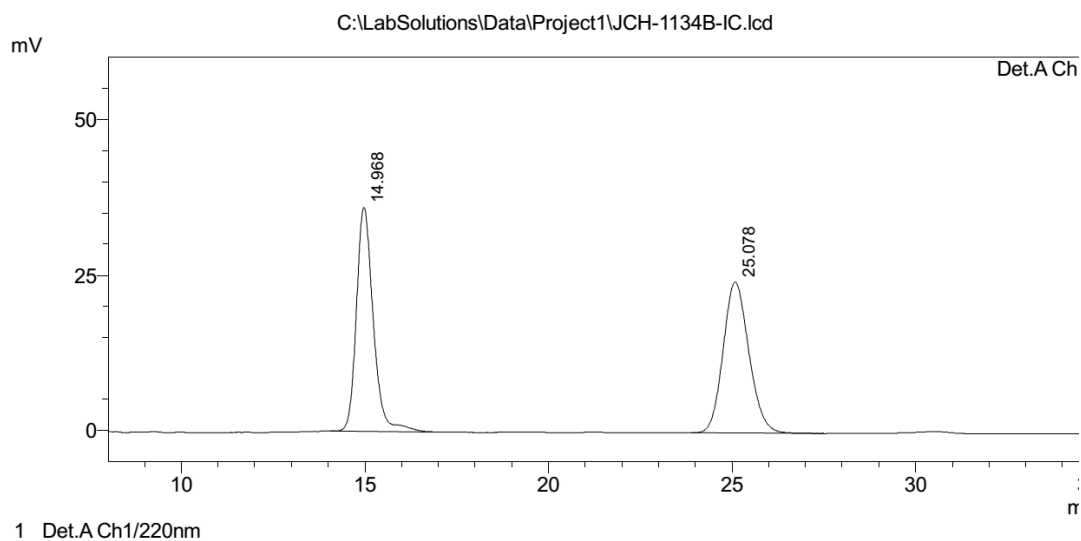
Peak#	Ret. Time	Area	Height	Area %	Height %
1	11.611	8298	178	0.067	0.061
2	16.608	12422350	293609	99.933	99.939
Total		12430648	293787	100.000	100.000

Enantiomerically enriched **2-20bz**

Compound 2-20cm. A colorless solid. $[\alpha]_D^{25} +9$ (c 0.78, CHCl_3). ^1H NMR (500 MHz, CDCl_3) δ 7.41–7.32 (m, 5H), 7.30 (tt, $J = 7.0, 1.2$ Hz, 1H), 7.22 (td, $J = 7.7, 1.2$ Hz, 1H), 7.14 (dd, $J = 7.9, 1.5$ Hz, 1H), 7.12 (dd, $J = 8.2, 1.2$ Hz, 1H), 5.01 (s, 1H), 2.45 (dq, $J = 14.5, 7.2$ Hz, 1H), 2.40 (dq, $J = 14.8, 7.4$ Hz, 1H), 1.01 (t, $J = 7.3$ Hz, 3H). ^{13}C NMR (125 MHz, CDCl_3) δ 150.8, 142.4, 129.5, 128.5, 128.4, 128.1, 126.7, 125.7, 125.3, 119.5, 68.4, 34.5, 8.6. The ee value was 99.5%, t_R (minor) = 15.8 min, t_R (major) = 25.8 min (Chiralpak IC, $\lambda = 220$ nm, hexane/ i -PrOH = 9/1, flow rate = 1.0

mL/min). HRMS (ESI) m/z calcd for $C_{15}H_{15}NO_3S$ (M-H)⁻ 288.0700, found 288.0701.

<Chromatogram>

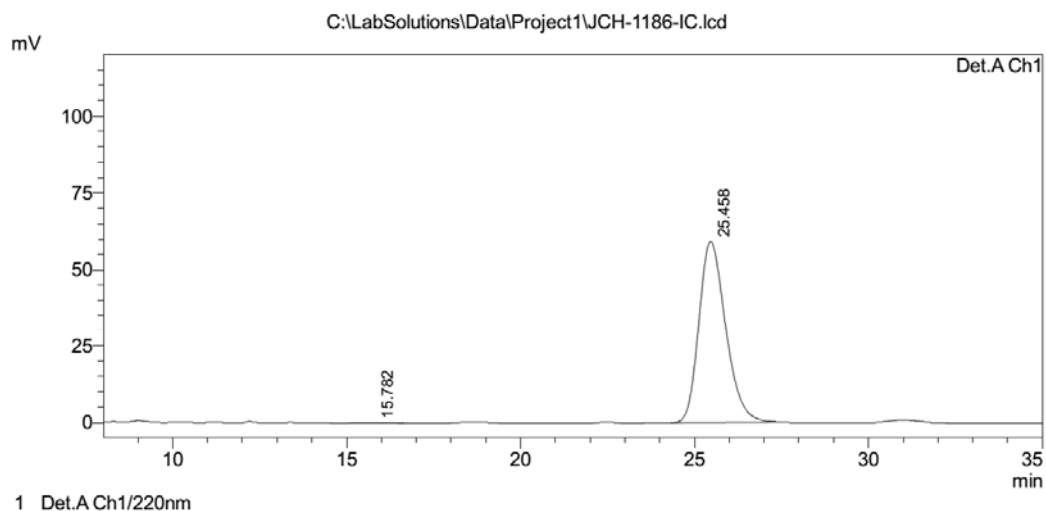


PeakTable

Peak#	Ret. Time	Area	Height	Area %	Height %
1	14.968	1153838	36085	49.236	59.716
2	25.078	1189625	24342	50.764	40.284
Total		2343463	60427	100.000	100.000

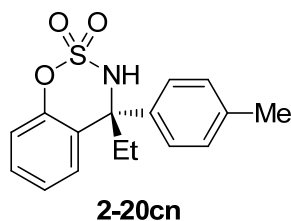
Racemic 2-20cm

<Chromatogram>



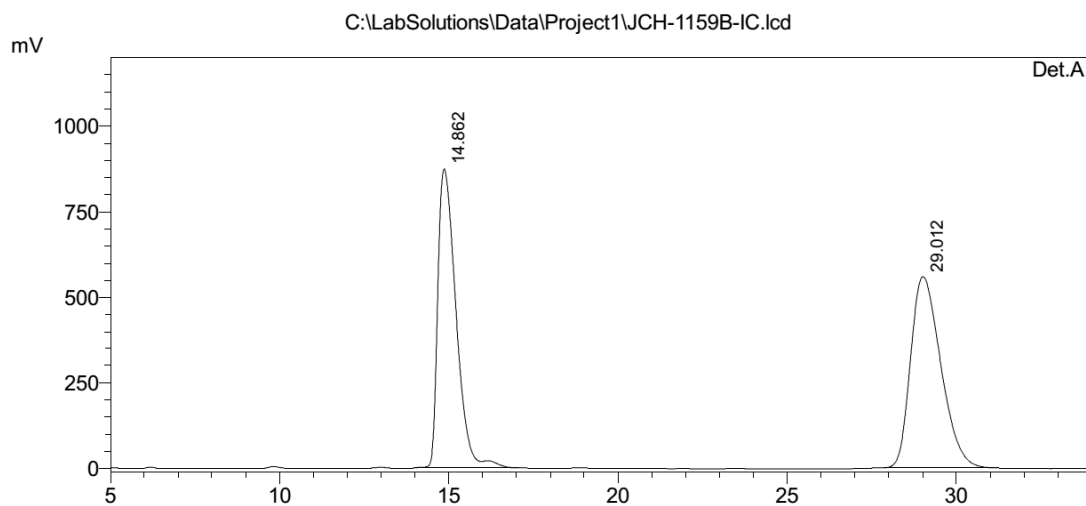
PeakTable

Peak#	Ret. Time	Area	Height	Area %	Height %
1	15.782	8292	172	0.261	0.289
2	25.458	3170165	59220	99.739	99.711
Total		3178458	59392	100.000	100.000

Enantiomerically enriched **2-20cn**

Compound 2-20cn. A colorless solid. $[\alpha]_D^{25} +3$ (*c* 1.1, CHCl₃). ¹H NMR (500 MHz, CDCl₃) δ 7.34 (td, *J* = 8.0, 1.4 Hz, 1H), 7.26 (d, *J* = 8.1 Hz, 2 H), 7.20 (t, *J* = 7.7 Hz, 1H), 7.16 (d, *J* = 8.1 Hz, 2H), 7.14–7.10 (m, 2H), 4.98 (s, 1H), 2.45 (dq, *J* = 14.8, 7.2 Hz, 1H), 2.40 (dq, *J* = 14.9, 7.5 Hz, 1H), 2.34 (s, 3H), 1.02 (t, *J* = 7.3 Hz, 3H). ¹³C NMR (125 MHz, CDCl₃) δ 150.7, 139.5, 138.0, 129.4, 129.3, 128.4, 126.7, 126.1, 125.3, 119.5, 68.3, 34.2, 21.0, 8.7. The *ee* value was 99.5%, *t_R* (minor) = 15.2 min, *t_R* (major) = 29.2 min (Chiralpak IC, λ = 220 nm, hexane/*i*-PrOH = 9/1, flow rate = 1.0 mL/min). HRMS (ESI) *m/z* calcd for C₁₆H₁₇NO₃S (M-H)⁻ 302.0856, found 302.0862.

<Chromatogram>



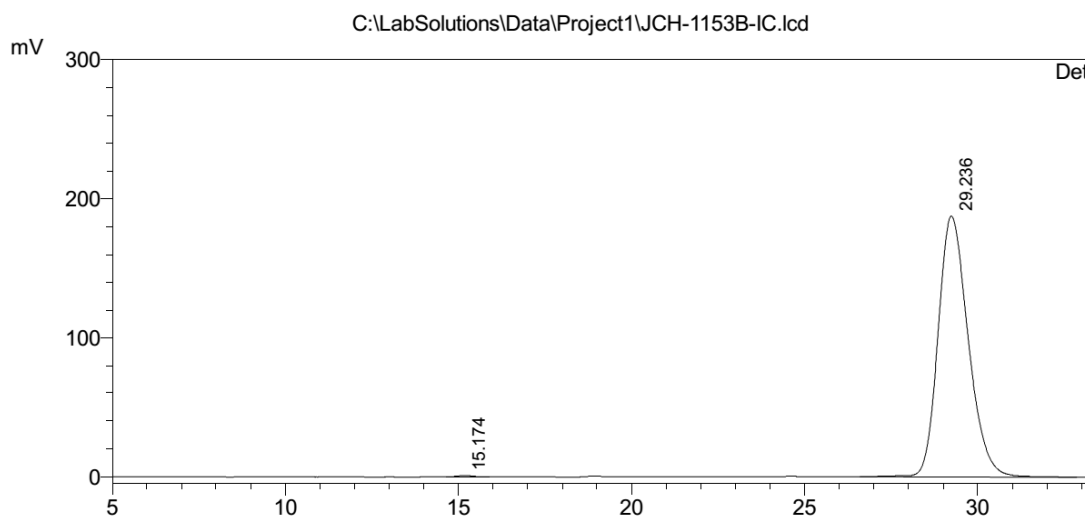
1 Det.A Ch1/220nm

PeakTable

Detector A Ch1 220nm					
Peak#	Ret. Time	Area	Height	Area %	Height %
1	14.862	32716472	874263	48.517	60.985
2	29.012	34717182	559299	51.483	39.015
Total		67433653	1433562	100.000	100.000

Racemic **2-20cn**

<Chromatogram>

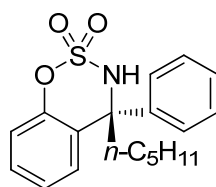


1 Det.A Ch1/220nm

PeakTable

Detector A Ch1 220nm

Peak#	Ret. Time	Area	Height	Area %	Height %
1	15.174	28963	992	0.254	0.525
2	29.236	11392412	187934	99.746	99.475
Total		11421375	188926	100.000	100.000

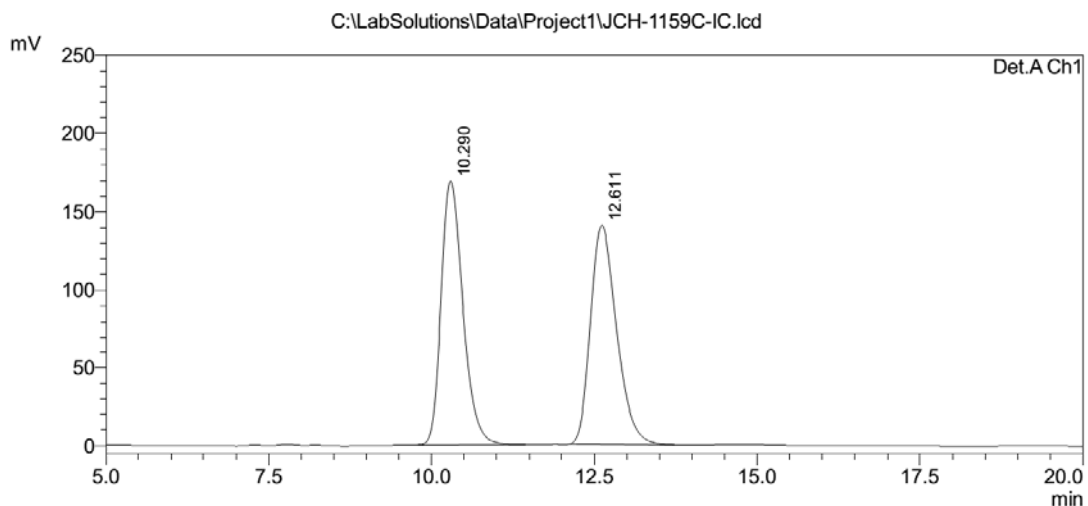
Enantiomerically enriched **2-20cn****2-20dm**

Compound 2-20dm. A colorless solid. $[\alpha]_D^{25} +21$ (*c* 0.53, CHCl₃). ¹H NMR (500 MHz, CDCl₃) δ 7.40–7.32 (m, 5H), 7.30 (tt, *J* = 6.8, 1.5 Hz, 1H), 7.23 (td, *J* = 7.7, 1.3 Hz, 1H), 7.15 (dd, *J* = 7.9, 1.6 Hz, 1H), 7.11 (dd, *J* = 8.2, 1.2 Hz, 1H), 5.02 (s, 1H), 2.34 (t, *J* = 7.1 Hz, 2H), 1.47–1.19 (m, 6H), 0.87 (t, *J* = 7.0 Hz, 3H). ¹³C NMR (125 MHz, CDCl₃) δ 150.7, 142.7, 129.5, 128.5, 128.4, 128.1, 126.7, 125.8, 125.3, 119.6, 68.1, 41.8, 31.6, 22.8, 22.3, 12.9. The *ee* value was 99.4%, *t_R* (minor) = 10.3 min, *t_R* (major)

= 12.6 min (Chiralpak IC, $\lambda = 220$ nm, hexane/*i*-PrOH = 9/1, flow rate = 1.0 mL/min).

HRMS (ESI) m/z calcd for $C_{18}H_{21}NO_3S$ (M-H)⁻ 330.1169, found 330.1171.

<Chromatogram>

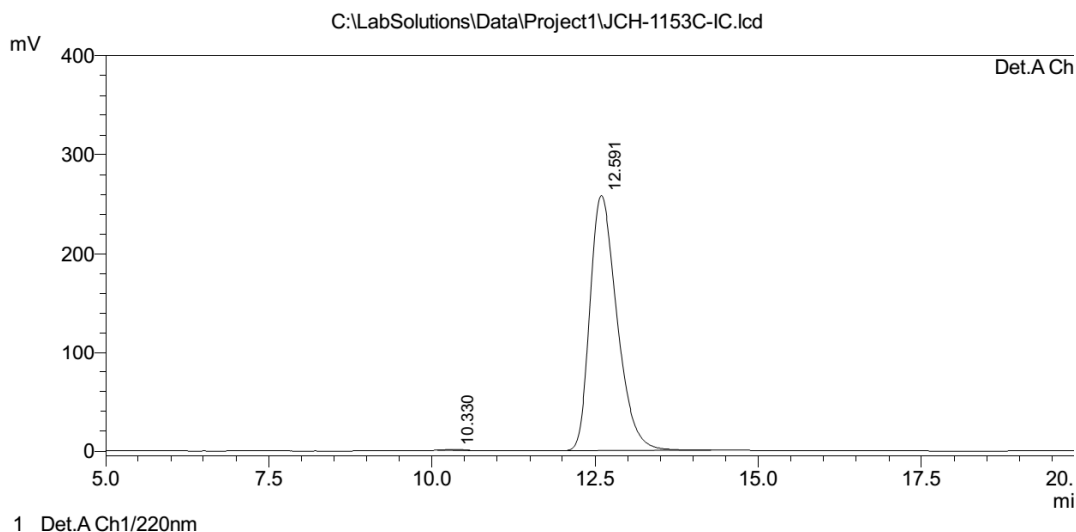


PeakTable

Peak#	Ret. Time	Area	Height	Area %	Height %
1	10.290	3933485	169120	50.142	54.638
2	12.611	3911152	140407	49.858	45.362
Total		7844636	309526	100.000	100.000

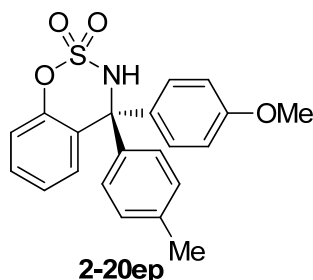
Racemic 2-20dm

<Chromatogram>



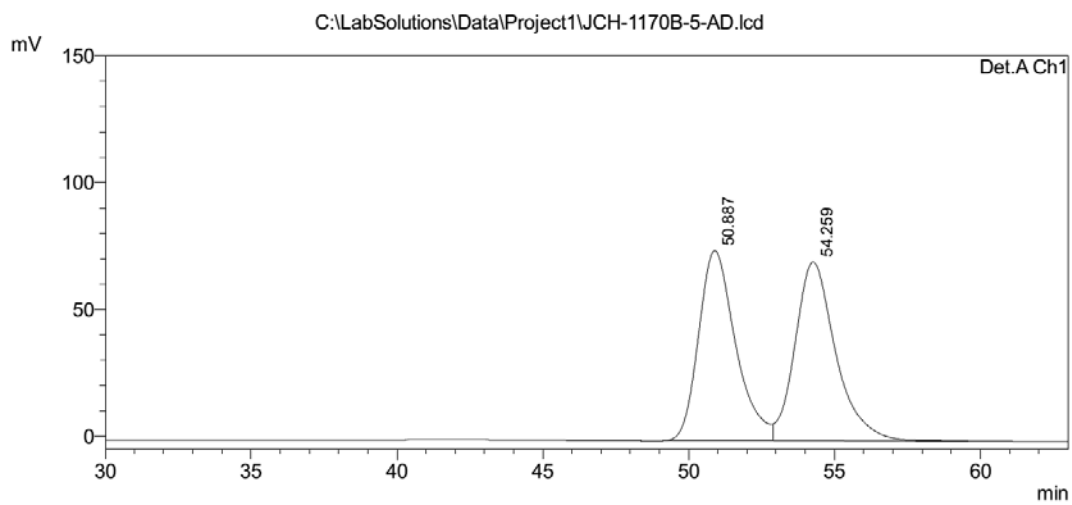
PeakTable

Peak#	Ret. Time	Area	Height	Area %	Height %
1	10.330	21563	1148	0.288	0.442
2	12.591	7475046	258642	99.712	99.558
Total		7496609	259790	100.000	100.000

Enantiomerically enriched **2-20dm**

Compound 2-20ep. A colorless solid. $[\alpha]_D^{25} +2$ (c 1.0, CHCl_3). ^1H NMR (500 MHz, CDCl_3) δ 7.37 (td, $J = 7.8, 1.6$ Hz, 1H), 7.17–7.11 (m, 6H), 7.13 (d, $J = 9.0$ Hz, 2H), 7.09 (d, $J = 8.4$ Hz, 2H), 6.86 (td, $J = 7.7, 1.3$ Hz, 1H), 6.86 (d, $J = 8.9$ Hz, 2H), 5.46 (s, 1H), 2.81 (s, 3H), 2.36 (s, 3H). ^{13}C NMR (125 MHz, CDCl_3) δ 159.4, 150.6, 139.4, 138.4, 134.1, 130.8, 129.8, 129.7, 129.2, 128.2, 127.3, 124.7, 119.4, 112.7, 71.6, 55.3, 21.0. The ee value was 99.2%, t_R (minor) = 50.9 min, t_R (major) = 54.2 min (Chiralpak AD-H, $\lambda = 220$ nm, hexane/ i -PrOH = 19/1, flow rate = 1.0 mL/min). HRMS (ESI) m/z calcd for $\text{C}_{21}\text{H}_{19}\text{NO}_4\text{S}$ (M-H) $^-$ 380.0962, found 380.0961.

<Chromatogram>



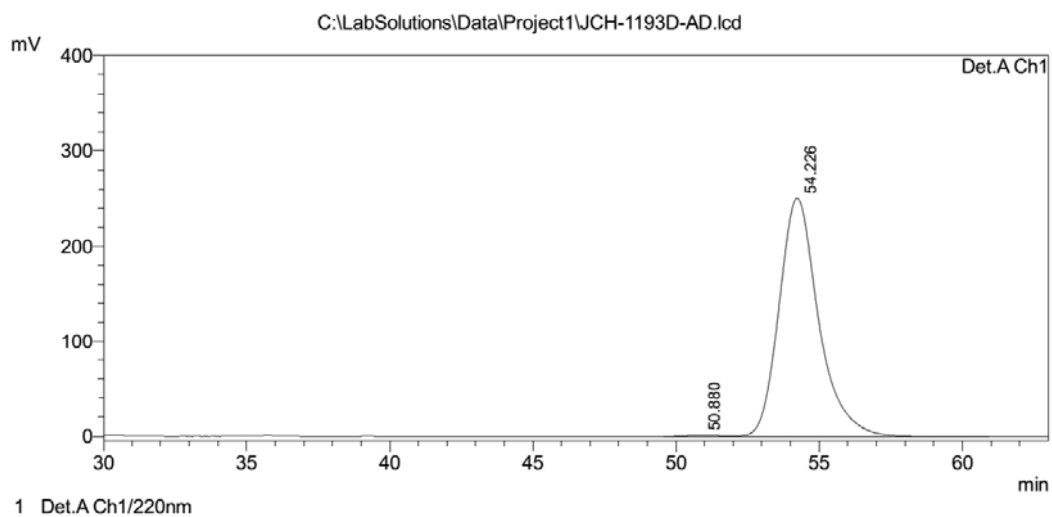
PeakTable

Detector A Ch1 220nm

Peak#	Ret. Time	Area	Height	Area %	Height %
1	50.887	6607787	75052	49.201	51.490
2	54.259	6822363	70708	50.799	48.510
Total		13430150	145760	100.000	100.000

Racemic **2-20ep**

<Chromatogram>

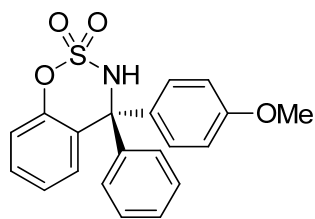


PeakTable

Detector A Ch1 220nm

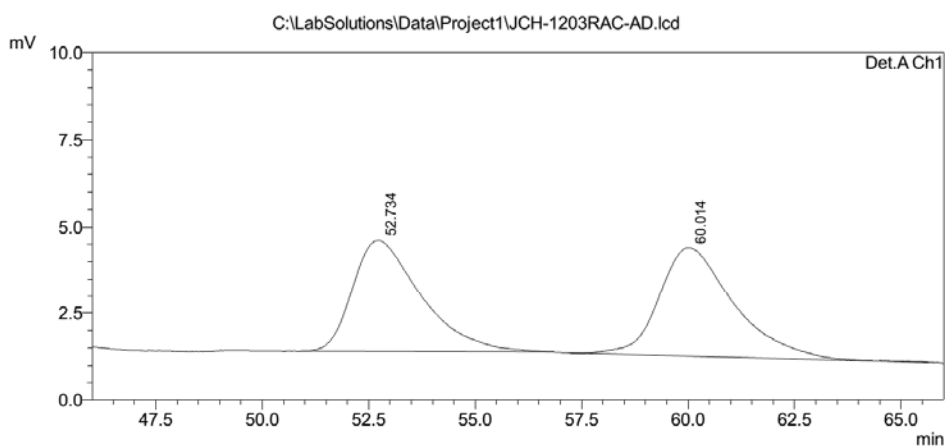
Peak#	Ret. Time	Area	Height	Area %	Height %
1	50.880	94965	1150	0.395	0.457
2	54.226	23976196	250670	99.605	99.543
Total		24071161	251821	100.000	100.000

Enantiomerically enriched **3ep**

**2-20fp**

Compound 2-20fp. A colorless solid. $[\alpha]_D^{25} -5$ (c 0.54, CHCl_3). ^1H NMR (500 MHz, CDCl_3) δ 7.38 (td, $J = 7.1, 1.5$ Hz, 1H), 7.38–7.35 (m, 3H), 7.25–7.22 (m, 2H), 7.16 (dd, $J = 8.3, 1.0$ Hz, 1H), 7.15 (td, $J = 7.5, 1.2$ Hz, 1H), 7.12 (d, $J = 8.9$ Hz, 2H), 6.87 (d, $J = 8.9$ Hz, 2H), 6.85 (dd, $J = 7.0, 2.0$ Hz, 1H), 5.44 (s, 1H), 2.81 (s, 3H). ^{13}C NMR (125 MHz, CDCl_3) δ 159.5, 150.7, 142.3, 134.1, 130.8, 129.9, 129.7, 128.49, 128.47, 128.36, 127.0, 124.8, 119.5, 112.8, 71.7, 55.2. The ee value was 99.6%, t_R (minor) = 52.4 min, t_R (major) = 59.7 min (Chiralpak AD-H, $\lambda = 220$ nm, hexane/ i -PrOH = 19/1, flow rate = 1.0 mL/min). HRMS (ESI) m/z calcd for $\text{C}_{20}\text{H}_{17}\text{NO}_4\text{S}$ (M-H) $^-$ 366.0806, found 366.0808.

<Chromatogram>

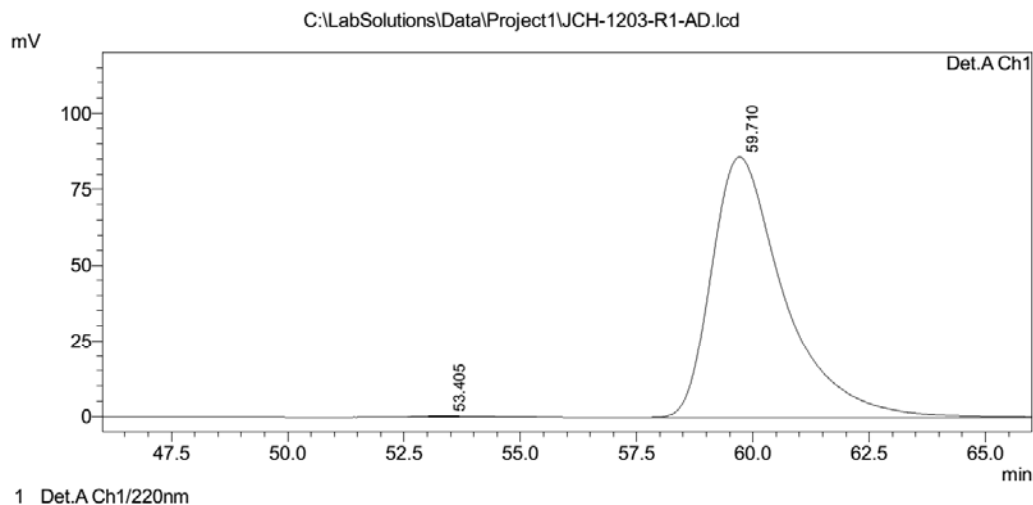


Peak Table

Peak#	Ret. Time	Area	Height	Area %	Height %
1	52.734	360033	3219	48.340	50.568
2	60.014	384759	3147	51.660	49.432
Total		744792	6365	100.000	100.000

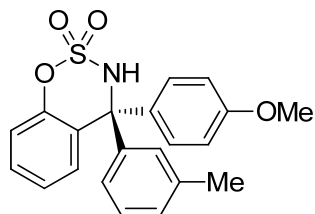
Racemic 2-20fp

<Chromatogram>



PeakTable

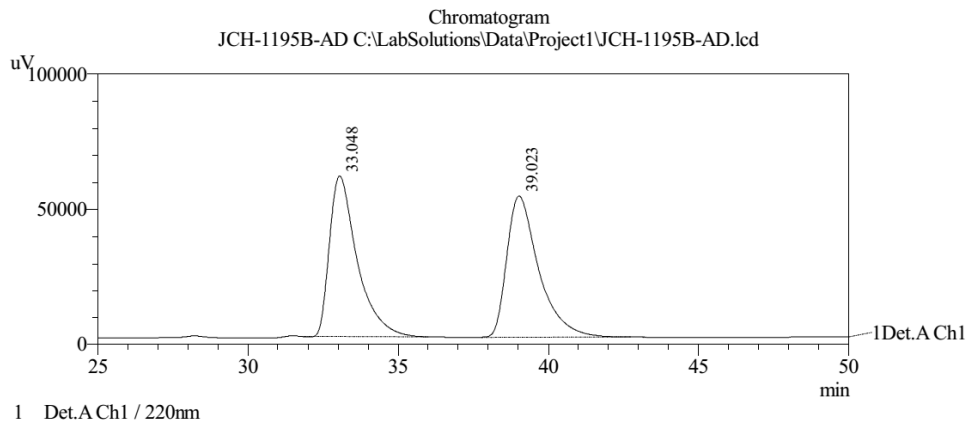
Peak#	Ret. Time	Area	Height	Area %	Height %
1	53.405	21346	275	0.227	0.319
2	59.710	9385354	85965	99.773	99.681
Total		9406700	86241	100.000	100.000

Enantiomerically enriched **2-20fp****2-20gp**

Compound 2-20gp. A colorless solid. $[\alpha]_D^{25} +7$ (c 1.1, CHCl_3). ^1H NMR (500 MHz, CDCl_3) δ 7.37 (td, $J = 7.8, 1.6$ Hz, 1H), 7.23 (t, $J = 7.7$, 1H), 7.16–7.13 (m, 3H), 7.13 (d, $J = 8.9$ Hz, 2H), 7.03 (s, 1H), 6.97 (d, $J = 7.9$ Hz, 1H), 6.87 (d, $J = 8.9$ Hz, 2H), 6.85 (dd, $J = 6.3, 1.6$ Hz, 1H), 5.45 (s, 1H), 2.81 (s, 3H), 2.32 (s, 3H). ^{13}C NMR (125 MHz, CDCl_3) δ 159.4, 150.6, 142.5, 138.3, 134.0, 130.8, 129.8, 129.3, 128.8, 128.3, 127.2, 125.5, 124.8, 119.5, 112.7, 105.0, 71.7, 55.3, 21.6. The ee value was 96%, t_R (minor) = 34.1 min, t_R (major) = 40.1 min (Chiralpak AD-H, $\lambda = 220$ nm,

hexane/*i*-PrOH = 19/1, flow rate = 1.0 mL/min). HRMS (ESI) m/z calcd for $C_{21}H_{19}NO_4S$ (M-H)⁻ 380.0962, found 380.0956.

<Chromatogram>



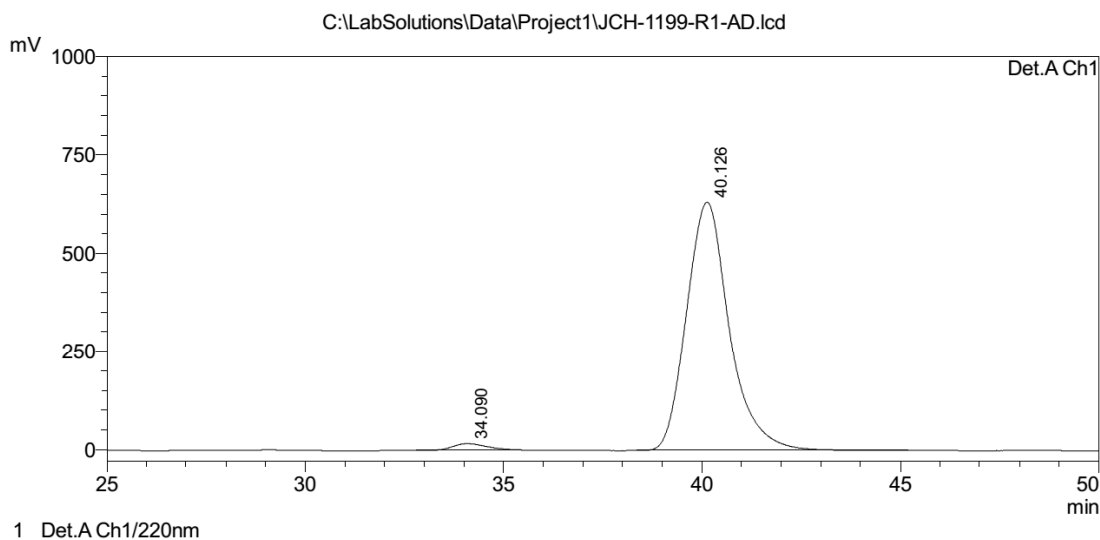
PeakTable

Detector A Ch1 220nm

Peak#	Ret. Time	Area	Height	Area %	Height %
1	33.048	3821486	59592	49.649	53.209
2	39.023	3875558	52404	50.351	46.791
Total		7697045	111996	100.000	100.000

Racemic 2-20gp

<Chromatogram>

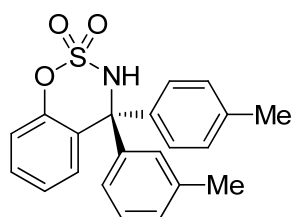


PeakTable

Detector A Ch1 220nm

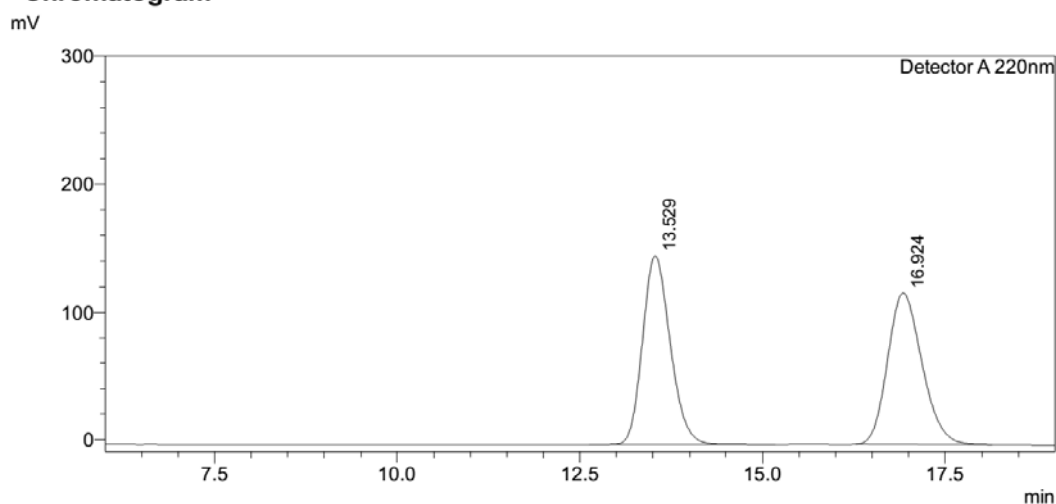
Peak#	Ret. Time	Area	Height	Area %	Height %
1	34.090	975605	16463	2.006	2.534
2	40.126	47647684	633288	97.994	97.466
Total		48623288	649751	100.000	100.000

Enantiomerically enriched 2-20gp

**2-20gn**

Compound 2-20gn. A colorless solid. $[\alpha]_D^{25} -2$ (c 0.84, CHCl_3). ^1H NMR (500 MHz, CDCl_3) δ 7.37 (td, $J = 7.8, 1.5$ Hz, 1H), 7.23 (t, $J = 7.7$ Hz, 1H), 7.19–7.13 (m, 3H), 7.16 (d, $J = 7.9$ Hz, 2H), 7.10 (d, $J = 8.3$ Hz, 2H), 7.03 (s, 1H), 6.97 (d, $J = 7.9$ Hz, 1H), 6.86 (dd, $J = 7.8, 1.4$ Hz, 1H), 5.46 (s, 1H), 2.36 (s, 3H), 2.32 (s, 3H). ^{13}C NMR (125 MHz, CDCl_3) δ 150.6, 142.3, 139.2, 138.3, 138.3, 130.9, 129.8, 129.3, 129.1, 128.9, 128.34, 128.28, 127.0, 125.6, 124.8, 119.5, 71.9, 21.6, 21.0. The *ee* value was 97%, t_R (minor) = 12.2 min, t_R (major) = 16.4 min (Chiralpak IC, $\lambda = 220$ nm, hexane/*i*-PrOH = 9/1, flow rate = 1.0 mL/min). HRMS (ESI) m/z calcd for $\text{C}_{21}\text{H}_{19}\text{NO}_3\text{S}$ (M-H) $^-$ 364.1013, found 364.1022.

<Chromatogram>

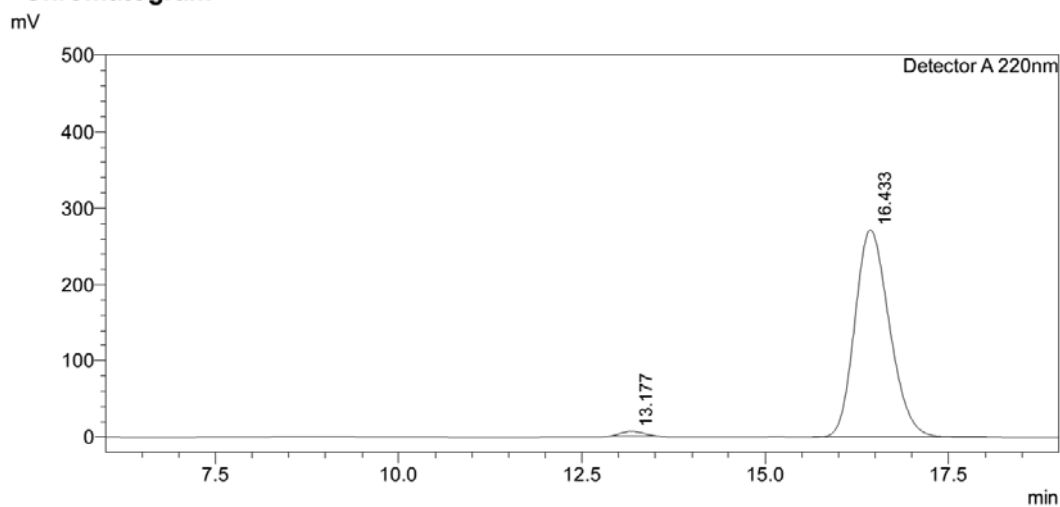


<Peak Table>

Detector A 220nm							
Peak#	Ret. Time	Area	Height	Conc.	Unit	Mark	Name
1	13.529	3938542	148243	50.281			
2	16.924	3894482	119106	49.719		M	
Total		7833024	267350				

Racemic 2-20gn

<Chromatogram>

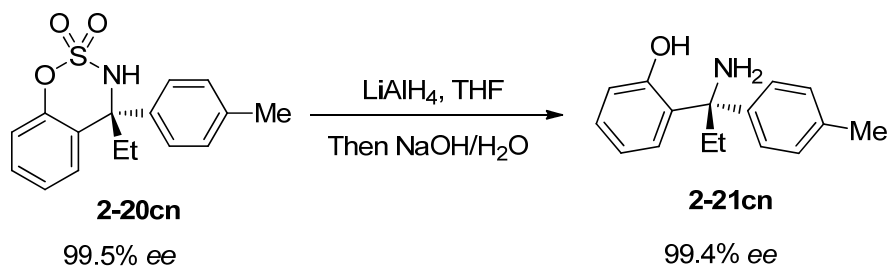


<Peak Table>

Detector A 220nm							
Peak#	Ret. Time	Area	Height	Conc.	Unit	Mark	Name
1	13.177	129006	6125	1.424		M	
2	16.433	8929110	271457	98.576		M	
Total		9058116	277582				

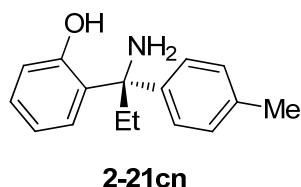
Enantiomerically enriched 2-20gn

2.4.4 Conversion of Arylation Products into Trialkylmethylamines



Transformation of 2-20cn to 4-20cn: The reaction was carried out according to the procedures reported for .^[72b] To a suspension of lithium aluminium hydride (12 mg, 0.30 mmol) in THF (2.0 mL) was added **2-20cn** (30.3 mg, 0.100 mmol, 99.5% ee), and the mixture was stirred under reflux for 6 h. The mixture was cooled to 0 °C, and water (60 μL) and 10% NaOH (20 μL) was carefully added. The resulting mixture was stirred at the same temperature for 30 min, and it was passed through a short column of celite with ethyl acetate as an eluent. The solvent was removed on a rotary evaporator and the residue was subjected to flash chromatography on silica gel using hexane/ethyl acetate (6:1) as an eluent to give **4-20cn** as a colorless solid (19.4 mg, 81% yield, 99.4% ee).

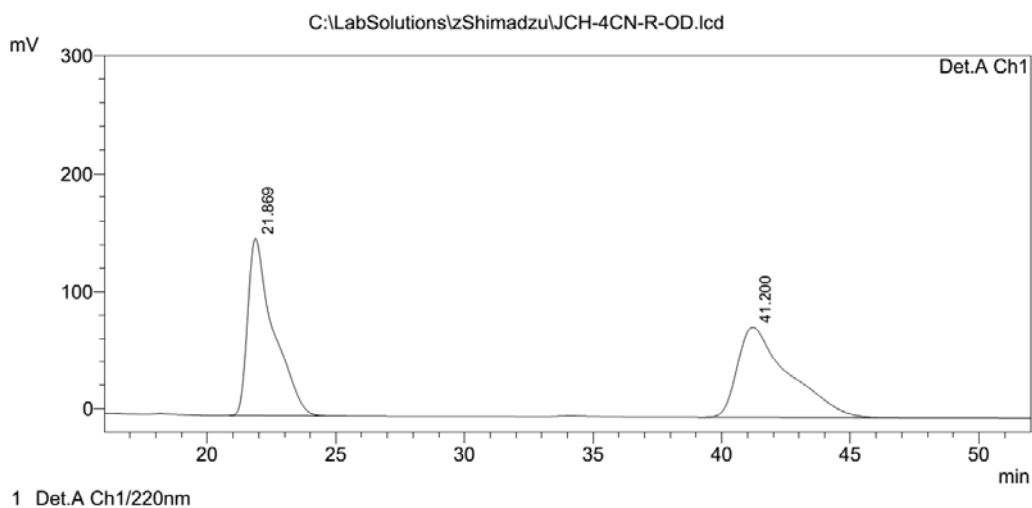
In a similar manner, treatment of **2-20gn** with lithium aluminium hydride in THF gave 75% yield of **2-21gn**.



Compound 2-21cn. A colorless solid. $[\alpha]_D^{25} +20$ (c 0.85, CHCl_3). $^1\text{H NMR}$ (500 MHz, CDCl_3) δ 7.19 (d, $J = 8.1$ Hz, 2H), 7.13 (t, $J = 7.3$ Hz, 1H), 7.13 (d, $J = 7.9$ Hz, 2H),

6.93 (d, $J = 7.7$ Hz, 1H), 6.82 (d, $J = 8.1$ Hz, 1H), 6.74 (t, $J = 7.5$ Hz, 1H), 2.39–2.19 (m, 2H), 2.32 (s, 3H), 0.92 (t, $J = 7.3$ Hz, 3H). ^{13}C NMR (125 MHz, CDCl_3) δ 158.0, 136.5, 129.3, 129.1, 128.9, 128.1, 126.7, 125.7, 118.5, 117.7, 62.8, 34.1, 20.9, 8.4. The ee value was 99.4%, t_R (minor) = 21.9 min, t_R (major) = 41.2 min (Chiralcel OD-H, $\lambda = 220$ nm, hexane/*i*-PrOH = 7/3, flow rate = 0.5 mL/min). HRMS (ESI) m/z calcd for $\text{C}_{16}\text{H}_{19}\text{NO}$ (M-H) $^-$ 240.1394, found 240.1397.

<Chromatogram>

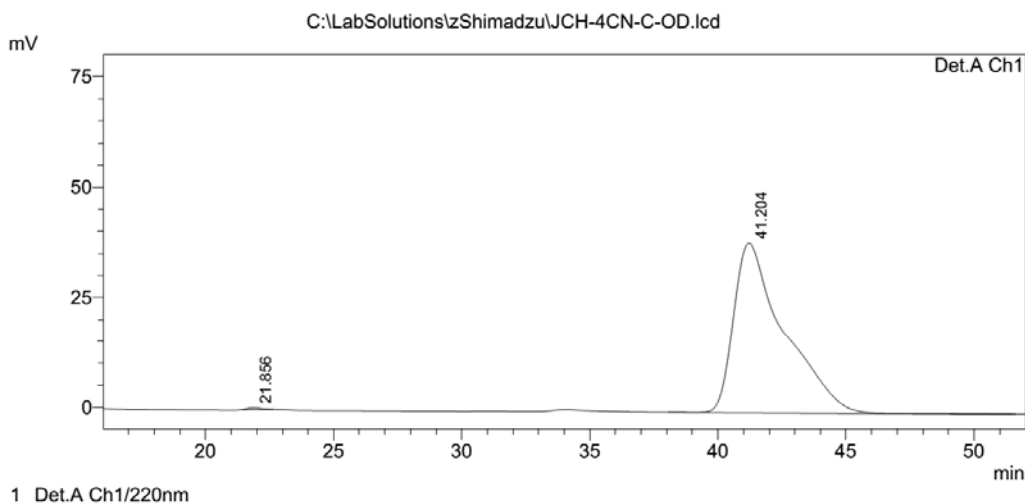


PeakTable

Peak#	Ret. Time	Area	Height	Area %	Height %
1	21.869	10526445	150555	49.977	66.147
2	41.200	10536047	77051	50.023	33.853
Total		21062492	227606	100.000	100.000

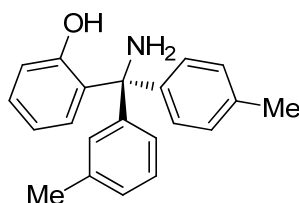
Racemic **2-21cn**

<Chromatogram>



PeakTable

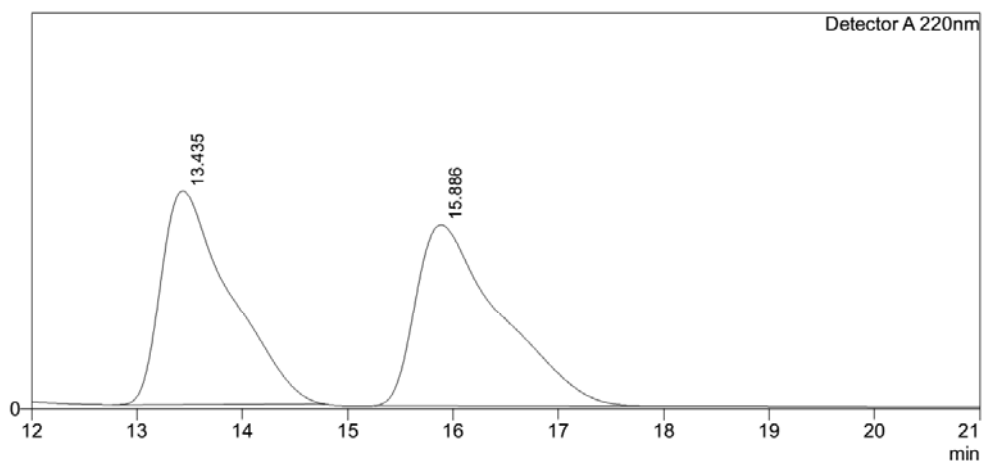
Peak#	Ret. Time	Area	Height	Area %	Height %
1	21.856	17131	442	0.324	1.133
2	41.204	5264903	38559	99.676	98.867
Total		5282034	39001	100.000	100.000

Enantiomerically enriched **2-21cn****2-21gn**

Compound 2-21gn. A colorless oil. $[\alpha]_D^{25} -0.4$ (c 1.0, CHCl_3). ^1H NMR (500 MHz, CDCl_3) δ 7.21–7.09 (m, 5H), 6.99 (d, $J = 8.1$ Hz, 2H), 6.96 (s, 1H), 6.88 (d, $J = 8.2$ Hz, 2H), 6.69 (t, $J = 7.5$ Hz, 1H), 6.55 (d, $J = 7.8$ Hz, 1H), 2.35 (s, 3H), 2.30 (s, 3H). ^{13}C NMR (125 MHz, CDCl_3) δ 158.1, 137.8, 136.9, 130.4, 130.3, 130.0, 129.3, 129.2, 128.9, 128.2, 128.1, 128.0, 127.5, 124.9, 118.3, 117.6, 67.1, 21.6, 21.0. The *ee* value was 97%, t_R (minor) = 12.3 min, t_R (major) = 15.8 min (Chiralcel OD-H, $\lambda = 220$ nm, hexane/*i*-PrOH = 7/3, flow rate = 0.5 mL/min). HRMS (ESI) m/z calcd for $\text{C}_{21}\text{H}_{21}\text{NO}$ (M-H) $^-$ 302.1550, found 302.1542.

<Chromatogram>

mV



<Peak Table>

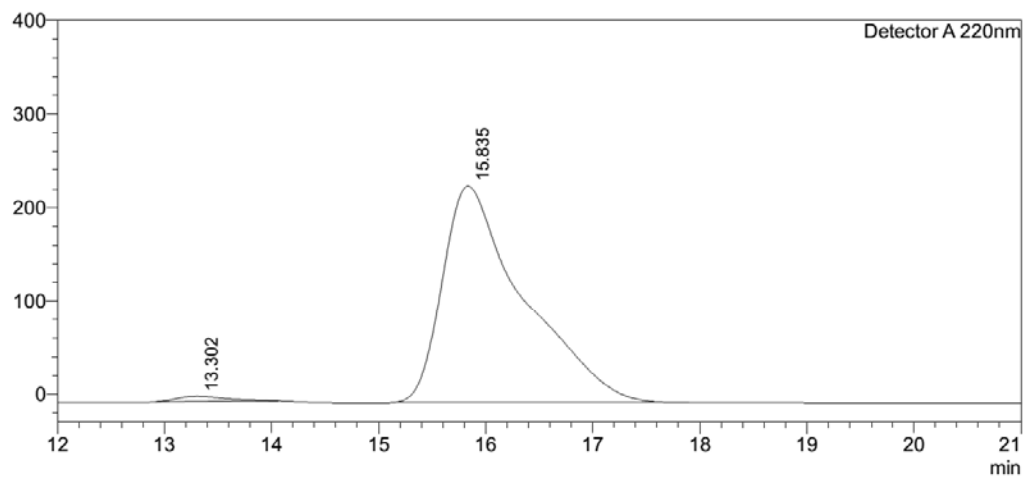
Detector A 220nm

Peak#	Ret. Time	Area	Height	Conc.	Unit	Mark	Name
1	13.435	99069453	2164875	49.302		M	
2	15.886	101875345	1834809	50.698		M	
Total		200944798	3999683				

Racemic **2-21gn**

<Chromatogram>

mV



<Peak Table>

Detector A 220nm

Peak#	Ret. Time	Area	Height	Conc.	Unit	Mark	Name
1	13.302	181556	5579	1.464		M	
2	15.835	12215648	231968	98.536		M	
Total		12397204	237548				

Enantiomerically enriched **2-21gn**

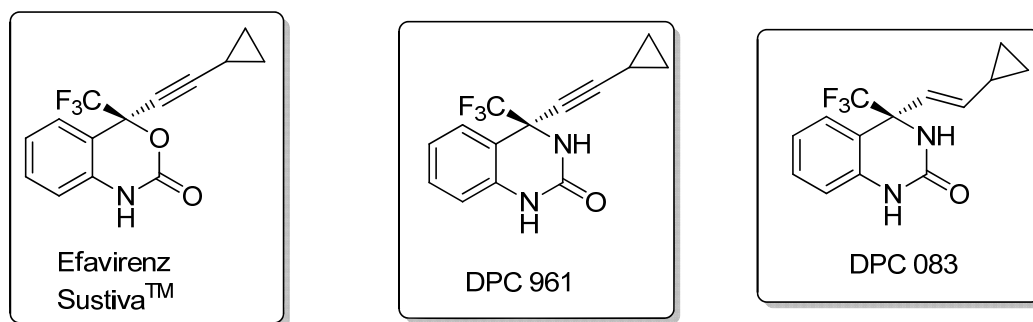
Chapter 3 Palladium(II)/PHOX Complex-Catalyzed Asymmetric Addition of Boron Reagents to Cyclic Trifluoromethyl Ketimines: An Efficient Preparation of Anti-HIV Drug Analogues

3.1 Introduction

Chiral nitrogen-containing compounds are widely distributed in nature and include many bioactive molecules. Among all of these compounds, dihydroquinazolines are taken as an important class of heterocyclic compounds due to their intriguing biological properties, such as antiviral, antiobesity activities and their use in the treatment in the cardiovascular diseases.⁸⁰ Notably, DPC 961 and DPC 083 of this class are second-generation HIV nonnucleoside reverse transcriptase inhibitors (NNRTIs) with enhanced potency when compared to Efavirenz (Sustiva) (Scheme 3.1).⁸¹ Therefore, enantioselectively synthesizing DPC 961 and DPC 083 analogues in efficient way has been attracting synthetic chemists since their high biological performances were discovered.

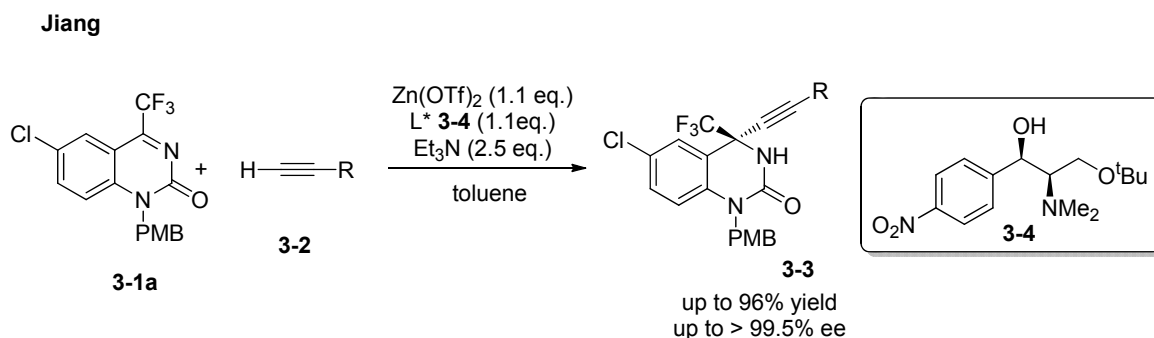
⁸⁰ a) J. W. Corbett, *Curr. Med. Chem.: Anti-Infect. Agents* **2002**, *1*, 119; b) S. G. Mueller, K. Rudolf, P. Lustenberger, D. Stenkamp, K. Arndt, H. Doods, G. Schaenzle, U.S. Pat. 20050234054, **2005**; c) H. Hasegawa, M. Muraoka, K. Matsui, A. Kojima, *Bioorg. Med. Chem. Lett.* **2003**, *13*, 3471.

⁸¹ J. W. Corbett, S. S. Ko, J. D. Rodgers, L. A. Gearhart, N. A. Magnus, L. T. Bachelier, S. Diamond, S. Jeffrey, R. M. Klabe, B. C. Cordova, S. Garber, K. Logue, G. L. Trainor, P. S. Anderson, S. K. Erickson-Viitanen, *J. Med. Chem.* **2000**, *43*, 2019.



Scheme 3.1 Structures of Efavirenz, DPC 961 and DPC 083

In 2004 Jiang group reported the first example of using achiral substrate **3-1a** to directly obtain DCP 961 and its analogues and stoichiometric amount of $\text{Zn}(\text{OTf})_2$ and derivatives of ephedrine **3-4** served as catalysts in this transformation (Scheme 3.2).⁸²

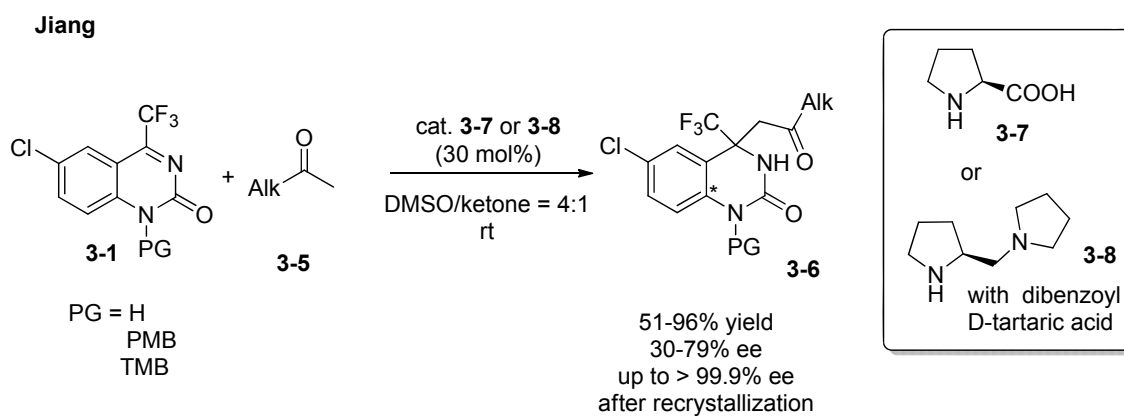


Scheme 3.2 $\text{Zn}(\text{OTf})_2$ promoted asymmetric alkylation of ketimine

Comparing with the metal-promoted reaction, organocatalysis was much more investigated to synthesize important intermediates of DPC 083 by applying different nucleophiles and activate models. Jiang group in 2008 demonstrated a high enantioselective construction of a quaternary carbon center of dihydroquinazoline **3-6** by an organocatalytic Mannich reaction with 30 mol% L-proline derivatives **3-7** or

⁸² B. Jiang, Y.-G. Si, *Angew. Chem. Int. Ed.* **2004**, *43*, 216

3-8 as catalyst (Scheme 3.3).⁸³

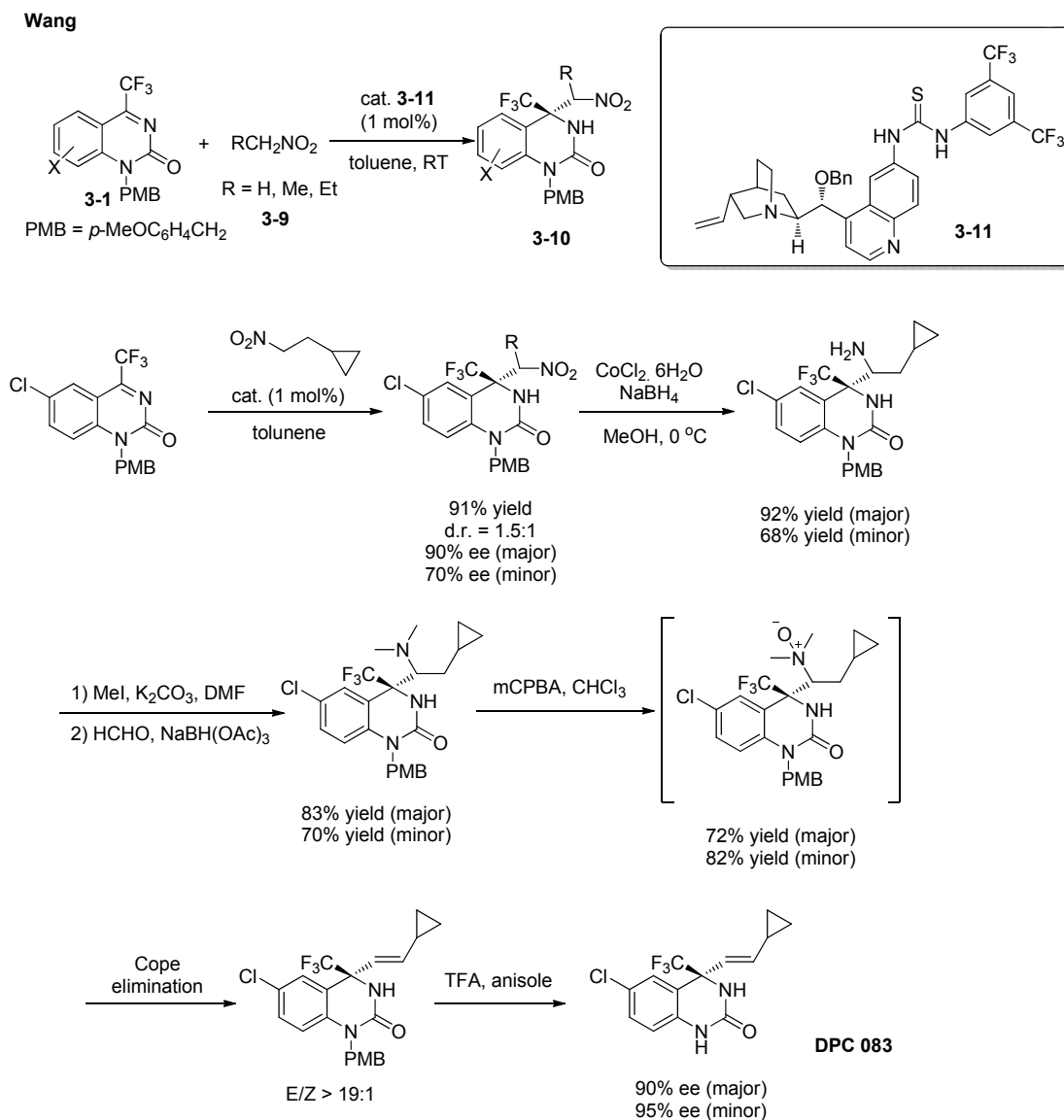


Scheme 3.3 Proline catalyzed asymmetric Mannich reaction of alkyl ketone and ketimine

Later on, Wang and coworkers developed a bifunctional cinchona alkaloid thiourea **3-11** catalyzed high efficient and enantioselective aza-Henry reaction of the cyclic trifluoromethyl ketimines **3-1** which served as a key step in the preparation of anti-HIV drug DPC 083 in 2011(Scheme 3.4).⁸⁴

⁸³ B. Jiang, J. J. Dong, Y. G. Si, X. L. Zhao, Z. G. Huang, M Xu, *Adv. Synth. Catal.* **2008**, 350, 1360.

⁸⁴ H. Xie, Y. Zhang, S. Zhang, X. Chen, W. Wang, *Angew. Chem. Int. Ed.* **2011**, 50, 11773.



Scheme 3.4 Bifunctional cinchona thiourea catalyzed asymmetric aza-Henry reaction of ketimines and derivation to DPC 083

In the recent two years, Ma group⁶ mainly worked on the important starting cyclic ketimine substrates and designed various organocatalytic asymmetric reactions based on hydrogen bond activation to achieve the anti-HTV drug analogues, such as Strecker reaction(2012),⁸⁵ decarboxylative Mannich reaction(2013)⁸⁶ and

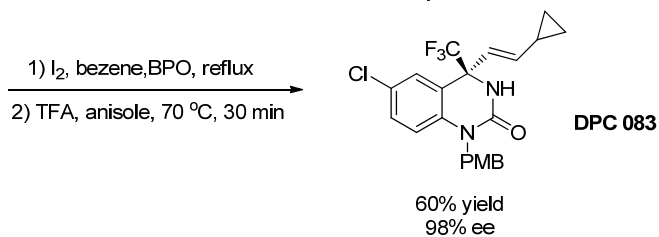
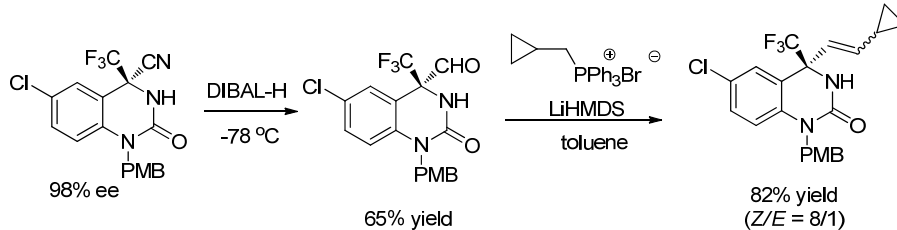
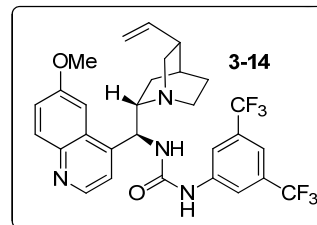
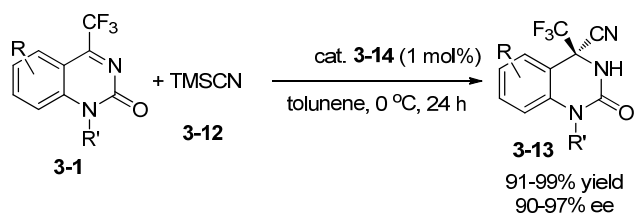
⁸⁵ F.-G. Zhang, X.-Y. Zhu, S. Li, J. Nie, J.-A. Ma, *Chem. Commun.* **2012**, 48, 11552.

⁸⁶ H.-N. Yuan, S. Wang, J. Nie, W. Meng, Q. Yao, J.-A. Ma, *Angew. Chem. Int. Ed.* **2013**, 52, 3869.

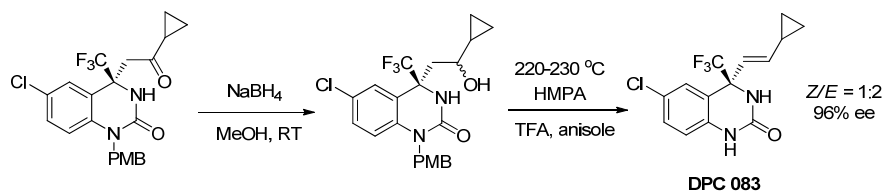
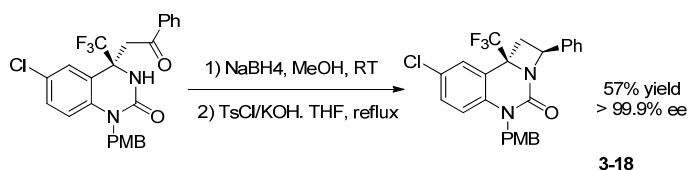
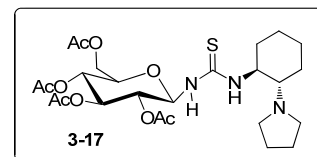
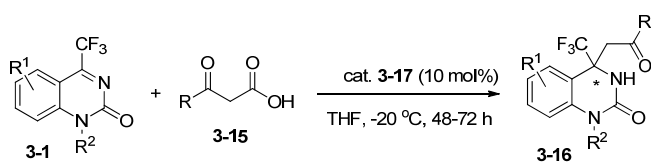
aza-Friedel-Crafts reaction(2013)⁸⁷ (Scheme 3.5).

Ma

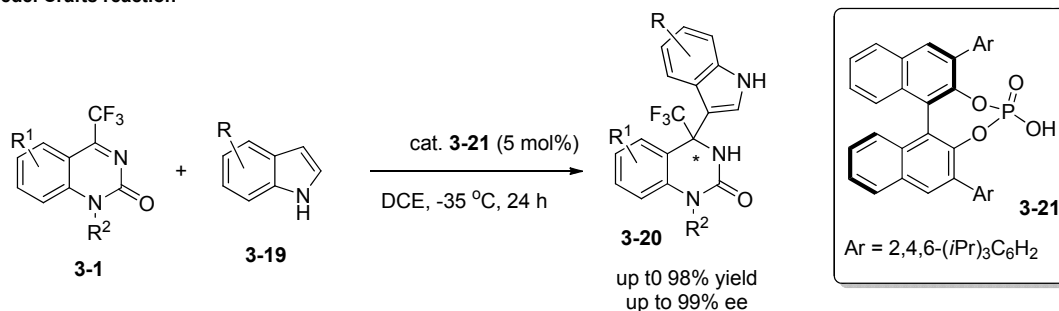
Strecker reaction



decarboxylative addition

⁸⁷ K.-F. Zhang, J. Nie, R. Guo, Y. Zheng, J.-A. Ma, *Adv. Synth. Catal.* **2008**, *350*, 1360.

Friedel Crafts reaction



Scheme 3.5 Ma's work on asymmetric reactions of ketimines and synthesis of DPC 083

From the above review, it can be generalized that most reported methods to synthesize anti-HIV drug analogues mainly focused on organo-catalytic asymmetric reactions. On the other hand, there was one only report about direct synthesis of DPC 961 analogues by metal promoted nucleophilic asymmetric addition to dihydroquinazolines. However, a stoichiometric amount catalyst loading was crucial to this chemical transformation.

Recently palladium- and Rhodium-catalyzed asymmetric additions of imines have emerged as a very important tool for generating disubstituted and trisubstituted amines with stereogenic carbon center.^[66] Our lab also reported the high performance of a palladium-PHOX catalyst in asymmetric arylation of cyclic *N*-sulfonyl ketimines.⁸⁸ To the best of our knowledge, no transition-metal-catalyzed asymmetric addition of cyclic trifluoromethyl ketimines was reported so far. Herein, we intend to apply transition-metal catalytic system in this transformation to obtain anti-HIV drug analogues.

⁸⁸ C. Jiang, Y. Lu, T. Hayashi, *Angew. Chem. Int. Ed.* **2014**, Early View. (DOI: 10.1002/anie.201406147)

3.2 Results and discussions

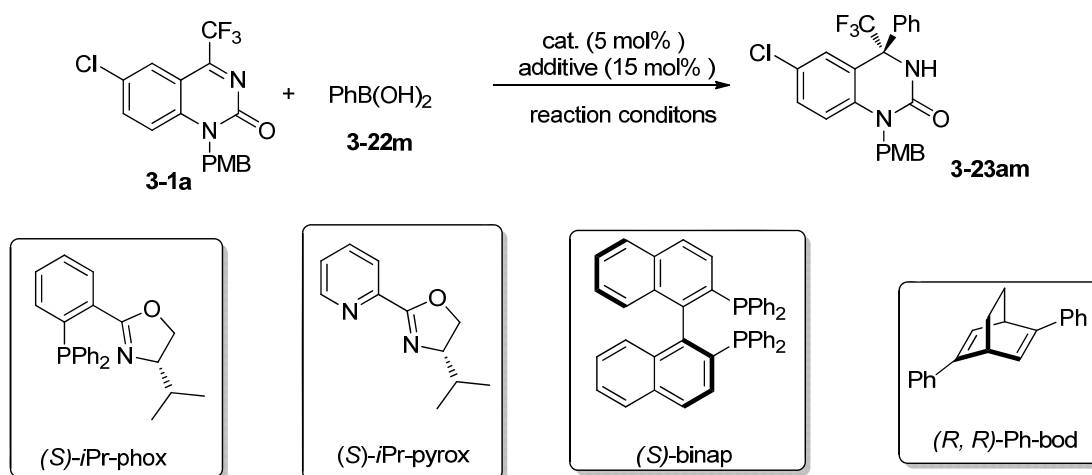
3.2.1 Catalyst screening

During our study on the catalytic asymmetric addition of organoboron reagents to cyclic trifluoromethyl ketimines **3-1**, it was found that the cationic palladium complex coordinated with a chiral phosphine-oxazoline ligand, which was proved to be efficient catalyst in asymmetric arylation of *N*-sulfonyl ketimines,⁸⁹ showed high catalytic activity and high enantioselectivity in the asymmetric addition of arylboronic acids to cyclic trifluoromethyl ketimines **3-1** to afford high yields of chiral dihydroquinazolines **3-23** which bear tetra-substituted stereogenic center.

We selected the asymmetric reaction of phenyl boronic acid **3-22m** to 6-chloro-1-(4-methoxybenzyl)-4-(trifluoromethyl)quinazolin-2(1H)-one **3-1a** as one of the model reactions, and a number of transition-metal catalytic systems were screened. The results are shown in Table 3.1.

Table 3.1 Catalytic Asymmetric Addition of Phenylboronic Acid to Cyclic *N*-trifluoromethyl ketimine ^[a]

⁸⁹ C. Jiang, Y. Lu, T. Hayashi, *Angew. Chem. Int. Ed.* **2014**, *53*, (DOI: 10.1002/anie.201406147).



	Cat. (5 mol%) additive	Solvent T [°C], t [h]	3-23am Yield ^[b] [%]	3-23am ee ^[c] [%]
1	PdCl ₂ [(S)-iPr-phox] AgBF ₄	ClCH ₂ CH ₂ Cl 65-70, 12	99	99.8, <i>R</i>
2	PdCl ₂ [(S)-iPr-phox] AgOTf	ClCH ₂ CH ₂ Cl 65-70, 12	90	99.8, <i>R</i>
3	PdCl ₂ [(S)-iPr-phox]	ClCH ₂ CH ₂ Cl 65-70, 12	0	-
4	PdCl ₂ [(S)-iPr-pyrox] AgBF ₄	ClCH ₂ CH ₂ Cl 65-70, 12	42	89
5	PdCl ₂ [(S)-binap] AgBF ₄	ClCH ₂ CH ₂ Cl 65-70, 12	0	-
6	[RhCl((R,R)-Ph-Bod)] ₂ K ₃ PO ₄ , t-amyl alcohol	dioxane 60, 12	67	93, <i>R</i>
7	PdCl ₂ [(S)-iPr-phox]	ClCH ₂ CH ₂ Cl	50	99.8, <i>R</i>

	AgBF ₄	25, 12		
8 ^[d]	PdCl ₂ [(<i>S</i>)- <i>i</i> Pr-phox]	ClCH ₂ CH ₂ Cl	99	99.8, <i>R</i>
	AgBF ₄	65-70, 12		

[a] Reaction conditions: **3-1a** (0.10 mmol), **3-22m** (0.20 mmol), catalyst (5 mol%), additive, solvent (1.0 mL) at a given temperature for 12 h. [b] Isolated yield of **3-23am**. [c] Determined by HPLC analysis with chiral columns. The absolute configuration of **3-23am** was determined by X-ray crystallographic analysis. [d] Catalyst (1 mol%) and additive (3 mol%) were employed.

The palladium-phosphineoxazoline complex with AgBF₄ as additive was firstly employed in this reaction. Excitingly, both excellent yield and ee were obtained under this catalytic system (entry 1). Less reactive additive AgOTf with Pd complex can also catalyze the transformation in lower yield (90%) and excellent ee (99.8%) (entry 2). It was found that generation of cationic palladium species is essential for the high catalytic activity. In the absence of AgBF₄, no additive product was observed (entry 3). To compare palladium-PHOX complex with other catalysts, those for the reaction in the presence of other palladium and rhodium complexes so far reported as effective catalysts were also examined. Palladium complex coordinated with chiral oxazoline-pyridine ligands can only give modest yield (42%) even though with good enantioselectivity (89% ee) (entry 4). Chiral Pd/BINAP system can not afford the desired product **3-23am** (entry 5). Chiral diene/rhodium catalyst, which was previously reported to be an efficient catalyst in asymmetric additions of organobron reagents catalyzed the phenylation of cyclic trifluoromethyl ketimine to

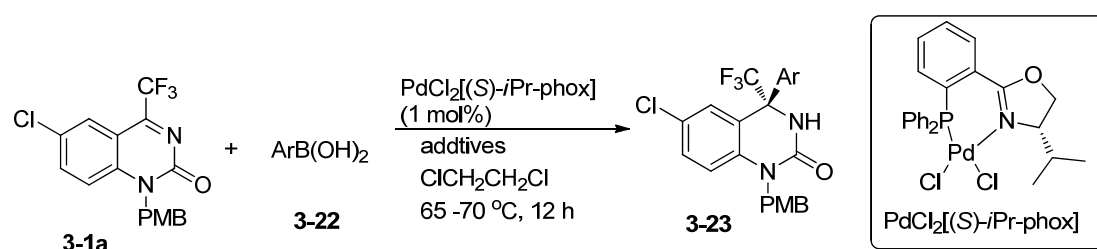
give product of high ee (93%) in a moderate yield (67%) (entry 6). Owing to high catalytic ability of Pd/PHOX complex, the reaction was further performed under room temperature, the enantioselectivity remained (99.8%) but yield dropped (50%) (entry 7). We were delighted to find the reaction proceed smoothly under 1 mol% catalyst loading under 65-70 °C (entry 8).

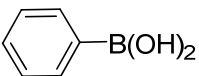
3.2.2 Substrate scope

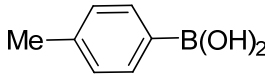
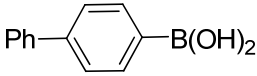
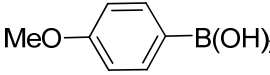
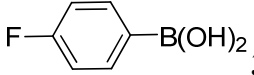
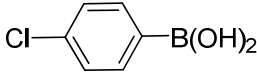
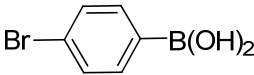
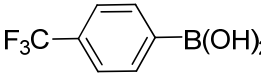
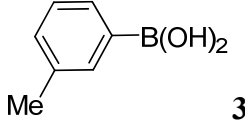
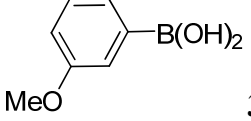
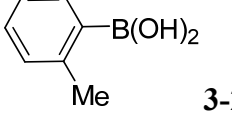
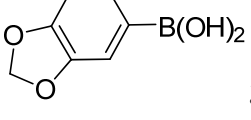
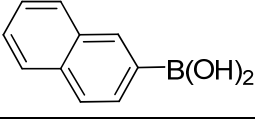
With the optimized condition in hand, we next studied the substrate scope of asymmetric addition of an array of different arylboronic acids **3-22** to the dihydroquinazoline **3-1a**.

Table 3.2 Catalytic Asymmetric Addition of Arylboronic Acid **3-22** to Cyclic

N-trifluoromethyl ketimine **3-1a** ^[a]



	additive	ArB(OH) ₂ 3-22	3-23 , yield	ee [%] ^[c]
			[%] ^[b]	
1	AgBF ₄	 3-22m	3-23am , 99	99.8, <i>R</i>

2	AgBF ₄		3-23an , 99	99.5, <i>R</i>
3	AgBF ₄		3-23ao , 82	99.9, <i>R</i>
4	AgBF ₄		3-23ap , 99	99.9, <i>R</i>
5	AgBF ₄		3-23aq , 87	99.9, <i>R</i>
6	AgBF ₄		3-23ar , 42	99.9, <i>R</i>
7	AgSbF ₆		3-23ar , 37	99.9, <i>R</i>
8	AgBF ₄		trace	-
9	AgBF ₄		trace	-
10	AgBF ₄		3-23au , 99	99.9, <i>R</i>
11	AgBF ₄		~20	-
12	AgBF ₄		3-23aw , 53	99.8, <i>R</i>
13	AgBF ₄		3-23ax , 97	99.5, <i>R</i>
14	AgBF ₄		~20	-

[a] Reaction conditions: **3-1a** (0.10 mmol), **3-22m** (0.20 mmol), catalyst (1 mol%), additive, solvent

(1.0 mL) at a given temperature for 12 h. [b] Isolated yield of **3-23**. [c] Determined by HPLC analysis with chiral columns.

The cationic palladium catalyst generated from PdCl₂[(*S*)-*i*-Pr-phox] and AgBF₄ was found to have wide applicability in the asymmetric addition of arylboronic acids **3-22** to the cyclic trifluoromethyl ketimine **3-1a**. The addition of phenylboronic acids substituted at para position with weak or strong electron-donating group methyl and methoxyl both gave the corresponding arylation products excellent enantioselectivity (99.5&99.9% ee) in excellent yield (99%) (entries 2 and 4). For those arylboronic acids which are with weak electron-withdrawing groups such as phenyl, bromo and chloro at para position, the enantioselectivity maintained very well (99.9% ee) but yields dropped as electron-withdrawing ability increasing (entries 3, 5 and 6). For para-substituted bromo and strong trifluoromethyl phenylboronic acids, the results were even worse and only trace amount of products can be observed (entries 8–9). Changing additive AgBF₄ to a more reactive AgSbF₆ could not influence the reactivity too much (entry 7). To our delight, under the standard condition both ortho- and meta-substituted phenylboronic acid with methyl group gave the product with high ee (99.9% and 99.8%) in moderate (53%) to excellent (99%) yields respectively (entries 12 and 10). From all of above results, it can be concluded that electron effects influence much more than steric effects in this transformation. It was found that the 3,4-(Methylenedioxy)phenylboronic acid performed better than 3-methoxyl-phenylboronic acid owing to the latter with a more electron-deficient

phenyl ring (entries 11 and 13). 1-Naphthylboronic acid was also tested and only low conversion (around 20%) to product can be afforded (entry 14).

3.2.3 Determination of absolute configuration

Furthermore, the absolute configuration of the product **3-23am** was determined to be *R* by X-ray crystallographic analysis (Figure 3.1).

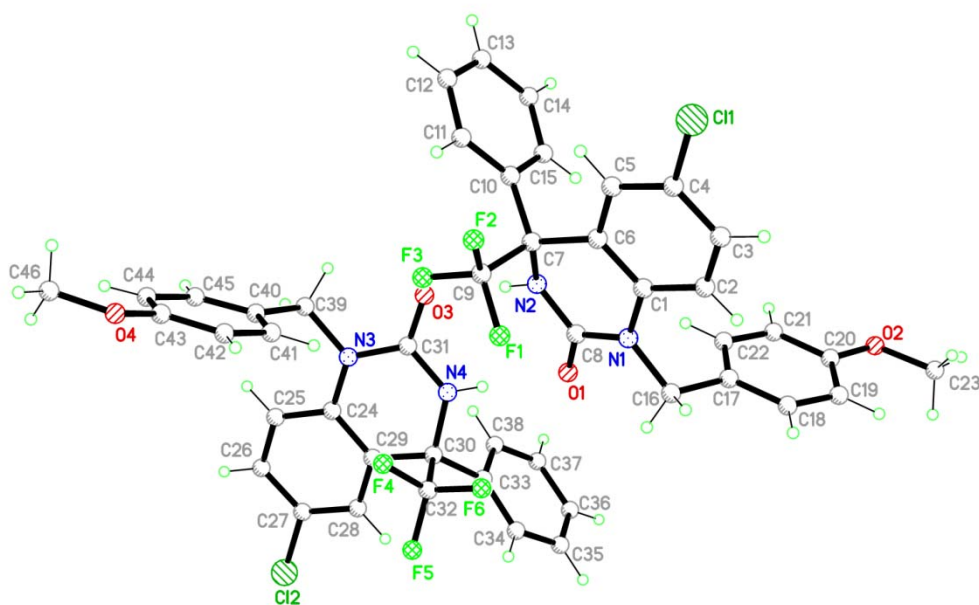


Figure 3.1 ORTEP structure of dihydroquinazoline **3-23am**

3.3 Conclusion

In conclusion, the first high enantioselective asymmetric addition of organoboron reagents to cyclic trifluoromethyl ketamine catalyzed by chiral palladium complex was described. The synthetic methodology reported provides easy access to chiral dihydroquinazolines bearing tetra-substituted stereogenic center which are also anti-HIV drug analogues. Further investigation on less reactive allylboron reagents

and direct synthesis of DPC 083 by this method are in progress.

3.4 Experimental section

3.4.1 General Information

All the starting materials were obtained from commercial sources and used without further purification unless otherwise stated. THF was dried and distilled from sodium benzophenone ketyl prior to use. DME and CH₂Cl₂ were distilled from CaH₂ prior to use. ¹H and ¹³C NMR spectra were recorded on a Bruker AMX500 (500 MHz) spectrometer. Chemical shifts were reported in parts per million (ppm), and the residual solvent peak was used as an internal reference: proton (chloroform δ 7.26), carbon (chloroform δ 77.0). Multiplicity was indicated as follows: s (singlet), d (doublet), t (triplet), q (quartet), m (multiplet), dd (doublet of doublet), and br s (broad singlet). Coupling constants were reported in Hertz (Hz). Low resolution mass spectra were obtained on a Finnigan/MAT LCQ spectrometer in ESI mode, and a Agilent Tech. 5975C inert MSD. All high resolution mass spectra were obtained on a Finnigan/MAT 95XL-T spectrometer. For thin layer chromatography (TLC), Merck pre-coated TLC plates (Merck 60 F254) were used, and compounds were visualized with a UV light at 254 nm. Further visualization was achieved by staining with iodine, or ceric ammonium molybdate followed by heating on a hot plate. Flash chromatographic separations were performed on Merck 60 (0.040-0.063 mm) mesh silica gel. The Enantiomerically excesses of products were determined by chiral-phase HPLC analysis, using a Daicel Chiralpak IC column (250 x 4.6 mm).

All the aryboronic acids are commercially available and used as received. The palladium complex PdCl₂[(*S*)-*i*Pr-phox]⁹⁰ was prepared from PdCl₂(MeCN)₂ and

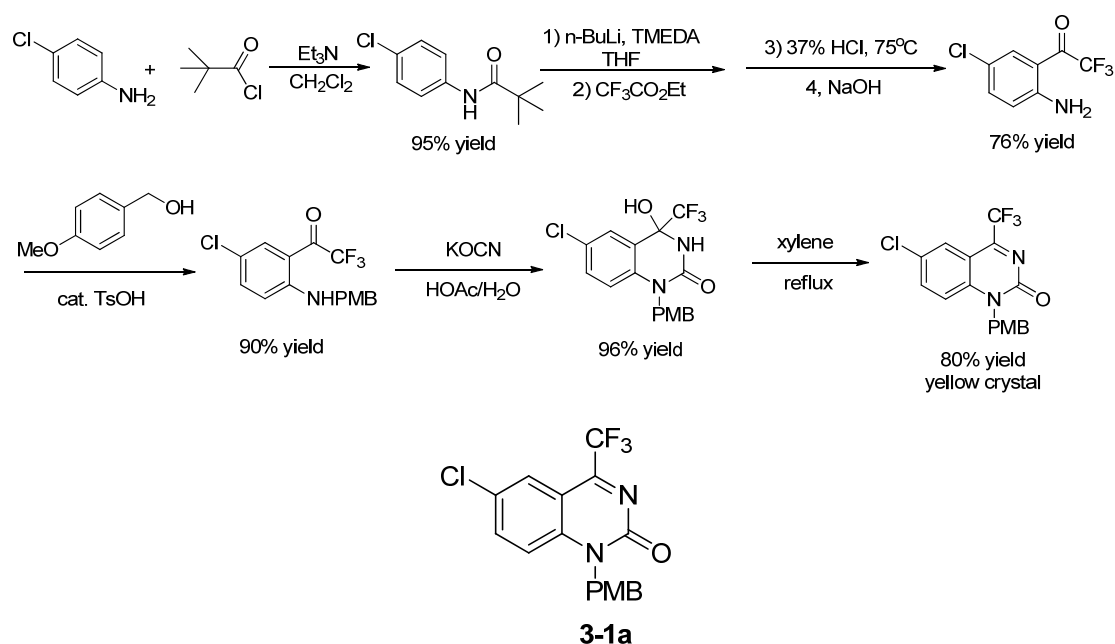
⁹⁰ Y. Uozumi, K. Kato, T. Hayashi, *Tetrahedron: Asymmetry* **1998**, *9*, 1065.

(*S*)-*i*Pr-phox (CAS: 148461-14-7, Strem Chemicals Inc.) in benzene according to the reported procedure.⁹⁰

3.4.2 Synthesis of cyclic *N*-trifluoromethyl ketimine

Following the published procedure, we synthesized the ketimine **3-1a** shown

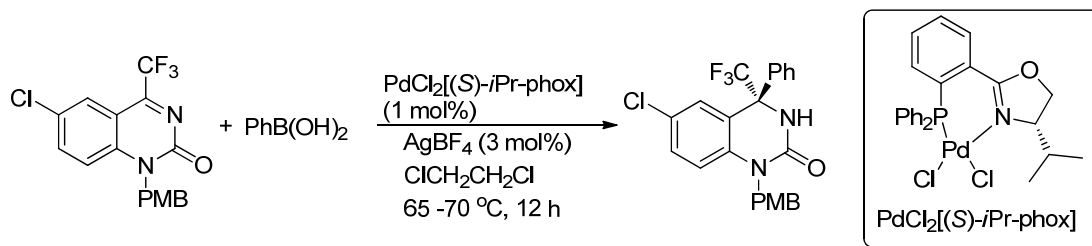
below.⁹¹



¹H NMR (500 MHz, CDCl₃): δ 7.97 (s, 1H), 7.67 (dd, *J* = 9.0, 2.0 Hz, 1H), 7.37 (d, *J* = 9.0 Hz, 1H), 7.21 (d, *J* = 8.5 Hz, 2H), 6.86 (d, *J* = 8.5 Hz, 2H), 5.47 (s, 2H), 3.77 (s, 3H).

3.4.3 Palladium-catalyzed asymmetric arylation of ketimines

⁹¹ N. A. Magnus, P. N. Confalone, L. Storace, M. Patel, C. C. Wood, W. P. Davis, R. L. Parsons, Jr., *J. Org. Chem.* **2003**, 68, 754.



$\text{PdCl}_2[(S)\text{-iPr-phox}]$ (2.9 mg, 0.0050 mmol), ketimine **xx** (36.8 mg, 0.100 mmol), and benzenboronic acid (**2-19m**) (24.4 mg, 0.200 mmol) were placed in Schlenk tube under nitrogen. To the tube, 1,2-dichloroethane (0.5 mL) was added, and then AgBF_4 (2.9 mg, 0.015 mmol) in 1,2-dichloroethane (0.5 mL) was added. The reaction mixture was stirred at 65–70 °C for 12 h, and the mixture was directly subjected to flash chromatography on silica gel using hexane/ethyl acetate (3:1) as an eluent to give **2-20bm** as a colorless solid (44.6 mg, 99% yield).

3.4.4 X-ray crystallographic analysis of 3-23am

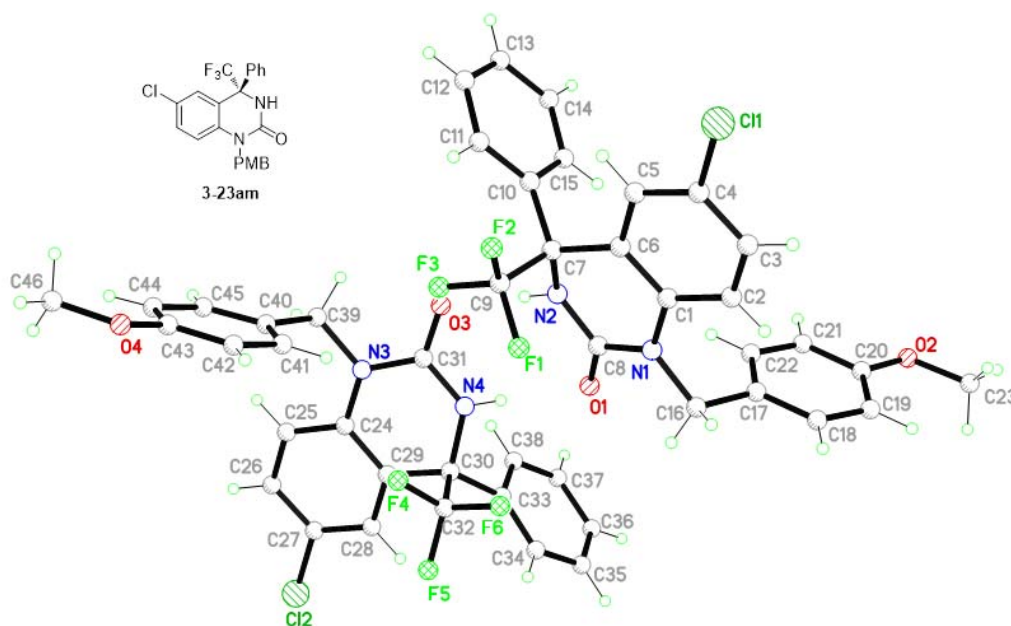


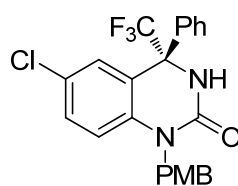
Figure 3.1 ORTEP structure of dihydroquinazoline **3-23am**

Table Crystal data

Identification code	E352
Empirical formula	C ₂₃ H ₁₈ Cl F ₃ N ₂ O ₂
Formula weight	446.84
Temperature	100(2) K
Wavelength	0.71073 Å
Crystal system	Orthorhombic
Space group	P2 ₁ 2 ₁ 2 ₁
Unit cell dimensions	a = 10.5894(4) Å α = 90°. b = 13.5143(5) Å β = 90°. c = 28.9569(11) Å γ = 90°.
Volume	4144.0(3) Å ³
Z	8
Density (calculated)	1.432 Mg/m ³
Absorption coefficient	0.234 mm ⁻¹
F(000)	1840
Crystal size	0.732 x 0.464 x 0.461 mm ³
Theta range for data collection	2.383 to 28.282°.
Index ranges	-14 ≤ h ≤ 13, -16 ≤ k ≤ 18, -38 ≤ l ≤ 36
Reflections collected	36385
Independent reflections	10230 [R(int) = 0.0234]

Completeness to theta = 25.242°	99.9 %
Absorption correction	Semi-empirical from equivalents
Max. and min. transmission	0.7457 and 0.6851
Refinement method	Full-matrix least-squares on F ²
Data / restraints / parameters	10230 / 0 / 569
Goodness-of-fit on F ²	1.039
Final R indices [I > 2sigma(I)]	R1 = 0.0299, wR2 = 0.0722
R indices (all data)	R1 = 0.0334, wR2 = 0.0741
Absolute structure parameter	-0.014(11)
Extinction coefficient	n/a
Largest diff. peak and hole	0.353 and -0.265 e.Å ⁻³

3.4.4 Analytical data of dihydroquinazoline 3-23



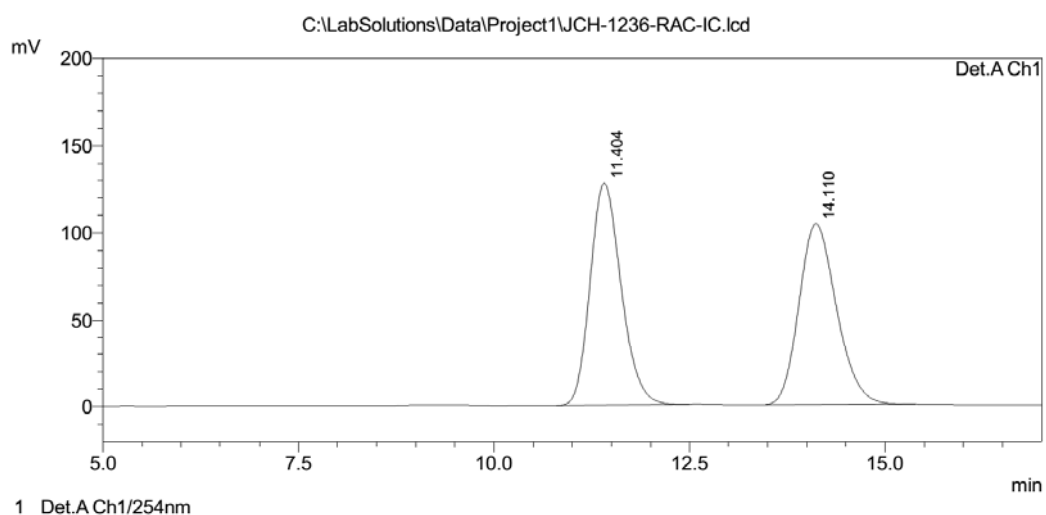
3-23am

Compound 3-23am. ¹H NMR (500 MHz, CDCl₃) δ 7.58 (d, *J* = 6.9 Hz, 2H), 7.46–7.39 (m, 3H), 7.18–7.13 (m, 3H), 6.85 (dd, *J* = 6.8, 4.7 Hz, 3H), 6.82 (d, *J* = 8.9 Hz, 1H), 5.95 (s, 1H), 5.20 (d, *J* = 16.3 Hz, 1H), 5.04 (d, *J* = 16.3 Hz, 1H), 3.78 (s, 3H).

¹³C NMR (126 MHz, CDCl₃) δ 158.86, 152.32, 137.81, 136.60, 130.12, 129.25, 129.15, 128.88, 128.14, 127.85, 127.83, 127.65, 127.53, 126.38, 124.09, 120.78,

116.00, 114.27, 65.98, 65.75, 55.23, 45.53. The *ee* value was 99.8%, t_R (major) = 11.7 min, t_R (minor) = 14.4 min (Chiralpak IC, $\lambda = 254$ nm, hexane/*i*-PrOH = 9/1, flow rate = 1.0 mL/min).

<Chromatogram>



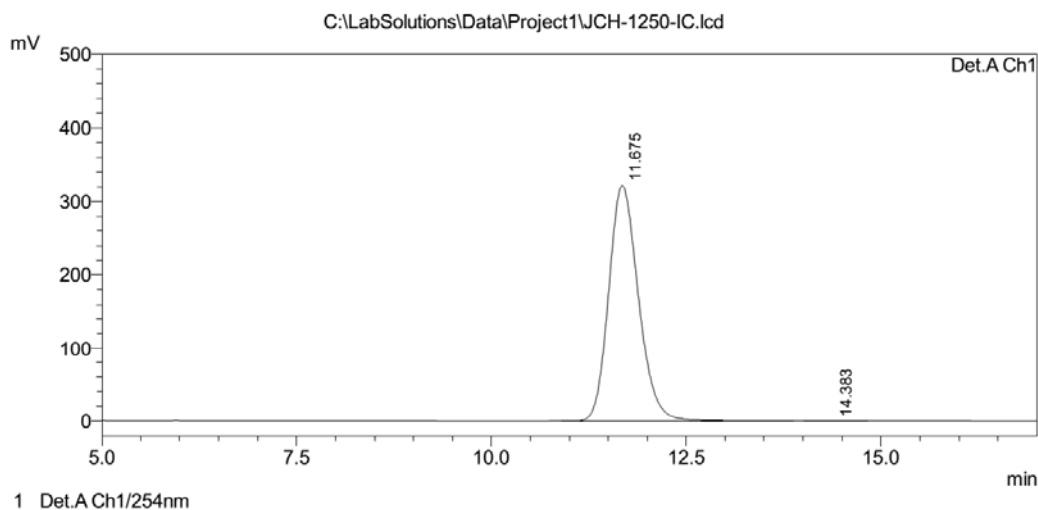
PeakTable

Detector A Ch1 254nm

Peak#	Ret. Time	Area	Height	Area %	Height %
1	11.404	3535647	127779	50.257	55.079
2	14.110	3499475	104214	49.743	44.921
Total		7035122	231993	100.000	100.000

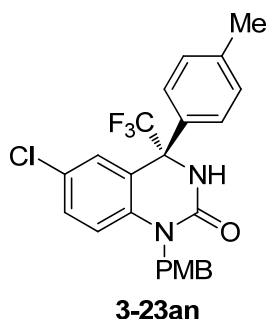
Racemic 3-23am

<Chromatogram>



PeakTable

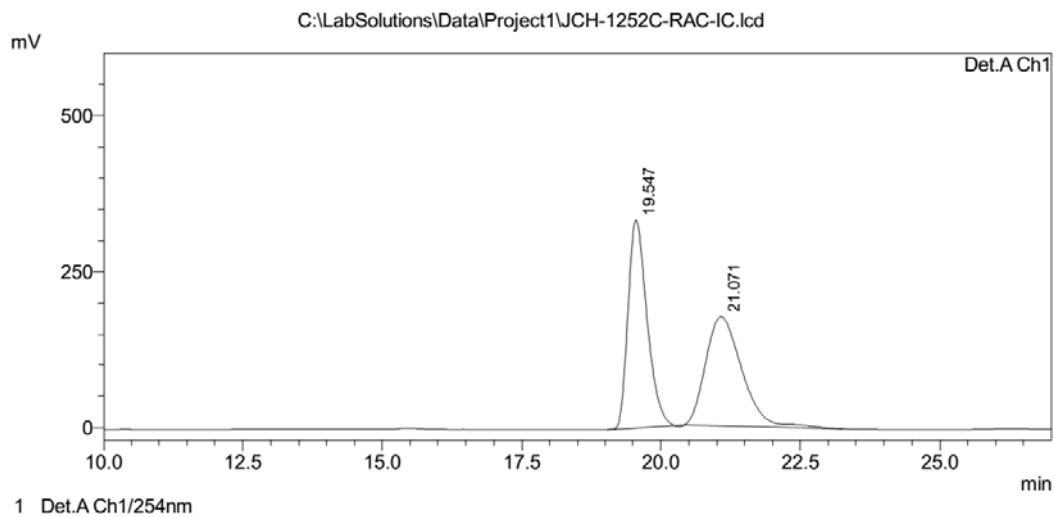
Peak#	Ret. Time	Area	Height	Area %	Height %
1	11.675	8561187	321415	99.842	99.841
2	14.383	13572	512	0.158	0.159
Total		8574758	321927	100.000	100.000

Enantiomerically enriched **3-23am**

Compound 3-23an. ^1H NMR (500 MHz, CDCl_3) δ 7.46 (d, $J = 7.9$ Hz, 2H), 7.22 (d, $J = 8.1$ Hz, 2H), 7.14 (dd, $J = 13.8, 5.2$ Hz, 3H), 6.85 (d, $J = 8.6$ Hz, 3H), 6.81 (d, $J = 8.9$ Hz, 1H), 5.94 (s, 1H), 5.21 (d, $J = 16.2$ Hz, 1H), 5.03 (d, $J = 16.3$ Hz, 1H), 3.78 (s, 3H), 2.38 (s, 3H). ^{13}C NMR (126 MHz, CDCl_3) δ 158.81, 152.37, 139.24, 136.56, 134.81, 130.02, 129.52, 129.17, 128.18, 127.68, 127.64, 127.44, 126.43, 124.13, 120.95, 115.92, 114.22, 65.78, 65.55, 55.21, 45.50, 21.00. The ee value was 99.5%, t_R (minor) = 20.0 min, t_R (major) = 21.6 min (Chiralpak IC, $\lambda = 254$ nm,

hexane/*i*-PrOH = 95/5, flow rate = 1.0 mL/min).

<Chromatogram>



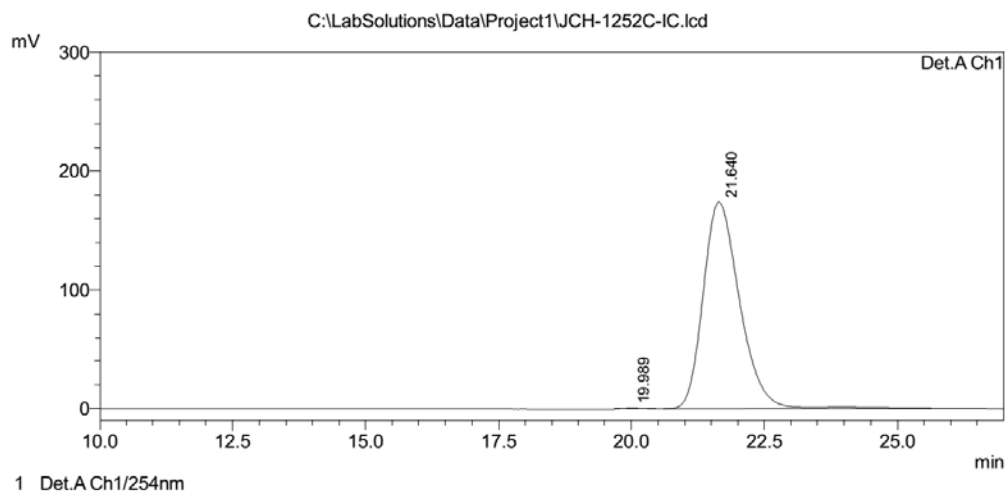
PeakTable

Detector A Ch1 254nm

Peak#	Ret. Time	Area	Height	Area %	Height %
1	19.547	7890566	333745	49.874	65.448
2	21.071	7930505	176191	50.126	34.552
Total		15821071	509936	100.000	100.000

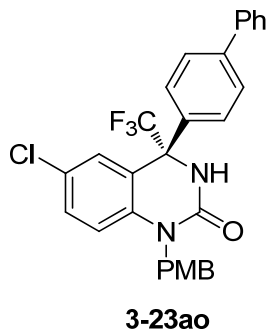
Racemic **3-23an**

<Chromatogram>



PeakTable

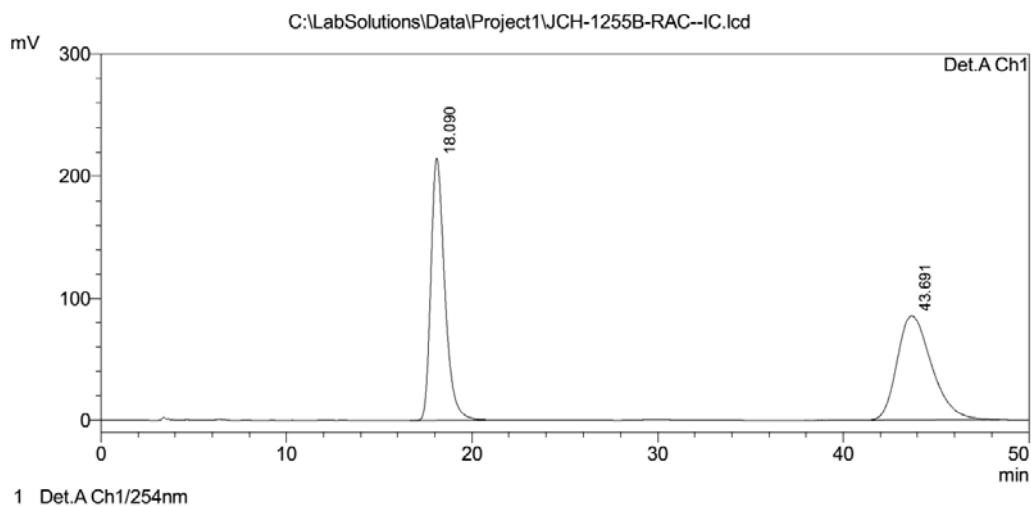
Peak#	Ret. Time	Area	Height	Area %	Height %
1	19.989	22749	934	0.272	0.533
2	21.640	8352126	174263	99.728	99.467
Total		8374875	175197	100.000	100.000

Enantiomerically enriched **3-23an**

Compound 3-23ao. ^1H NMR (500 MHz, CDCl_3) δ 7.65 (s, 4H), 7.61 (d, $J = 7.4$ Hz, 2H), 7.47 (t, $J = 7.6$ Hz, 2H), 7.40 (t, $J = 7.4$ Hz, 1H), 7.17 (dd, $J = 8.7, 3.6$ Hz, 3H), 6.90 (s, 1H), 6.84 (dd, $J = 8.5, 7.3$ Hz, 3H), 5.77 (s, 1H), 5.22 (d, $J = 16.2$ Hz, 1H), 5.07 (d, $J = 16.3$ Hz, 1H), 3.77 (s, 3H). ^{13}C NMR (126 MHz, CDCl_3) δ 158.88, 152.28, 142.12, 139.69, 136.62, 136.57, 130.22, 129.15, 128.94, 128.69, 128.29, 128.09, 127.96, 127.65, 127.63, 127.51, 127.13, 126.39, 124.10, 120.72, 116.07, 114.28, 65.89, 65.66, 55.24, 45.59. The *ee* value was 99.9%, t_{R} (major) = 18.2 min,

t_R (minor) = 44.0 min (Chiralpak IC, $\lambda = 254$ nm, hexane/*i*-PrOH = 9/1, flow rate = 1.0 mL/min).

<Chromatogram>



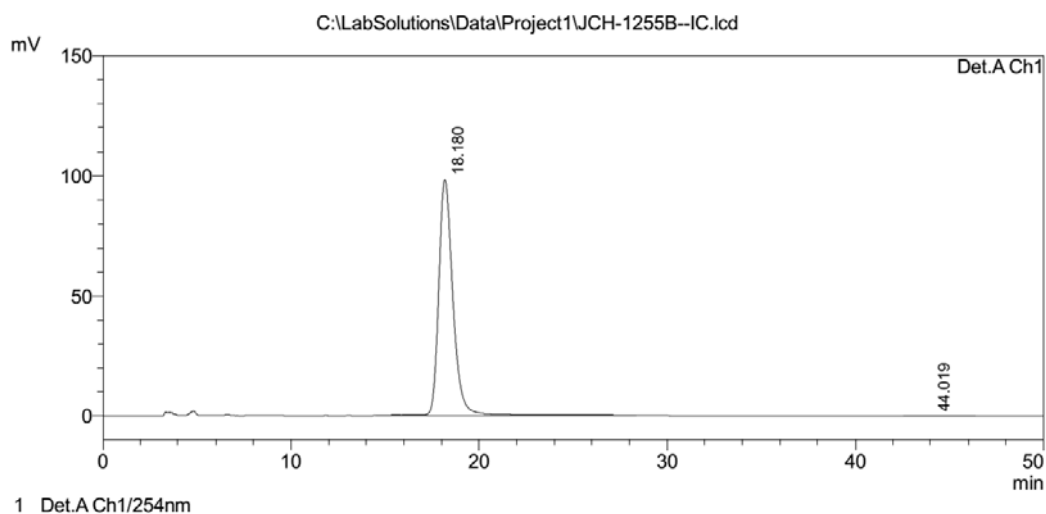
PeakTable

Detector A Ch1 254nm

Peak#	Ret. Time	Area	Height	Area %	Height %
1	18.090	11198745	214865	50.468	71.447
2	43.691	10991010	85868	49.532	28.553
Total		22189754	300733	100.000	100.000

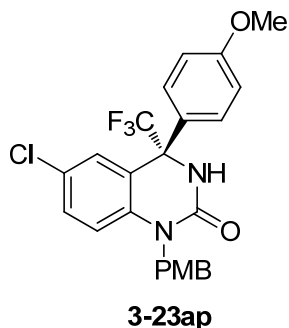
Racemic **3-23ao**

<Chromatogram>



PeakTable

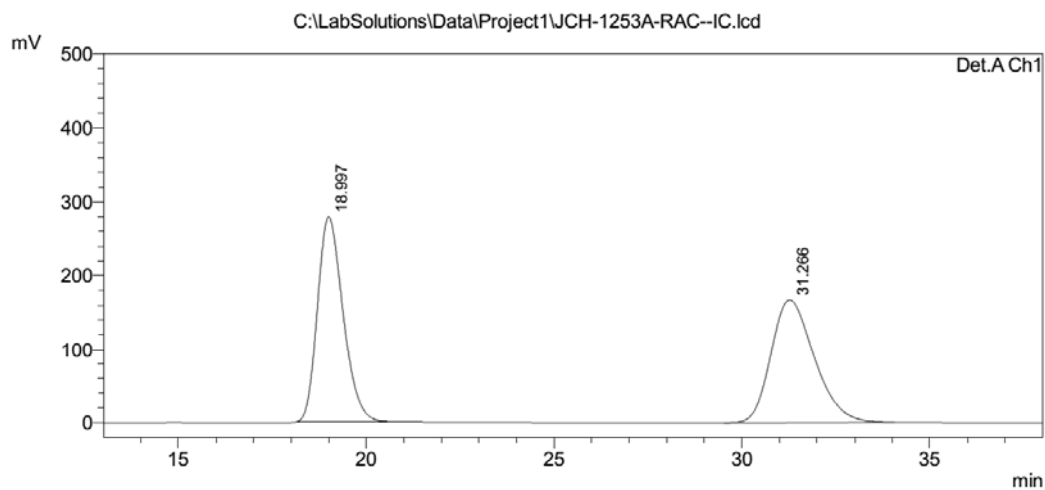
Peak#	Ret. Time	Area	Height	Area %	Height %
1	18.180	5246508	98545	99.924	99.954
2	44.019	4016	45	0.076	0.046
Total		5250524	98591	100.000	100.000

Enantiomerically enriched **3-23ao**

Compound 3-23ap. ^1H NMR (500 MHz, CDCl_3) δ 7.48 (d, $J = 8.6$ Hz, 2H), 7.14 (dd, $J = 11.8, 5.3$ Hz, 3H), 6.93 (d, $J = 8.9$ Hz, 2H), 6.87–6.77 (m, 4H), 5.93–5.85 (m, 1H), 5.20 (d, $J = 16.2$ Hz, 1H), 5.03 (d, $J = 16.2$ Hz, 1H), 3.83 (s, 3H), 3.78 (s, 3H). ^{13}C NMR (126 MHz, CDCl_3) δ 159.91, 158.82, 152.38, 136.56, 130.04, 129.67, 129.19, 128.17, 127.64, 127.47, 126.46, 124.16, 121.11, 115.93, 114.24, 114.13, 65.61, 65.38, 55.32, 55.22, 45.51. The *ee* value was 99.9%, t_{R} (major) = 20.2 min, t_{R} (minor) = 32.3 min (Chiralpak IC, $\lambda = 254$ nm, hexane/*i*-PrOH = 9/1, flow rate = 1.0

mL/min).

<Chromatogram>

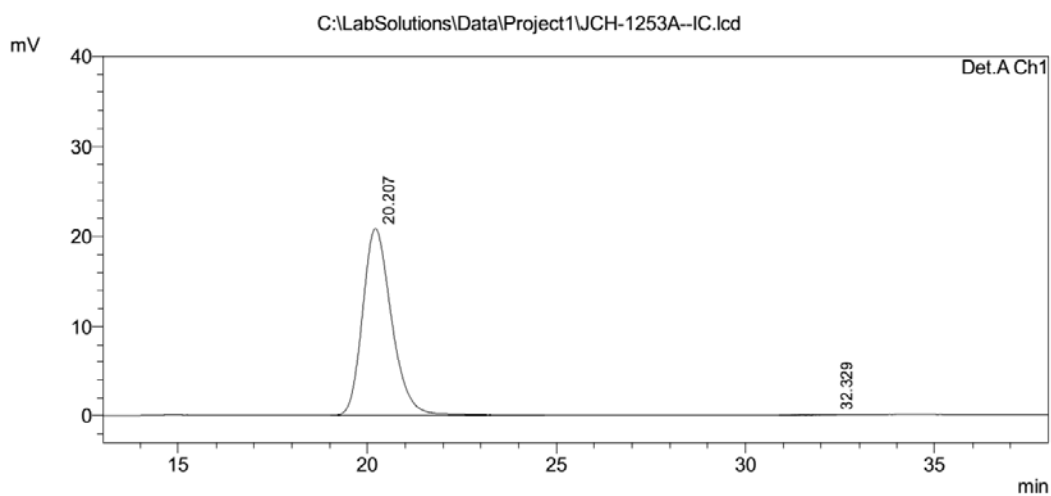


PeakTable

Peak#	Ret. Time	Area	Height	Area %	Height %
1	18.997	13228662	278528	49.696	62.456
2	31.266	13390300	167429	50.304	37.544
Total		26618962	445957	100.000	100.000

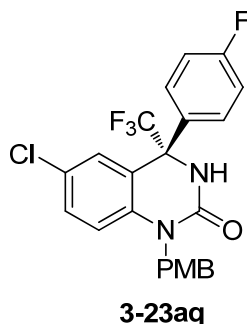
Racemic 3-23ap

<Chromatogram>



PeakTable

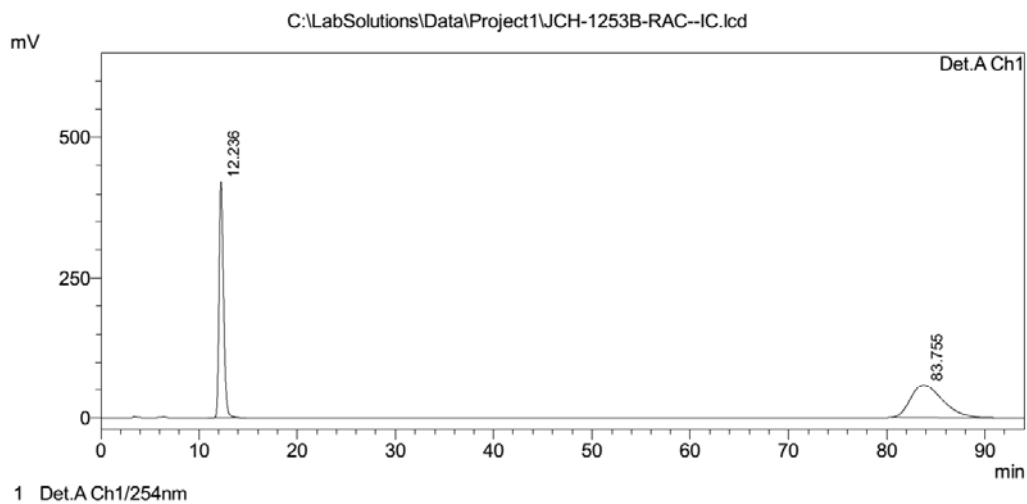
Peak#	Ret. Time	Area	Height	Area %	Height %
1	20.207	1111812	20843	99.989	99.975
2	32.329	121	5	0.011	0.025
Total		1111933	20848	100.000	100.000

Enantiomerically enriched **3-23ap**

Compound 3-23aq. ^1H NMR (500 MHz, CDCl_3) δ 7.57 (dd, $J = 8.2, 5.1$ Hz, 2H), 7.19–7.07 (m, 5H), 6.88 – 6.82 (m, 2H), 6.80 (d, $J = 10.1$ Hz, 1H), 6.13 (s, 1H), 5.18 (d, $J = 16.2$ Hz, 1H), 5.02 (d, $J = 16.3$ Hz, 1H), 3.78 (s, 3H). ^{13}C NMR (126 MHz, CDCl_3) δ 163.79, 161.80, 158.88, 152.33, 136.55, 133.69, 133.67, 130.28, 130.01, 129.96, 129.02, 128.03, 127.65, 126.29, 124.00, 120.59, 116.10, 116.00, 115.83, 114.26, 65.60, 65.37, 55.24, 45.54. The *ee* value was 99.8%, t_{R} (major) = 12.1 min, t_{R} (minor) = 81.5 min (Chiralpak IC, $\lambda = 254$ nm, hexane/*i*-PrOH = 9/1, flow rate =

1.0 mL/min).

<Chromatogram>

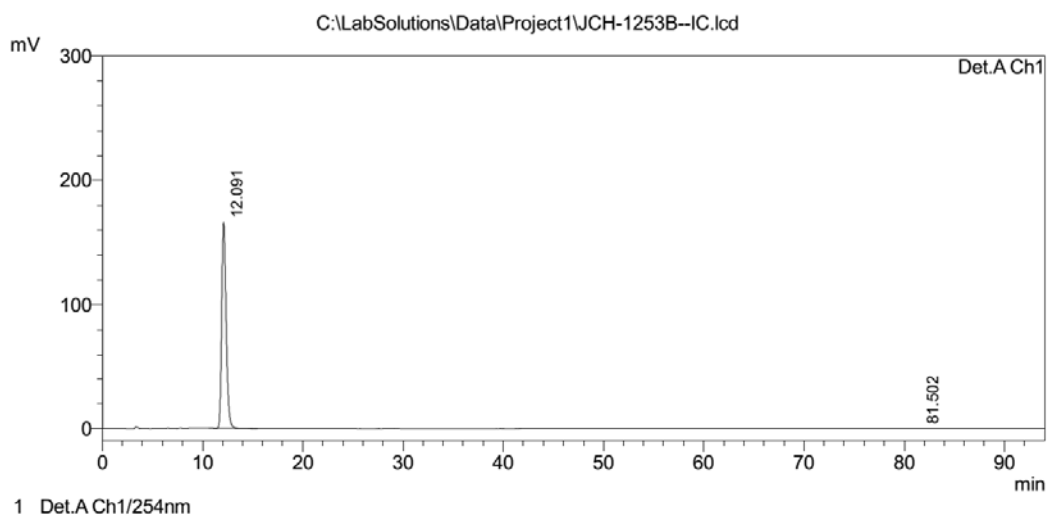


Peak Table

Peak#	Ret. Time	Area	Height	Area %	Height %
1	12.236	13390083	421436	50.521	87.830
2	83.755	13114169	58397	49.479	12.170
Total		26504252	479832	100.000	100.000

Racemic 3-23aq

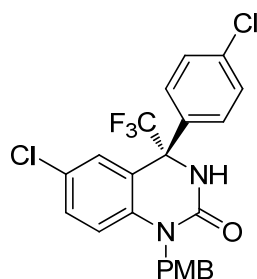
<Chromatogram>



Peak Table

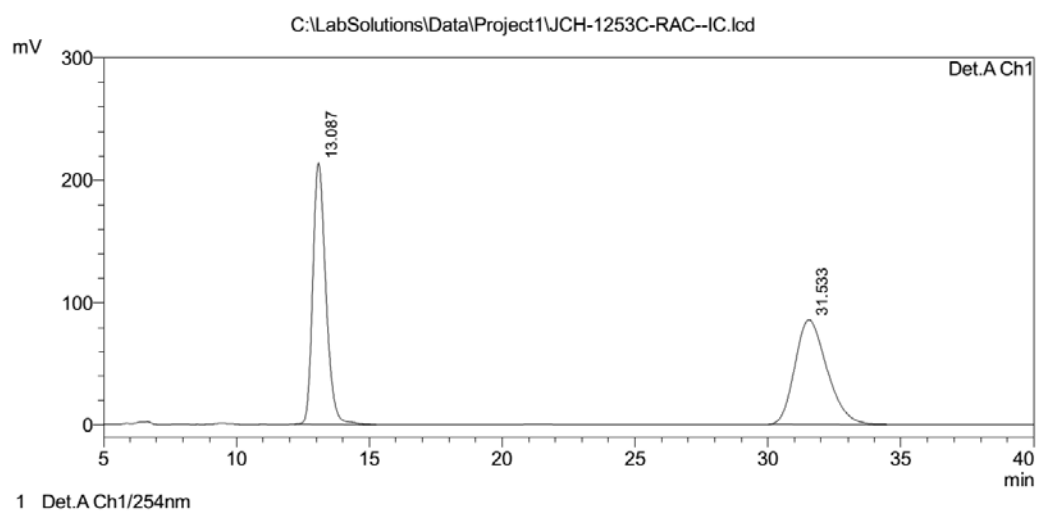
Detector A Ch1 254nm

Peak#	Ret. Time	Area	Height	Area %	Height %
1	12.091	5132146	166288	99.926	99.982
2	81.502	3818	29	0.074	0.018
Total		5135964	166318	100.000	100.000

Enantiomerically enriched **3-23aq****3-23ar**

Compound 3-23ar. $^1\text{H NMR}$ (500 MHz, CDCl_3) δ 7.52 (d, $J = 8.5$ Hz, 2H), 7.41 (d, $J = 8.7$ Hz, 2H), 7.17 (dd, $J = 8.9, 2.4$ Hz, 1H), 7.14 (d, $J = 8.6$ Hz, 2H), 6.84 (t, $J = 9.3$ Hz, 3H), 6.79 (s, 1H), 5.81 (s, 1H), 5.19 (d, $J = 16.2$ Hz, 1H), 5.03 (d, $J = 16.3$ Hz, 1H), 3.78 (s, 3H). The *ee* value was 99.9%, t_{R} (major) = 13.1 min, t_{R} (minor) = 31.6 min (Chiralpak IC, $\lambda = 254$ nm, hexane/*i*-PrOH = 9/1, flow rate = 1.0 mL/min).

<Chromatogram>

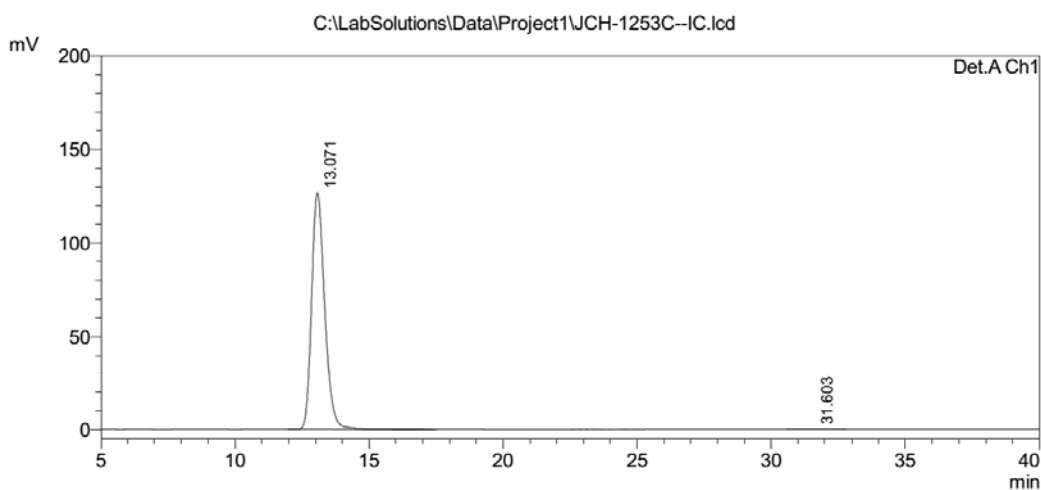


Peak Table

Peak#	Ret. Time	Area	Height	Area %	Height %
1	13.087	7307658	213834	50.278	71.299
2	31.533	7226813	86078	49.722	28.701
Total		14534471	299912	100.000	100.000

Racemic 3-23ar

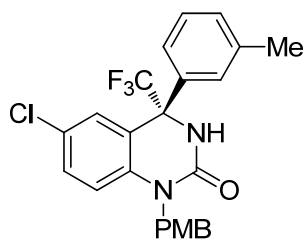
<Chromatogram>



PeakTable

Detector A Ch1 254nm

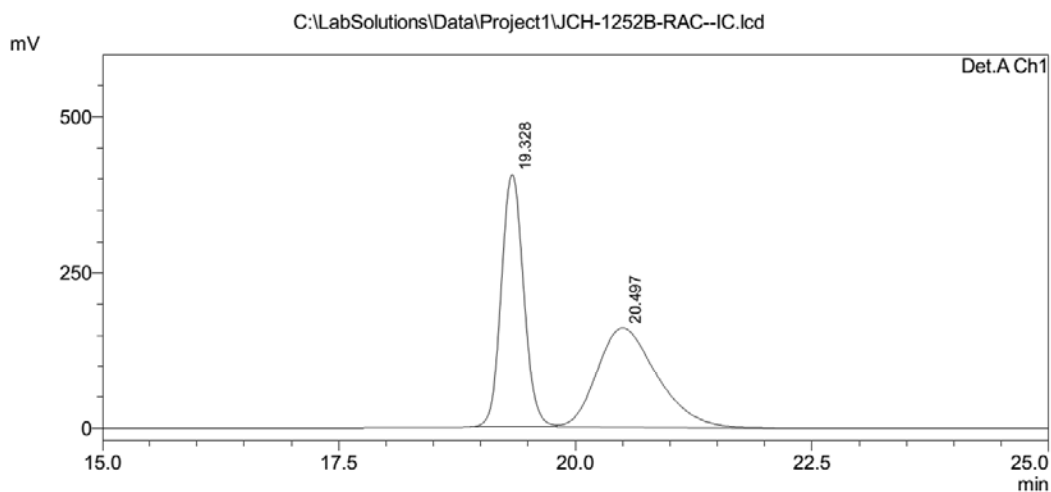
Peak#	Ret. Time	Area	Height	Area %	Height %
1	13.071	4300132	126842	99.945	99.966
2	31.603	2378	44	0.055	0.034
Total		4302510	126886	100.000	100.000

Enantiomerically enriched **3-23ar****3-23au**

Compound 3-23au. ^1H NMR (500 MHz, CDCl_3) δ 7.38 (d, $J = 9.9$ Hz, 2H), 7.31 (t, $J = 7.6$ Hz, 1H), 7.22 (d, $J = 7.4$ Hz, 1H), 7.20–7.12 (m, 3H), 6.85 (d, $J = 8.8$ Hz, 3H), 6.82 (d, $J = 8.9$ Hz, 1H), 5.91 (s, 1H), 5.23 (d, $J = 16.2$ Hz, 1H), 5.03 (d, $J = 16.3$ Hz, 1H), 3.78 (s, 3H), 2.38 (s, 3H). ^{13}C NMR (126 MHz, CDCl_3) δ 158.82, 152.33, 138.74, 137.70, 136.55, 130.07, 130.00, 129.20, 128.64, 128.50, 128.17, 127.65, 127.46, 126.41, 124.78, 124.11, 120.79, 115.93, 114.23, 65.93, 65.70, 55.21,

45.51, 21.59. The *ee* value was 99.9%, t_R (major) = 19.4 min, t_R (minor) = 21.7 min (Chiralpak IC, λ = 254 nm, hexane/*i*-PrOH = 95/5, flow rate = 1.0 mL/min).

<Chromatogram>



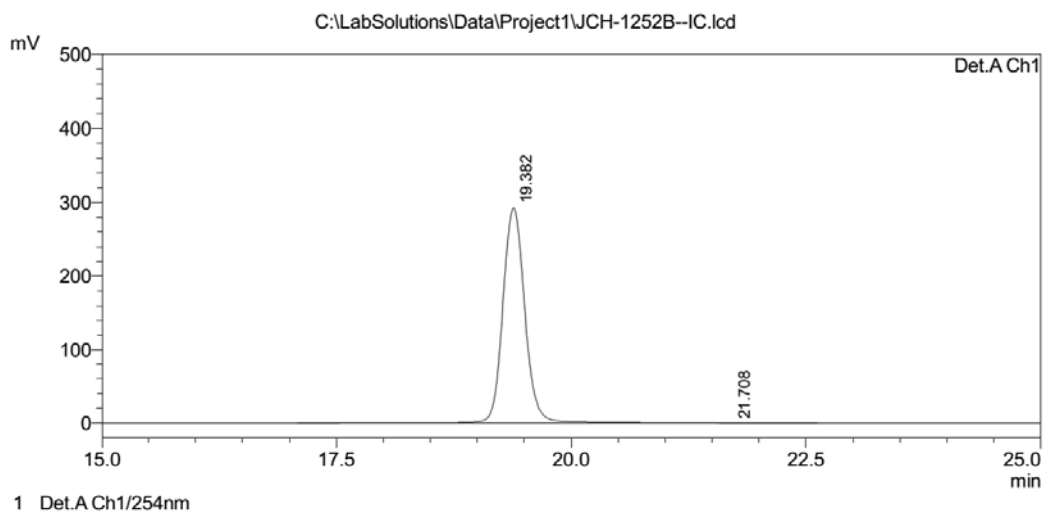
PeakTable

Detector A Ch1 254nm

Peak#	Ret. Time	Area	Height	Area %	Height %
1	19.328	6721425	406271	48.573	71.580
2	20.497	7116276	161304	51.427	28.420
Total		13837701	567575	100.000	100.000

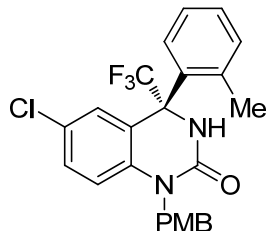
Racemic 3-23au

<Chromatogram>



Peak Table

Peak#	Ret. Time	Area	Height	Area %	Height %
1	19.382	4878195	292679	99.932	99.937
2	21.708	3318	184	0.068	0.063
Total		4881512	292863	100.000	100.000

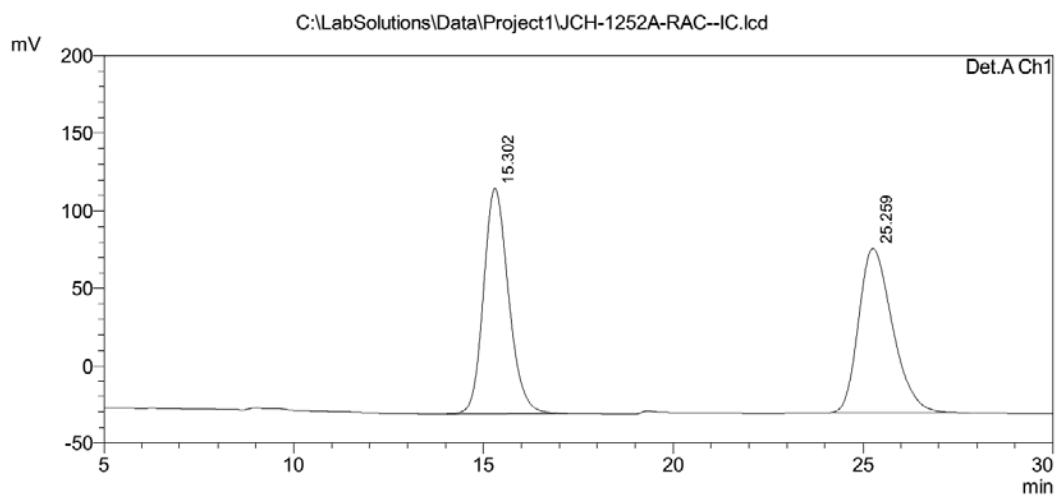
Enantiomerically enriched **3-23au****3-23aw**

Compound 3-23aw. ^1H NMR (500 MHz, CDCl_3) δ 7.62 (d, $J = 7.1$ Hz, 1H), 7.34 (t, $J = 7.1$ Hz, 1H), 7.29 (d, $J = 7.5$ Hz, 1H), 7.25 (d, $J = 14.3$ Hz, 1H), 7.20 (d, $J = 8.7$ Hz, 2H), 7.16 (dd, $J = 8.9, 2.3$ Hz, 1H), 6.87 (d, $J = 8.6$ Hz, 2H), 6.81 (d, $J = 8.9$ Hz, 1H), 6.72 (s, 1H), 5.63 (s, 1H), 5.21 (d, $J = 16.1$ Hz, 1H), 5.10 (d, $J = 16.2$ Hz, 1H), 3.78 (s, 3H), 2.05 (s, 3H). ^{13}C NMR (126 MHz, CDCl_3) δ 158.87, 151.94, 138.37, 137.07, 134.56, 134.10, 130.25, 129.60, 128.26, 128.24, 127.60, 127.57, 126.93, 126.90, 126.60, 125.81, 124.30, 119.50, 115.61, 114.29, 66.31, 66.09, 55.24, 45.62,

21.48. The *ee* value was 99.8%, t_R (major) = 15.2 min, t_R (minor) = 25.2 min

(Chiralpak IC, λ = 254 nm, hexane/*i*-PrOH = 95/5, flow rate = 1.0 mL/min).

<Chromatogram>

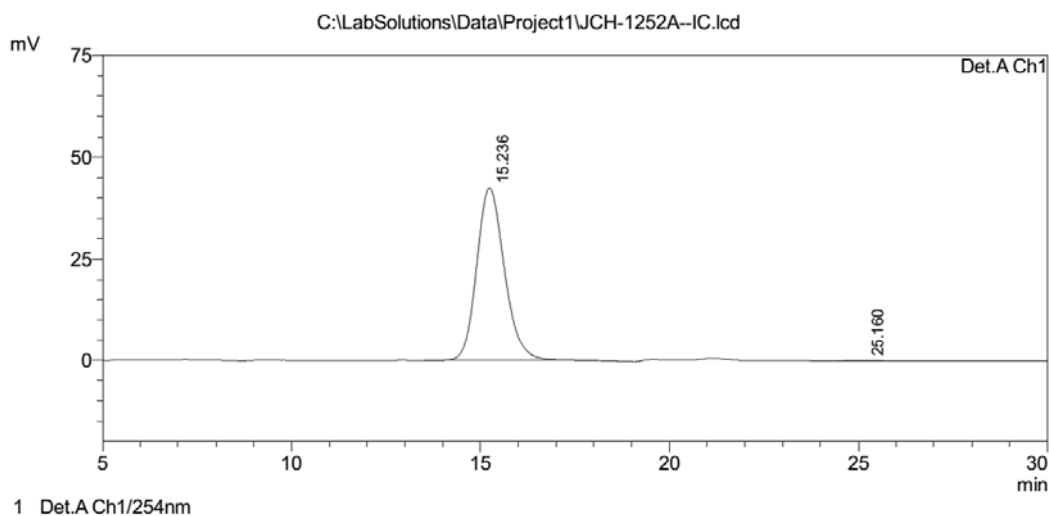


PeakTable

Peak#	Ret. Time	Area	Height	Area %	Height %
1	15.302	6687022	145759	50.173	57.759
2	25.259	6641017	106598	49.827	42.241
Total		13328039	252357	100.000	100.000

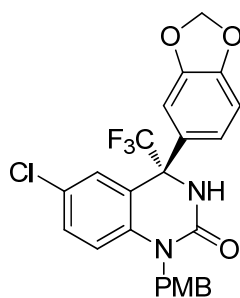
Racemic **3-23aw**

<Chromatogram>



PeakTable

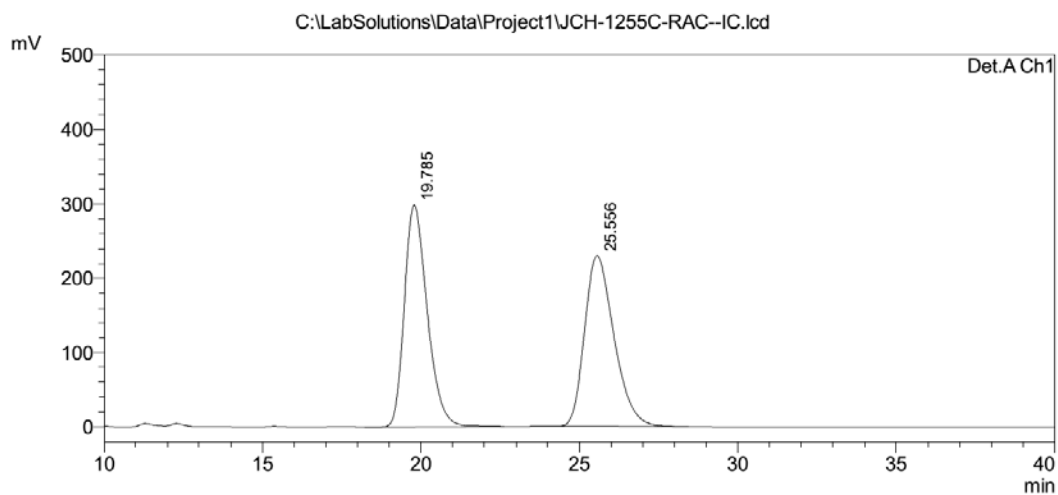
Peak#	Ret. Time	Area	Height	Area %	Height %
1	15.236	2202223	42614	99.876	99.857
2	25.160	2744	61	0.124	0.143
Total		2204967	42675	100.000	100.000

Enantiomerically enriched **3-23aw****3-23ax**

Compound 3-23ax. ^1H NMR (500 MHz, CDCl_3) δ 7.15 (d, $J = 8.6$ Hz, 3H), 7.08 (d, $J = 8.2$ Hz, 1H), 7.00 (s, 1H), 6.88 (s, 1H), 6.85 (d, $J = 8.6$ Hz, 2H), 6.83–6.79 (m, 2H), 6.00 (d, $J = 2.4$ Hz, 3H), 5.19 (d, $J = 16.2$ Hz, 1H), 5.02 (d, $J = 16.3$ Hz, 1H), 3.77 (s, 3H). ^{13}C NMR (126 MHz, CDCl_3) δ 158.83, 152.32, 148.21, 148.19, 136.49, 131.31, 130.13, 129.04, 128.11, 127.64, 127.53, 126.32, 124.03, 121.53, 120.81, 116.00, 114.24, 108.71, 108.04, 101.66, 65.81, 65.58, 55.22, 45.52. The *ee* value was 99.6%, t_{R} (major) = 19.9 min, t_{R} (minor) = 25.9 min (Chiralpak IC, $\lambda = 254$ nm,

hexane/*i*-PrOH = 9/1, flow rate = 1.0 mL/min).

<Chromatogram>



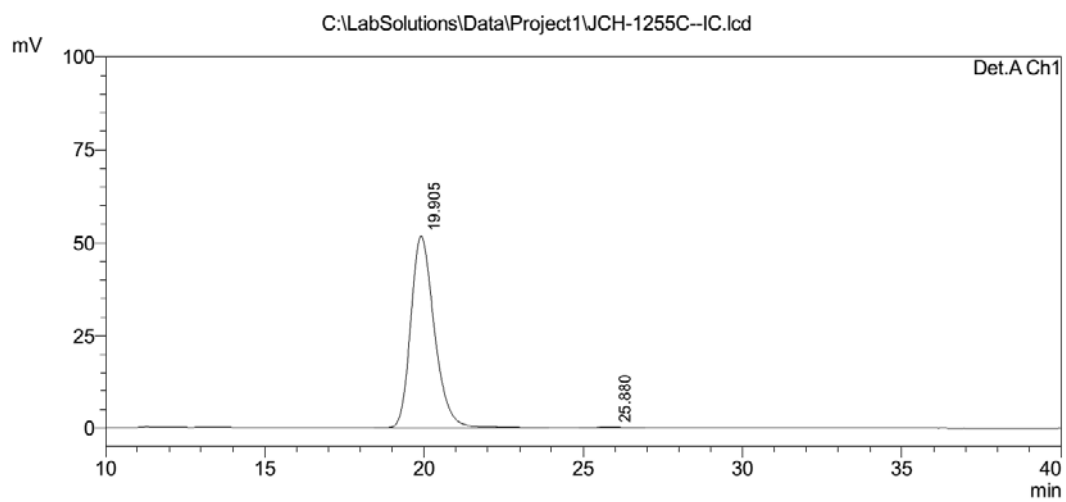
PeakTable

Detector A Ch1 254nm

Peak#	Ret. Time	Area	Height	Area %	Height %
1	19.785	14929020	297917	50.143	56.473
2	25.556	14843806	229622	49.857	43.527
Total		29772826	527538	100.000	100.000

Racemic 3-23ax

<Chromatogram>



PeakTable

Detector A Ch1 254nm

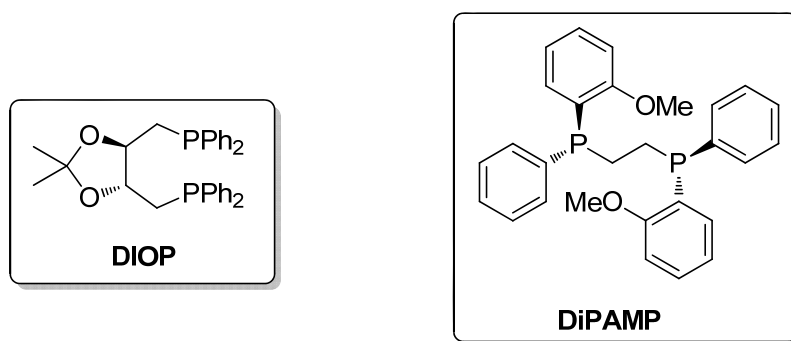
Peak#	Ret. Time	Area	Height	Area %	Height %
1	19.905	2666473	51785	99.770	99.799
2	25.880	6148	105	0.230	0.201
Total		2672621	51890	100.000	100.000

Enantiomerically enriched **3-23ax**

Chapter 4 Development of New Phosphine Ligands Derived from Amino Acids and Their Applications in Transition-Metal-Catalyzed Asymmetric Reactions

4.1 Introduction

The development of new chiral ligands always plays an important role in the discovery of asymmetric catalysts because the chiral ligands can support the metal ions and transfer their enantioselectivity in asymmetric reactions. Since its early invention of the chiral DIOP⁹² and DiPAMP⁹³ ligands (Scheme 4.1), continuous efforts have been put into this area and many thousands of chiral ligands have been synthesized. However, the development of new chiral ligands still remains a great task for synthetic chemists even today.

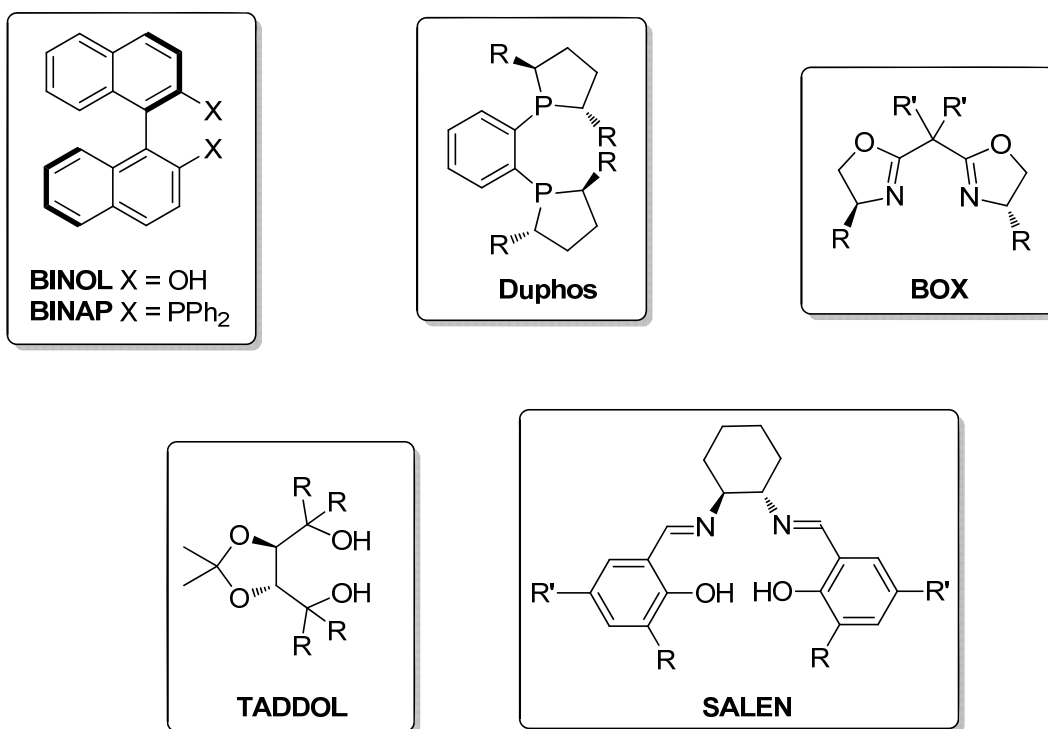


Scheme 4.1 Kagan's DIOP and Knowles' DiPAMP ligands

⁹² T. P. Dang, H. B. Kagan, *J. Chem. Soc. Chem. Commun.* **1971**, 481.

⁹³ B. D. Vineyard, W. S. Knowles, M. J. Sabacky, G. L. Bachman, D. J. Weinkauff, *J. Am. Chem. Soc.* **1977**, *99*, 5946.

The process of discovering new chiral ligand is empirical, which means rational design, systematic screening, and even intuition and chance are all playing important roles. Meanwhile, most of the developed chiral ligands have been tested in many different types of asymmetric reactions, but only a few classes of chiral compounds were identified to keep their enantioselective ability in a wide range of different asymmetric reactions. These ligands are so-called “privileged ligands” (Scheme 4.2).⁹⁴



Scheme 4.2 Examples of privileged chiral ligands

It is noteworthy that among all of the “privileged ligands”, phosphine based ligands are attracting tremendous attention for they are the most efficient ligands for

⁹⁴ a) T. P. Yoon, E. N. Jacobsen, *Science* **2003**, 299, 1691; b) A. Pfaltz, W. J. Drury III, *Proc. Natl. Acad. Sci. USA* **2004**, 101, 5723.

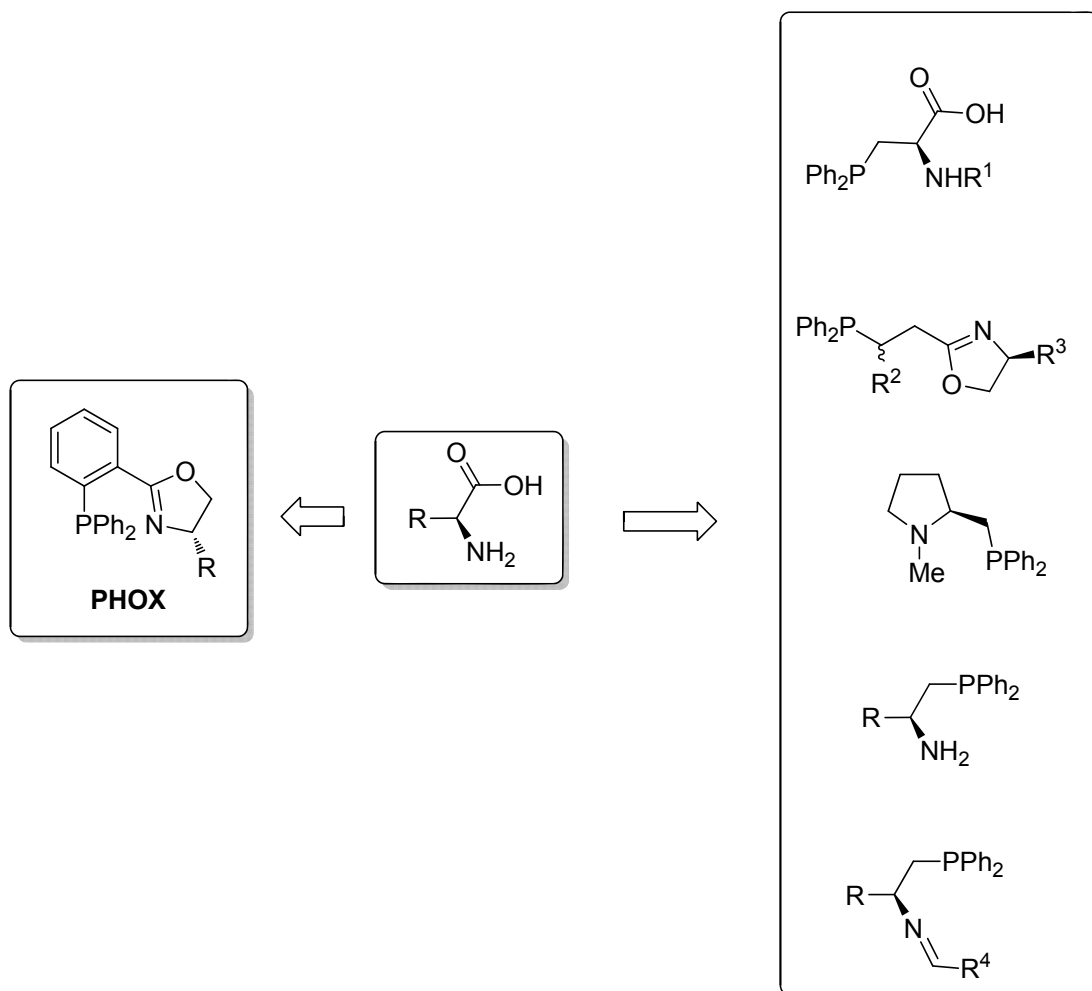
most homogeneous transition-metal catalysis. One of their advantages is that they can coordinate with the low-valent transition-metal intermediates and stabilize them to keep the high activity of catalysts which will influence the reaction efficiency in terms of catalytic activity and enantioselectivity.⁹⁵

On the other hand, amino acids are great naturally sources of chirality because they are readily available in enantiopure form, renewable and often of low cost. They have been employed as starting materials to produce many chiral compounds including the upper mentioned phosphine based ligands. One of the most famous ligand of them is phosphine-oxazoline (PHOX ligand).⁹⁶ The PHOX ligands are readily synthesized from the wide variety of commercial available amino alcohols and carboxylic acid derivatives, sharing scaffolds containing tri-aryl phosphines and oxazoline rings. Although they were originally designed for Pd-catalyzed asymmetric allylic substitution, they have been proved to be remarkably versatile ligands in a wide range of metal-catalyzed asymmetric reactions. Another typical phosphine ligands derived from amino acids have similar phosphine structures as the classical DIOP ligand, which the di-aryl phosphine groups are readily introduced onto the chiral scaffolds of amino acids. As a matter of fact, these types of phosphine ligands were less developed comparing PHOX ligands even though they also have been reported for many years since their first discovery. One of the main possible reason is their structures are usually much more flexible than the other commonly used ligands, which makes the coordination between metals and ligands weak and

⁹⁵ T. Hayashi, *Acc. Chem. Res.* **2000**, *33*, 354.

⁹⁶ G. Helmchen, A. Pfaltz, *Acc. Chem. Res.* **2000**, *33*, 336.

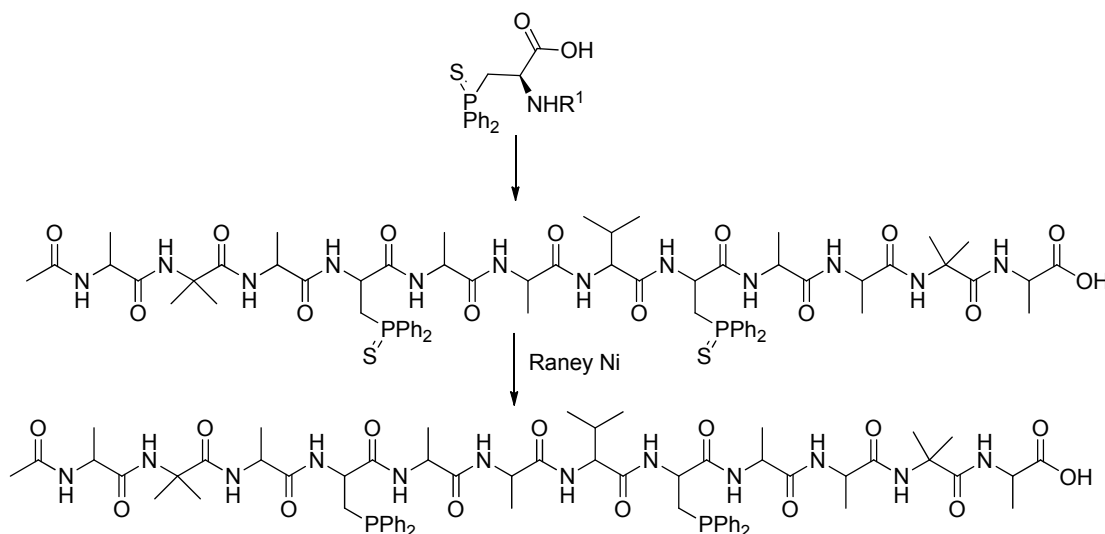
would further decrease both enantioselectivity and reaction efficiency (Scheme 4.3). One of the early studies of these flexible amino acid based phosphine ligands can be tracked back to Gilbertson's work in 1994. Gilbertson and co-workers developed a phosphorous containing derivative and used it as a key motif in synthesis of phosphine containing peptide, coordinating with rhodium to form a new metal peptide conjugate (Scheme 4.4).⁹⁷



⁹⁷ a) S. R. Gilbertson, G. Chen, M. McLoughlin, *J. Am. Chem. Soc.* **1994**, *116*, 4481; b) S. R. Gilbertson, X Wang, *J. Org. Chem.* **1996**, *61*, 434; c) S. R. Gilbertson, G.W. Starkey, *J. Org. Chem.* **1996**, *61*, 2922; d) S. R. Gilbertson, X. Wang, G. S. Hoge, C. A. Klung, J. Schaefer, *Organometallics*. **1996**, *15*, 6478; e) S. R. Gilbertson, G. Chen, J. Kao, A. Beatty, C.F. Campana, *J. Org. Chem.* **1997**, *62*, 5557; f) S. R. Gilbertson; C. T. Chang, *J. Org. Chem.* **1998**, *63*, 8424; g) S. R. Gilbertson, D. Xie, Z. Fu, *J. Org. Chem.* **2000**, *66*, 7240; f) G. Xu; S. R. Gilbertson, *Tetrahedron Lett.* **2002**, *43*, 2811; g) G. Xu, S. R. Gilbertson, *Tetrahedron Lett.* **2003**, *44*, 953.

Scheme 4.3 Amino acid derived chiral ligands: rigid versus flexible

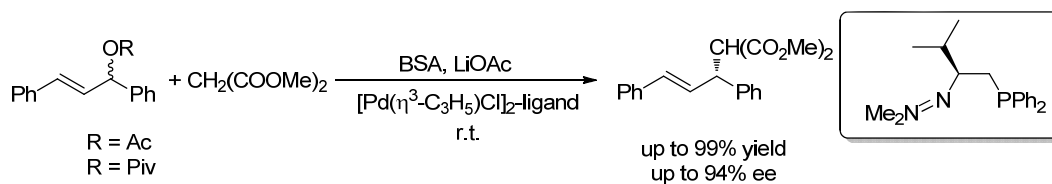
Gilbertson



Scheme 4.4 Gilbertson's phosphorus containing peptide ligands

Achiwa and co-workers in 1997 synthesized a new phosphorous containing amidine compound through several steps from L-valine, which was an excellent chiral ligand in the Pd-catalyzed asymmetric allylic alkylation (Scheme 4.5).⁹⁸

Achiwa



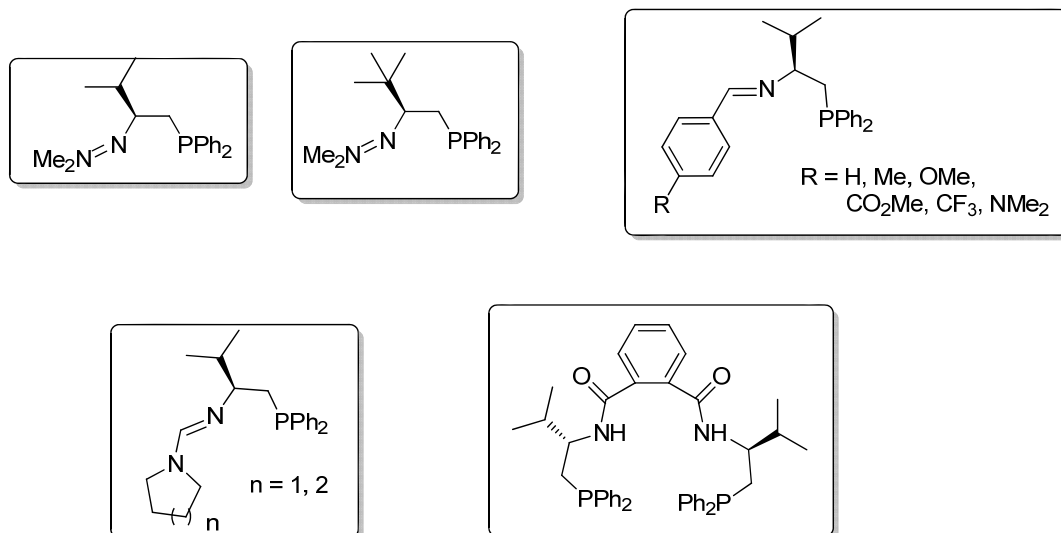
Scheme 4.5 Achiwa's phosphine-amidinate ligand in Pd-catalyzed AAA reaction

Later in 2000, Morimoto group modified the chiral amidine-phosphine ligand developed by Achiwa and produced a large library of these type bidentate ligands.

⁹⁸ A. Saitoh, T. Morimoto, K. Achiwa, *Tetrahedron: Asymmetry* **1997**, 8, 3567.

Furthermore, they studied the synthetic application and mechanism in the Pd-catalyzed asymmetric allylic substitutions (Scheme 4.6).⁹⁹

Morimoto



Scheme 4.6 Morimoto's extension of Achiwa's phosphine-amidinate ligand

Recently our group developed a new class of mono-phosphine catalysts which were proved to have excellent catalytic activity and enantioselectivity in many organo catalyzed asymmetric reactions.¹⁰⁰ These catalysts are all derived from natural amino acids and have flexible long-chained structures with amide functional groups. Inspired by these high structure similarities with the reported amino acid derived phosphine ligands, we decided to bring these organocatalysts as well as design some new derivatives into the metal-catalyzed asymmetric reaction serving as ligand partners.

To the best of our knowledge, no report has been published based on this proposed

⁹⁹ A. Saitoh, K. Achiwa, K. Tanaka, T. Morimoto, *J. Org. Chem.* **2000**, *65*, 4227.

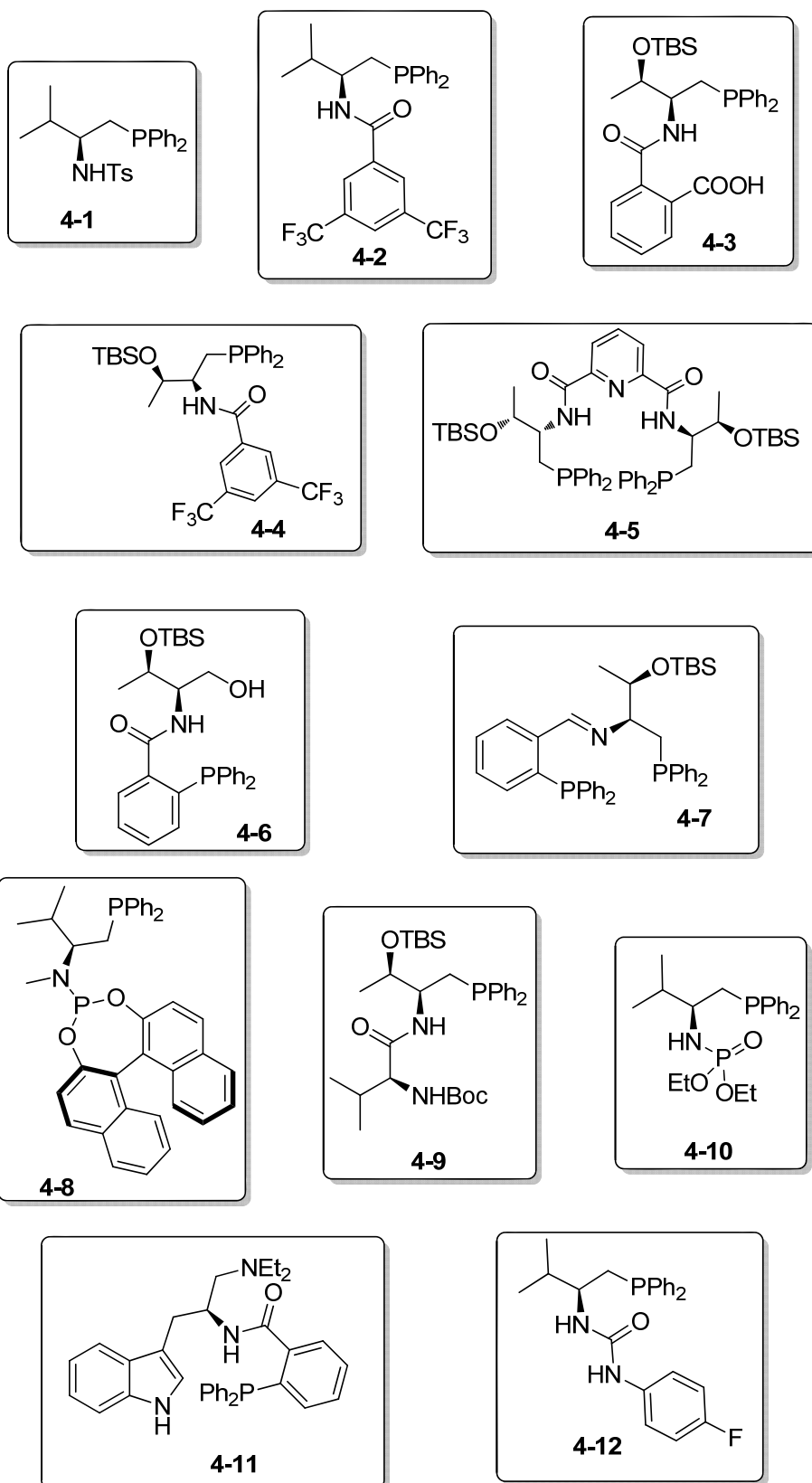
¹⁰⁰ a) X. Han, Y. Wang, F. Zhong, Y. Lu, *J. Am. Chem. Soc.* **2011**, *133*, 1726; b) F. Zhong, X. Han, Y. Wang, Y. Lu, *Angew. Chem. Int. Ed.* **2011**, *50*, 7837; c) F. Zhong, X. Han, Y. Wang, Y. Lu, *Chem. Sci.* **2012**, *3*, 1231; d) X. Han, F. Zhong, Y. Wang, Y. Lu, *Angew. Chem. Int. Ed.* **2012**, *51*, 767.

catalytic system so far. Herein, we developed a new type of phosphine ligand derived from amino acid and investigated its application in metal-catalyzed asymmetric reactions.

4.2 Results and discussions

4.2.1 Phosphine-amide ligands

At the beginning of our study, various phosphine amide ligands were synthesized from L-valine, L-threonine and L-troptophan, which are shown in Scheme 4.7.



Scheme 4.7 Phosphine-amide ligands derived from amino acids

We chose the Pd-catalyzed asymmetric allylic alkylation between dimethyl malonate **4-13** and (*E*)-1,3-diphenylallyl acetate **4-14** as the first model reaction (Table 4.1). This reaction was started by preparing the racemic product in the presence of Pd(PPh₃)₄ and found the desired product could be obtained in 92% yield. Then ligand **4-1** and [Pd(η³-C₃H₅)Cl]₂ was chosen as the catalyst partners, but no desired product was observed. Later, we tested the other three similar phosphine ligands **4-2**, **4-3** and **4-4** derived from L-valine and L-threonine respectively, none of them can afford the desired product. The same disappointing result occurred in the presence of phosphoramidite ligand **4-8**. Tri-aryl-phosphine based ligand **4-6** can finally give the product with around 60% conversion, but almost with no enantioselectivity. Bisphosphine ligands **4-5** and **4-7** were also used to improve the binding ability between ligands and palladium catalyst. However, the conversion was kept in modest level and no essential improvement of enantioselectivity.

Table 4.1 Phosphine ligands in Pd-catalyzed AAA reaction of malonate with allylic acetate^[a]

	Pd cat.	Ligand	Convesion ^[b]	ee ^[c] [%]
			[%]	
1	Pd(PPh ₃) ₄	–	92	–
2	[Pd(η ³ -C ₃ H ₅)Cl] ₂	4-1	0	–

3	$[\text{Pd}(\eta^3\text{-C}_3\text{H}_5)\text{Cl}]_2$	4-2	0	–
4	$[\text{Pd}(\eta^3\text{-C}_3\text{H}_5)\text{Cl}]_2$	4-3	0	–
5	$[\text{Pd}(\eta^3\text{-C}_3\text{H}_5)\text{Cl}]_2$	4-4	0	–
6	$[\text{Pd}(\eta^3\text{-C}_3\text{H}_5)\text{Cl}]_2$	4-5	50	10
7	$[\text{Pd}(\eta^3\text{-C}_3\text{H}_5)\text{Cl}]_2$	4-6	60	8
8	$[\text{Pd}(\eta^3\text{-C}_3\text{H}_5)\text{Cl}]_2$	4-7	67	30
9	$[\text{Pd}(\eta^3\text{-C}_3\text{H}_5)\text{Cl}]_2$	4-8	0	–

[a] Reaction conditions: **4-14** (0.10 mmol), **4-13** (0.15 mmol), palladium catalyst (5 mol%), ligand (10 mol%), Cs_2CO_3 (1.2 eq), THF (1.0 mL) at a room temperature for 24 h under Ar. [b]

Determined by TLC . [c] Determined by HPLC analysis with chiral columns.

After that, we changed the two reactants of allylic alkylation to α -substituted nitrophosphonate **4-16** and allylic carbamate **4-17** (Table 4.2). For preparing racemic products, it was found $\text{Pd}_2(\text{dba})_3$ is much more efficient than previous $[\text{Pd}(\eta^3\text{-C}_3\text{H}_5)\text{Cl}]_2$, affording the phosphonate product **4-18** in full conversion. Nonetheless, the same problem occurred when chiral phosphine ligands were applied, only tri-aryl phosphine amide ligand **4-6** could promote the transformation in 90% conversion but with only 15% ee. To make a complete comparison, (*R*)-BINAP was also examined and lower yield and ee were observed. It was shown that α -substituted nitrophosphonate is less reactive nucleophile possible owing to its steric hinder circumstance of nucleophilic carbon.

Table 4.2 Phosphine ligands in Pd-catalyzed AAA reaction of nitrophosphonate with allylic carbamate^[a]

Reaction scheme: **4-16** + **4-17** $\xrightarrow[\text{THF, r.t., Ar, 24h}]{\text{Pd cat. (5 mol%), L* (10 mol%)}}$ **4-18**

	Pd cat.	Ligand	Conversion ^[b] [%]	ee ^[c] [%]
1	[Pd(η^3 -C ₃ H ₅)Cl] ₂	PPh ₃	50	–
2	Pd ₂ (dba) ₃	PPh ₃	100	–
3	Pd ₂ (dba) ₃	4-1	0	–
4	Pd ₂ (dba) ₃	4-2	0	–
5	Pd ₂ (dba) ₃	4-3	0	–
6	Pd ₂ (dba) ₃	4-6	90	15
7	Pd ₂ (dba) ₃	4-8	0	–
8	Pd ₂ (dba) ₃	4-9	0	–
9	Pd ₂ (dba) ₃	4-10	0	–
10	Pd ₂ (dba) ₃	4-12	0	–
11	Pd ₂ (dba) ₃	(<i>R</i>)-BINAP	30	8

[a] Reaction conditions: **4-17** (0.10 mmol), **4-16** (0.12 mmol), palladium catalyst (5 mol%), ligand

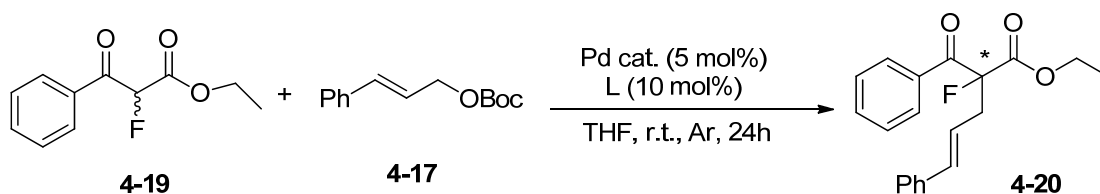
(10 mol%), THF (1.0 mL) at a room temperature for 24 h under Ar. [b] Determined by TLC. [c]

Determined by HPLC analysis with chiral columns.

Later, we selected α -fluoro- β -ketoester **4-19** and phthalide derivative **4-21** as

nucleophile independently under Pd/phosphine amide catalytic system (Table 4.3 & 4.4). Unfortunately, no essential change of either reactivity or enantioselectivity was observed. All obtained results implied Pd-catalyzed allylic alkylation is not a good model reaction for testing phosphine-amide ligands.

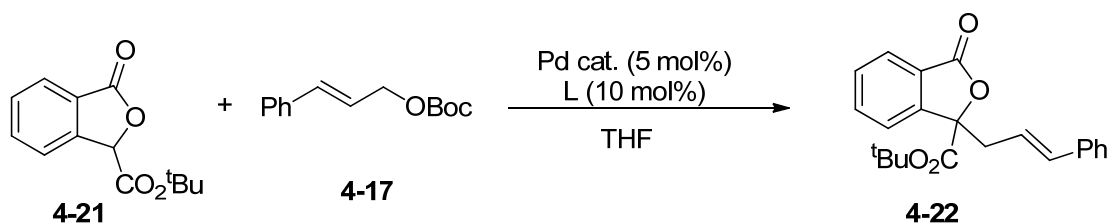
Table 4.3 Phosphine ligands in Pd-catalyzed AAA reaction of α -fluoro- β -ketoester with allylic carbamate^[a]



	Pd cat.	Ligand	Conversion ^[b] [%]	ee [%]
1	Pd(PPh ₃) ₄	–	95	0
2	[Pd(η^3 -C ₃ H ₅)Cl] ₂	4-6	0	–
3	[Pd(η^3 -C ₃ H ₅)Cl] ₂	4-11	0	–

[a] Reaction conditions: **4-17** (0.10 mmol), **4-19** (0.12 mmol), palladium catalyst (5 mol%), ligand (10 mol%), THF (1.0 mL) at a room temperature for 24 h under Ar. [b] Determined by TLC.

Table 4.4 Phosphine ligands in Pd-catalyzed AAA reaction of phthalide derivative with allylic carbamate^[a]



	Pd cat.	Ligand	Conversion ^[b] [%]	ee ^[c] [%]
1	Pd(PPh ₃) ₄	–	90	0
2	[Pd(η ³ -C ₃ H ₅)Cl] ₂	4-1	0	–
3	[Pd(η ³ -C ₃ H ₅)Cl] ₂	4-2	0	–
4	[Pd(η ³ -C ₃ H ₅)Cl] ₂	4-6	50	19
5	[Pd(η ³ -C ₃ H ₅)Cl] ₂	4-9	0	–
6	[Pd(η ³ -C ₃ H ₅)Cl] ₂	4-11	0	–
7	Pd ₂ (dba) ₃	4-1	0	–
8	Pd ₂ (dba) ₃	4-2	0	–
9	Pd ₂ (dba) ₃	4-9	0	–

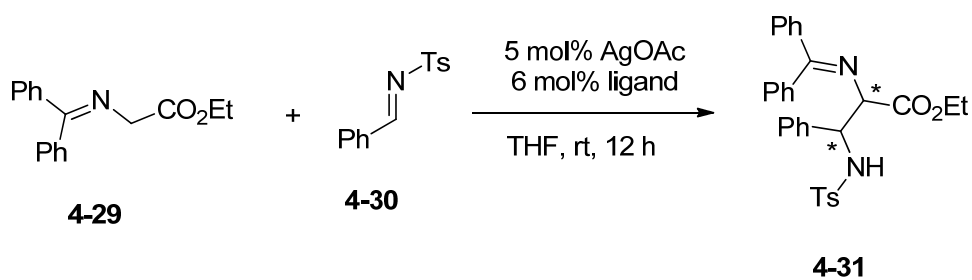
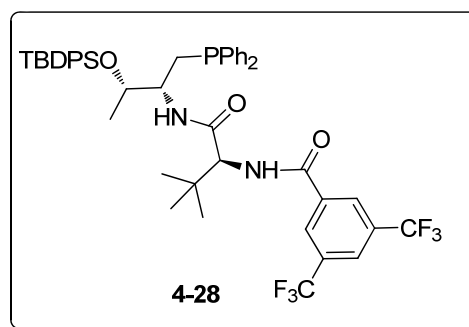
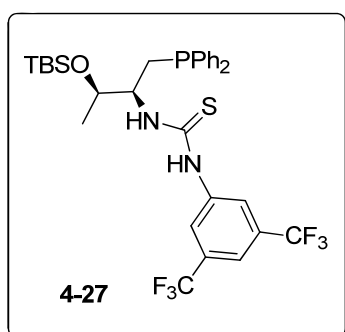
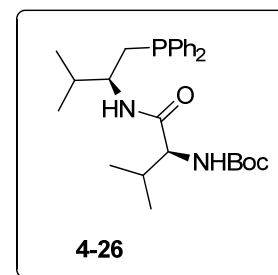
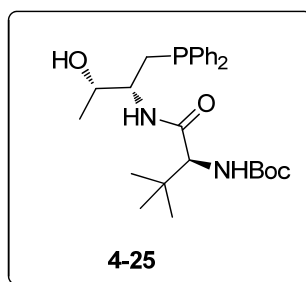
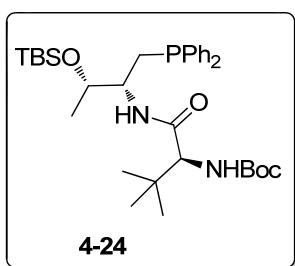
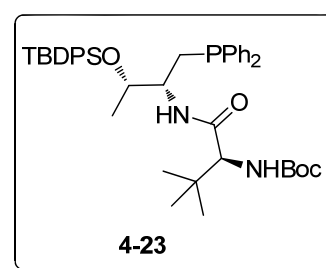
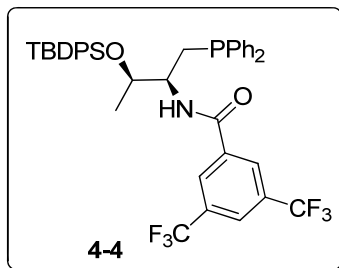
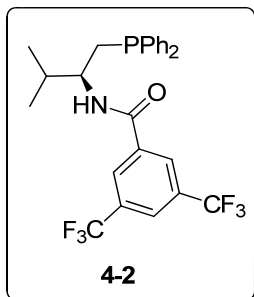
[a] Reaction conditions: **4-17** (0.10 mmol), **4-21** (0.12 mmol), palladium catalyst (5 mol%), ligand (10 mol%), THF (1.0 mL) at a room temperature for 24 h under Ar. [b] Determined by TLC. [c]

Determined by HPLC analysis with chiral columns.

Thus, we switched our interest onto silver-catalyzed enantioselective Mannich reaction of glycine derivatives **4-29** with imines **4-30** and a series of phosphine-amide ligands were examined (Table 4.5). The 3,5-di-trifluoromethyl phenyl amide phosphine ligand **4-2** was firstly employed in this reaction, using diphenyl glycine imine

derivative **4-29** and tosyl imine **4-30** as substrates. To our delight, the reaction proceeded very well under this condition and more than 90% conversion was achieved, although with low diastereoselectivity ($dr = 4.2:1$) and enantioselectivity (12% ee). After that, two modified ligands **4-4** and **4-26** were tested to verify the steric effect. It was found that modification of amide group to peptide bi-functional ligand could remarkably increase the enantioselectivity. Some phosphine-peptide ligands were then synthesized to optimize reaction conditions. Among all of these phosphine-peptide ligands, ligand **4-23** could afford the best result ($dr = 5.8:1$, ee = 81%). A phosphine-thiourea ligand **4-27** containing strong hydrogen bonding was also examined, but no desired product was achieved.

Table 4.5 Phosphine ligands in Ag-catalyzed asymmetric Mannich reaction^[a]



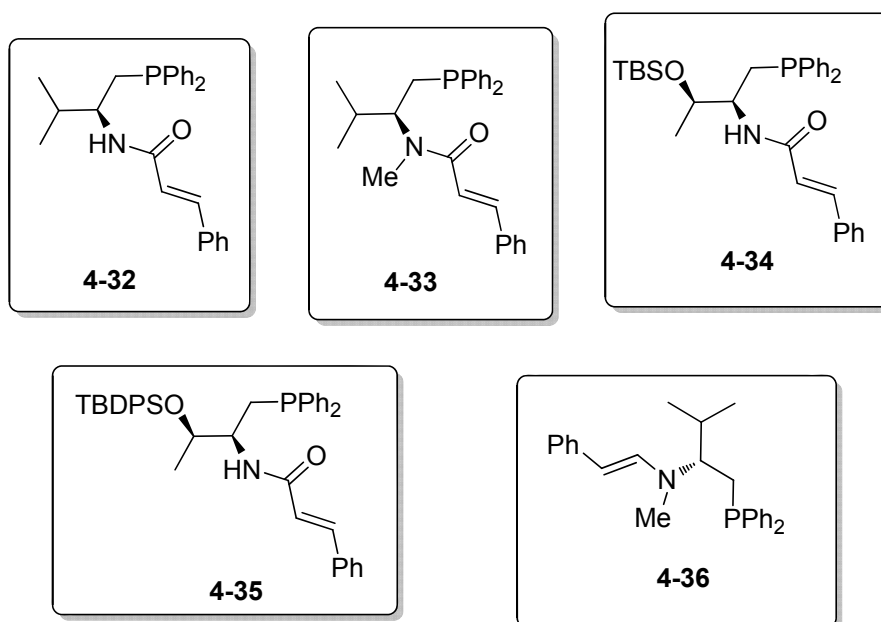
	Ligand	Conversion ^[b] [%]	dr ^[c]	ee(major) ^[d] [%]
1	PPh ₃	90	–	–
2	4-2	90	4.2:1	12

3	4-4	90	4.8:1	13
4	4-23	90	5.8:1	81
5	4-24	90	4.1:1	63
6	4-25	90	3.6:1	50
7	4-26	90	3.0:1	43
8	4-27	0	–	–
9	4-28	90	4.5:1	61

[a] Reaction conditions: **4-29** (0.10 mmol), **4-30** (0.12 mmol), silver catalyst (5 mol%), ligand (6 mol%), THF (1.0 mL) at a room temperature for 24 h under Ar. [b] Determined by TLC. [c] Determined by ^1H NMR. [d] Determined by HPLC analysis with chiral columns.

4.4.2 Phosphine-olefin ligands

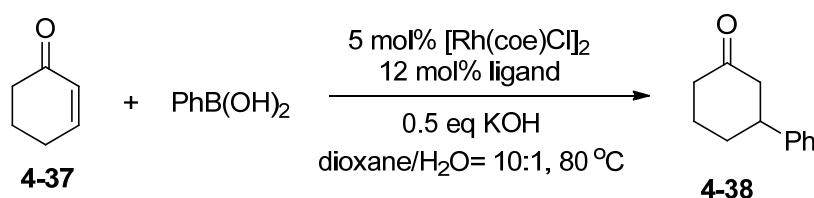
In addition to above phosphine-amide type ligands, a class of phosphine ligands containing olefin were synthesized as well (Scheme 4.8).



Scheme 4.8 Phosphine-olefin ligands derived from amino acids

Rh-catalyzed asymmetric 1,4-addition of organoboronic acid to cycloenone **4-37** were selected as a model reaction. Unfortunately, none of them could give the desired additive product under the standard condition (Table 4.6). By further NMR investigation, it implied that there was no coordination between olefin and rhodium catalyst, making the rhodium catalyst unstable in the reaction circumstance (Figure 4.1).

Table 4.6 Phosphine-olefin ligands in Rh-catalyzed 1,4-addition^[a]



	Ligand	Yield ^[b] [%]
1	4-32	0
2	4-33	0
3	4-34	0
4	4-35	0
5	4-36	0

[a] Reaction conditions: **4-37** (0.10 mmol), benzenboronic acid (0.2 mmol), rhodium catalyst (5 mol%), ligand (12 mol%), dioxane (1.0 mL) and KOH aq. (0.050 mmol, 0.1 mL) at 80 °C for 12 h under Ar. [b] Determined by TLC.

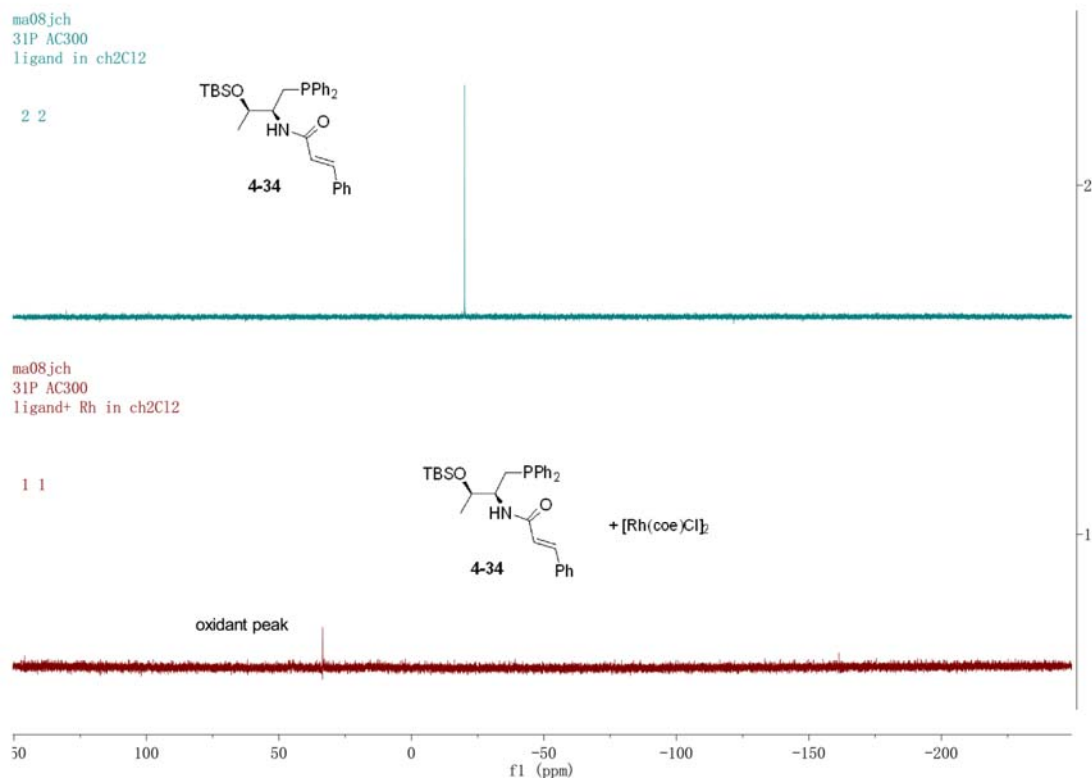
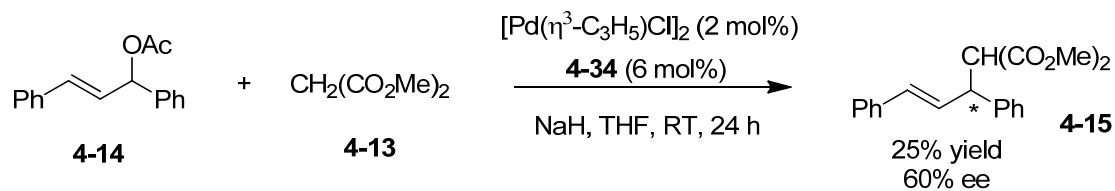


Figure 4.1 ³¹P NMR study on coordination between Rh catalyst and phosphine-olefin ligand

The phosphine-olefin ligand **4-34** was tried in asymmetric allylic alkylation.

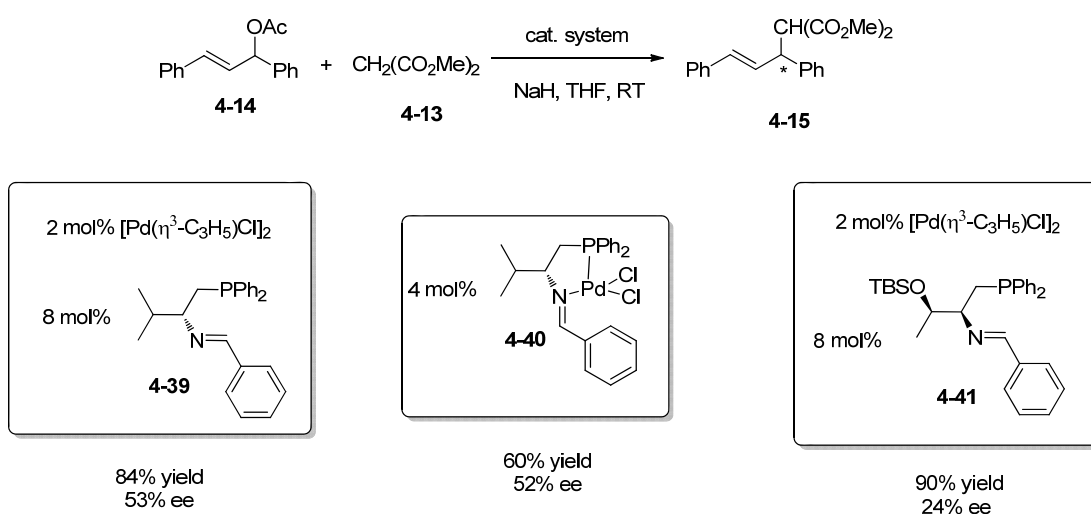
However, no impressive result was obtained (Scheme 4.9).



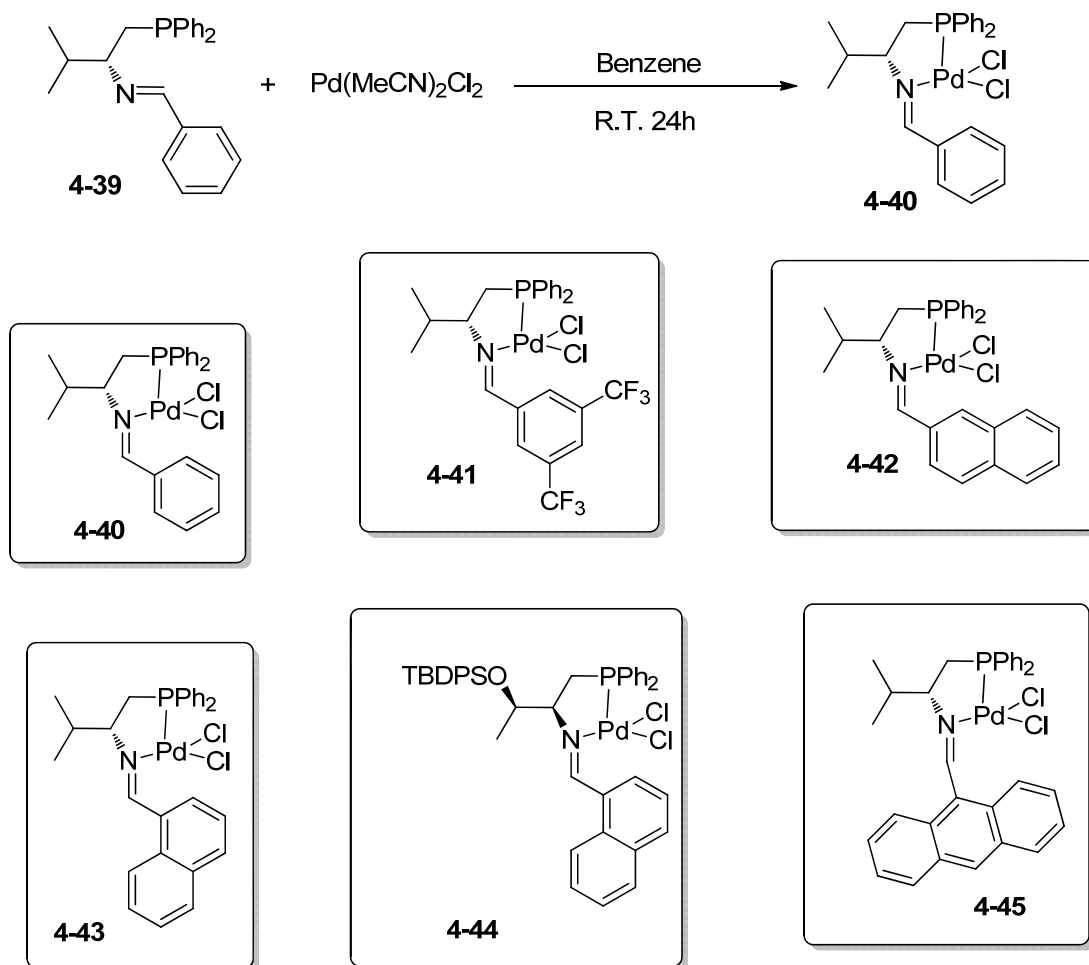
Scheme 4.9 Phosphine-olefin ligand in Pd-catalyzed AAA reaction

4.2.3 Phosphine-imine ligands

Last but not least, we developed some phosphine-imine ligands inspired from Morimoto's work in 2000. All of these phosphine-imine ligands could be easily derived from phosphine-amine precursors, leading to a facile modification of ligands. On account of the early applications of phosphine-imine ligands are Pd-catalyzed asymmetric allylic alkylations, we decided to select this reaction to test the reactivity of phosphine-imine ligands firstly. Substrates dimethyl malonate **4-13** and allyl acetate **4-14** could provide the desired product with good yield (84%) and modest ee (53%) in the presence of $[\text{Pd}(\eta^3\text{-C}_3\text{H}_5)\text{Cl}]_2$ and phosphine-imine ligand **4-39** under the standard condition. Interestingly, stable complex could generate between palladium catalyst precursor and phosphine-imine ligand **4-39** and the forming palladium complex **4-40** could also catalyze the transformation efficiently with approximate ee. Further optimization of bulky group at β -position even decreased the enantioselectivity (24% ee) (Scheme 4.10).

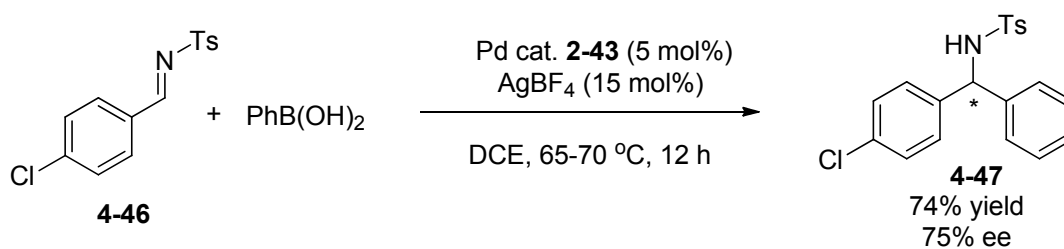


Scheme 4.10 Phosphine-imine ligands in Pd-catalyzed AAA reaction



Scheme 4.11 Pd/phosphine-imine complexes

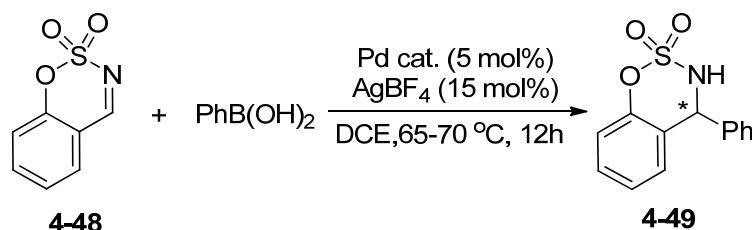
Pd-catalyzed asymmetric addition of imines is a well-established method for synthesizing chiral amine derivatives with tertiary or quaternary carbon center. We started screening the Pd/phosphine-imine complex **4-43** by using tosyl imines **4-46** as substrate for asymmetric phenylation. Desired adduct was obtained in 75% yield and 74% ee (Scheme 4.12).



Scheme 4.12 Pd/phosphine-imine complex catalyzed asymmetric arylation of tolsyl imine

Meanwhile, N-sulfonyl cyclic imines were found to be less investigated in this transformation. Hence we decided to test the reactivity of Pd/phosphine-imine complexes for these cyclic imines. The results were summarized in Table 4.7. We were delighted to find complex **4-40** can well promote the transformation in modest yield (58%) and with best ee (81%) so far. Later the aryl groups of imine parts were modified. While two CF₃ groups were introduced to *meta*-positions, catalytic activity increased dramatically (92% yield) but enantioselectivity slightly dropped (77% ee). it was also found that replacement of phenyl group by a bulky aryl group could increase the enantioselectivity and 1-naphthyl **4-43** performed better for improving yield than 4-naphthyl group **4-44**. Introducing a 9-anthracenyl group **4-45** caused almost no change about either activity or enantioselectivity. A further modification on β -position by OTBDPS group **4-44** even decreased the ee.

Table 4.7 Pd/phosphine-imine complex catalyzed asymmetric arylation of 6-membered cyclic imine^[a]



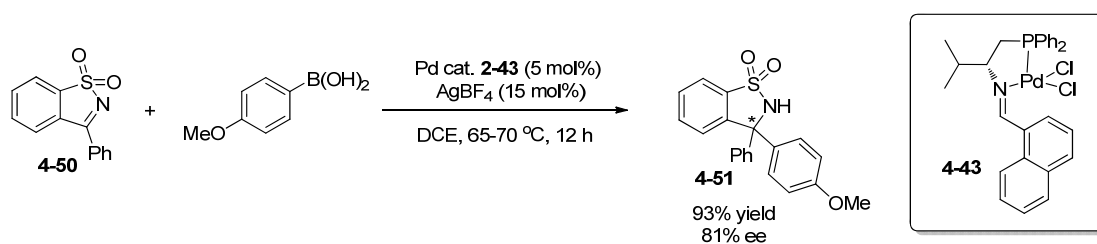
	Pd cat.	Yield ^[b] [%]	ee ^[c] [%]
1	4-40	58	81

2	4-41	92	77
3	4-42	58	87
4	4-43	98	91
5	4-44	99	53
6	4-45	98	92

[a] Reaction conditions: **4-48**(0.10 mmol), benzenboronic acid (0.20 mmol), catalyst (5 mol%), AgBF₄ (15 mol%), DCE (1.0 mL) at a given temperature for 12 h. [b] Isolated yield of **4-49**. [c]

Determined by HPLC analysis with chiral columns.

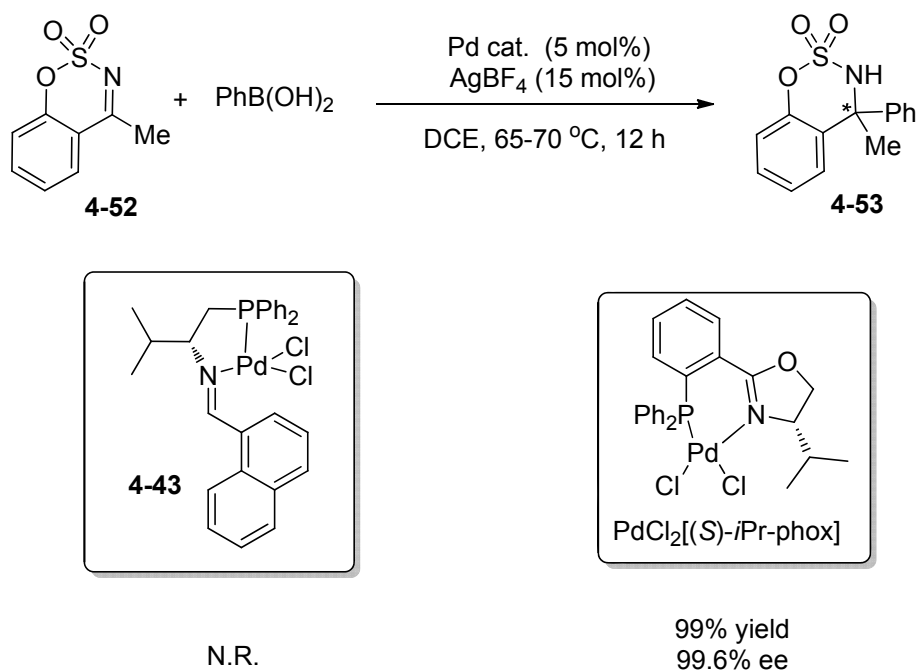
Besides unsubstituted cyclic imines, other substituted cyclic imines were examined as well. The arylation of five-membered ring cyclic imine **4-50** proceeded efficiently by applying the best catalyst **4-43**, providing the benzosultam **4-51** with 93% yield and 81% ee (Scheme 4.13).



Scheme 4.13 Pd/phosphine-imine complex catalyzed asymmetric arylation of 5-membered cyclic imine

However, the methyl substituted six-membered ring one didn't give any desired product under the same condition owing to its low reactivity. After that, we tested the

well-known PHOX ligand finding it is much more reactive comparing our developed phosphine-imine ligands (Scheme 4.14).



Scheme 4.14 Comparison between Pd/phosphine-imine and Pd/PHOX complexes

4.3 Conclusion

In conclusion, a series of phosphine-amide ligands, phosphine-olefin ligands and phosphine-imines ligands were prepared *via* a few steps from inexpensive amino acids. The applications of these new ligands in transition-metal-catalyzed asymmetric reactions were also examined. It was found that only a few of them can afford promising results, which are still not comparable with the reported methods.

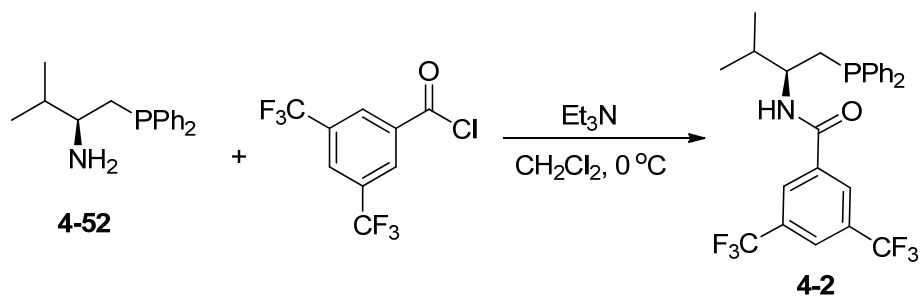
4.4 Experimental section

4.4.1 General Information

All the starting materials were obtained from commercial sources and used without further purification unless otherwise stated. THF was dried and distilled from sodium benzophenone ketyl prior to use. CH₂Cl₂ were distilled from CaH₂ prior to use. ¹H and ¹³C NMR spectra were recorded on a Bruker AMX500 (500 MHz) spectrometer. Chemical shifts were reported in parts per million (ppm), and the residual solvent peak was used as an internal reference: proton (chloroform δ 7.26), carbon (chloroform δ 77.0). Multiplicity was indicated as follows: s (singlet), d (doublet), t (triplet), q (quartet), m (multiplet), dd (doublet of doublet), and br s (broad singlet). Coupling constants were reported in Hertz (Hz). Low resolution mass spectra were obtained on a Finnigan/MAT LCQ spectrometer in ESI mode, and a Agilent Tech. 5975C inert MSD. All high resolution mass spectra were obtained on a Finnigan/MAT 95XL-T spectrometer. For thin layer chromatography (TLC), Merck pre-coated TLC plates (Merck 60 F254) were used, and compounds were visualized with a UV light at 254 nm. Further visualization was achieved by staining with iodine, or ceric ammonium molybdate followed by heating on a hot plate. Flash chromatographic separations were performed on Merck 60 (0.040-0.063 mm) mesh silica gel. The Enantiomerically excesses of products were determined by chiral-phase HPLC analysis, using a Daicel Chiralpak IA column (250 x 4.6 mm), Chiralpak AD-H column (250 x 4.6 mm), or Chiralcel IC column (250 x 4.6 mm).

4.4.2 General procedure for preparation of ligands

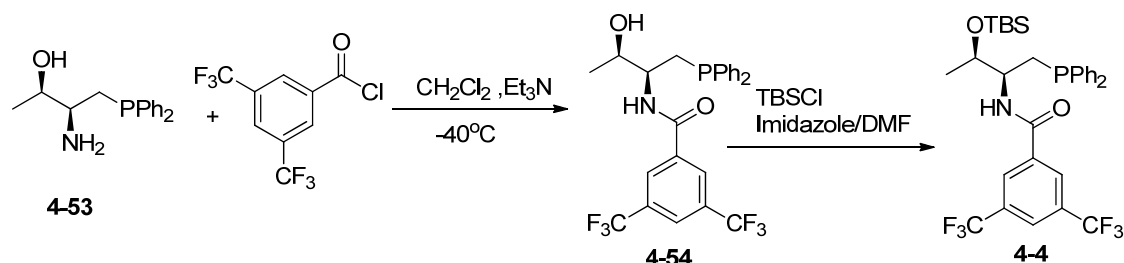
4.4.2.1 Phosphine-amide ligands from L-valine



To a solution of aminophosphine **4-52** (0.22 mmol) and Et₃N (62 μL, 0.44 mmol) in anhydrous CH₂Cl₂ (1.0 mL) was slowly added a solution of 3,5-bis(trifluoromethyl)benzoyl chloride (49 μL, 0.27 mmol) at 0 °C. The resulting mixture was stirred at the same temperature for 1h. Water (2 mL) was added and the organic layer was separated. The aqueous phase was extracted with CH₂Cl₂ (2x3 mL). The combined organic layers was washed with brine and dried over Na₂SO₄. Solvent was removed under vacuum and the residue was purified column chromatography on silica gel using hexane/ethyl acetate as an eluent to afford **4-2** (91 mg, 83% yield) as a white solid.

¹H NMR (500 MHz, CDCl₃) δ 1.46 (d, *J* = 7.0 Hz, 6H), 4.49 (d, *J* = 7.0 Hz, 2H), 4.44-4.50 (m, 1H), 6.08 (s, 1H), 7.25-7.34 (m, 6H), 7.42 (td, *J* = 7.6 Hz, 1.3 Hz, 2H), 7.49 (td, *J* = 7.6 Hz, 1.3 Hz, 2H), 7.96 (s, 3H); ¹³C NMR (125 MHz, CDCl₃) δ 24.20 (d, *J* = 10.0 Hz), 35.81 (d, *J* = 15.5 Hz), 45.28 (d, *J* = 15.7 Hz), 121.80, 123.97, 124.75 (d, *J* = 4.6 Hz), 127.12, 128.62 (d, *J* = 3.6 Hz), 128.68 (d, *J* = 3.6 Hz), 128.95 (d, *J* = 10.0 Hz), 131.95 (q, *J* = 34.6 Hz), 134.64 (d, *J* = 10.9 Hz), 134.79 (d, *J* = 14.3 Hz), 136.55, 137.70 (d, *J* = 10.9 Hz), 138.06 (d, *J* = 11.8 Hz), 163.56; ³¹P NMR (121 MHz, CDCl₃) δ -24.45; HRMS (ESI) *m/z* calcd for C₂₄H₂₀F₆NOP [M+H]⁺ = 497.1343, found = 497.1337.

4.4.2.2 Phosphine-amide ligands from L-threonine



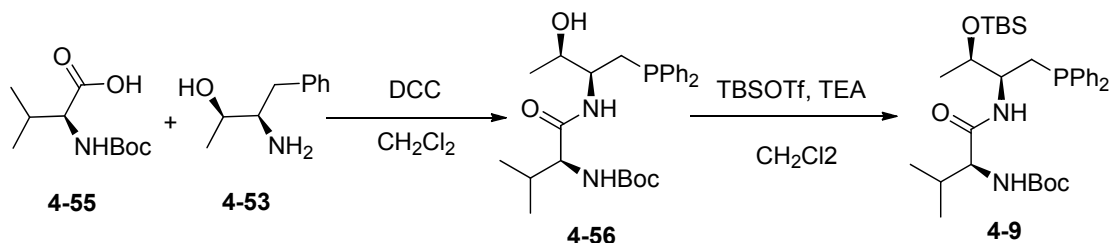
To a solution of **4-53** (546 mg, 2 mmol) and Et_3N (417 μL , 3 mmol) in anhydrous CH_2Cl_2 (30 mL) was slowly added a solution of 3,5-bis(trifluoromethyl)benzoyl chloride (360 μL , 2 mmol) in CH_2Cl_2 (30 mL) at -50°C over 30 min. The resulting mixture was stirred at the same temperature for 1h and then warmed to room temperature. Water (45 mL) was added and the organic layer was separated. The aqueous phase was extracted with CH_2Cl_2 (2 x 15 mL). The combined organic layers were washed with brine and dried over Na_2SO_4 . Solvent was removed under reduced pressure and the residue was purified by column chromatography on silica gel using hexane/ethyl acetate to afford **4-54** (630 mg, 62% yield) as a white solid.

To a solution of **4-54** (61 mg, 0.12 mmol) in dry DMF (28 μL , 0.36 mmol) was added imidazole (25 mg, 0.36 mmol) and *tert*-butyldimethylsilyl chloride (22 mg, 0.15 mmol) at room temperature under N_4 . The solution was stirred for 36 h, and the mixture was directly purified by column chromatography using hexane/ethyl acetate as eluent to afford **4-4** as a white solid (61 mg, 81 % yield).

^1H NMR (500 MHz, CDCl_3) δ 0.14 (s, 3H), 0.16 (s, 3H), 0.94 (s, 9H), 1.16 (d, $J = 7.7$

Hz, 3H), 4.27 (dd, $J = 7.6$ Hz, 13.3 Hz, 1H), 4.64-4.68 (m, 1H), 4.15-4.18 (m, 1H), 4.31-4.35 (m, 1H), 6.66 (d, $J = 8.9$ Hz, 1H), 7.30-7.38 (m, 6H), 7.39-7.41 (m, 2H), 7.56-7.59 (m, 2H), 7.99 (s, 1H), 8.11 (s, 2H); ^{13}C NMR (125 MHz, CDCl_3) δ 17.91, 21.26, 25.78, 29.65, 31.47 (d, $J = 13.7$ Hz), 53.40 (d, $J = 15.6$ Hz), 69.23 (d, $J = 10.9$ Hz), 123.99, 124.86, 127.08, 128.57 (d, $J = 7.3$ Hz), 128.69 (d, $J = 7.3$ Hz), 128.81, 129.18, 134.76 (q, $J = 28.8$ Hz), 136.52, 163.54; ^{31}P NMR (121 MHz, CDCl_3) δ -24.77; HRMS (ESI) m/z calcd for $\text{C}_{31}\text{H}_{36}\text{F}_6\text{NO}_2\text{PSi}$ $[\text{M}+\text{H}]^+ = 628.2230$, found = 628.2240.

4.4.2.3 Phosphine-peptide ligands from L- threonine



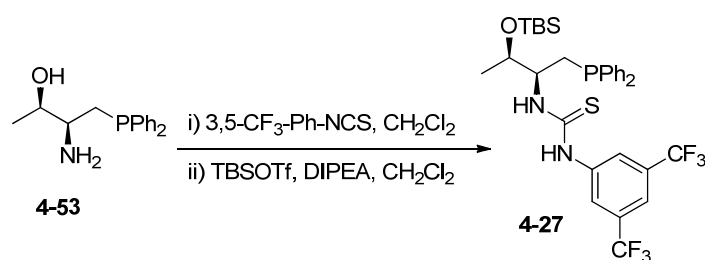
To a stirred solution of N-Boc L-valine **4-55** (0.176 g, 0.82 mmol) in anhydrous DCM (5 mL) was added DCC (84 mg, 0.41 mmol), and the resulting mixture was stirred at room temperature for 2 h. The solution was then cooled to 0 °C and a solution of (0.1 g, 0.37 mmol) in DCM (1 mL) was added dropwise over 2 minutes. The reaction mixture was stirred for additional 0.5 h at 0 °C and 0.5 h at room temperature. Water (10 mL) was added to quench the reaction, and the resulting mixture was extracted with DCM (3 x 10 mL). The combined organic extracts were dried over Na_2SO_4 , filtered, concentrated, and the residue was purified by column chromatography using hexane/EA as eluent to afford **4-56** (0.138 g, 79%) as a white solid. To a solution of **4-56** in anhydrous DCM (5 mL) at 0 °C was added TEA (61 μL , 0.44 mmol), followed by addition of TBSOTf (0.11 mL, 0.69 mmol) dropwise. Then the mixture was

allowed to warm to room temperature and continued stirring for additional 1 hour.

The reaction was quenched with saturated aqueous NaHCO₃ (10 mL) and extracted with DCM (2 × 20 mL). The combined organic extracts were washed with brine, and dried over Na₂SO₄. Purification by column chromatography using hexane/EA as eluent to afford **4-9** (0.140 g, 82% yield) as a white solid.

¹H NMR (300 MHz, CDCl₃) δ7.59-7.28 (m, 10H), 6.32 (s, 1H), 5.03 (s, 1H), 4.34-4.26 (m, 1H), 3.95-3.75 (m, 2H), 4.38 (dd, *J* = 3.9, 10.5 Hz, 1H), 4.20-4.12 (m, 2H), 1.42 (s, 9H), 1.07 (d, *J* = 6.0 Hz, 3H), 0.98-0.90 (m, 15H), 0.10 (d, *J* = 4.1 Hz, 6H); ¹³C NMR (75 MHz, CDCl₃) δ170.9, 138.6, 134.9, 134.7 (d), 134.5, 128.4 (dd), 79.6, 68.2(d), 60.0, 54.3 (d), 31.7 (d), 20.8, 19.2, 17.7 (d), -4.5; ³¹P NMR (121 MHz, CDCl₃) δ-23.9 (s); HRMS (ESI) *m/z* calcd for C₃₂H₅₂N₂O₄PSi [M+H]⁺ = 587.3428, found = 587.3449; [α]_D²⁵ = -19.7 (*c* 0.80, CHCl₃).

4.4.2.4 Phosphine-thiourea ligands from L-threonine



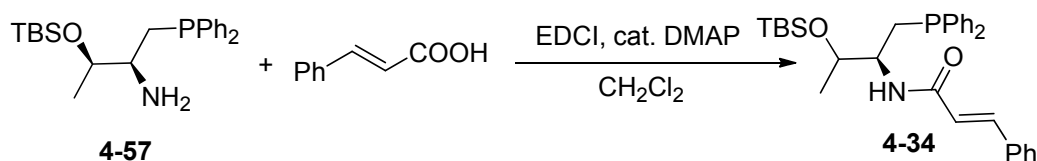
To a solution of the amino phosphine **4-53** (82 mg, 0.30 mmol) in CH₂Cl₂ (2 mL) was added 4-fluorophenyl isocyanate (46 mg, 0.33 mmol) under N₂ and the reaction mixture was stirred at room temperature for 2 hrs. Solvent was removed under reduced pressure and the residue was directly subjected to column chromatographic separation on silica gel using hexane/ethyl acetate as an eluent to afford white solid

intermediate (94 mg, 0.23 mmol). This intermediate was then dissolved in anhydrous CH_2Cl_2 (2 mL), followed by the addition of DIPEA (119 μL , 0.69 mmol) and *tert*-butyldimethylsilyl trifluoromethanesulfonate (63 μL , 0.28 mmol). The reaction mixture was stirred at room temperature for 1 h, and solvent was removed. The residue was directly purified by column chromatography on silica gel using hexane/ethyl acetate as an eluent to afford **4-27** as a white solid (107 mg, 68% yield).

A white solid; 61% yield;

^1H NMR (500 MHz, CDCl_3) δ 0.04 (s, 6H), 0.66 (s, 9H), 1.13 (d, $J = 3.6$ Hz, 3H), 4.16 (br, 1H), 4.68 (br, 1H), 4.34-4.40 (m, 2H), 6.46 (br, 1H), 7.30-7.40 (m, 8H), 7.61 (br, 2H), 7.71 (br, 3H), 8.40 (s, 1H); ^{13}C NMR (125 MHz, CDCl_3) δ -4.72, -4.70, -4.35, 17.69, 21.32, 25.53, 31.57 (d, $J = 14.7$ Hz), 58.72 (d, $J = 16.7$ Hz), 68.60 (d, $J = 10.2$ Hz), 120.05, 121.61, 123.78, 124.91, 128.48, 128.53, 128.72, 128.99, 134.65, 134.80, 133.02, 133.17, 137.05, 138.39, 180.30; ^{31}P NMR (121 MHz, CDCl_3) δ -24.12; HRMS (ESI) m/z calcd for $\text{C}_{31}\text{H}_{37}\text{F}_6\text{N}_2\text{OPSSi}$ $[\text{M}+\text{H}]^+ = 659.2110$, found = 659.2114.

4.4.2.5 Phosphine-olefin ligands

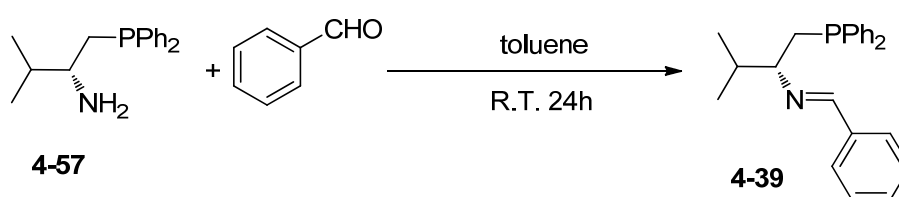


To a stirred solution of cinnamic acid (0.82 mmol) in anhydrous DCM (5 mL) was added EDCI (0.41 mmol), and the resulting mixture was stirred at room temperature for 2 h. The solution was then cooled down to 0 $^\circ\text{C}$ and a solution of aminophosphine **4-57** (0.37 mmol) in DCM (1 mL) was added dropwise over 2 minutes. The reaction mixture was stirred for additional 0.5 h at 0 $^\circ\text{C}$ and 0.5 h at room temperature. Water

(10 mL) was added to quench the reaction, and the resulting mixture was extracted with DCM (3 x 10 mL). The combined organic extracts were dried over Na₂SO₄, filtered, concentrated, and the residue was purified by column chromatography using hexane/EA as eluent to afford **4-34** (0.18 g, 82%) as a white solid.

¹H NMR (500 MHz, CDCl₃) δ 7.65–7.55 (m, 3H), 7.50 (dd, *J* = 7.6, 1.4 Hz, 2H), 7.37 (qt, *J* = 7.8, 4.6 Hz, 8H), 7.32 (dd, *J* = 13.0, 3.3 Hz, 3H), 6.30 (d, *J* = 15.6 Hz, 1H), 5.93 (d, *J* = 7.9 Hz, 1H), 4.30 (q, *J* = 6.1 Hz, 1H), 4.19–3.95 (m, 1H), 4.61–4.41 (m, 1H), 4.37–4.18 (m, 1H), 1.12 (d, *J* = 6.2 Hz, 3H), 0.93 (s, 10H), 0.13 (d, *J* = 4.3 Hz, 7H); ¹³C NMR (126 MHz, CDCl₃) δ 165.40, 140.90, 134.90, 133.00, 134.85, 134.81, 134.66, 129.56, 128.87, 128.74, 128.67, 128.61, 128.49, 128.43, 127.78, 120.77, 68.92, 68.83, 54.60, 54.48, 31.62, 31.52, 25.94, 25.63, 20.77, 18.04, -4.23, -4.53. ³¹P NMR (202 MHz, CDCl₃) δ -23.03.

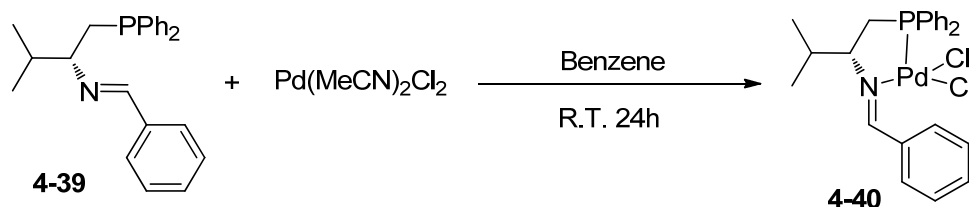
4.4.2.6 Phosphine-imine ligands



To a solution of the amino phosphine **4-57** (82 mg, 0.30 mmol) in toluene (2 mL) was added benzyl aldehyde (30 μL, 0.3 mmol) under N₂ and the reaction mixture was stirred at room temperature for 6 h. Solvent was removed under reduced pressure and the residue was used without purification.

¹H NMR (500 MHz, CDCl₃) δ 8.05 (s, 1H), 7.62 (d, *J* = 6.3 Hz, 2H), 7.52 – 7.44 (m, 2H), 7.43 – 7.32 (m, 8H), 7.24 (d, *J* = 6.5 Hz, 3H), 3.04 (dq, *J* = 14.6, 6.2 Hz, 1H),

4.51 (d, $J = 6.6$ Hz, 2H), 4.01 (dq, $J = 13.1, 6.6$ Hz, 1H), 0.94 (t, $J = 7.2$ Hz, 6H).; ^{31}P NMR (202 MHz, CDCl_3) δ -19.98.

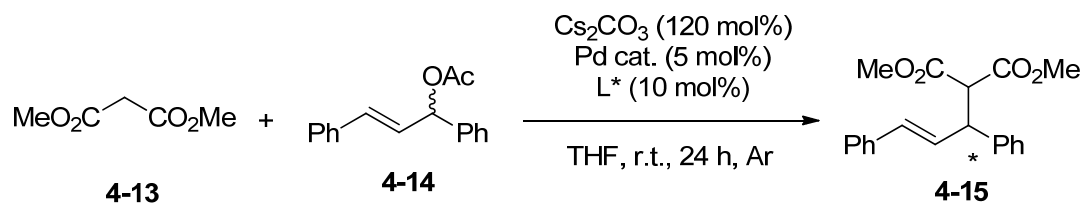


To a solution of the $\text{Pd}(\text{MeCN})_2\text{Cl}_2$ (51 mg, 0.20 mmol) in benzene (2 mL) was added a solution of the phosphine-imine ligand **4-39** (80 mg, 0.22 mmol) under N_2 and the reaction mixture was stirred at room temperature for 3 h. The precipitate was collected by filtration to afford Pd complex **4-40** in 82% yield as a yellow solid.

^1H NMR (300 MHz, CDCl_3) δ 8.58 (s, 1H), 8.51 (d, $J = 7.4$ Hz, 2H), 8.11 – 7.95 (m, 2H), 7.88 (dd, $J = 14.4, 7.1$ Hz, 2H), 7.64 – 7.31 (m, 12H), 3.67 (d, $J = 41.8$ Hz, 1H), 3.00 (s, 1H), 4.72 (d, $J = 11.5$ Hz, 2H), 1.17 (d, $J = 6.2$ Hz, 3H), 0.81 (d, $J = 6.3$ Hz, 3H).; ^{31}P NMR (121 MHz, Acetone) δ 40.44.

4.4.3 General procedures for transition-metal-catalyzed reactions

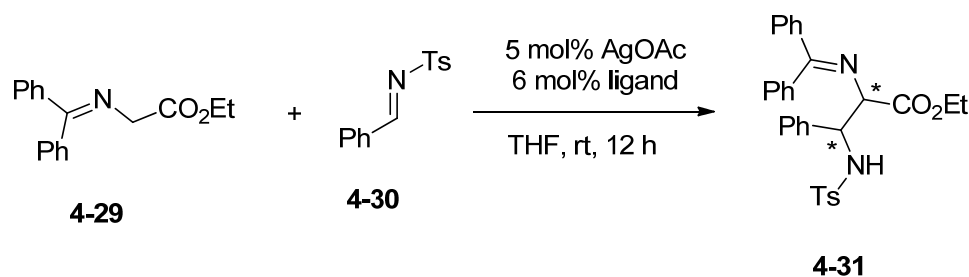
4.4.3.1 Pd-catalyzed AAA reaction



To a catalyst solution of palladium catalyst (0.005 mmol) and phosphine ligand (0.01 mmol) in THF (0.1 mL) were added allylic acetate **4-14** (0.1 mmol), Cs_2CO_3 (0.12

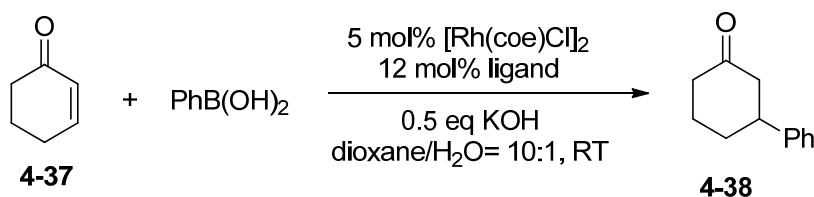
mmol) and dimethyl malonate **4-13** (0.15 mol) subsequently under Ar. The resulting mixture was allowed to stir at room temperature for 24 h and the mixture was directly subjected to column chromatographic separation on silica gel using hexane/ethyl acetate as an eluent to afford allylic product **4-15**. The *ee* value of **4-15** was determined by HPLC analysis under the condition (Chiralpak IA, $\lambda = 254$ nm, hexane/*i*-PrOH = 95/5, flow rate = 1.0 mL/min).

4.4.3.2 Ag-catalyzed Mannich reaction



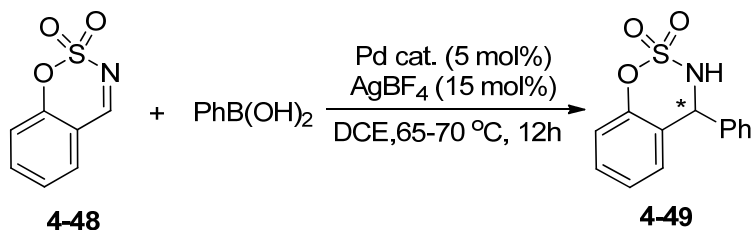
To a catalyst solution of silver catalyst (0.005 mmol) and phosphine-amide ligand (0.006 mmol) in THF (0.1 mL) were added glycine imine derivative **4-29** (0.1 mmol) and tosyl imine **4-30** (0.12 mol) subsequently under N_2 . The resulting mixture was allowed to stir at room temperature for 12 h and the mixture was directly subjected to column chromatographic separation on silica gel using hexane/ethyl acetate as an eluent to afford Mannich product **4-31**. The d.r. was determined by ^1H NMR analysis. The *ee* value of **4-31** was determined by HPLC analysis under the condition (Chiralpak AD-H, $\lambda = 254$ nm, hexane/*i*-PrOH = 9/1, flow rate = 1.0 mL/min).

4.4.4.3 Rh-catalyzed 1,4-addition



To a catalyst solution of $[\text{Rh}(\text{coe})\text{Cl}]_2$ (0.005 mmol) and phosphine-olefin ligand (0.012 mmol) in dioxane (0.5 mL) were added cyclohexenone **4-37** (0.1 mmol), benzeneboronic acid and potassium hydroxide aqueous solution (0.05 mmol) subsequently under N_2 . The resulting mixture was allowed to stir at room temperature for 12 h and the mixture was directly subjected to column chromatographic separation on silica gel using hexane/ethyl acetate as an eluent to afford adduct product **4-38**.

4.4.4.4 Pd catalyzed 1,2-addition



Palladium complex (0.0050 mmol), ketamine **4-48** (0.100 mmol), and benzeneboronic acid (24.4 mg, 0.200 mmol) were placed in Schlenk tube under nitrogen. To the tube, 1,2-dichloroethane (0.5 mL) was added, and then AgBF_4 (0.015 mmol) in 1,2-dichloroethane (0.5 mL) was added. The reaction mixture was stirred at 65–70 °C for 12 h, and the mixture was directly subjected to flash chromatography on silica gel using hexane/ethyl acetate (4:1) as an eluent to give **4-49** as a colorless solid. The *ee* value of **4-49** was determined by HPLC analysis under the condition (Chiralpak IC, $\lambda = 220 \text{ nm}$, hexane/*i*-PrOH = 9/1, flow rate = 1.0 mL/min).